



**HAL**  
open science

# Nouveaux polyesters biosourcés comme additifs pour moduler les propriétés rhéologiques des lubrifiants

Hélène Meheust

► **To cite this version:**

Hélène Meheust. Nouveaux polyesters biosourcés comme additifs pour moduler les propriétés rhéologiques des lubrifiants. Polymers. Université de Bordeaux, 2018. English. NNT: 2018BORD0291 . tel-03402978

**HAL Id: tel-03402978**

**<https://theses.hal.science/tel-03402978>**

Submitted on 26 Oct 2021

**HAL** is a multi-disciplinary open access archive for the deposit and dissemination of scientific research documents, whether they are published or not. The documents may come from teaching and research institutions in France or abroad, or from public or private research centers.

L'archive ouverte pluridisciplinaire **HAL**, est destinée au dépôt et à la diffusion de documents scientifiques de niveau recherche, publiés ou non, émanant des établissements d'enseignement et de recherche français ou étrangers, des laboratoires publics ou privés.

THÈSE PRÉSENTÉE  
POUR OBTENIR LE GRADE DE

**DOCTEUR DE**  
**L'UNIVERSITÉ DE BORDEAUX**

ÉCOLE DOCTORALE DES SCIENCES CHIMIQUES  
SPÉCIALITÉ: POLYMÈRES

Par **Hélène MEHEUST**

**NEW FATTY ACID-BASED POLYESTERS AS VISCOSITY  
CONTROL ADDITIVES FOR LUBRICANTS**

**Nouveaux polyesters biosourcés comme additifs pour moduler les propriétés  
rhéologiques des lubrifiants**

Sous la direction de : Pr. Henri CRAMAIL  
Co-encadrant : Dr. Etienne GRAU

Soutenance le 06/12/2018

Membres du jury :

Mme NEGRELL, Claire  
M. NICOL, Erwan  
M. NICOLAY, Renaud  
M. SANDRE, Olivier  
M. GRAU, Etienne  
M. CRAMAIL, Henri  
Mme VOUILLON, Nathalie  
M. CHOLLET, Guillaume

Ingénieure d'étude CNRS, HDR, ICG Montpellier  
Maître de conférences, HDR, Le Mans Université  
Professeur, ESPCI Paris Tech  
Directeur de recherche, INC Bordeaux  
Maître de conférences, Université de Bordeaux  
Professeur, Université de Bordeaux  
Docteur, SAS PIVERT, Compiègne  
Docteur, ITERG, Bordeaux

Rapportrice  
Rapporteur  
Examineur  
Président du jury  
Examineur  
Directeur de thèse  
Invitée  
Invité



***Disclaimer***

*« Ce document est confidentiel, et a été réalisé dans le cadre du programme de recherche GENESYS de la SAS PIVERT. Il ne peut être ni reproduit ni exploité sans l'autorisation expresse de la SAS PIVERT. »*

***Disclaimer***

*"This document is confidential and was prepared within the frame of the GENESYS research program of the SAS PIVERT. No copy, no distribution, and no exploitation are allowed without the authorization of the SAS PIVERT."*



*« On n'est jamais à l'abri d'une bonne surprise »*



## Remerciements

---

Ce manuscrit est l'aboutissement de trois ans de travail au sein du LCPO qui auraient été bien difficiles à vivre sans l'aide et le soutien de nombreuses personnes que j'aimerais remercier ici.

Je tiens en premier lieu à exprimer ma profonde reconnaissance et ma gratitude à mes deux encadrants de thèse, Henri Cramail et Etienne Grau qui m'ont accordé leur confiance pendant ces trois années. Votre encadrement à tous les deux est complémentaire et ça a été un plaisir de travailler avec vous. Merci Henri pour vos conseils avisés et pour votre soutien, particulièrement lors de la rédaction. Merci Etienne, pour avoir été toujours disponible pour moi, pour tes idées qui jaillissent de ton cerveau en permanence et pour avoir su calmer mes doutes et me faire prendre du recul sur mon projet.

Je suis également à exprimer ma reconnaissance à Claire Négrell et Erwan Nicol d'avoir accepté d'être les rapporteurs de cette thèse ainsi qu'à Renaud Nicolaÿ et Olivier Sandre d'avoir examiné ces travaux. Merci à l'ensemble du jury pour la discussion instructive et enrichissante que nous avons eu lors de la soutenance.

Je souhaiterais remercier la SAS PIVERT pour avoir financé ces travaux de thèse au sein du projet POLYADD, et particulièrement Nathalie Vouillon qui a suivi ce projet activement. Merci à Guillaume Chollet, chef de projet à l'ITERG et chef de file de POLYADD ainsi que tout l'équipe de l'IAM (Sylvain Caillol, Claire Négrell, Vincent Lapinte et Jean-Jacques Robin) pour leurs conseils pendant nos réunions et leur bienveillance. Un clin d'œil particulier pour Juliette, ça a été un réel plaisir d'échanger avec toi, on a su rester en contact et se soutenir pendant ces trois années !

Un énorme merci à Jean-François Le Meins pour son aide précieuse ! Je ne suis toujours pas une experte rhéo mais j'ai énormément progressé grâce à toi. Tu as toujours répondu à mes multiples questions avec une grande patience et de la pédagogie, sans oublier une jolie pointe d'humour ! Je tiens également à remercier Annie Brulet du CEA de Saclay pour les analyses de SANS et Olivier Sandre pour son aide impliquée et pédagogue pour l'interprétation de ces

résultats. Je souhaiterais aussi remercier Eric Laurichesse du CRPP qui m'a permis de faire quelques tests préliminaires sur leurs rhéomètres en attendant l'arrivée de celui du LCPO.

Merci aux experts en caractérisation du LCPO, toujours aidants et disponibles. Anne-Laure pour les RMNs, Gérard pour les DSC et TGA, Manu pour mes essais un peu ratés en microscopie, Christophe pour la SLS, Eric pour la Flash qui était plus que capricieuse, Amélie que j'ai beaucoup sollicitée pour la SEC avec mes nombreuses tentatives de détermination des dn/dc et autres et Cédric enfin, pour la DSC, la rhéo, la visco et tout le reste !

Un grand merci également à Dominique, Corinne, Claude, Bernadette et Loïc sans qui ce labo ne tournerait pas aussi bien. Vous êtes aussi sympathiques qu'efficaces.

Je voudrais aussi remercier Lucie et Camille, mes deux stagiaires, pour leur aide, leur motivation et surtout leur envie d'apprendre.

Ce fut un plaisir de travailler au sein de la « fatty team » pendant ces trois ans. D'abord avec les « vieux », Océane, Geoffrey, P'tit Sav, Dounia, Laurence, P-L et Léa. Puis avec les nouveaux entrants : Fiona, Martin, Boris (tout plein de discussions intéressantes), Nicolas, Christopher, Sylwia (Time flies !!) Léa, Guillaume, ... Un gros merci à P-L et Léa qui ont un peu été mes mentors, P-L, ta bonhomie m'a sacrément manquée quand tu es parti ! Et Léa, on a su rester en contact et on est restées sacrément copines toutes les deux, surtout ne change pas ! QP, on a commencé ensemble et on s'est suivi pendant ces trois ans, d'avoir dans le bureau cette dernière année a vraiment été un plaisir ! Et merci Thomas (pépète amicale de 2018), merci pour tes conseils, pour ton aide et pour m'avoir écouté radoter sans moufter !

Mais le LCPO, ce n'est pas que la « fatty team », il doit sa bonne ambiance à une foule de gens avec qui j'ai pu partager des bons moments : Marie (et sa bonne humeur perpétuelle au CAES), Leila, Pauline, Antoine, Jérémy, Jérémie (Hé salut !!!), Berto, Michou, Romain, Anne, Martin F., Tim, Michèle, Monica, Camille G., Beste, Amélie, Cédric. Une énorme pensée pour vous « les gars » : Arthur Vénère, Bakka, Quentin, Louis, compagnons de tous les instants. Cette thèse n'aurait pas été la même sans vous (et, même si ça me fait mal de le dire, merci de m'avoir attendu, et merci d'avoir écouté mes histoires presque jusqu'au bout). Julien B., tu es

parti dans l'Est mais c'était super chouette de t'avoir rencontré ! David, garde ta curiosité et continue à accroître ta culture incroyable. Audrey, tu fais trop de sport et moi, ça me fait culpabiliser (un peu) mais je suis bien contente de t'avoir rencontrée Ariane, tu es bien la seule qui aime que je chante Ursule alors sincèrement merci ! Julien R. et bien que dire sinon merci et que j'ai été bluffée devant tant de gentillesse ! Et Gauvin, copain d'avant et de maintenant, merci pour toutes ces discussions (scientifiques ou pas d'ailleurs) sur les plots de l'école.

Je voudrais aussi remercier tous mes copains de Bretagne, de prépa ou de Mulhouse et plus récemment de Bordeaux qui ont été là pour moi pendant de nombreuses années et avec qui j'ai passé vraiment de bons moments. A part un amour commun de la nourriture, vous êtes tous différents et vous m'avez beaucoup apporté ! Particulièrement toi Audrey, depuis quoi, 24 ans ? Sincèrement, merci d'être toi. Merci aussi à mes copines de CAES, Louisiane, Marie et surtout Céline et Hélène. Vous êtes aussi drôles qu'intéressantes toutes les deux. Je pense que je dois aussi remercier chaleureusement mes colocs, Eric, Julie, Thibault, Aurélien et Mathieu de m'avoir supporté au quotidien pendant 3 ans ! Et puis merci à toi Geoffrey, et à ta joie de vivre, à mes côtés depuis 2 ans. Enfin, un énorme merci à mes parents et à ma sœur, pour leur amour et leur soutien. On ne choisit pas sa famille mais moi je suis sacrément bien tombée, sans vous je ne serais pas celle que je suis aujourd'hui.







# General table of content

---

List of abbreviations.....	
Résumé.....	<b>1</b>
General introduction.....	<b>11</b>

## Chapter I: Viscosity control additives for lubricants: from petroleum- to bio-based polymers

Introduction to the lubricants.....	21
1. Lubricants: a complex formulation.....	22
1.1. Lubricant base oils.....	23
1.1.1. API base stock classification.....	23
1.1.2. Mineral base oil: API group I, II and III.....	24
1.1.3. Synthetic base oils: API Group IV and V.....	25
1.1.4. Bio-sourced base oils.....	28
1.2. Most common additives in lubricants.....	30
2. Viscosity modifiers from petroleum resources.....	34
2.1. Viscosity modifiers function relative to the lubricant requirements.....	34
2.1.1. Viscosity and VM thickening properties.....	34
2.1.2. Viscosity-Temperature (V-T) relationship.....	37
2.1.3. Shear stability.....	39
2.2. Chemistry of viscosity modifiers.....	41
2.2.1. Olefin copolymers (OCP).....	41
2.2.2. Poly(alkyl methacrylate)s (PAMAs).....	44
2.2.3. Hydrogenated Styrene-Diene (HSD) copolymers.....	46
2.2.4. PAMA-OCPs comb copolymers.....	48
2.2.5. Other polymers.....	48
2.3. Viscosity Index improver impact on oil V-T behavior.....	50
2.3.1. Coil expansion of the polymer chain.....	51
2.3.2. Interaction between polymer chains: aggregation - disaggregation.....	53
2.3.3. Other secondary mechanisms through polymer-solvent interactions.....	56

2.4. Summary and outlook.....	57
3. Pour point depressants .....	58
3.1. Pour point depressant function and mechanisms.....	58
3.1.1. <i>Low-temperature behavior of base oils</i> .....	58
3.1.2. <i>PPD function and mechanisms of action</i> .....	60
3.2. Main pour point depressant chemical structures .....	62
3.2.1. <i>Poly(alkylmethacrylate) comb polymers (PAMAs)</i> .....	62
3.2.2. <i>Other polymers</i> .....	64
3.3. Summary and outlook.....	66
4. Bio-based viscosity control additives for lubricants .....	66
4.1. Strategies to enhance bio-based part in lubricants.....	66
4.2. Short overview of bio-based additives .....	67
4.3. Bio-based viscosity modifiers .....	68
4.3.1. <i>Bio-based viscosity modifiers for petroleum-based oils</i> .....	68
4.3.2. <i>Viscosity modifiers for fully bio-based lubricants</i> .....	71
4.4. Bio-based pour point depressant .....	72
4.4.1. <i>Bio-based PPD for petroleum-based oils</i> .....	72
4.4.2. <i>PPD for fully bio-based lubricants</i> .....	73
Conclusion .....	74
References.....	76

## Chapter II: Poly(methyl ricinoleate) as bio-based viscosity modifiers: synthesis, optimization and characterization

Introduction.....	89
1. Poly(methyl ricinoleate): State of the art.....	90
1.1. From castor oil to methyl ester ricinoleate .....	90
1.2. Methyl ester ricinoleate as a monomer for polyesters .....	92
2. Poly(methyl ricinoleate) synthesis optimization.....	95
2.1. Monomer purity.....	95
2.2. Screening of catalyst and temperature .....	96
2.3. Polymerization kinetic .....	100

2.4. Magnetic versus mechanical stirring .....	101
2.5. Conclusion: polymerization by transesterification optimization .....	102
3. PRic characterization .....	103
3.1. Chemical structure .....	103
3.1.1. <i>Poly(methyl ricinoleate)</i> .....	103
3.1.2. <i>Poly(methyl-12-hydroxystearate)</i> .....	106
3.2. Molecular weights determination .....	107
3.3. Thermal properties .....	109
3.3.1. <i>Degradation temperature</i> .....	109
3.3.2. <i>Thermo-mechanical properties</i> .....	110
4. Melt poly(methyl ricinoleate) rheological behavior .....	112
4.1. Dynamic mechanical analysis .....	113
4.1.1. <i>Linear domain</i> .....	113
4.1.2. <i>Complex viscosity as function of angular frequency, Time-temperature superposition (TTS)</i> .....	114
4.2. Viscosity determination by creep tests .....	118
4.3. Viscosity as a function of molecular weights.....	120
5. PRic and PHS behavior in solution .....	122
5.1. Preliminary study .....	122
5.1.1. <i>Choice of the mineral and organic base oils</i> .....	122
5.1.2. <i>Choice of the commercial additives</i> .....	126
5.1.3. <i>Determination of the appropriate additive concentration</i> .....	127
5.2. Effect of the PRic and PHS on oil viscosity.....	129
5.2.1. <i>Solubility on oils depending on the molecular weights</i> .....	129
5.2.2. <i>Effect on oil viscosity: towards thickening agents</i> .....	130
5.3. Conclusion.....	133
Conclusion .....	134
References.....	135
Experimental .....	137
Appendix.....	138

## Chapter III: Structural modification of bio-based polyesters: from linear to comb polymers

Introduction.....	145
1. From linear to comb bio-based polyesters .....	145
1.1. Synthesis of A-B monomer from renewable resources.....	146
1.1.1. 2-Mercaptoethanol addition on methyl-10-undecanoate .....	146
1.1.2. 2-Mercaptoethanol addition of methyl oleate.....	147
1.1.3. Dodecane-1-thiol addition on methyl ricinoleate.....	148
1.2. Polyesters synthesis by transesterification .....	150
1.3. Effect of the various architectures on polyester properties .....	155
1.3.1. Thermal properties .....	156
1.3.2. Polyester behavior in base oil.....	158
1.4. Conclusion.....	161
2. Comb poly(9-alkyl 12-hydroxystearate)s with various dangling chains.....	162
2.1. Synthesis of comb poly(9-alkyl 12-hydroxystearate)s with various side chains .....	163
2.1.1. Methyl ricinoleate functionalization by thiol-ene addition .....	163
2.1.2. Polymerization of the functionalized monomers .....	164
2.2. Comb poly(9-alkyl 12-hydroxystearate) thermal properties.....	167
2.3 Investigation of comb poly(9-alkyl 12-hydroxystearate)s as viscosity modifiers.....	168
2.3.1. Comb poly(9-alkyl 12-hydroxystearate)s behavior in organic oil.....	168
2.3.2. Comb poly(9-alkyl 12-hydroxystearate)s behavior in mineral oil .....	171
2.4. Investigation of comb poly(9-alkyl 12-hydroxystearate)s as pour point depressants	174
2.4.1. Evaluation of some comb poly(9-alkyl 12-hydroxystearate)s as potential PPD ...	174
2.4.2. Influence of the polymer concentration on oil pour point.....	175
2.4.3. Influence of the molecular weight on additive efficiency as PPD.....	177
2.4.4. Comb versus semi-crystalline polyesters .....	178
2.4.5. Comb poly(9-octadecyl 12-hydroxystearate) investigation as PPD in organic oil	180
Conclusion .....	181
References.....	183
Experimental .....	184
Appendix.....	188

## Chapter IV: *Comb copoly(9-alkyl 12-hydroxystearate)s: from thickeners towards Viscosity Index improvers*

Introduction.....	193
1. Comb copoly(9-phenyl ethyl 12-hydroxystearate- <i>r</i> -9-dodecyl 12-hydroxystearate)s P(Ric-Ph- <i>r</i> -Ric-C12).....	194
1.1. First series of comb P(Ric-Ph- <i>r</i> -Ric-C12)s with $M_w \approx 10 \text{ kg}\cdot\text{mol}^{-1}$ .....	195
1.1.1. Copolymers synthesis .....	195
1.1.2. Thermal properties .....	197
1.1.3. Solubility and behavior in mineral oil regarding to the temperature .....	199
1.1.4. Conclusion .....	200
1.2. Second series of comb copolyesters with $M_w > 50 \text{ kg}\cdot\text{mol}^{-1}$ .....	201
1.2.1. Copoly(9-alkyl 12-hydroxystearate)s synthesis .....	201
1.2.2. Behavior in oil with temperature .....	202
1.3. Conclusion.....	203
2. Variation of copolyesters pendant chain moieties .....	204
2.1. Copoly(9-alkyl 12-hydroxystearate)s synthesis and solubility in oil.....	205
2.1.1. Copolymers with phenyl ethyl pendant chains and various soluble pendant chains .....	205
2.1.2. Copolymers with butyl pendant chains and various soluble pendant chains .....	207
2.2. Copoly(9-alkyl 12-hydroxystearate)s behavior in Yubase 4+ with temperature .....	209
2.3. Conclusion.....	211
3. Study in model solvent: conformational behavior.....	212
3. 1. Behavior of homo- and copoly(9-alkyl 12-hydroxystearate)s in dodecane with the temperature.....	213
3.2. Evolution of the intrinsic viscosity regarding to the temperature .....	215
3.2.1. Determination of the dilute regime .....	215
3.2.2. Intrinsic viscosity determination .....	217
3.3. Determination of the polymer size with respect to the temperature .....	219
Conclusion .....	221
References.....	223
Experimental .....	224
Appendix.....	226

<b>General conclusion and perspectives .....</b>	<b>231</b>
<b>Materials and methods .....</b>	<b>237</b>
1. Materials .....	237
2. Methods.....	237

## List of abbreviations

---

### **Techniques:**

COSY: homonuclear correlation spectroscopy  
DEPT: distortionless enhanced polarization transfer spectroscopy  
DLS: dynamic light scattering  
DSC: differential scanning calorimetry  
MD: molecular dynamics simulations  
NMR: nuclear magnetic resonance spectroscopy  
SANS: small angle neutrons scattering  
SEC: size exclusion chromatography  
SLS: static light scattering  
TGA: thermogravimetric analysis chromatography  
TTS: Time temperature superposition  
WAXS: Wide-angle X-ray scattering  
XRD: X-ray diffraction

### **Characteristic**

$\phi$ : coil diameter  
 $[\eta]$ : intrinsic viscosity  
aT: translation factor  
C\*: overlap concentration  
CP: cloud point  
D: dispersity  
DP<sub>n</sub>: degree of polymerization  
E<sub>a</sub>: activation energy  
G': storage modulus  
G'': loss modulus  
k<sub>H</sub>: Huggins constant  
M<sub>c</sub>: critical molecular weight of entanglement  
M<sub>n</sub>: number average molar mass  
M<sub>w</sub>: mass average molar mass  
N<sub>a</sub>: Avogadro number  
 $\eta_0$ : Newtonian steady-state shear viscosity  
 $\eta^*$ : complex viscosity  
 $\eta_{abs}$ : absolute viscosity  
 $\eta_{dyn}$ : dynamic viscosity  
 $\eta_{kin}$ : kinematic viscosity  
 $\eta_{rel}$ : relative viscosity  
 $\eta_{sp}$ : specific viscosity  
 $\rho$ : volumetric mass density  
 $p$ : monomer conversion  
PP: pour point  
Q value: specific viscosity at 40°C / specific viscosity at 100°C  
R: universal gas constant.  
R<sub>g</sub>: radius of gyration

R<sub>H</sub>: Hydrodynamic radius  
T<sub>cris</sub>: crystallization temperature  
T<sub>d5wt.%</sub>: temperature corresponding to 5 wt.% loss  
TE: thickening efficiency  
T<sub>g</sub>: glass transition temperature  
T<sub>m</sub>: melting temperature  
T<sub>Ref</sub>: reference temperature  
V<sub>e</sub>: hydrodynamic volume  
VI: viscosity index  
WAT: wax appearance temperature  
 $\omega$ : angular frequency  
 $\gamma$ : shear strain

### **Chemicals:**

CAL-B: candida antarctica lipase B  
CO: castor oil  
DA: dodecyl acrylate  
DMPA: 2,2-dimethoxy-2-phenylacetophenone  
EC: ethyl cellulose  
EO: ethylene oxide  
EPDM: ethylene-propylene-diene monomer  
EVA: ethylene vinyl acetate copolymers  
FA: fatty acids  
FAME: fatty acid methyl ester  
HBPE: highly branched polyethylene  
HEMA: 2-hydroxyethyl methacrylate  
HOSO: high oleic sunflower oil  
HSB: styrene-hydrogenated butadiene copolymer  
HSD: hydrogenated styrene-diene copolymers  
IM-CA: immobilized lipase from Pseudomonas cepacia  
MA: methyl acrylate  
MAEO: 2-(methacryloyloxy)ethyl oleate  
MDI: methylene diphenyl diisocyanate  
Me<sub>3</sub>SiONa: trimethyl- silanolate sodium  
MMA: methyl methacrylate  
ME: 2-mercaptoethanol  
MO: methyl oleate  
MO-ME: methyl 10-(2-hydroxyethylthio) stearate  
MRic: methyl ricinoleate  
MRic-C12: methyl 10-(dodecylthio) 12-hydroxystearate  
MRic-Ph: methyl 10-(phenylethylthio) 12-hydroxystearate  
MU: methyl-10-undecenoate

MU-ME: methyl 11-(2-hydroxyethylthio) undecanoate  
NaH: sodium hydride  
NaOMe: sodium methoxide  
OCP: olefin copolymers  
P: priolube 3986  
PA-11: polyamide 11  
PA-6,10: polyamide 6,10  
PAG: polyalkylene glycols  
PAMA: poly(alkylmethacrylate)  
PAO: poly(alphaolefin)s  
PET: poly(ethylene terephthalate)  
PHS: poly(methyl-12-hydroxystearate)  
PIB: polyisobutene  
PLA: poly(lactic acid)  
P(MA-MAn): methacrylate-maleic anhydride copolymers  
PMAEO: poly(2-(methacryloyloxy)ethyl oleate)  
PO: propylene oxide  
P(RA): poly(ricinoleic acid)  
PRic: Polyricinoleate  
P(Ric-C12): poly(methyl 10-(dodecylthio) 12-hydroxystearate)  
PRic-Ph: poly(methyl 10-(phenylethylthio) 12-hydroxystearate)  
P(Ric-Ph-*r*-Ric-C12): random poly(methyl 10-(phenylethylthio) 12-hydroxystearate - *r* - methyl 10-(dodecylthio) 12-hydroxystearate)  
PS: polystyrene  
PU: polyurethane  
R: radialube 7368  
SBO: soybean oil  
SFO: sunflower oil

Sn(Oct)<sub>2</sub>: tin octoate  
TBD: 1,5,7-triazabicyclo[4.4.0]dec-5-ene  
Ti(OiPr)<sub>4</sub>: titanium (IV) isopropoxide  
VP: viscoplex 10-250  
Y: yubase 4+  
Y(OiPr)<sub>3</sub>: yttrium isopropoxide  
ZnDTP: zinc dithiophosphates  
Zn(OAc)<sub>2</sub>: zinc acetate

***Polymerization techniques:***

ATRP: atom transfer radical polymerization  
CRP: controlled radical polymerization  
NMP: nitroxide-mediated polymerization  
FRP: free radical polymerization  
RAFT: reversible addition-fragmentation chain-transfer polymerization  
ROMP: ring opening metathesis polymerization

***Miscellaneous:***

API: American petroleum institute  
DCC: dynamic covalent chemistry  
EP: extreme pressure  
E/P: ethylene/propylene ratio  
PPD: pour point depressants  
VM: viscosity modifiers  
VII: viscosity index improvers  
V-T: viscosity – temperature  
WLF: William, Landel and Ferry mode

## Résumé

---

Un lubrifiant est un produit qui, interposé entre deux surfaces d'un mécanisme, en facilite le fonctionnement.<sup>1</sup> Le rôle d'un lubrifiant est donc de créer un film protecteur entre deux pièces en mouvement d'un moteur ou d'une machine afin de réduire le frottement, ce qui permet d'économiser de l'énergie.<sup>2</sup> Un lubrifiant doit également dissiper la chaleur produite lors des frottements et protéger les surfaces contre la corrosion ou des contaminations extérieures. Son action permet de diminuer l'usure des machines et ainsi d'augmenter considérablement leur durée de vie.<sup>3-5</sup> Pour assurer toutes ces fonctions, des formulations de plus en plus complexes ont été développées au cours des années. Aujourd'hui, la majorité des lubrifiants sont des liquides comprenant une huile de base, de type minéral, synthétique ou organique et de nombreux additifs.<sup>6</sup>

Actuellement, les 36 millions de tonnes de lubrifiants produites chaque année sont utilisées dans de nombreuses applications telles que les moteurs de véhicules, les équipements industriels, la marine, l'aéronautique, etc.<sup>5,7</sup> Malheureusement, 40 à 50% des lubrifiants finissent dans les sols ou dans l'eau ce qui représente une importante source de pollution.<sup>3,5</sup> La priorité est donc de développer des lubrifiants moins nocifs pour l'environnement. Certains efforts ont déjà été faits. Les lubrifiants sont de plus en plus utilisés en circuit fermé par exemple, des lubrifiants formulés à partir d'esters synthétiques biodégradables sont également utilisés.<sup>5,8</sup> Néanmoins de nombreux progrès restent à faire. Une des solutions innovantes serait de développer des lubrifiants à partir de la biomasse. Cela conduirait à des formulations moins toxiques, biodégradables et renouvelables. Dans ce sens, des huiles végétales sont utilisées comme huiles de base pour lubrifiants.<sup>8,9</sup> C'est d'ailleurs un marché grandissant, avec une croissance annuelle estimée de 6% entre 2018 et 2025 en termes de revenus.<sup>10</sup> En revanche, peu d'additifs sont biodégradables et encore moins proviennent de ressources renouvelables.<sup>9,11</sup>

C'est dans ce contexte que s'inscrit ce sujet de thèse qui vise à développer de nouveaux additifs bio-sourcés pour les lubrifiants. Ces travaux, réalisés au sein du Laboratoire de Chimie des Polymères Organiques (LCPO) font partie du projet POLYADD financé par la SAS PIVERT en

collaboration avec le Centre Technique Industriel des Huiles et Corps Gras (ITERG) et l'Institut Charles Gerhardt de Montpellier (ICGM). Plus particulièrement, parmi les nombreux additifs utilisés dans les lubrifiants, un type d'additif a été visé : les additifs de contrôle de la viscosité. Ces additifs polymères représentent actuellement 25% du volume total d'additifs pour lubrifiants produits chaque année et incluent les modificateurs de viscosité (VM) et les abaisseurs de point d'écoulement (PPD).<sup>6,12</sup> Comme illustré en Figure 1, la viscosité d'une huile diminue drastiquement lorsque la température augmente. Ce comportement pose deux problèmes majeurs pour son utilisation en tant qu'huile lubrifiante. Premièrement, à haute température, l'huile ne peut plus assurer de film protecteur efficace en raison de sa trop faible viscosité. Pour pallier ce problème, les modificateurs de viscosité sont ajoutés afin d'épaissir l'huile à haute température, voir Figure 1 (2).<sup>6,13,14</sup> Deuxièmement, au-dessous d'une certaine température, appelé point d'écoulement, l'huile va se gélifier par cristallisation ce qui entraîne une importante prise en viscosité. Le lubrifiant ne peut plus s'écouler ce qui entrave le bon fonctionnement de la machine. Les abaisseurs de point d'écoulement sont alors ajoutés dans les formulations afin de diminuer la température de gélification de l'huile, permettant son utilisation à des plus basses températures, voir Figure 1 (3).<sup>15</sup>

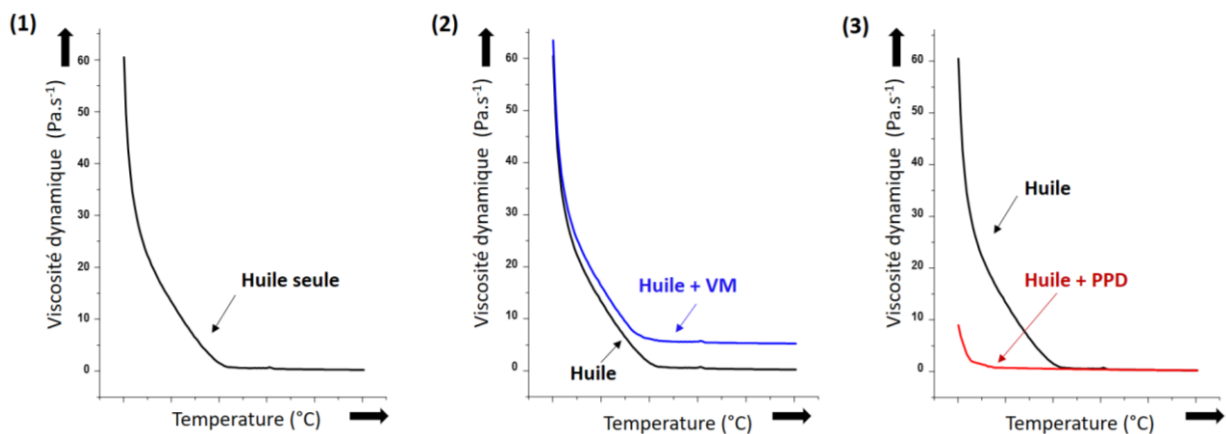


Figure 1: Illustration de la viscosité en fonction de la température pour (1) une huile seule, (2) une huile additivée d'un modificateur de viscosité et (3) une huile additivée d'un abaisseur de point d'écoulement

Dans un premier temps, une étude bibliographique sur les additifs de contrôle de la viscosité a été réalisée. Ces additifs étant utilisés depuis plus de 60 ans, de nombreuses études ont déjà été décrites sur le sujet.<sup>3-5,14,16,17</sup> L'objectif ici n'était donc pas de fournir un examen exhaustif de tous les additifs de contrôle de viscosité mais plutôt de mettre en évidence les fonctions et propriétés requises, les principales structures chimiques utilisées ainsi que leurs modes de

fonctionnement en solution. L'utilisation de composés bio-sourcés étant très peu décrite, cette étude s'est premièrement tournée vers les additifs provenant de ressources fossiles.

Les modificateurs de viscosité doivent posséder un fort pouvoir épaississant comme c'est le cas des polymères aliphatiques linéaires tels les poly(alphaolefine)s (OCP).<sup>18-20</sup> Au vu des importantes contraintes de cisaillement présentes dans les applications de lubrifiants, ces additifs doivent également être résistants au cisaillement. Cette propriété est principalement reliée à l'architecture du polymère. En effet, il est apparu que plus la chaîne polymère est ramifiée, plus celle-ci sera stable vis-à-vis du cisaillement.<sup>21,22</sup> Les polymères en étoile et hyper-ramifiés sont donc les plus résistants, suivi des polymères en peigne et enfin des polymères linéaires. En revanche, le pouvoir épaississant est inversement proportionnel à la stabilité au cisaillement. En ce sens, les polymères en peigne semblent être un bon compromis en regard de ces deux propriétés requises.<sup>23</sup> Finalement, les modificateurs de viscosité doivent plus impacter la viscosité de l'huile à haute température qu'à basse température, c'est à dire modifier l'indice de viscosité (VI).<sup>17,24</sup> Ce dernier traduit le comportement de la viscosité d'une huile en fonction de la température. Plus le VI est haut, moins la viscosité de l'huile diminuera avec la température, ce qui est souhaité pour l'application. Il est alors important de distinguer les deux types de modificateurs de viscosité : les épaississants, comme les OCPs, et les additifs améliorant l'indice de viscosité (VII) tels que les poly(alkylmethacrylate)s (PAMAs) et les copolymères à blocs styrène-diène hydrogéné (HSD).<sup>14,25</sup> Les VII vont plus augmenter la viscosité de l'huile à haute température qu'à basse température par un phénomène d'expansion de chaînes, comme les PAMAs<sup>26-28</sup>, ou par un phénomène d'agrégation/désagrégation, tels les HSD.<sup>29-31</sup>

En ce qui concerne les abaisseurs de point d'écoulement, ce sont principalement des polymères en peigne avec de longues chaînes alkyle comme les PAMAs et des polymères semi-cristallins tels que certains OCP et les copolymères éthylène - acétate de vinyle.<sup>6,15</sup> Les longues chaînes pendantes des PAMAs ainsi que les parties cristallines des polymères semi-cristallins sont capables de co-cristalliser avec les composés cristallins de l'huile à basse température alors que la partie amorphe de ces polymères permet la dispersion des cristaux, retardant ainsi le phénomène de gélation.<sup>32</sup>

Un état de l'art a ensuite été réalisé sur les mêmes additifs provenant cette fois de ressources renouvelables. Il est apparu que la grande majorité des additifs bio-sourcés proviennent de ressources végétales.<sup>8,33</sup> Comme illustré en Figure 2, les huiles végétales, extraites des plantes par un procédé de bioraffinerie sont principalement composées de triglycérides qui peuvent être modifiées par transestérification afin d'obtenir des acides gras. Ces derniers, en raison de la présence de fonctions ester et de doubles liaisons, représentent des précurseurs prometteurs pour la synthèse de polymères bio-sourcés.<sup>34,35</sup>

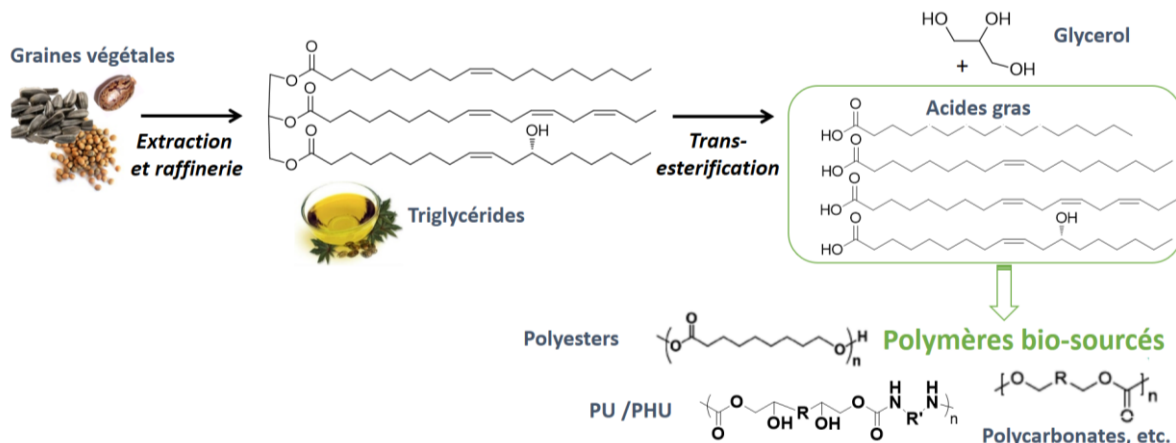


Figure 2: Illustration du développement de polymères bio-sourcés à partir de plantes

Au regard de cette étude bibliographique et devant la nécessité de développer des additifs biodégradables pour les lubrifiants, notre choix s'est porté sur le polyricinoleate, un polyester aliphatique pouvant être obtenu par polycondensation directe de l'ester méthylique de ricin, un acide gras issu de l'huile de ricin. Ce monomère de type AB possédant une fonction hydroxyle et une fonction ester, ainsi que son homologue saturé, le 12-hydroxystéarate de méthyle, ont été polymérisés *via* transestérification. Une optimisation des conditions expérimentales a permis d'obtenir une gamme de masses molaires de 10 à 130 kg.mol<sup>-1</sup>. Le polyricinoleate (PRic) est apparu être un polymère amorphe avec une température de transition vitreuse de -60° C alors que le polyhydroxystéarate (PHS) est semi-cristallin avec une température de cristallisation de -34 °C (T<sub>m</sub> = -22 °C) et une T<sub>g</sub> de -40°C. Leurs structures respectives sont présentées en Figure 3.

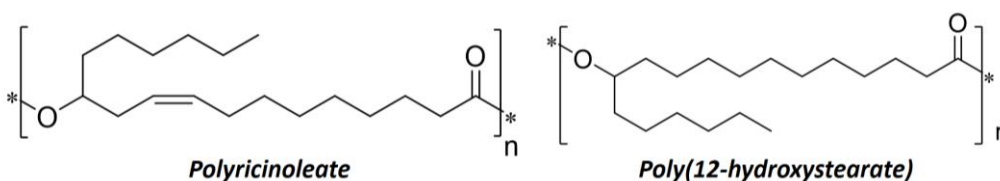


Figure 3: Structures chimiques du PRic et du PHS

Une étude rhéologique en masse du PRic a permis de montrer la présence d'un enchevêtrement pour des masses molaires supérieures à  $25 \text{ kg.mol}^{-1}$ . Ces polymères ont ensuite été évalués comme modificateurs de viscosité dans une huile minérale, la Yubase 4+ et une huile végétale, la Radialube 7368. Bien que le PHS soit parfaitement soluble dans chacune des huiles, le PRic perd sa solubilité lorsque ses masses molaires deviennent trop élevées. Ainsi, uniquement les polyricinoleates avec  $M_w < 30 \text{ kg.mol}^{-1}$  et  $M_w < 40 \text{ kg.mol}^{-1}$  ont pu être solubilisés dans la Yubase 4+ et la Radialube 7368, respectivement. Un important pouvoir épaississant a été démontré pour le PHS dans les deux huiles, avec une augmentation de la viscosité des huiles par deux et une augmentation de l'indice de viscosité de 152 à 204 pour l'huile végétale et de 145 à 209 pour l'huile minérale. Toutefois, les polymères évalués n'ont pas eu d'effet sur le comportement des huiles en fonction de la température.

Il a été également montré dans la littérature que la structure du polymère avait une grande importance sur l'efficacité de ce dernier en tant que modificateur de viscosité. Pour cette raison, l'impact de l'architecture d'un polyester sur son comportement en solution a été évalué. Pour cela, trois précurseurs bio-sourcés ont été fonctionnalisés par addition thiol-ène. Des monomères AB linéaire et avec une chaîne alkyle pendante ont été obtenus par réaction du 2-mercaptoethanol (ME) avec l'undécénoate de méthyle (MU) et l'oléate de méthyle (MO), respectivement. Le monomère AB avec deux chaînes pendantes, soit le 9-dodécyle 12-hydroxystéarate de méthyle, a été obtenu par addition thiol-ène du 1-dodécane-thiol sur l'ester méthylique de ricin. Ces monomères ont ensuite été polymérisés suivant les conditions établies lors de l'étude précédente, les structures obtenues sont présentées en Figure 4.

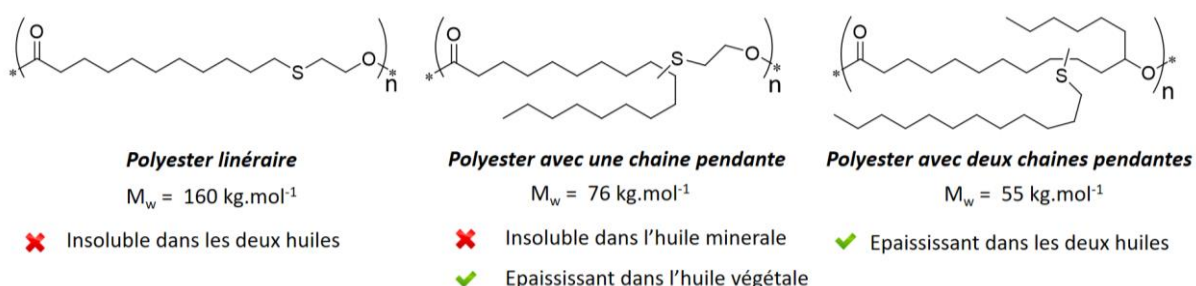


Figure 4: Polyesters avec différentes architectures soit P(MU-ME) linéaire, P(MO-ME) avec une chaîne pendante et P(Ric-C12) avec deux chaînes pendantes

Comme attendu, il a été montré que la cinétique de polymérisation est affectée par la nature de la fonction alcool (primaire ou secondaire) et la présence de chaînes pendantes. Les plus hautes masses molaires ont donc été obtenues lors de la polymérisation du monomère

linéaire. La présence d'une liaison thioéther ainsi que celle des chaînes pendantes dans l'unité de répétition du polymère ont un fort impact sur les propriétés thermiques de ce dernier. Par exemple, le polyester linéaire est semi-cristallin ( $T_g = -33\text{ °C}$ ,  $T_m = 53\text{ °C}$  and  $T_{cris} = 35\text{ °C}$ ) alors que le polyester en peigne, avec deux chaînes pendantes est amorphe ( $T_g = -61\text{ °C}$ ). Afin d'évaluer leur comportement en solution, les polyesters préparés ont été ajoutés dans la Yubase 4+, une huile minérale et la Radialube 7368, organique. Il est apparu que le polyester linéaire est insoluble dans les deux huiles. L'ajout d'une chaîne pendante a permis la solubilisation du P(MO-ME) dans l'huile végétale. Seul le poly(9-dodécyl 12-hydroxystéarate) (PRic-C12) avec deux chaînes pendantes s'est avéré soluble dans les deux huiles. Cette architecture a donc été retenue pour la suite de l'étude.

Par la suite, différentes natures de chaînes alkyle pendantes ont été ajoutées sur l'ester méthylique de ricin par addition thiol-ène, comme illustré en Figure 5.

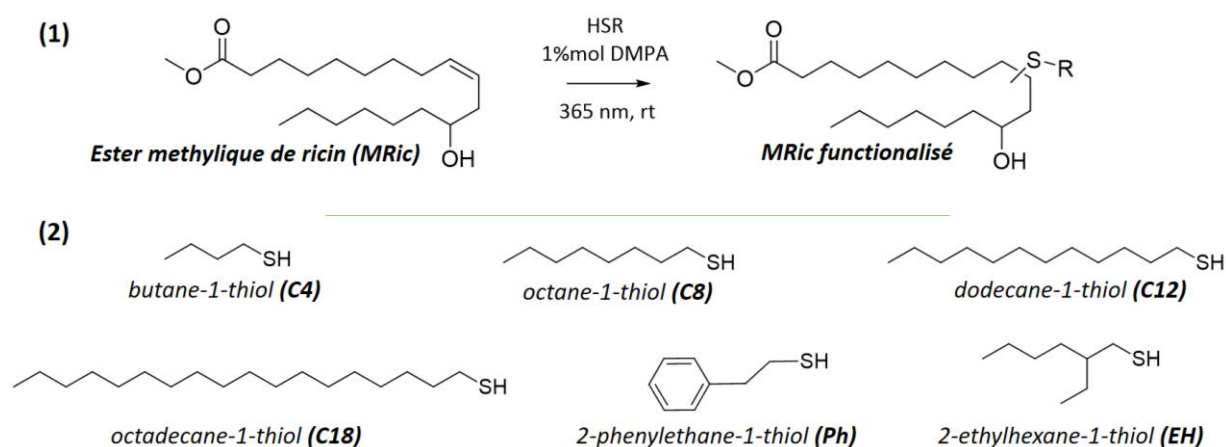


Figure 5: (1) Fonctionnalisation de l'ester méthylique de ricin par addition thiol-ène. (2) Composés thiolés ajoutés comme chaînes pendantes sur l'ester méthylique de ricin

Les propriétés des différents poly(9-alkyl 12-hydroxystéarate)s en peigne obtenus ont été évalués par analyse thermique. Il est apparu que la nature de la chaîne pendante greffée avait un impact sur le comportement thermique du polymère. En effet, plus la chaîne pendante est longue, plus la  $T_g$  est élevée. Par exemple, le poly(9-butyl 12-hydroxystéarate)s, P(Ric-C4), possède une  $T_g$  de  $-66\text{ °C}$  alors que le P(Ric-C12) a une  $T_g = -61\text{ °C}$ . Il a également été observé que le P(Ric-C18) est de nature semi-cristalline, avec une température de cristallisation de  $-12\text{ °C}$  et une  $T_g$  de  $-28\text{ °C}$  environ. La chaîne polymère étant amorphe, cette cristallisation en masse provient de la chaîne alkyle pendante, assez longue pour s'arranger aux faibles températures. Il s'est d'ailleurs avéré que ce polymère en particulier possède des propriétés

d'abaisseur du point d'écoulement. En effet, l'addition de P(Ric-C18) dans l'huile minérale a permis une diminution du point d'écoulement de l'huile de 11 °C. Les autres polymères en peigne amorphes n'ont, quant à eux, pas montré cet effet.

Les différents poly(9-alkyl 12-hydroxystéarate)s en peigne ont ensuite été évalués en tant que modificateurs de viscosité. Dans l'huile minérale, tous ont montré un pouvoir épaississant, quelle que soit la nature de la chaîne pendante. En revanche, dans l'huile minérale, les polymères possédant des chaînes courtes de type thiobutyl- ou thiophényléthyl- se sont avérés insolubles. Les autres poly(9-alkyl 12-hydroxystéarate)s, solubles, ont montré un effet épaississant. Le P(Ric-EH) est apparu comme ayant le plus grand pouvoir épaississant avec une augmentation de la viscosité par 1,4 et une augmentation de l'indice de viscosité de 145 à 190. Cependant, aucun effet de l'ajout de ces polyesters sur le comportement de la viscosité de l'huile au regard de la température n'a été observé.

En conclusion, les polyesters bio-sourcés synthétisés sont des épaississants prometteurs, notamment le PHS et le P(Ric-EH) qui ont permis de doubler la viscosité de l'huile par exemple. De plus, le poly(9-octadécyl 12-hydroxystéarate), P(Ric-C18), s'est avéré être également un prometteur abaisseur de point d'écoulement. En revanche, aucun des polymères synthétisés n'a permis d'améliorer le comportement de la viscosité de l'huile vis-à-vis de la température (effet VII). L'obtention de VII bio-sourcés a donc été l'objectif de cette dernière étude.

Dans le cas précédent, il a été montré que certains poly(9-alkyl 12-hydroxystéarate)s en peigne étaient solubles ou non suivant la nature de la chaîne pendante greffée par addition thiol-ène. Par conséquent, des copoly(9-alkyl 12-hydroxystéarate)s ont été synthétisés avec différents ratios de chaînes pendantes « insolubles » comme les chaînes phényléthyle ou butyle et « solubles » (dodécyle et éthylhexyle par exemple) afin de diminuer la solubilité des copolymères à température ambiante. Ces copolyesters sont présentés en Figure 6.

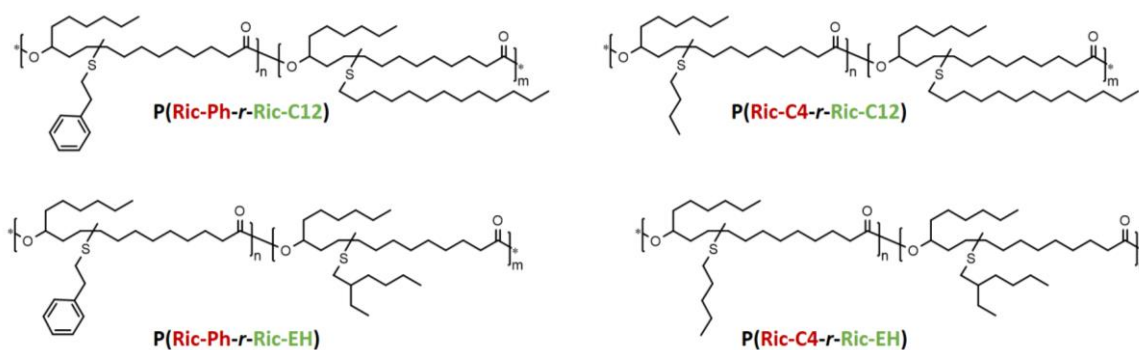


Figure 6: Structure chimique des différents copoly(10-alkyl 12-hydroxystéarate)s peignes synthétisés

Dans un premier temps, plusieurs copolymères P(Ric-Ph-*r*-Ric-C12) avec différents ratios de chaînes pendantes phényléthyle et dodécyle ont été synthétisés et mélangés à 3% en masse avec la Yubase 4+. Il est apparu que les copolymères perdent leur solubilité lorsque le pourcentage de monomère fonctionnalisé avec des chaînes phényléthyle dépasse 25%. Pour les autres systèmes, une augmentation de la viscosité relative lors de l'augmentation de la température a été observée, confirmant l'impact de ces copolymères sur la relation viscosité-température de l'huile. Par la suite, les autres copoly(9-alkyl 12-hydroxystéarate)s présentés ont été synthétisés avec des ratios de chaînes pendantes variables et testés en solution. Le copolymère avec 55%<sub>massique</sub> de chaînes butyle et 45% de chaînes dodécyle a également montré un effet VII. En revanche, cet effet n'a pas été observé avec les polymères possédant des chaînes éthylhexyle comme partie « soluble ». Cela a été hypothétiquement attribué à la gêne stérique induite par ces chaînes ramifiées qui pourraient empêcher les interactions des chaînes pendantes non solubles.

Dans une dernière étude, l'homopoly(9-dodécyle 12-hydroxystéarate), P(Ric-C12) et un copoly(9-alkyl 12-hydroxystéarate), le P(Ric-Ph<sub>0,25</sub>-*r*-Ric-C12<sub>0,75</sub>), ont été étudiés dans un solvant modèle, le dodécane. De façon surprenante, ces deux polymères impactent favorablement la viscosité du dodécane vis-à-vis de la température avec des valeurs de Q supérieures à 1. La viscosité intrinsèque  $[\eta]$  de ces deux polymères augmente avec la température tandis que leur constante de Huggins  $K_H$  diminue. Par exemple,  $[\eta]$  passe de 13 à 17 mL.g<sup>-1</sup> et  $K_H$  diminue de 3 à 0.6 lorsque la température passe de 40 °C à 100 °C dans le cas du P(Ric-C12). Cet effet est d'autant plus important dans le cas du copolymère P(Ric-Ph<sub>0,25</sub>-*r*-Ric-C12<sub>0,75</sub>) avec une augmentation de  $[\eta]$  de 8 à 15 mL.g<sup>-1</sup> et une diminution de  $K_H$  de 12 à 3 pour les mêmes températures. De plus, une diminution de leurs rayons de giration avec

l'augmentation de la température a été observée. Au regard de ces résultats, il a été supposé que ces deux polymères s'agrègent à température ambiante et se désagrègent progressivement avec l'augmentation de la température. Cette désagrégation entraîne une augmentation progressive la viscosité relative du dodécane avec la température, impactant donc favorablement sa relation V-T.

Pour conclure, différents dérivés du polyricinoléate ont été obtenus par des procédés de synthèse simples. Ces procédés ont été développés de façon à respecter les principes de la chimie verte autant que faire se peut. Ainsi, l'addition thiol-ène a été sélectionnée car elle ne nécessite pas de solvant, est rapide et ne requiert pas d'apport d'énergie thermique. La polymérisation a été faite en masse et ne nécessite pas de purification. Les polyesters bio-sourcés obtenus sont probablement biodégradables.<sup>36</sup> Testés en solution, ils ont montré un pouvoir épaississant aussi bien dans l'huile minérale que végétale. Certains copoly(9-alkyl 12-hydroxystéarate), comme le P(Ric-Ph<sub>0,25</sub>-*r*-Ric-C12<sub>0,75</sub>) par exemple, sont également capables d'impacter favorablement la relation viscosité-température de l'huile minérale. Ils peuvent donc être considérés comme de prometteurs modificateurs de viscosité pour les lubrifiants, aussi bien en tant qu'épaississant que VII. Le poly(9-octadécyl 12-hydroxystéarate), est également apparu comme un abaisseur du point d'écoulement efficace. Ainsi, ces polymères bio-sourcés peuvent être considérés comme de prometteurs additifs de contrôle de la viscosité et répondent aux nouvelles exigences environnementales des lubrifiants. De par leurs structures, il est possible que ces polymères possèdent des propriétés pouvant les amener à être utilisés comme modificateurs de frictions ou dispersants. Il serait donc intéressant d'évaluer également ces propriétés dans le futur.

## Références

- 1 J. Ayel, *Lubrifiants; Techniques de l'ingénieur*, 1996, vol. 33.
- 2 K. C. Ludema, *Friction, wear, lubrication*, University of Michigan, 1996.
- 3 S. Q. a Rizvi, *A Comprehensive Review of Lubricant Chemistry, Technology, Selection and Design*, 2009.
- 4 R. M. Mortier, M. F. Fox and S. T. Orszulik, *Chemistry and Technology of Lubricants*, 2010.
- 5 D. M. Pirro, M. Webster and E. Daschner, *Lubrication Fundamentals, Third edition*, 2016.
- 6 L. R. Rudnick, *Lubricant Additives: Chemistry and Applications*, Taylor and Francis, 2017.
- 7 Fuchs group, Evolve magazine, <https://www.fuchs.com/group/magazine/en/topics/detail-view/do-disruptions-damage-durability-1/>.
- 8 J. P. Davim, *Ecotribology*, Springer, 2016.
- 9 G. Biresaw and B. K. Sharma, *Environmentally friendly and biobased lubricants*, Taylor and Francis, 2017.
- 10 Report Buyer, Bio-Lubricant Market - Global Forecast to 2022, <https://www.reportbuyer.com/product/4090177/bio-lubricant-market-by-base-oil-type-application-end-use-global-forecast-to-2022.html>.
- 11 P. Nagendramma and S. Kaul, *Renew. Sustain. Energy Rev.*, 2012, **16**, 764–774.
- 12 GrandViewResearch, Lubricant Additives Market, <https://www.grandviewresearch.com/industry-analysis/lubricant-additives-market>.
- 13 N. S. Ahmed and A. M. Nassar, *Tribol. Lubr. Lubr.*, 2011, 301–315.
- 14 A. Martini, U. S. Ramasamy and M. Len, *Tribol. Lett.*, 2018, **66**, 58.
- 15 F. Yang, Y. Zhao, J. Sjöblom, C. Li and K. G. Paso, *J. Dispers. Sci. Technol.*, 2015, **36**, 213–225.
- 16 L. R. Rudnick, *Synthetics, Mineral Oils, and Bio-Based Lubricants - Second edition*, CRC Press., 2013.
- 17 T. Mang and W. Dresel, *Lubr. Lubr. Second Ed.*, 2007, 1–850.
- 18 K. Marsden, *Lubr. Sci.*, 1989, **1**, 265–280.
- 19 A. Sen and I. D. Rubin, *Macromolecules*, 1990, **23**, 2519–2524.
- 20 I. D. Rubin and M. M. Kapuscinski, *J. Appl. Polym. Sci.*, 1993, **49**, 111–115.
- 21 J. Wang, Z. Ye and S. Zhu, *Ind. Eng. Chem. Res.*, 2007, **46**, 1174–1178.
- 22 L. Cosimbescu, J. W. Robinson and J. P. Page, *Ind. Eng. Chem. Res.*, 2018, 1–28.
- 23 T. Stöhr, B. Eisenberg and M. Müller, *SAE Int. J. Fuels Lubr.*, 2008, **1**, 2008-01–2462.
- 24 ASTMInternational D2270-10, in *Annual Book of ASTM Standards*, 2015.
- 25 M. J. Covitch and K. J. Trickett, *Adv. Chem. Eng. Sci.*, 2015, **5**, 134–151.
- 26 M. J. Covitch, *SAE Tech. Pap. Ser.*, 1998, 14–30.
- 27 D. LaRiviere, A. F. A. Asfour, A. Hage and J. Z. Gao, *Lubr. Sci.*, 2000, **12**, 133–143.
- 28 C. Mary, D. Philippon, L. Lafarge, D. Laurent, F. Rondelez, S. Bair and P. Vergne, *Tribol. Lett.*, 2013, **52**, 357–369.
- 29 P. Bezot, B. Elmakoudi, B. Constans, D. Faure and P. Hoornaert, *J. Appl. Polym. Sci.*, 1994, **51**, 1715–1725.
- 30 C. Price and D. Woods, *Polymer (Guildf.)*, 1974, **15**, 389–392.
- 31 M. T. Savoji, D. Zhao, R. J. Muisener, K. Schimossek, K. Schoeller, T. P. Lodge and M. A. Hillmyer, *Ind. Eng. Chem. Res.*, 2018, **57**, 1840–1850.
- 32 W. Chen, Z. Zhao and C. Yin, *Fuel*, 2010, **89**, 1127–1132.
- 33 G. Karmakar and P. Ghosh, *ACS Sustain. Chem. Eng.*, 2013, **1**, 1364–1370.
- 34 A. Gandini and T. M. Lacerda, *Polymers from Plant Oils*, 2015.
- 35 L. Maisonneuve, T. Lebarbé, E. Grau and H. Cramail, *Polym. Chem.*, 2013, **4**, 5472.
- 36 K. R. Kunduru, A. Basu, M. Haim Zada and A. J. Domb, *Biomacromolecules*, 2015, **16**, 2572–2587.

## General introduction

Lubricants are used in modern engines, industrial machines and equipment in order to ensure a protective film between two metal pieces.<sup>1</sup> Their utilization prevents wear, corrosion and equipment failure. Consequently, they are intensively required for numerous applications and represented in 2017 a production around 36 million tons.<sup>2,3</sup> Lubricants are subjected to severe conditions, such as important load and shear and have to ensure a proper lubrication under a wide range of temperature. As a result, they are constituted of complex formulations mainly including a base oil and several additives to reach the properties required for a given application.<sup>4-6</sup>

One of the major class of lubricant additives are the viscosity control additives, including viscosity modifiers and pour point depressants.<sup>7</sup> These polymeric materials represent nowadays 25% of the total additives, in terms of volume. As illustrated in Figure i-1, the oil viscosity naturally drops with temperature. As a result, at high temperature, the lubricant viscosity is too low to ensure a protective film between metal pieces.

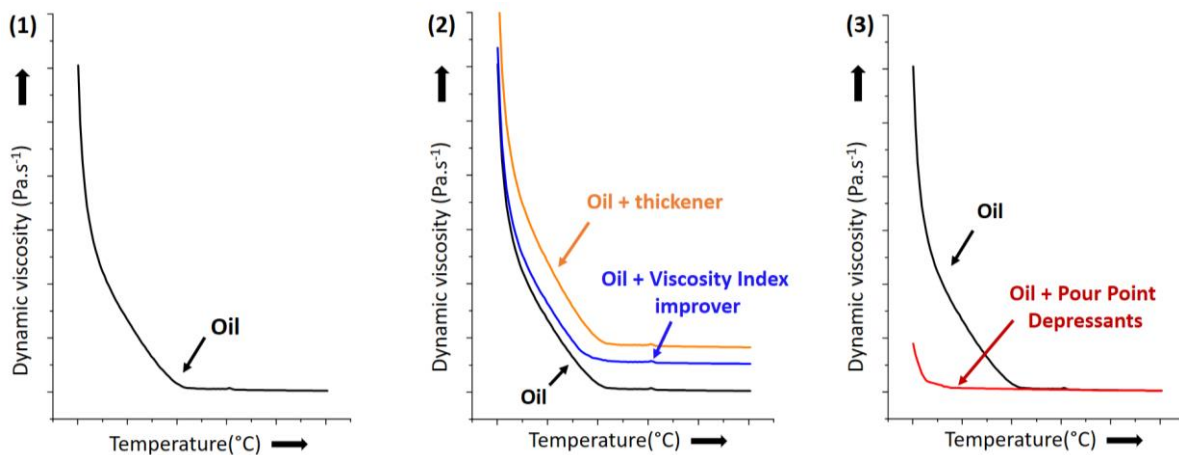


Figure i-1: Viscosity as a function of the temperature (1) Vegetable oil as example (2) Oil blended with a viscosity modifier and (3) Oil blended with a pour point depressant

Viscosity modifiers are then used in lubricant formulations to enhance the oil viscosity at high temperature resulting in the conservation of the protective film. Viscosity modifiers are then separated in two categories: thickeners and Viscosity Index improvers. The first thicken the oil regardless to the temperature while the latter thicken more the oil viscosity at high than at low temperature.

Conversely, at low temperature, the oil generally tends to crystallize leading to an exponential increase of the viscosity which can impede the lubricant flow and block the engine movement. The addition of pour point depressants permits to delay the oil crystallization and thus to reduce the oil viscosity and ensure a proper lubricant flow over lower temperature.

Thanks to the viscosity control additives, the lubricant remains efficient over a wider range of temperature.<sup>4-7</sup> Several polymers have been developed for this application but the most used are poly(alkylmethacrylate)s, poly(αolefin)s, hydrogenated styrene diene copolymers and ethyl vinyl acetate copolymers, all petroleum-based and not biodegradable.<sup>7</sup>

The improvement of oils and additives through the years led to the development of high performance lubricants, allowing maintenance reduction and higher operating speed, temperature and pressure.<sup>4,8</sup> However, another challenge today is to reduce the negative impact of lubricants on the environment. Every year, 40-50% of the lubricants end up polluting water and soils.<sup>5,9</sup> One of the major way to drastically decrease this pollution is to develop biodegradable and non-toxic lubricants.<sup>10</sup> In addition, most of the lubricant oils and additives are produced from fossil resources which are limited. Most of the current lubricants are then not valuable in terms of durability and sustainability. To tackle all these challenges, bio-based resources appeared to be promising substrates for the development of environmentally friendly and sustainable lubricant oils and additives.<sup>11,12</sup>

Bio-based resources offer a regeneration time of the carbon source which is measured in years in comparison to hundreds of millions of years for fossil resources. This largely available feedstock includes lignin, cellulose, starch, proteins and plant oils.<sup>13,14</sup> The latter, extracted from seeds, are naturally liquid which can be used as lubricant base oil.<sup>12</sup> They are constituted of triglycerides composed of glycerol and fatty acids with alkyl chains from 8 to 22 carbons. As illustrated in Figure i-2, the biorefinery of this natural resource gives access to a large palette of aliphatic fatty acids, which can be polymerized through their reactive functions, i.e. carboxylic esters, hydroxyl groups and double bonds.<sup>13,14</sup> Consequently, this research project aims at designing bio-based polymeric materials as lubricant additives such as viscosity control additives.

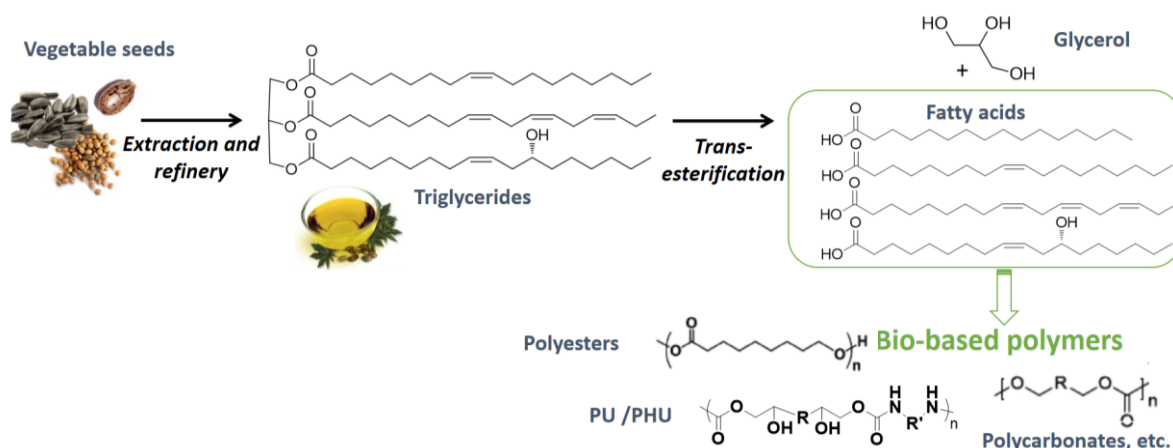


Figure i-2: Schematic illustration of the development of fatty acid-based polymers which could be used as lubricant additives through vegetable oil modifications

This thesis, performed at the Laboratoire de Chimie des Polymères Organiques (LCPO), took place in the frame of POLYADD project supported by the SAS PIVERT, in collaboration with the Centre Technique Industriel des Huiles et Corps Gras (ITERG) and the Institut Charles Gerhardt at Montpellier (ICGM). The aim of the project was to design bio-based polymeric viscosity control additives for lubricants. In this thesis, polyesters stemming from fatty acids were developed and evaluated both as viscosity modifiers and pour point depressants.

The present manuscript is composed of four chapters. The first chapter is devoted to the state of the art on the viscosity control additives. A short overview of the lubricant formulations is first performed, mentioning the main oils and the principal additives used. Then, a bibliographic survey on viscosity modifiers and pour point depressants is presented, with the aim not to provide a full comprehensive review but rather to highlight the main properties required for each additive and to investigate their action on oil viscosity with respect to their chemical structure and dimension. Finally, the already existing bio-based viscosity control additives will be discussed.

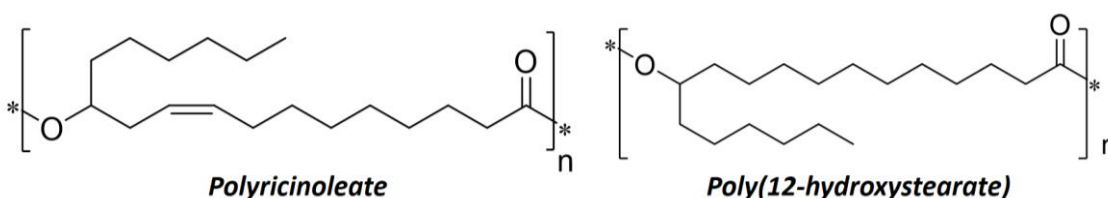


Figure i-3: PRic and PHS chemical structures

In the second chapter, a short review of the polymers developed from fatty acids will be first presented. Polyricinoleate (PRic), a biodegradable aliphatic polyester was selected as potential viscosity modifier. Its synthesis through polycondensation was optimized in order to obtain PRic and its saturated homologous, poly(hydroxystearate), with various molecular weights, see Figure i-3. The impact of PRic molecular weight on thermal and rheological properties was first investigated and, finally, these polyesters were evaluated as viscosity modifiers in lubricant oils.

Then, in Chapter III, bio-based linear and comb polyricinoleate derivatives were designed through successive thiol-ene addition and polycondensation. Again, the impact of the polymer architecture on its efficiency as viscosity modifier was investigated. Comb poly(9-alkyl 12-hydroxystearate) were then synthesized with various pendant alkyl chains and evaluated both as viscosity modifiers and pour point depressants.

Finally, in the fourth chapter, copoly(9-alkyl 12-hydroxystearate) composed of various pendant alkyl chains were prepared. The copolymer composition was tuned with the objective to control the polymer solubility in oil as a function of the temperature. Finally, a selected comb copoly(9-alkyl 12-hydroxystearate) was evaluated in dodecane, used as a model solvent of mineral oil, in order to understand its behavior in oil as a function of the temperature.

In this thesis, the impact of the structure of fatty acid-based polyesters on the rheological properties of oils was performed. The effect of the chemical structure, presence of dangling alkyl chains and molecular weight was rationalized. Polyricinoleate and its derivatives exhibit promising properties as thickeners. The presence of crystalline pendant chains brings PPD efficiency to the polymer family. Finally, comb copoly(9-alkyl 12-hydroxystearate)s represent promising Viscosity Index improvers.

## References

- 1 K. C. Ludema, *Friction, wear, lubrication*, CRC Press, 1996.
- 2 Fuchs group, Evolve magazine, <https://www.fuchs.com/group/magazine/en/topics/detail-view/do-disruptions-damage-durability-1/>.
- 3 P. Nagendramma and S. Kaul, *Renew. Sustain. Energy Rev.*, 2012, **16**, 764–774.
- 4 D. M. Pirro, M. Webster and E. Daschner, *Lubrication Fundamentals, Third edition*, CRC Press, 2016.
- 5 S. Q. a Rizvi, *A Comprehensive Review of Lubricant Chemistry, Technology, Selection and Design*, ASTM International, 2009.
- 6 R. M. Mortier, M. F. Fox and S. T. Orszulik, *Chemistry and Technology of Lubricants*, Springer, 2010.
- 7 L. R. Rudnick, *Lubricant Additives: Chemistry and Applications*, Taylor and Francis, 2017.
- 8 V. W. Wong and S. C. Tung, *Friction*, 2016, **4**, 1–28.
- 9 T. Mang and W. Dresel, in *Ullmann's Encyclopedia of Industrial Chemistry*, Wiley, 2007, pp. 1–850.
- 10 J. P. Davim, *Ecotribology*, Springer, 2016.
- 11 R. Nasser, N. Ahmed and A. Nassar, *Pet. coil*, 2016, **58**, 687–694.
- 12 G. Biresaw and B. K. Sharma, *Environmentally friendly and biobased lubricants*, Taylor and Francis, 2017.
- 13 A. Gandini and T. M. Lacerda, *Polymers from Plant Oils*, 2015.
- 14 D. K. Schneiderman and M. A. Hillmyer, *Macromolecules*, 2017, **50**, 3733–3749.



# Chapter I:

*Viscosity control additives for lubricants: from petroleum- to bio-based polymers*

## Table of content

Introduction to the lubricants .....	21
1. Lubricants: a complex formulation .....	22
1.1. Lubricant base oils .....	23
1.1.1. API base stock classification .....	23
1.1.2. Mineral base oil: API group I, II and III .....	24
1.1.3. Synthetic base oils: API Group IV and V .....	25
1.1.4. Bio-sourced base oils .....	28
1.2. Most common additives in lubricants .....	30
2. Viscosity modifiers from petroleum resources .....	34
2.1. Viscosity modifiers function relative to the lubricant requirements .....	34
2.1.1. Viscosity and VM thickening properties .....	34
2.1.2. Viscosity-Temperature (V-T) relationship.....	37
2.1.3. Shear stability.....	39
2.2. Chemistry of viscosity modifiers.....	41
2.2.1. Olefin copolymers (OCP).....	41
2.2.2. Poly(alkyl methacrylate)s (PAMAs) .....	44
2.2.3. Hydrogenated Styrene-Diene (HSD) copolymers.....	46
2.2.4. PAMA-OCPs comb copolymers .....	48
2.2.5. Other polymers .....	48
2.3. Viscosity Index improver impact on oil V-T behavior .....	50
2.3.1. Coil expansion of the polymer chain .....	51
2.3.2. Interaction between polymer chains: aggregation - disaggregation .....	53
2.3.3. Other secondary mechanisms through polymer-solvent interactions .....	56
2.4. Summary and outlook.....	57
3. Pour point depressants .....	58
3.1. Pour point depressant function and mechanisms.....	58
3.1.1. Low-temperature behavior of base oils .....	58
3.1.2. PPD function and mechanisms of action.....	60
3.2. Main pour point depressant chemical structures .....	62
3.2.1. Poly(alkylmethacrylate) comb polymers (PAMAs) .....	62

3.2.2. <i>Other polymers</i> .....	64
3.3. Summary and outlook.....	66
4. Bio-based viscosity control additives for lubricants .....	66
4.1. Strategies to enhance bio-based part in lubricants.....	66
4.2. Short overview of bio-based additives .....	67
4.3. Bio-based viscosity modifiers .....	68
4.3.1. <i>Bio-based viscosity modifiers for petroleum-based oils</i> .....	68
4.3.2. <i>Viscosity modifiers for fully bio-based lubricants</i> .....	71
4.4. Bio-based pour point depressant .....	72
4.4.1. <i>Bio-based PPD for petroleum-based oils</i> .....	72
4.4.2. <i>PPD for fully bio-based lubricants</i> .....	73
Conclusion .....	74
References.....	76



## Introduction to the lubricants

---

By definition, the lubrication is the principle of supporting a sliding load by applying a film which reduces friction. The substance that composes the film is a lubricant which can be a solid, a liquid or a gas.<sup>1</sup> The lubricant is usually placed between two metal parts moving against one another limiting the friction and thus the wear.<sup>2</sup> It has also to perform number of critical functions such as cooling, cleaning and protecting metal surfaces of modern equipment in order to generally prolong the engine lifetime.<sup>1-5</sup> Therefore, a lubricant formulation should attend proper low and high temperature viscosity, low volatility, low flash point and non-flammability, good thermo-oxidative and chemical stabilities.<sup>3,6,7</sup> These properties, and many others, are mandatory to tackle to a good engine lubrication, especially the viscosity which is probably the most important single property of a lubricating oil.<sup>3,8</sup> Indeed, it affects heat generation in bearings, cylinders or gears, governs the sealing effect of the oil and the rate of consumption or loss.<sup>2,8</sup>

Mineral, synthetic and even organic oils are used as lubricant base oils but cannot attend all the required properties discussed above. For these reasons, additives are added to the base oil.<sup>9,10</sup> The function of an additive is to enhance an already-existing property of the base oil or to add a new one in order to impart the lubricant properties necessary to perform effectively in the intended application.<sup>10</sup> The complete formulation depends on the specific application targeted. Therefore, between 5000 and 10 000 different lubricant formulations are necessary to satisfy more than 90% of all lubricant applications.<sup>3,4,8</sup>

For the last 10 years, the global production of lubricants remains stable around 36 million tons.<sup>11,12</sup> In terms of volume, Pacific Asia became recently the most important lubricant-consuming area with 43% of the global production of lubricants, compared to 35% ten years ago. Europe and North America consume both 18%. As illustrated in Figure I-1, engine oils accounted for approximatively 53% of the year 2016 lubricant use. Then, 42% were used for industrial applications, including classical industrial lubricants and process lubricants. Industrial lubricants are added in the engine or machinery without any contact with the

product. Conversely, process oils are added to the formulation of a product to both enhance manufacturing process and improve “end-product” performance and quality.<sup>4, 3,4,11</sup>

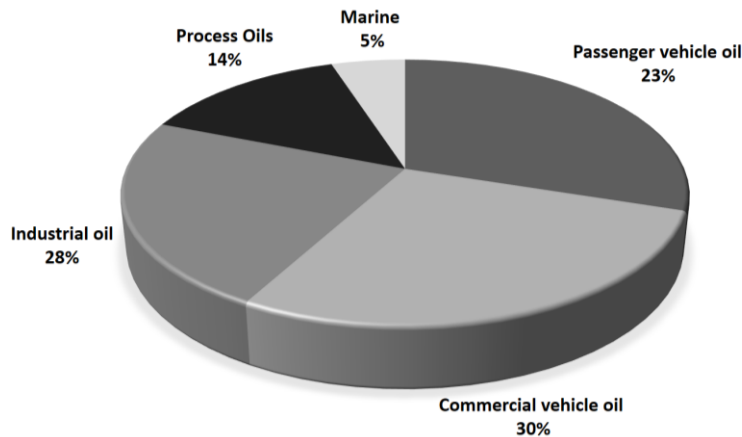


Figure I-1: Worldwide lubricant utilization <sup>4</sup>

The twenty-first century continues to see advances in equipment technology. New demands are particularly placed on output and environmental performances.<sup>4,13,14</sup> A lot of emphasis is put on engines and machines capabilities in terms of life-time extension, energy saving and emission reduction. As a result, lubricants with improved performances are required.<sup>15,16</sup> Moreover, every year, about 40-50% of the used lubricants in the world end up polluting the environment.<sup>8</sup> The environmental concerns urge then to develop biodegradable lubricants with low toxicity, such as bio-based and biodegradable synthetic lubricants.<sup>13,15,17</sup> From 2018 to 2025, an annual growth rate of 2.5% for synthetic lubricants market<sup>18</sup> and above 6% for bio-based lubricants market<sup>19,20</sup> is expected in terms of revenues. This forecast shows that the trend towards ever-greater performance and even better environmental compatibility is expected to continue, despite their higher price.<sup>8,9,21</sup>

## 1. Lubricants: a complex formulation

---

This section proposes to shortly introduce the different base oils and additives currently used in lubricants. For more details, lubricant chemistries, properties and functions have been extensively reviewed in several books.<sup>3,6-8,10,22,23</sup> Oil based lubricants are extensively used compared to other lubricant types such as solid or grease lubricants.<sup>3</sup> Therefore, only oil based lubricants will be considered here. Different types of base oils and most common additives will be mentioned in this chapter.

## 1.1. Lubricant base oils

In a lubricant, the amount of base oil can be from 70% to greater than 99%.<sup>3</sup> It depends on the desired performance level and the severity of the end-use requirement. Since lubricants are mainly composed of the base oil, the properties of this latter greatly impact the final properties of the lubricants. Base oils are derived from three sources: mineral, synthetic and biological, i.e. from plants or animals.<sup>3,4,8</sup>

### 1.1.1. API base stock classification

Base stock oils have been classified by the American Petroleum Institute (API).<sup>24</sup> This simple classification illustrated in Table I-1 was originally intended to help regulators interpret performance data for the licensing and certification of lubricants.<sup>3,4</sup>

Table I-1: API Base oil classification<sup>4</sup>

Group	Saturates (%)		Sulfur (%)	Viscosity Index
Group I	<90	and/or	> 0.03	80 to <120
Group II	≥90	and	≤ 0.03	80 to <120
Group III	≥90	and	≤ 0.03	≥ 120
Group IV	All polyalphaolefins (PAOs)			
Group V	All other not included in above groups			

Groups I, II and III are mineral oil-based. Group IV is reserved solely for PAOs which are synthetic in origin, being built up from gaseous hydrocarbons such as ethylene. Group V have been added after the classification establishment in 1995. This group is a “catch-all” category for all base oils not included in the first four groups. That includes synthetic base oils such as polyglycols, silicones, synthetic esters as well as organic base oils.

Mineral oils are classified regarding to the percentage of compounds without unsaturation, percentage of sulfur and Viscosity Index value.<sup>3,4,8</sup> As unsaturated compounds are sensitive to oxidation, they are not desired in base oils. As a result, high percentage of saturated compounds is required in mineral base oil to reach good oxidation properties.<sup>25</sup> Modern base oils are required to have a low sulfur percentage. The presence of sulfur in oil is controversial. In contact with air, water or particular additives, it can form weak acids which damage engines metal piece in the long term.<sup>6,8</sup> However, for many years the presence of sulfur in base oil was required because the organo-sulfur compounds have an antioxidant and antiseptic activity.<sup>3,25</sup>

Nowadays, sulfur percentage required in base oil is low but sulfur-containing additives are often used in these oils in order to improve their oxidative stability and anti-wear performance.<sup>3,4</sup> Finally, the classification is based on oil Viscosity Index (VI). It is a measure of the viscosity-temperature relationship, i.e. it indicates the rate of loss in viscosity depending on the temperature.<sup>26</sup> The lower the VI value, the most important the viscosity loss. As engines are used at a large range of temperature, a low decrease rate of the viscosity, i.e. a high VI, is preferred in most applications.<sup>3,4,6,8</sup> The main properties of lubricants depending on their classification are compared in Table I-2.<sup>4</sup>

Table I-2: Base oils properties comparison

Group	Mineral oil			PAO, Esters
	I	II	III	IV, V
<b>Kinematic viscosity (mm<sup>2</sup> s-1)</b>	20-540	20-130	20-54	20-1500
<b>Oxidation stability</b>	Good	Good	Very good	Excellent
<b>Volatility</b>	Fair	Good	Very good	Excellent
<b>Solvency</b>	Very good	Poor/good	Poor	Poor-Excellent
<b>Low-temperature characteristics</b>	Fair	Good	Very good	Excellent

In the next section, the different base oils will be introduced in three groups: mineral, synthetic and organic base oils.

### **1.1.2. Mineral base oil: API group I, II and III**

A large majority of lubricants are based on mineral oils, because of their low cost, ready availability and overall adequate performances. The properties of mineral base oils depend on their source and degree of refining.<sup>27</sup> As illustrated in Figure I-2, the latter are composed of a mix of paraffinic, naphthenic and aromatic hydrocarbon types.<sup>3,28,29</sup> Paraffinic compounds are linear aliphatic alkane chains or with branched side chains. With high degree of branching, the term isoparaffinic is used. Naphthalene compounds are cycloalkanes with aliphatic carbons chains. Aromatic compounds are not desired because of the unsaturation of the benzyl moieties.<sup>28</sup> Paraffinic and especially isoparaffinic compounds have a viscosity relatively stable regarding to the temperature compared to naphthalene ones.<sup>30</sup>

Group I base stock comes from traditional petroleum refining techniques. It is composed mainly of naphthenic compounds leading to large variations of the viscosity with temperature.<sup>28</sup> As a result, Viscosity Index of Group I oils are low. Moreover, it has the highest amount of unsaturated hydrocarbons and sulfur. Despite its use in marine or some industrial

applications, Group I market is in a steady decline. Its low properties do not meet market needs as well as Group II and Group III mineral oils. <sup>3,4,8</sup>

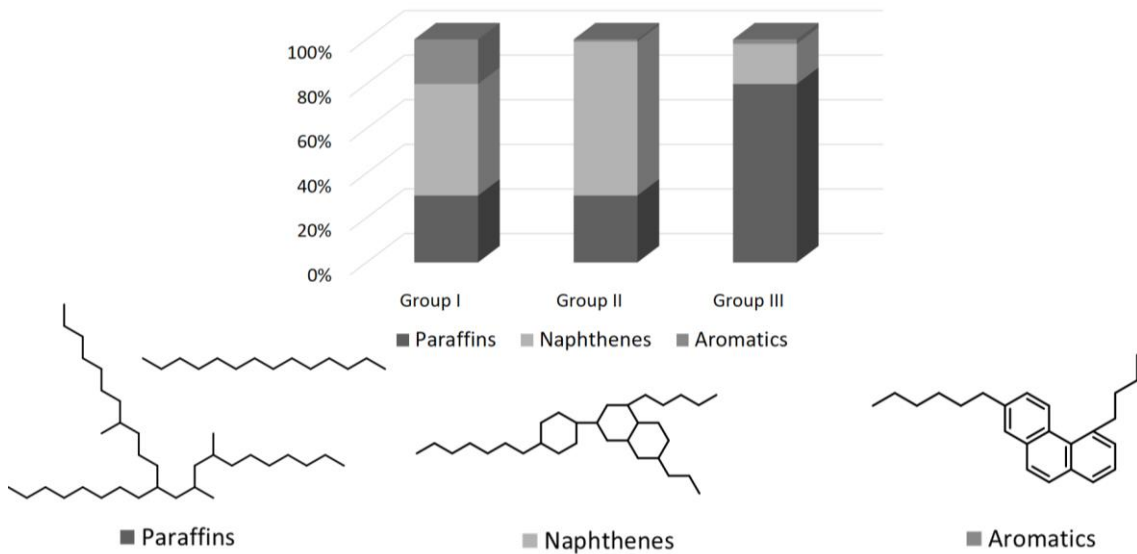


Figure I-2: Typical composition of the mineral oils with the chemical structures associated <sup>3,29</sup>

Group II and Group III base oils refining is typically done by vacuum distillation, hydrogenation and catalytic dewaxing. These techniques allow removing impurities that could affect oxidation stability, leading to small percentage of aromatic and sulfur compounds. <sup>3,27</sup>

Compared to Group I, these base oils have better thermal stability and low temperature performance. <sup>4,6,27</sup> In case of Group III base oil, the oil refining includes an isomerization step in order to increase the amount of isoparaffin and then increase base oil VI. <sup>27,30</sup> These mineral oils are mostly used for passenger vehicles and heavy-duty commercial lubricants. Recently, lubricant manufactures developed Group II+ and Group III+ base oils. They reach the top of the Viscosity Index of each category, i.e. 120 and more than 140 respectively. That allows Group III+ to fill the performance gap between the best mineral based oils and Group IV and V base oils. <sup>4</sup> Consequently, Group III+ is extensively used to meet the increasingly demanding performance requirement of the lubricants. <sup>4,31</sup>

### 1.1.3. Synthetic base oils: API Group IV and V

By definition, a synthetic base oil is a material produced by combining or building individual component into a unified entity. <sup>3</sup> Unlike mineral oils which are a mixture of naturally occurring hydrocarbons, synthetic base oils are man-made and tailored to have predictable properties. <sup>4,7,22</sup> Synthetic lubricants possess additional performance advantages such as better thermo-oxidative stability and chemical stability than mineral oils. <sup>3-5</sup> The three main

classes of synthetic oils are synthetic hydrocarbons fluids, synthetic esters and polyglycols.<sup>6,7</sup> An example of their common structures is illustrated in Figure I-3. Other synthetic fluids such as silicones, halogenated hydrocarbons and polyphenylethers are also used, mainly for very specific applications.<sup>3,4,8</sup>

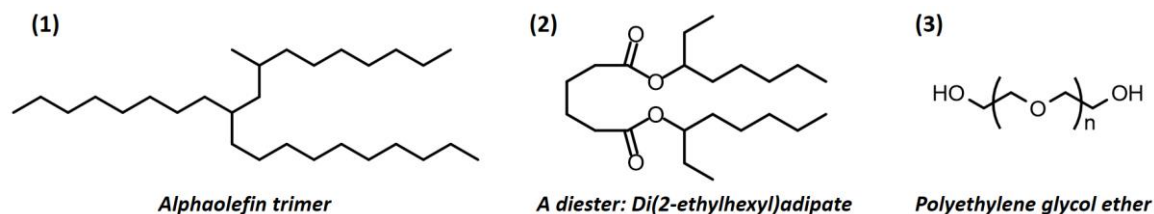


Figure I-3: Examples of the chemical structure of (1) a PAO (2) a synthetic ester and (3) a polyglycol

### 1.1.3.1. Synthetic hydrocarbon fluids

Poly(alphaolefin)s, or PAOs, represent the most important family of synthetic hydrocarbon fluids and the entire group IV of lubricant base oils. These isoparaffinic compounds, see Figure I-3 (1), are obtained from ethylene within two steps: oligomerization then hydrogenation.<sup>7,32-34</sup> The obtained PAOs are similar to mineral base oils, but without the presence of naphthenic and aromatic structures as well as sulfur or nitrogen compounds, that negatively impacts the base oil properties. Consequently, PAOs have VI from 135 up to 200, good shear and oxidation stability and can reach a large range of viscosity.<sup>3,8,35</sup> PAOs are fully apolar leading to anti-foam and de-emulsifying properties. However, PAO apolar feature decreases significantly the solvency power and affinity with metals.<sup>7,8</sup> PAOs are used for the same applications than mineral oils, for instance as automotive and industrial lubricants.<sup>6,22,36</sup>

### 1.1.3.2. Synthetic esters

The other main type of synthetic base oil is based on ester chemistry. Ester-based oils are more polar than mineral ones, have lower volatility, higher flash point and better solvency.<sup>7,36</sup> In addition, the presence of the ester group increases the thermal stability, the lubricity but decreases the hydrolysis stability. One other interest for synthetic esters is their biodegradability.<sup>7,8</sup> The most commonly used classes of synthetic esters are diesters, polyol esters and phosphate esters. Structures are displayed in Figure I-4.

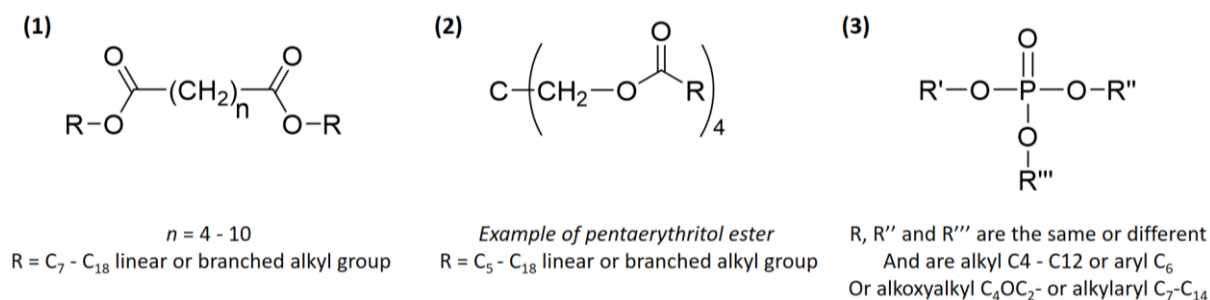


Figure I-4: Chemical structure of (1) diester, (2) polyol ester and (3) phosphate ester

Diesters viscosity and low temperature properties mainly depend on the carbon chain length of the initial diacid and monoalcohol compound, see Figure I-4 (1). The longer the chain, the higher the viscosity.<sup>3</sup> Because of higher requirements for some technologies such as aeronautic, polyol esters have been developed, see an example in Figure I-4 (2).<sup>7</sup> Vegetable oils fall under the class of polyol esters but will be discussed separately since they are not synthetic in origin.<sup>8</sup> Finally, phosphate esters, illustrated in Figure I-4 (3) are usually prepared by reacting an alcohol or a phenol with phosphoryl chloride. One of the major features of phosphate esters is their fire resistance.<sup>7,8</sup> They also have good lubricity and good oxidation resistance. On the other hand, they have poor viscosity-temperature characteristics, their thermal stability is fair and their decomposition products can be corrosive. These drawbacks preclude their widespread use as lubricants.<sup>4,8</sup>

### 1.1.3.3. Polyalkylene glycols (PAGs)

Polyalkylene glycols are also named polyethers, polyalkylene glycol ethers and polyglycols, see Figure I-3 (3). These polymers are made by ring-opening polymerization of ethylene oxide (EO), propylene oxide (PO) or their derivatives initiated by water or alcohol.<sup>3,6,8,36</sup> Depending on the EO/PO ratio, the final copolymer can be water-soluble or not.<sup>3</sup> The structure, hence properties, can be tailored using various groups and molecular weights. The polar nature of PAGs gives the oils strong affinity with metals, hence very good lubricity, even at extreme pressure and good heat transfer capacities. Water soluble PAGs with high EO contents are up to 80% biodegradable.<sup>8</sup> Because of their low toxicity, polyglycols find applications in the food, pharmaceutical and cosmetics industries.<sup>6,8</sup> Water-soluble PAGs are also largely used in hydraulic brake fluids, metalworking lubricants and fire-resistant lubricants.<sup>4</sup> Water-insoluble polyglycols are mostly used as heat transfer fluids in high-temperature gear and bearing oils. They are also included in refrigerants and compressors.<sup>4</sup>

Synthetic base oils have been tailored in order to have predictable and specific properties. Thank to that, they are able to fulfill the high performance requirement of numerous specific applications. Besides PAO, polyesters are the most commonly used synthetic lubricants, mainly because of their biodegradability. Despite their higher cost, the market for synthetic lubricants is growing while mineral market is stagnating.

#### 1.1.4. Bio-sourced base oils

Bio-based oils such as vegetable oils were the original lubricants.<sup>4</sup> They were mostly replaced by mineral and synthetic oils in the past. However, environmental concerns, particularly related to the effects of oils entering the soil and the water, lead, nowadays, to a growing interest for natural oils.<sup>37,38</sup> The naturally biodegradable oils have very low toxicity while possessing very good lubricity characteristics.<sup>17,39</sup> Some reviews<sup>12,17,37,40–43</sup> and books<sup>7,38,39</sup> already explored extensively the subject. Today, the most important renewable base oils are natural vegetable oils, and derivatized vegetable oils. This derivatization can be performed by epoxidation or esterification leading to polyolesters or estolides for instance.<sup>37,44,45</sup> The structures of the given examples are illustrated in Figure I-5.

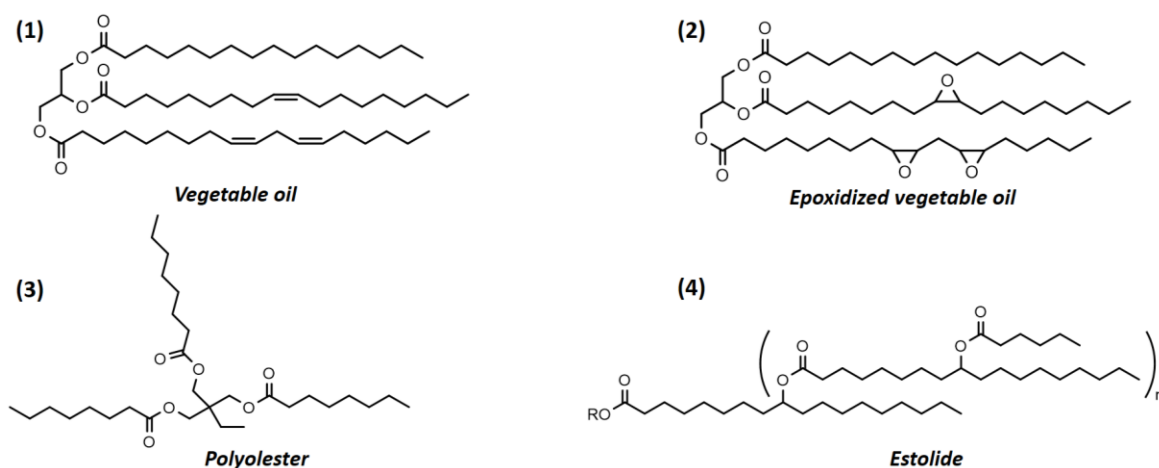


Figure I-5: Chemical structure of some examples of bio-based lubricants with (1) raw vegetable oil (2) derivatized vegetable oil and (3) polyolester and (4) estolide

As illustrated in Figure I-5 (1), vegetable oils are composed of different triglycerides resulting from the esterification of glycerol with three fatty acids (FA). Fatty acids content is characteristic of each plant oil and FAs present various chain lengths and number of unsaturations.<sup>40,46,47</sup> A large variety of vegetable oils can be used to formulate bio-lubricant such as canola, rapeseed and soybean oils.<sup>23,38,48</sup> Besides biodegradability and non-toxicity, vegetable oils have a number of other advantages. Their polarity permits affinity with metal

and then an excellent lubricity.<sup>17,42,49</sup> Their viscosity indices are much higher than those of mineral oils. For instance, soybean oil has a VI of 223 in comparison to 90 or 100 for most conventional mineral oils.<sup>42,49</sup> On the other hand, vegetable oils suffer from disadvantages, mainly thermo-oxidative stability, sensitivity to water and relatively high melting point.<sup>50-52</sup>

One of the approaches to improve oxidation stability is to lower the amount of unsaturation by hydrogenation. Unfortunately, saturated structures show higher melting points, which increase drastically the oil pour point, i.e. the temperature at which the oil stops to pour.<sup>38</sup> To circumvent this issue, strains were selected that boost mono-unsaturated content, such as high oleic sunflower oil (HOSO).<sup>3,8</sup> It is also possible to blend vegetable oils with synthetic esters.<sup>39</sup> Such blends have improved oxidation stability and lower melting points than vegetable oils alone and are already used as hydraulic fluids for instance.<sup>38,40</sup>

Another strategy with respect to vegetable oils is to chemically modify them. Chemical reactions can occur on the carboxyl or olefinic functionalities.<sup>50</sup> By transesterification, it is possible to change the glycerol portion of the triglycerides structure and then to obtain derivatized vegetable oils.<sup>3,50</sup> Epoxidation (see Figure I-5 (2)) or acetylation are also used to decrease vegetable oils sensitivity to hydrolysis and oxidative attacks. Moreover, low-temperature properties and VI coefficients can be improved.<sup>38,42</sup>

Finally, some synthetic esters are made from natural fatty acids and alcohols alike oleic acids and oleic alcohol. Examples of a polyolester and an estolide are given in Figure I-5 (3) and (4), respectively. They usually combine the superior viscosity properties of vegetable oils with the excellent low-temperature fluidity of the synthetic esters while keeping their biodegradability and non-toxicity. Polyolesters are usually formed by esterifying polyalcohols with fatty acids.<sup>37</sup> They present higher temperature stability than classic vegetable oils<sup>38,53,54</sup> Their branched structure avoid early crystallization. Some bio-based synthetic esters are nowadays commercial, such as Radialube base oil, from Oleon.<sup>55</sup> Recently, Narine *et al.*<sup>56-58</sup> developed a series of synthetic esters based on fatty acids that exhibited large range of viscosity depending on the chain length and low melting point with a minimum of -70 °C. Research on these lubricant base oils is active and several developed compounds seem promising such as estolides, illustrated in Figure I-5 (4).<sup>38,50</sup> These oligoesters of fatty acids have VI above 200 and show strength in the areas of oxidative stability and wear protection.<sup>38,59-61</sup>

Therefore, vegetable oils and bio-based synthetic esters are currently used as lubricant base oil in agriculture, forestry, construction, off-shore drilling and marine industries.<sup>3,4,38</sup> The modified vegetable oils and bio-based synthetic esters can be used in higher performance requirement applications such as hydraulic fluids<sup>38</sup>, cutting fluids<sup>62</sup> or automotive lubricants.<sup>17,38,41</sup>

To conclude this section, many lubricant base oils have been developed through years and research on this subject is still active. Mineral base oils are currently the most used, followed by synthetic ones such as PAOs and synthetic esters. The environmental concerns lead to a novel development of bio-based lubricants. Despite the improvement of base oil properties, additives are still mandatory in order to enhance their performances and fulfil the modern engine lubricant requirements.

## 1.2. Most common additives in lubricants

Additives are chemical compounds that impart specific properties of lubricants when added in base stock.<sup>3,63,64</sup> The amount of additives varies from less than 1 wt.% up to 30 wt.% or even more depending on the application.<sup>4</sup>

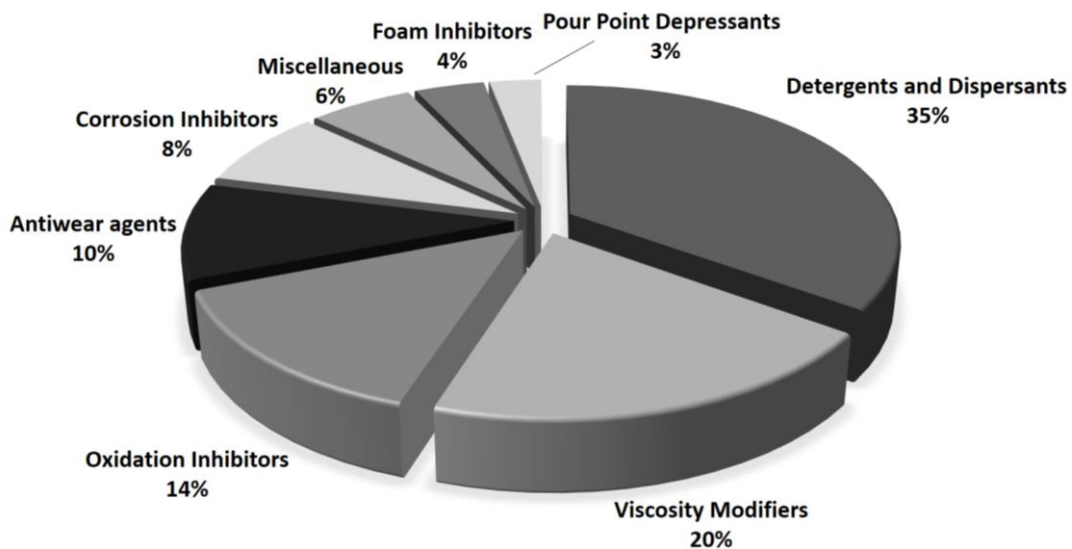


Figure I-6: Estimated additive use by additive type, in terms of volume<sup>3</sup>

Additives are categorized depending on the properties they impart to the base oil. The most common are dispersants and detergents, viscosity modifiers, oxidation inhibitors, anti-wear agents, corrosion inhibitors, foam inhibitors and pour point depressants.<sup>3,4,10</sup> Figure I-6 displays the use of additives in 2006 depending on their type and is still relevant nowadays.<sup>3,65</sup>

The additives annual production is expected to grow from 900 kTon in 2016 up to one million ton in 2020.<sup>66</sup>

In this section, a short description of the most common additives is proposed. As the main objective of this work is to design bio-based viscosity modifiers and pour point depressants, these two types of additives will be investigated more in details in the next section.

- **Oxidation inhibitors**

The aging and the degradation of lubricants are mainly due to oxidation process under oxygen.<sup>8,10</sup> Radicals and peroxides produced by oxidation of hydrocarbons lead to the creation of varnish-like deposits and harmful compounds that can cause corrosive wear.<sup>23,67–70</sup> Oxidative inhibitors are added in oil in order to trap the radicals and peroxides. The most common antioxidant additives are the zinc dithiophosphates (ZnDTP), see Figure I-7.<sup>3,10,71</sup> They render free radicals and peroxides innocuous by oxidation-reduction reaction. Other compounds, such as hindered phenolics and aromatic amines act *via* hydrogen transfer.

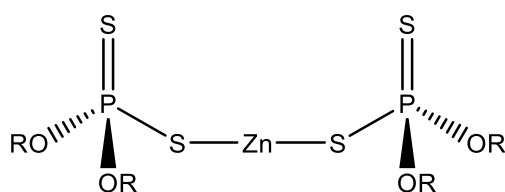


Figure I-7: Chemical structure of Zinc dialkyldithiophosphate ZnDTP<sup>8</sup>

- **Detergents and dispersants**

Lubricant contaminants, such as sludge, resin or varnish are formed by oil oxidation and combustion.<sup>72,73</sup> Consequently, detergents and dispersants are added in the base oil in order to keep oil contaminants in suspension and to prevent them from agglomerating into solid particles.<sup>8,74</sup> They also minimize particle-related abrasive wear and viscosity increase.<sup>10,72,75</sup> Detergents and dispersants are generally amphiphilic molecules. They envelop contaminants by forming micelles, keeping them in suspension. Detergents chemically neutralize contaminants while dispersants avoid their deposit on metal surface by forming suspension. Detergents and dispersants work in synergy with each other.<sup>4,63</sup>

Detergents are metal salts of organic acids such as sulfonates, phenates and salicylates with alkaline metals, mainly calcium and magnesium.<sup>10,76,77</sup> Dispersants are metal-free amphiphilic macromolecules with  $M_w$  from 3 kg.mol<sup>-1</sup> to more than 25 kg.mol<sup>-1</sup>. Various polyolefins are

used as dispersants.<sup>3,10,75</sup> Usually, a polar moiety, usually nitrogen- or oxygen-derived, is introduced to the polymer backbone to bring amphiphilic properties.<sup>10</sup>

- **Antiwear and other film-forming additives**

Under severe conditions such as high local temperature or load, the lubricant oil film becomes progressively thinner. At a certain point, contact between two metal pieces through the oil film can occur leading to wear. In order to avoid this undesirable contact, film-forming additives are used. Three classes of film-forming additives were developed depending on the severity of the lubricant requirement: the friction modifiers, antiwear agents and extreme-pressure (EP) additives, see Figure I-8 (1).<sup>4,10,64</sup>

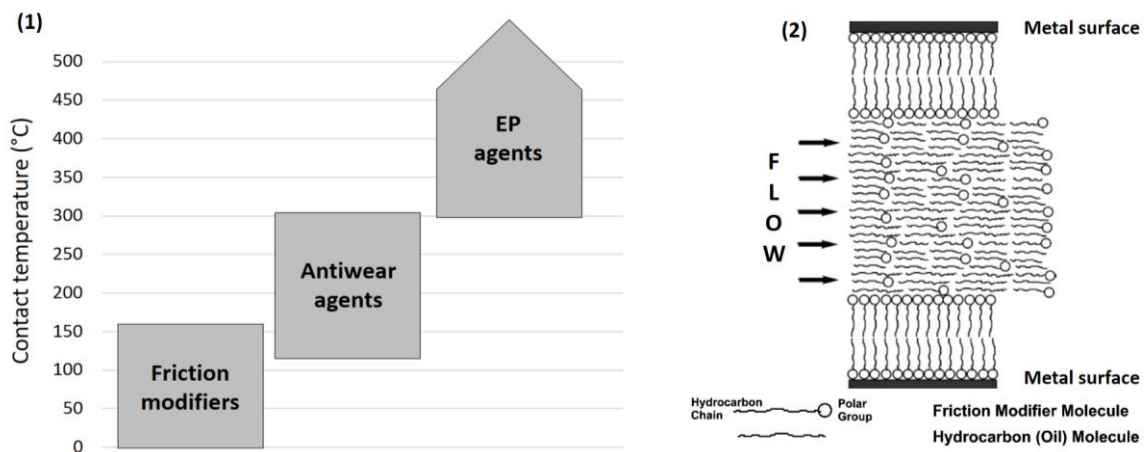


Figure I-8: (1) Classes of film-forming agents depending on the contact temperature range of their application<sup>66</sup> and (2) Friction modifier mechanism of action

Friction modifiers have a polar head which is anchored to the surface, through hydrogen adhesive bonding or physical interaction with the metal, see Figure I-8 (2). The hydrocarbon tail is solubilized in the oil.<sup>6,10,78</sup> Usually, phosphoric and phosphonic acid derivatives as well as fatty acids such as stearic acid are used as friction modifiers.<sup>4,10,79,80</sup>

Antiwear and EP additives act as friction modifiers, their polar nature leads to the formation of a layer on the metal surface but their hydrocarbon tails are much shorter and thermally labile which make them more surface active.<sup>3</sup> Moreover, when the temperature increases, the additives thermally decompose to yield compounds to react with the metal surface, forming consequently a new chemically-bonded layer to the surface.<sup>8,9</sup> EP additives typically require higher activation temperature and load than antiwear additives.<sup>3</sup> The most important antiwear additives for decades are ZnDTP, see Figure I-7.<sup>81-83</sup>

- ***Rust and corrosion inhibitors***

The metal surfaces under severe conditions can undergo corrosion.<sup>3</sup> As a result, corrosion inhibitors are used and can be categorized as acid neutralizers or scavengers and film-formers.<sup>3,64</sup> Acid neutralizing agents function is to neutralize aggressive materials in solution and make them innocuous. Their mechanism of action is the same as detergents. As a result, it appears that basic detergents such as alkaline materials are excellent corrosion inhibitors.<sup>3,8,10</sup> Film formers attach their polar head to the metal surface to form impenetrable protective films following the same mechanism as friction modifiers.<sup>3,84</sup> The chemical type of corrosion inhibitors depends on the metal surface. For instance, ZnDTP inhibits copper-lead bearing corrosion but causes silver corrosion damage because of the presence of sulfur.<sup>3</sup> For ferrous metals, sulfonate and phosphates derivatives are used for example while thiadiazole and triazole are preferred for nonferrous devices.<sup>3,8,84</sup>

- ***Antifoams additives***

During use, air can be incorporated into the lubricant, causing foam. The foaming of lubricant is undesirable because it can include possible fluid overflow leading to equipment failure but also impair power and heat transfer lubricant capabilities and enhance oxidation.<sup>85-88</sup> Antifoams are added in lubricants at very low concentration, typically 10-100 ppm and take the form of small (less than 100 $\mu$ m) and insoluble liquid droplets that are dispersed in the oil.<sup>8,10,89</sup> Antifoam agents have to be chemically inert and to have a lower surface tension than the oil.<sup>10</sup> With their particularly low surface tension, liquid silicones are consequently the most efficient antifoam agents used nowadays.<sup>4,8,10</sup> Demulsifiers work the same way to avoid water in oil emulsions as well as oil in water emulsions in case of water based lubricants. They are mainly anionic surfactants such as alkyl-naphthalene sulfonates but alkyl-phenol “resins” and block copolymers are also used.<sup>6</sup>

Other additives such as dyes, diluent or surfactant emulsifiers in some cases are also barely used. All the additives describe are mandatory to reach the required lubricant properties. However, additives need to be carefully formulated, making use of synergistic effect and avoiding any antagonism.<sup>3,6</sup> Viscosity modifiers and pour point depressants have also a predominant role in lubricant formulation and will be discussed in detailed in the next section.

## 2. Viscosity modifiers from petroleum resources

Viscosity modifiers (VM) represent more than 25% of the total additives used in terms of volume.<sup>3,65</sup> Engine lubricants are, by far, their largest commercial application followed by automatic transmission fluids, hydraulic fluids, turbine engine oils, etc.<sup>4,6</sup> Their use in lubricant formulations mainly permits to provide satisfactory lubrication over a wider temperature range than it is possible with base oil allowing for instance developing multi-grade oils also called “all seasons oils”.<sup>3,6,90</sup> Moreover, the better control of oil viscosity over the temperature through additive effect results in a decrease of lubricant oil as well as fuel consumption.<sup>6,91</sup>

Viscosity modifiers have to display several functions related to the lubricant properties required. These functions will be presented in the first section. Then, the major classes of polymers used as VM will be described. Benchmarking with respect to their performances as VMs is difficult as the latter are used in several base oils at different concentrations. Finally, the mechanism of VM action proposed in literature will be reviewed.

### 2.1. Viscosity modifiers function relative to the lubricant requirements

#### 2.1.1. Viscosity and VM thickening properties

##### Definition of the viscosity

Viscosity is defined as a fluid’s resistance to flow.<sup>3</sup> Viscosity measures the internal friction within a liquid, reflecting the way molecules interact to resist motion.<sup>6</sup> A simple model is illustrated in Figure I-9.

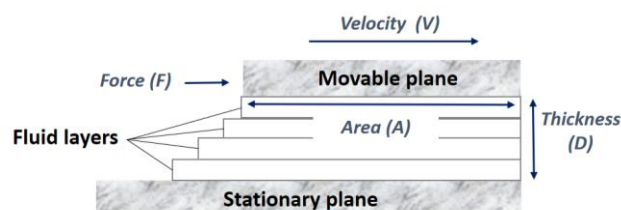


Figure I-9: Schematic lubricant laminar flow between shearing planes<sup>3,6</sup>

In the model, the fluid forms parallel layers between a stationary plane and a movable plane. When a force  $F$ , i.e. the shear, is applied, the plane moves at a constant velocity  $V$ . Because the fluid usually wets or adheres to the surface, the layer in contact with the moving plane will move at the same velocity  $V$ . However, the movement is transmitted through different fluid

layers in a dissipating manner until the fluid velocity approaches zero near the stationary plane. The decrease in movement occurs because of the friction between the fluid layers. The overall effect is the fluid resistance to free flow, namely the viscosity. Newton defined the absolute viscosity or dynamic viscosity according to equation (I-1).<sup>6</sup>

$$\eta_{dyn} = \eta_{abs} = \frac{\tau}{s} = \frac{F/A}{V/D} \quad (I-1)$$

where  $\eta_{abs}$ , the absolute viscosity is defined as the ratio between the applied shear stress  $\tau$  and the resulting shear rate  $s$ . As illustrated in Figure I-9, the shear stress is the force  $F$  applied to the movable plate, divided by the area  $A$  of the plate. The resulting shear rate is the velocity  $V$  of the moving plate divided by the film thickness  $D$ .<sup>3,6</sup>

The absolute viscosity is the Pascal second (Pa.s) or centipoise (cP), where 1 Pa.s = 10<sup>3</sup> cP. Dynamic or absolute viscosity is independent of the gravity. The viscosity under influence of gravity is called kinematic viscosity and is defined according to equation (I-2).

$$\eta_{kin} = \frac{\eta_{dyn}}{\rho} \quad (I-2)$$

where the kinematic viscosity,  $\eta_{kin}$ , is the dynamic viscosity,  $\eta_{dyn}$ , divided by the liquid density  $\rho$ . The SI unit of  $\eta_{kin}$  is m<sup>2</sup>.s<sup>-1</sup> and centistoke, cSt, are also used, where 1 cSt = 10<sup>-6</sup> m<sup>2</sup>.s<sup>-1</sup>.

Newtonian fluids have, by definition, a viscosity which is independent of the shear rate. Conversely, non-Newtonian fluids viscosity vary with the shear rate. Usually, mineral base oils are Newtonian while the finished lubricant formulations are non-Newtonian because of the addition of polymers such as viscosity modifiers or dispersants.<sup>3</sup>

### Function of viscosity modifiers

The function of the viscosity modifiers is to thicken the base oil. Because their molecular weight is higher than the ones of base oils, polymers have a natural thickening effect. Larger molecules in solution, i.e. polymeric viscosity modifiers, move less readily. Then they restrain the progress of the smaller oil molecules during the flow leading to a viscosity increase.<sup>92</sup> The amount of polymer that has to be used in a lubricant formulation to reach a desired viscosity is defined as thickening efficiency.<sup>93,94</sup> It can be evaluated by using relative or specific viscosity, according to equation (I-3) and (I-4)

$$\eta_{rel} = \eta_r = \frac{\eta}{\eta_0} \quad (I-3)$$

$$\eta_{sp} = \frac{\eta - \eta_0}{\eta_0} \quad (I-4)$$

with the relative viscosity  $\eta_{rel}$ , also called reduced viscosity  $\eta_r$ ,  $\eta_{sp}$  the specific viscosity,  $\eta$ , the viscosity of the blend of the oil with the polymer and  $\eta_0$  the oil viscosity. Those can be dynamic or kinematic viscosities.

The contribution of a polymer to the viscosity of a solution is also quantified by its intrinsic viscosity. This feature is related to its molecular weight, the nature of both the polymer and the base oil, the size of polymer in solution and the polymer concentration in oil. It has been rationalized by Mark-Houwink-Sakurada<sup>95</sup> equation (I-5) and Einstein<sup>96</sup> equation (I-6).

$$[\eta] = KM_v^a \quad (I-5)$$

$$[\eta] = \frac{M_w V_e}{2.5 N_a} \quad (I-6)$$

with  $[\eta]$  is the intrinsic viscosity;  $M_v$  is the viscosity average molecular weight;  $K$  and  $a$  are constants that depend on the polymer and solvent.  $V_e$  is the hydrodynamic volume of the polymer in solution,  $M_w$  its molecular weight and  $N_a$  the Avogadro number. Then the relation between the polymer intrinsic viscosity and the blend viscosity was rationalized by Huggins<sup>97</sup> and Kraemer<sup>95</sup> according to equations (I-7) and (I-8) respectively.

$$\frac{\eta_{sp}}{c} = [\eta] + k'[\eta]^2 c \quad (I-7)$$

$$\frac{\ln(\eta_r)}{c} = [\eta] - k''[\eta]^2 c \quad (I-8)$$

where  $c$  the polymer concentration;  $k'$  and  $k''$  are constants that depend on the polymer and the solvent. These relationships are available for  $c < c^*$ , the overlap concentration, i.e. in a dilute solution where the polymer chains act as single particles. The overlap concentration is defined according to equation (9)

$$c^* = \frac{3M_w}{4\pi N_a R_g^3} \quad (I-9)$$

where  $R_g$  is the radius of gyration. These equations imply an increase of the solution viscosity with molecular weight and concentration. This is typically observed for viscosity modifiers.<sup>90,98-101</sup> Concentration is a key parameter: the highest the concentration, the highest the base oil thickening. As illustrated in Figure I-10, above  $c^*$ , polymer coils are in contact with each other. Then the polymer chains can inter-penetrated, i.e. entangled.<sup>102</sup> Viscosity modifiers act as aggregates of multiple chains and the rate of viscosity increase with concentration is larger than in dilute solutions.<sup>93,103</sup>

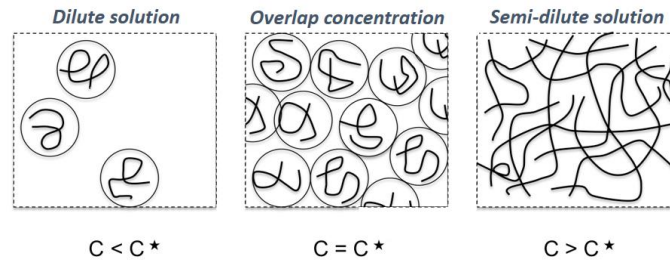


Figure I-10: Illustration of the different dilution regimes depending on the concentration

However, polymers are expensive relative to base oil and high polymer concentration can affect negatively other oil properties. Consequently, it is required to use as little polymer additive as possible, i.e. to maximize the thickening efficiency. To do so, the use of a polymer with high intrinsic viscosity is required and thus with high  $M_w$  and good solubility in the oil. It has been also shown that the polymer backbone nature and architecture have obviously an impact on the thickening efficiency.<sup>3,6</sup> This will be further investigated in the section about VMs chemistry.

### 2.1.2. Viscosity-Temperature (V-T) relationship

The second function of viscosity modifiers is to change the behavior of an oil regarding to the temperature, i.e. the viscosity-temperature (V-T) relationship or V-T behavior. Indeed, naturally, a fluid viscosity dramatically decreases by increasing the temperature. An example of the V-T relationship for usual base oils is illustrated in Figure I-11.<sup>3,8</sup> The three oils present an exponential viscosity drop with temperature change. This V-T behavior can be plotted as semi logarithmic trace which permit an easier comparison of the different behaviors. For instance, the viscosity resistance to the temperature is as follows: rapeseed > paraffinic (Group III) > naphtenic oils (Group I).<sup>8</sup>

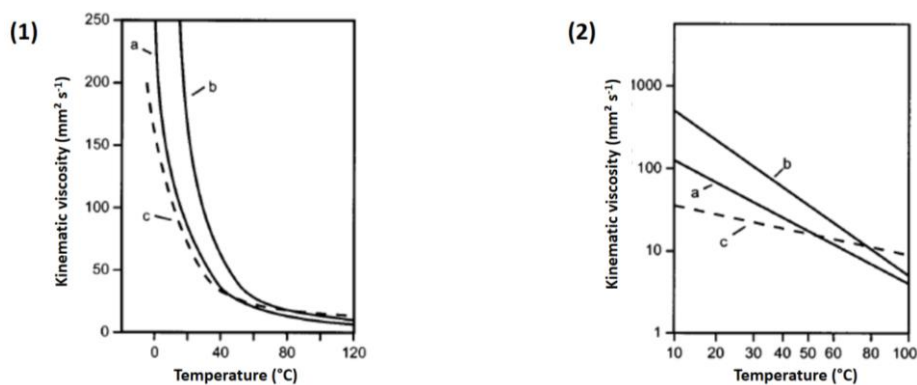


Figure I-11: V-T behavior of various oils (1) Linear, (2) Double logarithmic plot; a-Paraffinic oil; b-Naphtenic oil and c-Rapeseed oil<sup>8</sup>

This V-T relationship is problematic for lubricant applications. At low temperature, a high viscosity induces a lot of viscous friction, resulting in energy loss. Conversely, at high temperature, a low viscosity, i.e. high fluidity, results in a lower lubricant thickness which may not be able to ensure its lubricating properties such as wear and friction reduction. In order to avoid this issue, viscosity modifiers are added in solution to give higher thickness to the oil at high temperature. Nevertheless, the thickening improvement should occur more at high temperature than at low temperature to avoid additional viscous friction. As a result, a viscosity modifier has to impact the V-T behavior of a base oil. <sup>3,10</sup>

There are several ways to evaluate the V-T relationship. The most common method in lubricants is to calculate the Viscosity Index (VI).<sup>3,6,10</sup> To do so, the kinematic viscosity of the sample oil is measured at 40 °C and 100 °C and the viscosity change is compared with an empirical reference scale.<sup>6</sup> The VI is defined by ASTM D2270<sup>26</sup> as equation (I-10)

$$VI = 100 \frac{(L-U)}{(L-H)} \quad (I-10)$$

with  $U$  the kinematic viscosity of the sample oil at 40 °C and  $L$  and  $H$  the viscosities of reference oils at 40 °C with VIs of 0 and 100, respectively, having the same viscosity as the sample oil at 100 °C.<sup>26</sup> This calculation is schematically plotted in Figure I-12. In general, larger VI means a smaller decrease of the viscosity with temperature. Currently, all the lubricant V-T behaviors are defined by their Viscosity Index.<sup>24</sup> Moreover, a viscosity modifier which is able to enhance the V-T behavior of a base oil is called a Viscosity Index improver (VII). Its efficiency is evaluated regarding to the increase of the base oil VI within the VII addition. <sup>6</sup>

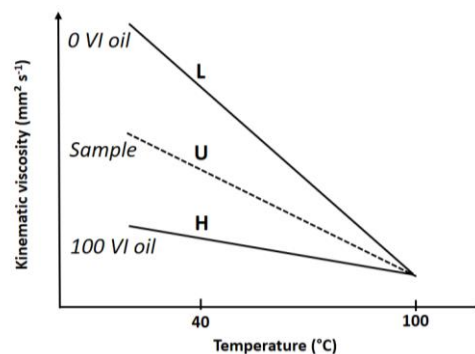


Figure I-12: Schematic illustration of VI calculation, double logarithmic plot<sup>6</sup>

As a result, VI is a useful tool to compare the V-T behavior of lubricants. It also allows evaluating the impact of a VM on the V-T behavior of a lubricant oil. Nevertheless, it has some drawbacks.<sup>104,105</sup> First, the  $L$  and  $H$  data are given at 100 °C for a kinematic viscosity from 2

$\text{mm}^2.\text{s}^{-1}$  up to  $70 \text{ mm}^2.\text{s}^{-1}$ .<sup>26</sup> But there are modern lubricants with viscosities below and above this data range.<sup>105</sup> Moreover, it has been observed that the lowest viscosity oil often has a lower VI than the higher viscosity oil, even if their V-T behaviors are the same.<sup>3,6,104</sup> VI is not only related to the V-T behavior but also to the whole oil viscosity. Other ways to evaluate the V-T behavior have been proposed, including the Dynamic Viscosity Index and the Proportional Viscosity Index.<sup>104,106</sup> These methods have not been widely adopted and will not be further detailed here.<sup>93</sup> VI is still the most used method to compare base oils and finished lubricant V-T relationship as well as VM efficiency. However, in order to have a complete overview of the VM efficiency, it is recommended to take into account both VI and the evolution of specific or relative viscosities as a function of the temperature.<sup>107,108</sup>

All the viscosity modifiers have a thickening effect when added in base oil. Conversely, only some kinds of VM will really affect the V-T behavior of a base oil. As a result, viscosity modifiers are separated into two categories: thickeners and Viscosity Index improvers.<sup>6,108</sup> Both are high molecular weight polymers but only VII have an impact on V-T behavior. This VII function is mainly related to the chemical structure and the architecture of the VII polymers.<sup>3,93</sup> Their mechanisms of action are not well understood nowadays and are still investigated.<sup>109,110</sup> They will be described more in details in the section 2.3. The  $Q$  value, defined according to equation (I-11) can be used to distinguish Viscosity Index improvers from thickeners.<sup>93,107,108</sup>

$$Q = \frac{\eta_{sp\ 100\ ^\circ C}}{\eta_{sp\ 40\ ^\circ C}} \quad (\text{I-11})$$

where  $\eta_{sp\ 40\ ^\circ C}$  and  $\eta_{sp\ 100\ ^\circ C}$  are the specific viscosities at  $40\ ^\circ\text{C}$  and  $100\ ^\circ\text{C}$ , respectively. Specifically,  $0 < Q < 1$  indicates the thickening power of the VM is less significant at high temperature. As a result, the viscosity modifier is a thickener. Conversely,  $Q > 1$  indicates the thickening power is more prominent at high temperature. The viscosity modifier is then a Viscosity Index improver and has a positive effect on the oil V-T behavior.<sup>107,111</sup>

### **2.1.3. Shear stability**

In most of the lubricant applications, the formulated oils sustain extreme shear forces during their use. Shear stress can cause a degradation of these molecules such as VMs thereby leading to a viscosity loss.<sup>92</sup> This results in a temporary or permanent decrease in viscosity,

often called shear thinning. The shear stability is the resistance of a polymer solution to thinning. It is the third and last key feature required for efficient VM. <sup>3,93,112</sup>

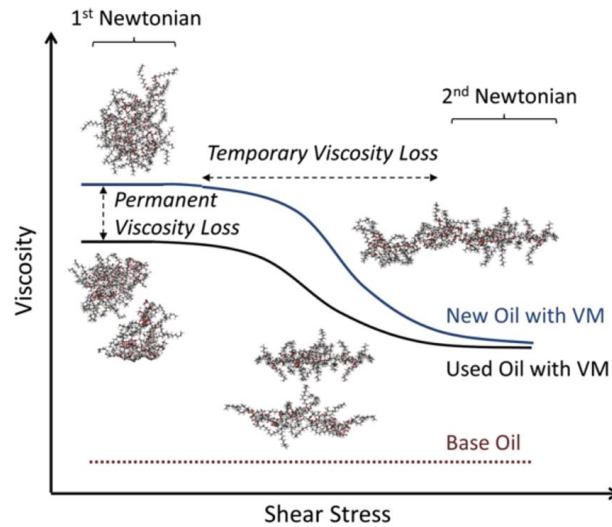


Figure I-13: Illustration of temporary and permanent viscosity loss. The insets show the corresponding elongation and scission of a model PAMA molecule obtained from a molecular simulation.<sup>93</sup>

The shear-related viscosity loss in a finished lubricant can be temporary or permanent, as illustrated in Figure I-13. The shear stress induces conformational changes in the polymer, which lead to a temporary viscosity loss. When the shear rate decreases, the polymer returns to its initial conformation and the lubricant returns to its original viscosity value. Conversely, when the shear is too high, permanent viscosity loss occurs. It is due to polymer chain scission and it is non-reversible.<sup>3,112</sup>

The shear-induced viscosity loss upon VMs depends on numerous factors. That includes the polymeric nature of VMs<sup>113,114</sup>, their molecular weight<sup>115</sup> as well as their dispersity<sup>116</sup> and architecture<sup>117</sup>. Other factors such as the polarity of the base oil and the other additives included in the lubricant formulation have also an impact.<sup>118,119</sup> The most predominant factor in determining a polymer shear resistance is the molecular weight.<sup>115,116</sup> More precisely, chain scission of long polymer backbone will induce a higher viscosity loss than chain scission of shorter polymer backbone.<sup>6,93,112</sup> For this reason, comb and multibranched polymer architectures generally show higher shear stability than linear ones for the same  $M_w$ .<sup>117,120–122</sup> This suggests that smaller polymers maximize shear stability. Unfortunately, shorter polymers typically have less thickening efficiency. Consequently, one of the current challenges of VM research is to provide a maximum thickening efficiency polymer with a maximum shear stability.<sup>123</sup>

To conclude this section, viscosity modifiers have to display a good thickening efficiency in order to improve the base oil viscosity towards the desirable value at 100 °C. This thickening should occur at high temperature while the VM addition doesn't affect too much the oil viscosity at low temperature. This is the second function of VM, i.e. impact positively the oil V-T behavior. In that sense, it is important to distinguish thickeners from Viscosity Index improvers. Finally, viscosity modifiers must fulfil these two functions while maintaining a good shear stability. Consequently, VMs polymer have to be designed regarding to their molecular weight, nature and architecture. No current VM is able to deliver optimum performance in all the three areas. Consequently, the choice of a VM depends on which properties are the most important for a given application.

## 2.2. Chemistry of viscosity modifiers

A wide variety of polymers have been explored as viscosity modifiers, which are already well reviewed in literature.<sup>6,10,93</sup> The most commonly used ones are Olefin copolymers (OCP), poly(alkylmethacrylate)s (PAMAs) and Hydrogenated Styrene-Diene copolymers (HSD), as illustrated in Figure I-14 (1). In each family, several polymer topologies have been investigated, see Figure I-14 (2).

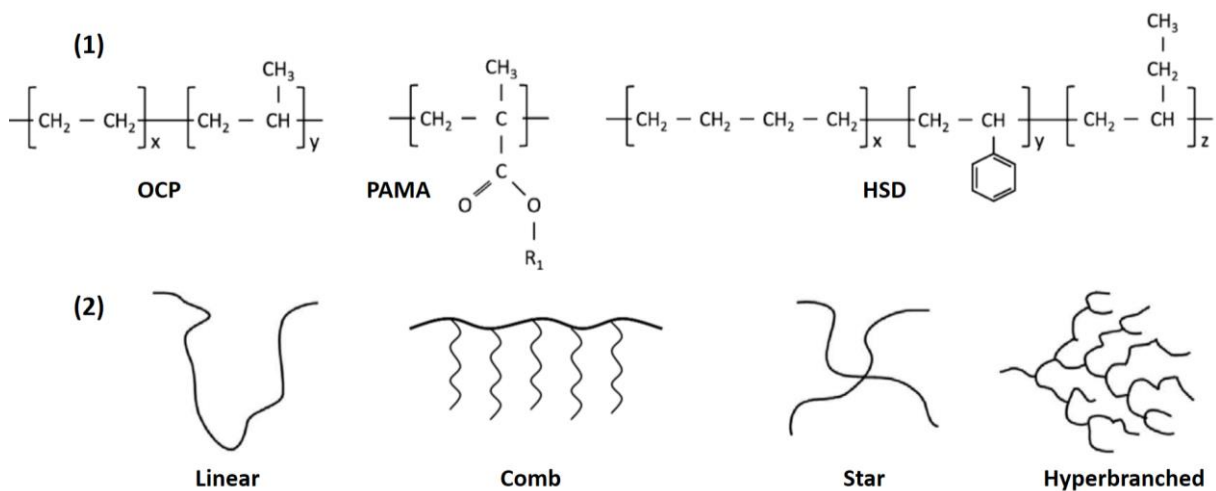


Figure I-14: (1) Most common types of viscosity modifiers and (2) viscosity modifiers architectures

### 2.2.1. Olefin copolymers (OCP)

Olefin copolymers, OCPs, are oil soluble viscosity modifiers. They are obtained by the copolymerization of ethylene, propylene and sometimes a non-conjugated diene as third monomer. Introduced as a viscosity modifier additive in the 1960's by Exxon, OCPs are

nowadays one of the largest classes of viscosity modifiers thanks to their low prices and high thickening properties.<sup>10</sup>

### Chemistry of conventional OCPs

The first commercially OCPs were synthesized via Ziegler-Natta polymerization.<sup>10,124</sup> OCPs can also be obtained using homogeneous metallocene catalyzed polymerization.<sup>125</sup> This chemistry permits a better control on composition and microstructure as well as the design of OCPs with narrow molecular weight distribution.<sup>126</sup> Olefins multiblock copolymers (OCBs) have been also developed using this methodology to be used as VM.<sup>127,128</sup> Other olefins like polymers can be obtained by anionic polymerization such as hydrogenated star shaped polymer.<sup>129,130</sup>

Nowadays, it exists a high variety of OCPs, the latter can be solid or viscous liquids depending on the ethylene/propylene ratio (E/P) and molecular weight. The usual E/P for OCP viscosity modifier is in the range 45/55 – 60/40. Below 55/45 ratio, the polymer is amorphous and flows at room temperature. Above, it is semi-crystalline in nature and remains solid at ambient conditions. More rarely, OCP viscosity modifiers in the range of E/P = 40/60 up to E/P = 10/90 have also been reported.<sup>131,132</sup> Non-conjugated dienes can be used as third monomer leading to the terpolymer Ethylene-Propylene-Diene Monomer (EPDM). They are incorporated in order to reduce the tackiness of the polymer for ease of manufacture and handling.<sup>10,133</sup> Finally, hyper branched and star-shaped polyethylene were also investigated as promising VM.<sup>120,123,130,134</sup>

### Properties and performance

Firstly, the E/P ratio has an important influence on the polymer properties. The OCP thickening efficiency increases with the increase of ethylene content, see Figure I-15 (1). Nevertheless, when the ratio of ethylene is too high, the copolymer is crystalline and losses its solubility in base oil.<sup>6,10</sup> Indeed, Rubin *et al.*<sup>135</sup> demonstrated that intrinsic viscosity of semicrystalline OCPs undergo a dramatically drop under  $T = 10\text{ }^{\circ}\text{C}$ , leading to a loss of solubility, see Figure I-15 (2).<sup>99,135,136</sup> In addition, the ethylene content can interact with oil waxes at low temperature and decrease the oil pour point.<sup>10,124</sup> Conversely, the increase of the propylene ratio decreases

the OCP oxidative stability. This is due to the presence of a labile tertiary proton in the propylene monomer unit.<sup>10</sup>

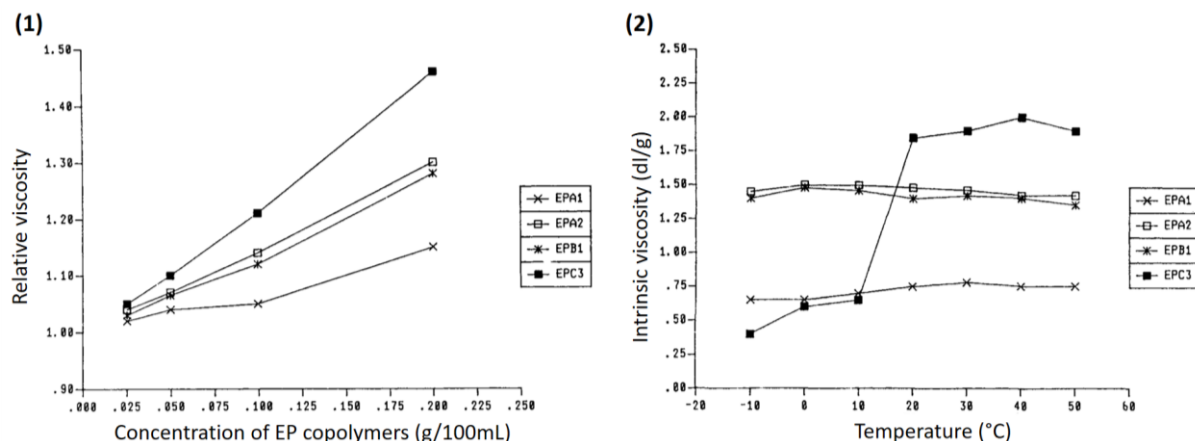


Figure I-15: (1) Relative viscosity versus polymer concentration and (2) Intrinsic viscosity versus temperature of EP copolymers in mineral oil. With EPA1 60/40 E/P  $M_w = 148 \text{ kg}\cdot\text{mol}^{-1}$ ; EPA2 58/42 E/P,  $M_w = 251 \text{ kg}\cdot\text{mol}^{-1}$ ; EPB1 70/30 E/P,  $M_w = 192 \text{ kg}\cdot\text{mol}^{-1}$ ; EPC3 80/20 E/P,  $M_w = 321 \text{ kg}\cdot\text{mol}^{-1}$ ,  $T_m = 43 \text{ }^\circ\text{C}$ .<sup>135</sup>

The monomer distribution has also an impact on OCP properties. For instance, block olefin copolymers show an improved thickening efficiency while the large sequences or ethylene block result in microcrystalline regions with undesirable low temperature properties.<sup>93,137</sup> As already mentioned, OCP with increase  $M_w$  leads to a better thickening efficiency but a decrease of shear stability.<sup>10,124,138</sup> Finally, EPDM presents lower thickening efficiency than a E/P copolymer of similar  $M_w$ , although low levels of vinyl norbornene or norbornadiene are claimed to improve low temperature properties such as shear stability without loss in thickening efficiency.<sup>139</sup>

Finally, the OCP topology strongly affects their performance as viscosity modifiers. For instance, Ye *et al.*<sup>120,123,134</sup> showed that hyperbranched polyethylenes are considerably more resistant to shear stress than the linear homologous with similar  $M_w$  while the thickening efficiency is reduced because of their compact structure. It has been shown that the intrinsic viscosity of EP star polymers depends only on the arm length but not on the number of arms.<sup>130,140</sup> Moreover, Cosimbescu *et al.*<sup>141</sup> showed that highly branched polyethylene could also reduce the friction coefficient in lubrication.

Overall, with a good compromise in E/P ratio, OCPs are good cost effective viscosity modifiers. Their excellent thickening properties lead to use them as thickeners. Moreover, they do not show a significant effect on the V-T behavior of base oils. They are mainly used in engine oil

application. For applications with higher shear stability required, highly branched polyethylene could be promising VM.

### 2.2.2. Poly(alkyl methacrylate)s (PAMAs)

Poly(alkyl methacrylate)s are used as viscosity modifiers in numerous lubricant formulations. Compare to OCP, they exhibit less thickening efficiency for similar molecular weight but have particularly good V-T behavior in solution. Moreover, PAMAs can also be highly efficient pour point depressant for lube oil, which will be mentioned in PPD section. In this part, the PAMA chemistry and synthesis will be discussed as well as their VM properties.

#### PAMAs chemistry

Typically, poly(alkylmethacrylate)s are obtained combining alkyl methacrylate monomers with different chain lengths which are mixed together and polymerized using Free Radical Polymerization (FRP). Since the reactivity ratios of alkyl methacrylates are quite similar, random copolymers are easily obtained as illustrated in Figure I-16.<sup>6,10</sup> In most cases, the molecular weight is controlled by chain transfer agents. Commercial products have  $M_w$  from  $20 \text{ kg}\cdot\text{mol}^{-1}$  up to  $750 \text{ kg}\cdot\text{mol}^{-1}$ .<sup>10</sup>

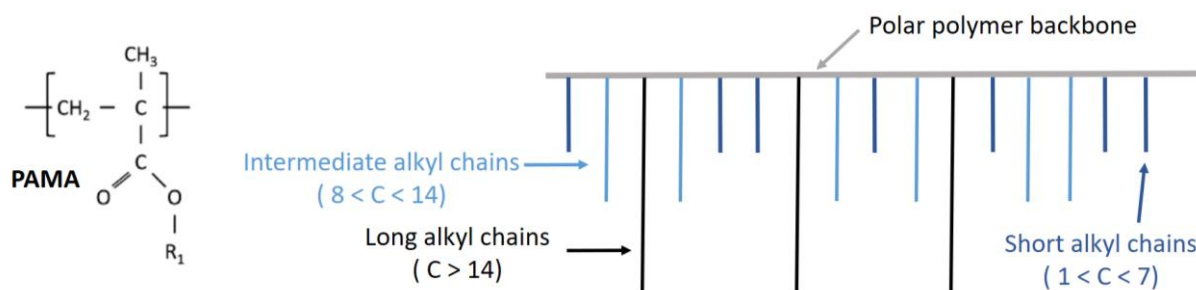


Figure I-16 : Schematic representation of PAMA structures with various side alkyl chain lengths

Nowadays, PAMAs polymer architecture is actively investigated. Block, comb, branched, star-shaped structures and narrow dispersity poly(alkylmethacrylate)s were obtained *via* controlled radical polymerization (CRP), such as atom transfer radical polymerization (ATRP) or nitroxide-mediated polymerization (NMP).<sup>122,142–145</sup> PAMAs with polar monomers in block or polar/apolar branched structures were also prepared by ATRP.<sup>146–149</sup>

PAMAs properties and performances

PAMAs thickening efficiency is mainly monitored by their coil size in solution.<sup>150</sup> Short alkyl side chains, i.e. with less than 7 carbons, enhance PAMA coil size and thus thickening efficiency while intermediate alkyl side chains ( $8 < C < 14$ ) ensure solubility in oil.<sup>3</sup> Long alkyl side chains ( $C > 14$  carbons) are also well soluble in oil but are added in order to interact with oil wax at low temperature and thus provide PPD properties.<sup>6,10</sup> Alike OCPs, the highest their  $M_w$ , the highest the thickening efficiency.<sup>3,10</sup> It is claimed that PAMAs are effective as Viscosity Index improvers because they contribute more in viscosity at high temperature than at low temperature.<sup>10,90,93,109</sup> This is mainly explained by PAMAs chemical composition of relatively polar backbone and a mixture of oil-immiscible/miscible side-chain moieties.<sup>146,151</sup> As a lot of polymers, they are susceptible to mechanical shear, especially for high molecular weight PAMAs.<sup>10,90,152</sup>

New developments in PAMAs architecture allow enhancing their properties. A narrow molecular weight distribution improves the thickening efficiency/shear stability balance.<sup>143</sup> Star shaped poly(alkylmethacrylate)s ensure excellent shear stability while maintaining high VI contribution.<sup>144,147,148</sup> As well as block PAMAs with polar moieties, they also effectively reduce the lubricant friction coefficient and enhance thin film formation properties<sup>117,146–149</sup> Recently, Nicolay *et al.*<sup>153,154</sup> with Total corporation developed innovative viscosity modifiers based on dynamic covalent chemistry (DCC). First, acrylate monomers were functionalized with a diol moiety in the one hand and boronic ester in the other hand. Functionalized monomers were then copolymerized with long chain acrylates using FRP or CRP.

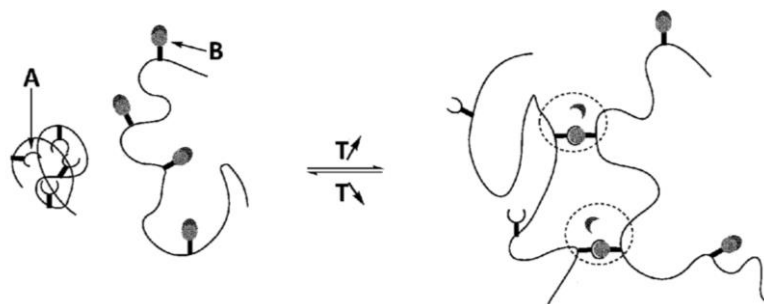


Figure I-17: Thermoreversible association of a statistical copolymer having diol function (A) with a statistical copolymer having boronic ester functions (B) via a transesterification reaction<sup>154</sup>

As illustrated in Figure I-17, the diol functionalized copolymer is then able to associate with the boronic ester functionalized copolymer with the temperature. In solution, this association leads to an increase of the viscosity at high temperature while the viscosity at low temperature

is less impacted. Consequently, when added in oil, additives enhance considerably the base oil V-T behavior. Moreover, as the polymer association is based on DCC, systems present high shear stability.

Overall, poly(alkylmethacrylate)s are chemically inert and exhibit good oxidation and thermostability. However, some depolymerisation can occur when the temperature reaches 235 °C.<sup>10,93</sup> The combination of good chemical properties with thickening efficiency and particularly good V-T behavior explain their extensive use as VII in widespread applications, such as automotive engine oils, hydraulic fluids and industrial oils.<sup>4,10</sup>

### **2.2.3. Hydrogenated Styrene-Diene (HSD) copolymers**

Hydrogenated Styrene-Diene copolymers are typically made using alkenyl aromatics, e.g. styrene and conjugated diene monomers, e.g. isoprene and butadiene.<sup>6,69,93</sup> Anionic polymerization offers the best route to make different architectures, such as random, block or star-shaped polymers.<sup>155–158</sup> Typical  $M_w$  are in the range of 75 – 200 kg.mol<sup>-1</sup> with  $\bar{D} < 1.5$ .<sup>6</sup> The final product is obtained by hydrogenation of the diene-derived unsaturation whilst the styrene is not affected.<sup>159,160</sup>

The basic HSD is a random copolymer of styrene and butadiene with styrene/ butadiene (S/B) ratio from 50/50 up to 60/40.<sup>6,161</sup> Styrene monomer improved the thermal, oxidative and shear stability but is oil insoluble. Consequently, the solubility of HSD depends on the content of diene units. It appears that the highest thickening efficiency is obtained with 1,4 butadiene units. However, to prevent 1,4 butadiene unit crystallization, 30-40% of 1,2 butadiene units are incorporated in the composition in order to obtain a fully amorphous polymer with good low temperature properties.<sup>6,93</sup>

Diblocks A-B and triblocks A-B-A HSD are also used commercially, where A represents polyisoprene and B polystyrene.<sup>10,155,162</sup> Typically, the styrene block has  $M_w$  of 10 – 50 kg.mol<sup>-1</sup> while the isoprene blocks are in the range of 50 – 100 kg.mol<sup>-1</sup>.<sup>6,163</sup> Since the polystyrene block is insoluble in base oil, the block copolymer functions as associative thickener which can impact the oil V-T behavior.<sup>164</sup> This mechanism will be detailed further. As illustrated in Figure I-18, through this association mechanism, the concentration impacts strongly the thickening efficiency of the HSD block copolymers.<sup>165,166</sup>

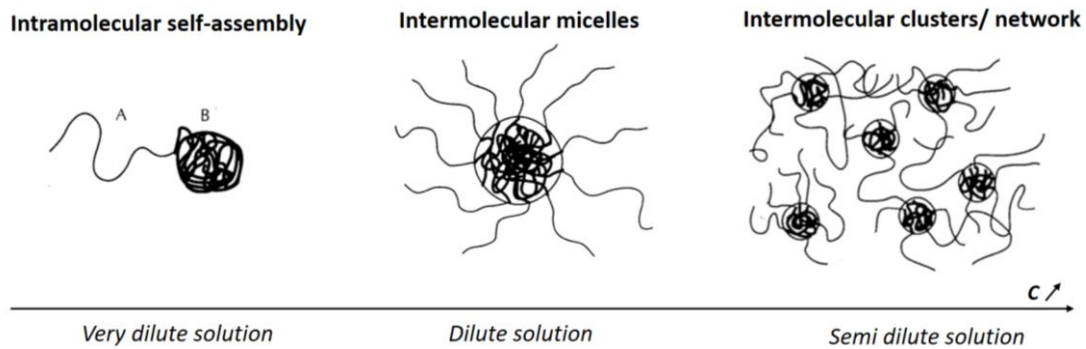


Figure I-18 : Association conformation of an associative block copolymer in selective solvent as a function of the concentration

For instance, Coutinho and coll.<sup>167</sup> studied the thickening effect of a EPDM and a HSD copolymer against the concentration in a mineral oil. For concentration  $C \leq 1$  wt.%, EPDM has a higher thickening efficiency (TE) than HSD copolymer. For  $C > 3$  wt.%, TE of HSD was superior to EPDM one. It was assumed that OCP chains act as dispersed coil while HSD ones are aggregated at low concentration. With concentration above the  $C^*$ , HSD behaves alike an associated network, leading to a dramatic increase of the oil viscosity. The same behavior was observed by Paula and coll.<sup>164</sup> At high concentration, the authors considered the formation of a loose network due to the styrene blocks. Consequently, block HSD copolymers are alike to self-assemble in solution.<sup>168,169</sup>

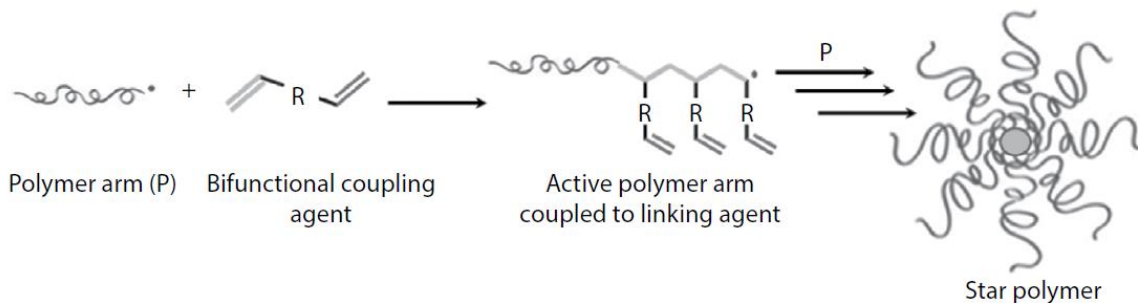


Figure I-18: Formation of a star copolymer using difunctional coupling agent<sup>10</sup>

Highly branched block copolymers or star shaped copolymers are as effective as block copolymers as Viscosity Index improvers.<sup>6,10,157,170,171</sup> The arms can be either random or block copolymers. As illustrated in Figure I-19, to prepare the star-shaped copolymer, a linear polymer chain is firstly synthesized and then coupled with a polyfunctional core such as divinylbenzene or polyisocyanates. The number of arms is controlled by the amount and type of the polyfunctional linking compound. It varies typically in the 10-20 range.<sup>6,10,129,157</sup> Star polymers are more compact in solution, thus they present lower thickening efficiency than linear HSD copolymers.<sup>172,173</sup> Nevertheless, their shear stability is much higher than their linear homologous.<sup>10</sup>

#### **2.2.4. PAMA-OCPs comb copolymers**

OCPs and PAMAs represent the two of the three largest types of viscosity modifiers. Recently, another new polymer architecture of interest has been developed: comb polymers with polyolefin and PAMAs segments. It was reported that blends of PAMAs with OCPs can provide intermediate properties to the individual ones or even synergistic effect.<sup>10,93,174,175</sup> For instance, OCP provides efficient thickening while PAMA imparts high VI. However, OCP/PAMA mixture is found to be immiscible.<sup>174</sup> This problem can be overcome by the use of a graft polymer of PAMA to OCP, as compatibilizer.<sup>176</sup> Then, comb polymers were added as themselves in base oil and appeared as promising viscosity modifiers.<sup>93,94,110</sup>

Takigawa *et al.*<sup>177</sup> developed random grafted copolymers by grafting a methacrylate moiety onto olefinic copolymer using FRP. The same group also developed block copolymers using anionic polymerization.<sup>177</sup> Eisenberg *et al.*<sup>94,176,178–180</sup> developed large varieties of comb polymers based on a PAMA backbone and polyolefin side chains with  $M_w$  in the range 1 to 10  $\text{kg}\cdot\text{mol}^{-1}$ . Conversely, Hillmyer *et al.*<sup>110</sup> synthesized comb polymers with an olefinic backbone obtained by ROMP and PAMAs side chains grafted by ATRP.

Eisenberg *et al.*<sup>94</sup> compared comb PAMA-OCPs with conventional PAMAs. It appears that the use of comb polymers results in Viscosity Index about 220 – 310 while VI of 140 - 160 were obtained with conventional PAMAs. Shear stability was also better for PAMA-OCPs than PAMAs due to the long comb structure.<sup>94</sup> Takigawa<sup>177</sup> observed the same improvement of the V-T behavior with his comb systems. Hillmyer *et al.*<sup>110</sup> also observed that the presence of side chains favorably impacts the performance of graft copolymers as VM, both in terms of thickening efficiency than V-T behavior.<sup>110</sup> Finally, it has been shown that PAMA-OCPs comb polymers as VM also allow reducing fuel consumption as well as internal friction reducing and anti-wear effect.<sup>178–180</sup>

#### **2.2.5. Other polymers**

##### **Polyisobutene PIB**

Polyisobutene was one of the first polymer used as viscosity modifiers.<sup>6,181,182</sup> It is made from a mixture of butene isomers, mainly isobutylene and is synthesized through a Lewis acid-

catalyzed polymerization. In the past, PIBs were widely used in lubricants due to properties such as high thickening efficiency, low toxicity and low deposit.<sup>3,183</sup> However, their popularity decreased due to poor oxidative and mechanical stability. Nowadays, some PIBs are still used in two-stroke engines, gear oils and hydraulic fluids.<sup>3,93</sup>

### Styrene based copolymers

Styrene ester polymers, with molecular weights in the range of 350 – 700 kg.mol<sup>-1</sup>, were developed as VM.<sup>3,6,184</sup> Styrene-ester polymers have lower thickening efficiency than typical OCPs and PAMAs.<sup>3</sup> Nowadays, styrene-ester polymers are used exclusively in automatic transmission fluids and tractor fluids but are replaced progressively by PAMAs additives.<sup>6</sup>

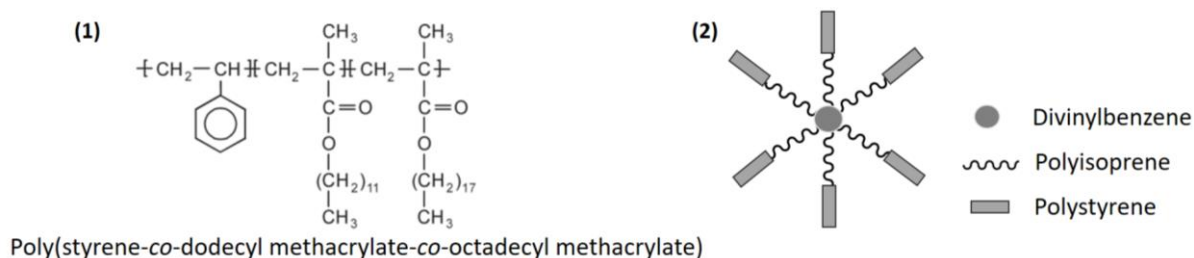


Figure I-19: (1) Example of a PS-PAMA copolymer<sup>185</sup> and (2) Star-shaped polystyrene-b-poly(ethylene-co-propylene)<sup>186</sup>

Jarrin and coll.<sup>185</sup> developed random copolymers containing 10 to 35% of styrene and 65 to 90% of acrylate moieties with different side chain lengths. A good compromise between various properties required for VM such as thickening efficiency and shear stability was observed for these compositions. Terpolymers of styrene / dodecyl methacrylate / octadecyl methacrylate were also evaluated as VI improvers, see Figure I-20 (1).<sup>187,188</sup> Good thickening efficiency and V-T behavior are provided by acrylates while styrene enhances shear and thermal stability. However, the VI and solubility decrease by increasing the styrene content. Finally, Wang and coll.<sup>186</sup> developed star-shaped PS-OCP block copolymers as illustrated in Figure I-20 (2) and observed an increase of the thermal decomposition of 50 °C compared to star shape OCPs, independently of the arm length or the degree of branching.

### Polyesters

Polyesters have been barely described in literature as viscosity modifiers. Oil-soluble polyesters were first developed as dispersants<sup>189</sup> then functionalized with sulfur and used as antiwear agents.<sup>190</sup> Rare examples of polyesters as VMs were obtained by polycondensation

of a dicarboxylic acid and a diol.<sup>191,192</sup> The prepared polyesters have good shear stability and VI improving.<sup>192</sup> Recently, Cosimbescu *et al.*<sup>193,194</sup> prepared hyperbranched aryl polyester containing aromatic core and long aliphatic arms to provide lipophilicity in apolar base oil, as illustrated in Figure I-21. These polyester additives demonstrated an improved VI and reduced friction coefficient. The authors<sup>195</sup> also developed a derivatization of this system, from comb to hyperbranched polyesters with functionalization of the side chains or arms chain ends with alkyl methacrylates, for instance.

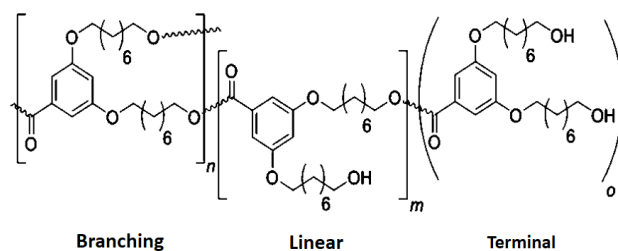


Figure I-20: Schematic illustration of hyper branched aryl polyester<sup>193</sup>

To conclude this section, many polymer chemistries and topologies have been investigated to design performant viscosity modifiers in terms of thickening efficiency, impact on V-T behavior and shear stability. Investigations were also performed in order to understand how VM impact oil viscosity.

### 2.3. Viscosity Index improver impact on oil V-T behavior

As it has been already mentioned in the previous sections, the thickening effect of VM on base oil viscosity is related to many features such as molecular weight, polymer architecture and chemistry.<sup>196</sup> Viscosity modifier can also affect oil viscosity by other means through interactions between polymer chains and between polymer chains and oil molecules.<sup>197</sup> While thickening effects are well understood using polymer in solution theories, the Viscosity Index improver mechanism remain unclear. Surprisingly, there are only scattered fundamental studies that report on the impact of VI improvers on oil V-T behavior. Still, some mechanisms have been proposed such as coil expansion or association/aggregation. Some other secondary mechanisms have been also described.<sup>93,109,148</sup>

### 2.3.1. Coil expansion of the polymer chain

The most widely reported mechanism of how polymers affect the oil V-T relationship is the coil expansion. First introduced by Selby<sup>92</sup> in 1958, it describes the inherent property of a polymer molecule in solution to expand with temperature and thus increase the viscosity. This concept is illustrated in Figure I-22.

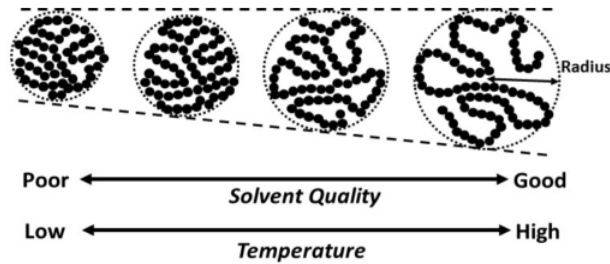


Figure I-21: Illustration of the coil expansion mechanism: a polymer coil expands as temperature and solvent quality increases<sup>109</sup>

Selby's mechanism refers to the work by Flory who stated that the radius of gyration,  $R_g$ , of polymer chains depend on their interactions with the solvent molecules.<sup>95</sup> Basically, in poor solvent, the attractive interactions between the polymer chains are prominent. As a result, the polymer chains collapse into compact polymer globules. Conversely, in a good solvent, the solvent-polymer chain segment interactions dominate resulting on a random polymer coil. Generally, the solvent becomes more effective by increasing the temperature. Then, an increase of the temperature can induce a globule-to-random coil transition due to the solvent quality increase.<sup>92,93,109</sup>

In dilute solution, the polymer coil size is directly related to its intrinsic viscosity in solution. It is then possible to evaluate the coil expansion by following  $[\eta]$  as a function of the temperature. The coil size can also be measured using direct experimental techniques such as dynamic or static light scattering (DLS and SLS) and small angle neutron scattering (SANS).<sup>93,109</sup>

Some studies reported in literature compared the behavior in solution of usual commercial viscosity modifiers such as OCP, PAMAs and HSD copolymers. For instance, Müller<sup>107</sup> investigated the behavior of four types of viscosity modifiers in mineral oil regarding to the temperature. The data show that intrinsic viscosity decreases by increasing the temperature in the case of OCP, HSD and styrene-ethylene-propylene copolymer. When added at 2 wt.% in mineral oil, Q values of 0.78, 0.85 and 0.85 were obtained, respectively. On the other hand, mineral oil containing PAMA show a  $[\eta]$  increase with temperature (Q = 1.35 at 2 wt.%). Gao

*et al.*<sup>198</sup> investigated dilute polymer solution of OCP, HSD and PAMAs in Group II base oil. Based on intrinsic viscosity data illustrated in Figure I-23, it was concluded that OCP and HSD random copolymer coil size remain constant independently of the temperature while PAMAs expand with the temperature.

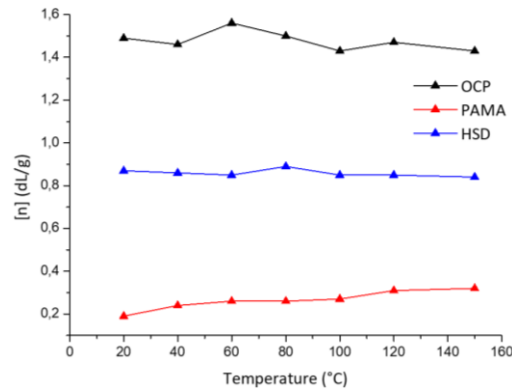


Figure I-22: Intrinsic viscosity as a function of the temperature for OCP, PAMA and HSD polymers in mineral oil (adapted from Gao *et al.*<sup>198</sup> paper)

Rubin *et al.*<sup>135</sup> studied the intrinsic viscosity of five different OCP polymers in methylcyclohexane. It appeared that their hydrodynamic volumes, calculated from  $[\eta]$ , decreased by about 15% - 20% with increasing temperature between -10 °C and 50 °C. Vergne *et al.*<sup>108,151</sup> performed a rheological study of mineral base oils blended with an OCP, a PAMA and a star-shaped HSD polymer, i.e. a poly(isoprene-styrene) hydrogenated (PISH), under high pressure in a range of temperature from 40 °C to 150 °C. As illustrated in Figure I-24, PAMAs coil size increases with temperature while OCP and HSD coil sizes remain stable whatever the temperature.

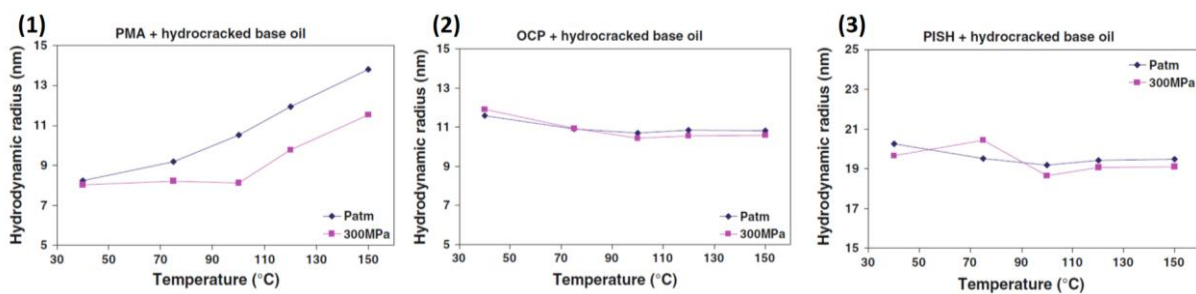


Figure I-23: Hydrodynamic radius as a function of the temperature of (1)PMA, (2)OCP and (3)PISH, i.e. HSD polymers blended at 1.2 wt.% in a mineral base oil<sup>151</sup>

Recently, Covitch *et al.*<sup>109</sup> evaluated OCP and PAMAs viscosity modifiers behavior in dilute solution with temperature. Intrinsic viscosity was determined in mineral oil and radius of gyration,  $R_g$ , were measured in dodecane by SANS. As illustrated in Figure I-25, PAMAs show a coil expansion with  $[\eta]$  and  $R_g$  increase while OCP  $[\eta]$  and  $R_g$  decrease between 40°C and 100

°C. It was also observed that the highest the percentage of methacrylate short and insoluble side alkyl chains, the largest the coil expansion.

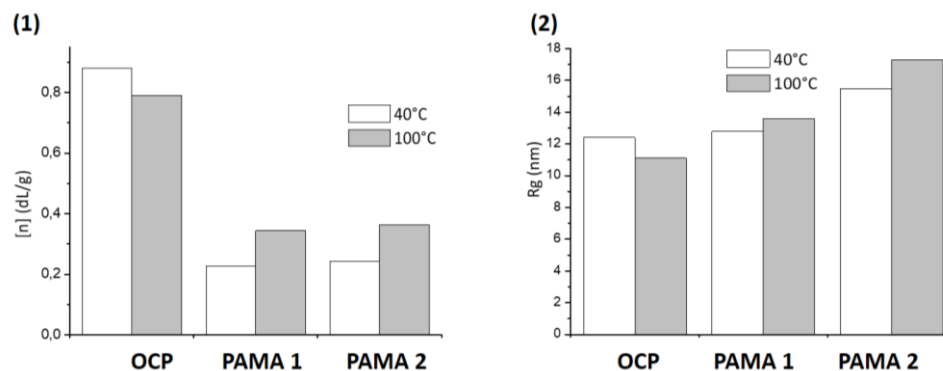


Figure I-24: (1) Intrinsic viscosity and (2) Radius of gyration of OCP, PAMA 1 and PAMA 2 in mineral oil and dodecane, respectively. PAMA 1 is a copolymer of C12-C18 alkylmethacrylate monomers and PAMA 2 is a copolymer of methylmethacrylate and C12-C15 alkylmethacrylate (adapted from Covitch et al. paper<sup>109</sup>)

Martini *et al.*<sup>199</sup> used MD simulations to predict that PAMA will increase in size with temperature while OCP will not. All these studies converge to confirm that only PAMA viscosity modifiers seem to impact the mineral oil V-T behavior by coil expansion mechanism.

### 2.3.2. Interaction between polymer chains: aggregation - disaggregation

It is well-known that some polymer chains with attracting groups can associate through the formation of intra and intermolecular physical bonds. They are called associative polymers.<sup>200</sup> This class includes charged polymers (ionomers, polyelectrolytes and polyampholites), polymers with hydrogen bonding and block/grafted copolymers in selective solvent.<sup>200–202</sup> Block or grafted copolymers of AB or ABA types in dilute solution may phase separate.<sup>169,203</sup> In selective solvent, i.e. a good solvent for block A and poor for block B, copolymer usually self-assembled as micellar aggregates.<sup>204,205</sup> The occurrence of association depends on the polymer nature, the block size, concentration, temperature and solvent quality.<sup>10,169,200,203</sup> This behavior was observed for some viscosity modifiers and largely described for block styrene-diene copolymers (HSD) in hydrocarbon solvents such as decane, dodecane or mineral base oil.<sup>6,10,201</sup> Polydiene block ensures the polymer solubility in solvent while insoluble polystyrene blocks associate and self-assemble, forming the core of the micelle.<sup>200,203,206</sup>

The polymer association is strongly related to the temperature. As illustrated in Figure I-26, at low temperature, insoluble part of the copolymer formed micelles but by increasing the

temperature, the blocks dissociate and the structures disaggregate.<sup>169,200,206</sup> It is called the association-dissociation process.

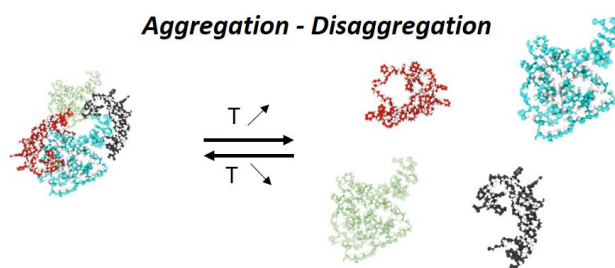


Figure I-25: Schematic representation of the aggregation - disaggregation behavior

Studies were performed on model solvents such as decane or docecane and less in lubricant base oils. Price and Woods<sup>207</sup> studied dilute solutions of block and grafted copoly(styrene-isoprene) in decane. As illustrated in Figure I-27, the copolymer hydrodynamic radius decreases while the intrinsic viscosity increases with the temperature increase. Authors interpreted this behavior as an aggregation – disaggregation behavior. The intrinsic viscosity is determined by extrapolation of viscosities values considering that concentration tends to zero, well below the critical aggregation concentration. As a result, the intrinsic viscosity describes the behavior of a single chain in solution. Conversely, the  $R_H$  correspond to the size of the global object observed by DLS. As a result, by increasing the temperature, the polymer solubility increases and a single chain expands naturally following the Selby coil expansion despite its aggregation with other chains and its intrinsic viscosity increase. Consequently, the aggregate progressively disaggregates leading to a global decrease of the  $R_H$ . This behavior is enhanced by increasing the percentage of polystyrene part in the HSD composition.

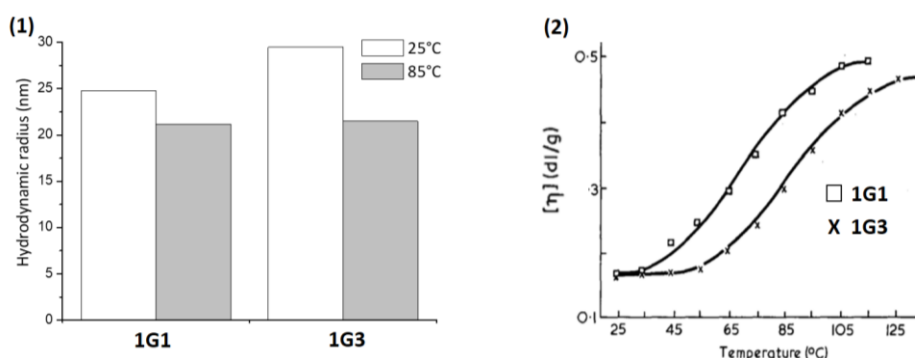


Figure I-26: (1) Hydrodynamic radius and (1) intrinsic viscosity as a function of the temperature for two grafted HSD copolymers in decane : 1G1 with 29 wt.% of PS and  $M_n = 550 \text{ kg.mol}^{-1}$  and 1G3 with 38 wt.% of PS and  $M_n = 550 \text{ kg.mol}^{-1}$ .<sup>206</sup>

Mandema and coll.<sup>203,208</sup> evaluated the behavior of a hydrogenated poly(styrene-isoprene) in decane. The existence of large aggregates at 25 °C which dissociate with the temperature was demonstrated. However, the intrinsic viscosity showed a gradual and continuous decrease with the temperature. The two copolymers tested, with both 38% of polystyrene block but different  $M_w$  showed similar behaviors. Lodge *et al.*<sup>209–211</sup> studied extensively the micelle conformation regarding on the temperature of poly(styrene-ethylene-propylene) in squalane. A dramatic increase of the solvent fraction in the micelle core was observed just below the critical micelle temperature. At higher temperature, a decrease of the  $R_H$  was observed, corresponding to the particle dissociation. Bezot and coll.<sup>212</sup> investigated the behavior of a Styrene-Hydrogenated Butadiene (HSB) polymer VM in different hydrocarbon solvents as a function of the temperature under dilute conditions. The polymer coil diameter ( $\phi$ ) in solution was obtained by DLS and confirmed by SLS. In cyclohexane, which is a good solvent for styrene block, the HSB coil diameter ( $\phi$ ) was below 25 nm corresponding to an isolated polymer in solution, irrespective of the temperature. Conversely, as illustrated in Figure I-28, in mineral oil, both  $\phi$  and Huggins coefficient  $k_H$  decrease while  $[\eta]$  increases with the temperature. The authors interpreted these results as a formation of HSB micelles in poor solvent such as mineral oil then dissociate with the temperature.

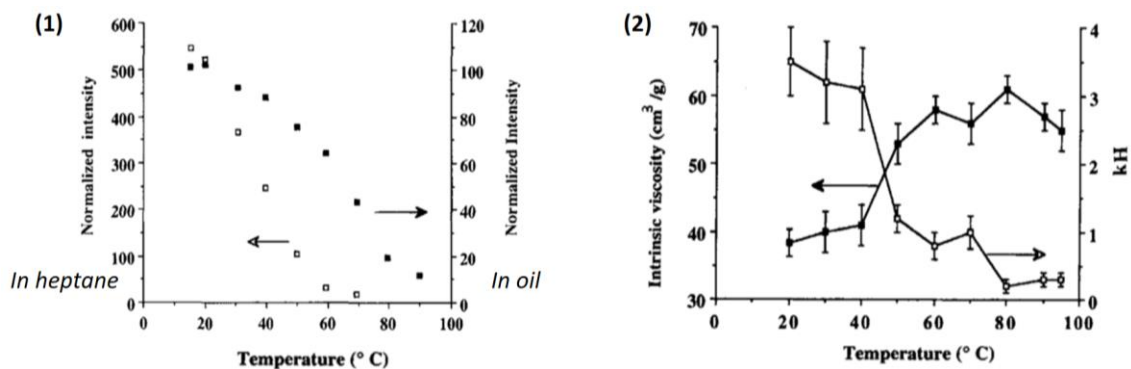


Figure I-27 : (1) Scattering intensity for SHB in heptane and mineral oil VS the temperature and (2) intrinsic viscosity and Huggins coefficient of HSB copolymer in mineral oil VS temperature<sup>212</sup>

This associative-dissociative behavior has been mainly observed for block HSD copolymers. Recently, Hillmyer *et al.*<sup>110</sup> synthesized polyolefin with grafted poly(alkyl methacrylate) side chains. Blended with a paraffinic base oil, this OCP-PAMA copolymer exhibits a positive impact on the oil V-T behavior. For the most promising copolymer, the  $[\eta]$  increased from 68 mL.g<sup>-1</sup> to 95 mL.g<sup>-1</sup> between 0 °C and 140 °C. Both  $R_H$  and  $R_g$  decreased with temperature, with a  $R_H$  drop of 40% between 40 °C and 100 °C for instance. The authors suggested that the copolymer chains may form aggregates at lower temperature due the low solubility of the methacrylate

side chains. The solubility of the side chain increases with the temperature, thus leading to disaggregation of the chain cluster into single chains, alike an association – dissociation mechanism leading to an increase of the solution viscosity with the temperature.

To conclude, the association – dissociation mechanism was described for some viscosity modifiers such as block HSD and more recently, grafted OCP-PAMAs copolymers. In most cases, an increase of the polymer intrinsic viscosity occurred similarly with the disaggregation of the particles with the temperature, impacting positively the oil V-T behavior. Such as coil expansion; this mechanism is related to the polymer solubility in oil.

### 2.3.3. Other secondary mechanisms through polymer-solvent interactions

The two previously discussed mechanisms are the most commonly cited in the VM literature. Still, polymers may also affect the oil V-T behavior through polymer-solvent interactions. It was proposed that polymers can increase viscosity indirectly, through their effect on nearby solvent molecules. This theory was proposed a long time ago by Rouse.<sup>213</sup> Specifically, the polymer may cause a disturbance to the velocity field through the force it exerts on the solvent, which should increase the viscosity.<sup>213,214</sup> To the best of our knowledge, this mechanism was barely investigated experimentally for viscosity modifiers systems. A recent modelling developed by Martini *et al.*<sup>215</sup> showed that PAO molecules close to polyisobutylene (PIB) may be less aligned with the flow direction than the solvent molecules further away from the PIB, contributing to PIB thickening efficiency.

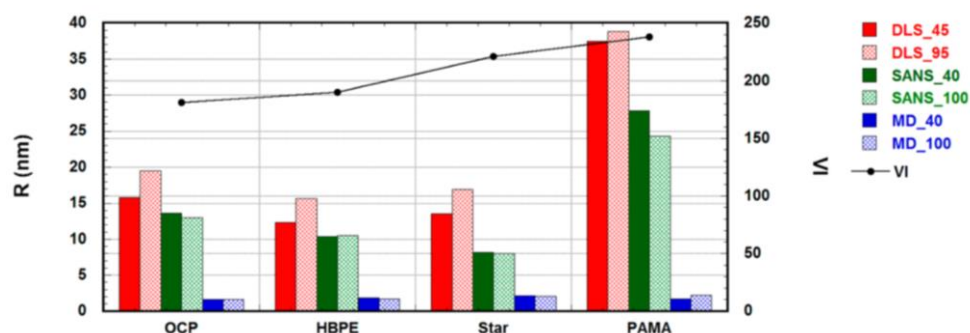


Figure I-28: Comparison between DLS  $R_H$ , SANS  $R_g$  and MD simulations  $R_g$  values for OCP, hyperbranched polyethylene (HBPE), star PAMA and PAMA viscosity modifiers<sup>197</sup>

Cosimbescu *et al.*<sup>197</sup> studied the correlations between size changes with temperature of lipophilic polymers in solution and Viscosity Index trends. As illustrated in Figure I-29,  $R_H$  values obtained by DLS measurement increased with the temperature. Conversely, the  $R_g$  values,

obtained by SANS decreased with the temperature for OCP and highly branched polyethylene (HBPE). The authors assume that changes in  $R_H$  may correspond to changes in solvent interactions, while changes in  $R_g$  may correspond to change in the polymer conformation itself. Therefore, an increase in  $R_H$  may correspond to an increase in solvent-polymer chain interactions, which leads to an increase of the viscosity in accordance with the VI increase observed.

Overall, both coil expansion for PAMAs and association-dissociation for block and grafted polymers seem to play a major role on the VM impact on oil V-T behavior. The polymer-solvent interaction can also act positively on oil V-T relationship.

## 2.4. Summary and outlook

A viscosity modifier function is to enhance oil viscosity at high temperature while limiting the viscosity increase at low temperature. As a result, VMs should have a high thickening efficiency and an impact on oil V-T behavior. The concentration, molecular weight and chemical structure of the polymer are crucial to ensure these requirements. As a lubricant is subject to high shear, VM should display a good shear stability. It has been shown here that the terminology to express VM performance is confusing, specifically about the Viscosity Index. It is still the most used tool to evaluate the V-T behavior of an oil. However, other features have to be investigated, such as relative or specific viscosities and Q value, to properly evaluate the VM impact on oil viscosity.

Many polymer structures and topologies have been investigated in order to design efficient viscosity modifiers such as OCPs, PAMAs and HSD copolymers. It appears that an efficient VM should have high molecular weight to ensure good thickening efficiency. Its structure should be designed to resist to high shear such as star polymer while keeping a good thickening efficiency, i.e. a high intrinsic viscosity in solution, such as OCPs linear polymers. Comb polymer such as PAMAs seems to be a good compromise between thickening efficiency and shear stability. The VM polymer composition is also an important feature. VM should be designed with polar backbone such as PAMAs to enhance oil V-T behavior by coil expansion. A polymer containing insoluble parts can also be an option, such as HSD and some grafted

OCP-PAMA copolymers which affect also positively the oil V-T behavior by aggregation-disaggregation mechanism.

The need for optimized VMs will continue to become more important as lubricants are asked to provide better performances under a wide range of operating conditions. It has been shown that viscosity modifiers could provide additional benefits as friction modifiers, dispersants and pour point depressants.<sup>6,93,149</sup> The development of multifunctional additive is also needed to limit the use and the drawback of additives as well as the possible opposite effects between them. Finally, due to the environmental concerns, viscosity modifiers have to be biodegradable and non-toxic as much as possible.

### 3. Pour point depressants

---

At low temperature, many lubricants become too viscous to flow easily or might even be gelled. As a result, the lubricant would not move through the system or machine requiring lubrication. The temperature at which an oil stops to pour is defined as Pour Point temperature. Pour point depressants (PPDs) are small or polymeric molecules added in lubricant base oils to improve the cold-flow properties or low temperature properties of the oil, i.e. to decrease the oil pour point. PPD are engineered for different lubricant applications such as automotive engine oils, gear oils, automatic transmission fluids and hydraulic fluids. In this section, the oil behavior at low temperature as well as the mechanism of PPD on oil will be described. Then, the most common PPDs used in lubricants will be reviewed.

#### 3.1. Pour point depressant function and mechanisms

##### 3.1.1. Low-temperature behavior of base oils

Some base oils such as mineral paraffinic oils and vegetable oils contain aliphatic chains. These species are recognized as waxy components and can crystallize under a certain temperature, i.e. cloud point (CP) or wax appearance temperature (WAT).<sup>10,216</sup> The wax tends to precipitate in oil as crystals which can trap a substantial amount of oil *via* association, thereby inhibiting the oil flow and dramatically increasing the oil viscosity as illustrated in Figure I-30. For this reason, Pour Point is closely linked to Cloud Point.<sup>3,217,218</sup> Most lubricant base oils are refined

in order to remove waxy compounds. However, the removal of the last traces of wax from oil is expensive and difficult. <sup>218,219</sup>

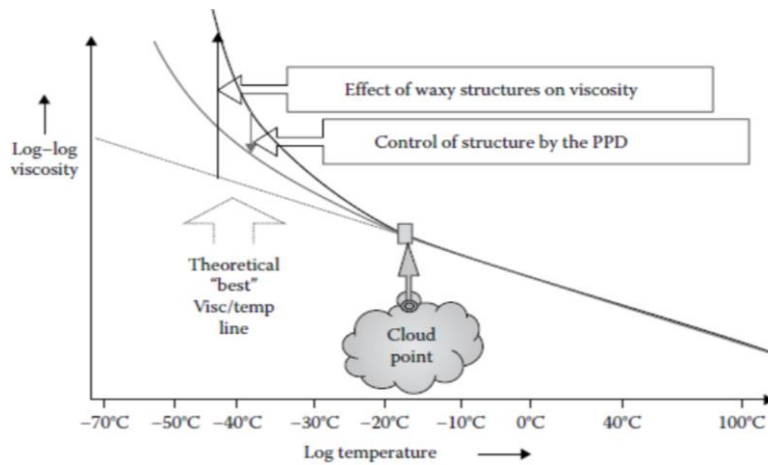


Figure I-29: Relation between temperature and oil viscosity<sup>10</sup>

As display in Figure I-30, transition is observed from a Newtonian behavior above the Cloud Point to a non-Newtonian behavior below CP. The latter is related to the wax crystallization process which can be divided in three stages: the nucleation, the growth and the agglomeration. In the first stage, nuclei appear due to super-saturation of paraffin waxes in the oil phase. Then the nuclei growth through an epitaxy mechanism leading to the formation of two-dimensional crystals (platelets) leading to needle-like structures, as illustrated in Figure I-31. Finally, during the agglomeration process, these structures form a gel network that traps the non-crystalline oil molecules, which impedes drastically the oil to flow. This process is known as gelation. The waxy molecules can also co-crystallize, without formation of a strongly organized network. These co-crystals have enough hydrodynamic volume to impede the oil flow and greatly increase the oil viscosity. <sup>10,216,220</sup>

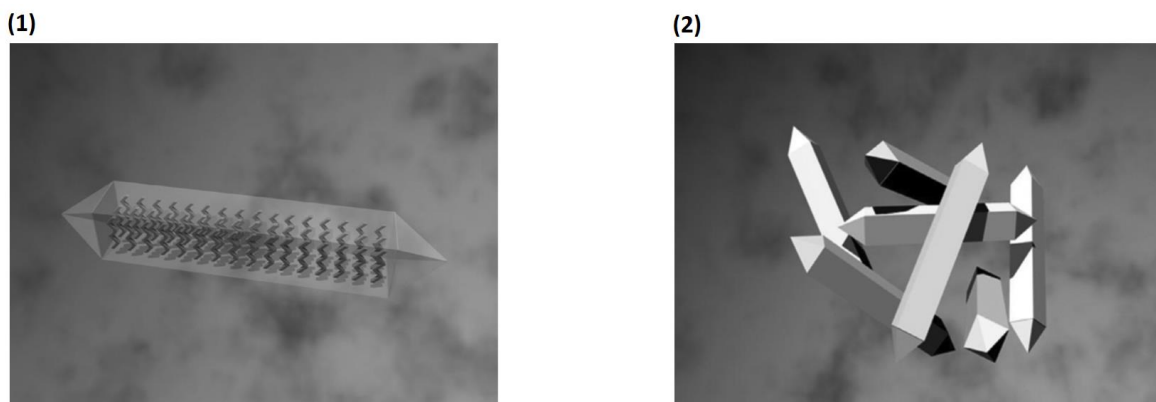


Figure I-30: Schematic view of wax crystallization in (1) Needle-like structure and (2) 3D gel network of needle-like structures<sup>10</sup>

It is important to note that the oil can stop to flow for another reason, unrelated to wax crystal formation. Indeed, all fluids become more viscous by decreasing the temperature. It can eventually reach a viscosity where the fluid cannot flow anymore. This temperature is called the Viscous Pour Point and cannot be changed or improved by PPD addition.<sup>10,216</sup>

The cloud point is defined as the temperature at which some of the waxy components start to crystallize and precipitate from solution, leading to a hazy appearance.<sup>10</sup> The visual evidence of the onset wax crystal can be tested using ASTM D2500.<sup>221</sup> However, in most cases, this transition is evaluated in terms of pour point.<sup>10,217</sup> It marks the temperature at which the rheological properties of oil sharply change from those of a liquid to those of a rigid semi-solid. The crystal growth in solution is strongly related to the cooling profile as well as to the shear rate. As the crystallization is a slow process, a fast cooling can affect the number of crystals formed and their relative size, distorting results.<sup>216,222,223</sup> In addition, a high shear rate can break crystal formation leading to a lower pour point than in real conditions. Numerous methods have been developed to evaluate pour point (ASTM D3829, D4684 and D5293 for instance) but the ASTM D97 is still the most used, despite a rapid and unrealistic cooling rate for wax crystal growth.<sup>10,90,217</sup> It is also possible to evaluate it by Differential Scattering Calorimetry (DSC) and rheology. Crystal growth can also be observed using microscopy, light scattering and X-ray diffraction (XRD).<sup>216,220,224,225</sup>

The crystallization behavior occurs in lubricating base oils but also in fuel or in crude oils. In the latter, the phenomenon is amplified due to the higher amount of wax compounds. It is particularly problematic during pipeline transport where paraffin precipitation leads to wax deposition, flow reduction and gel formation. To circumvent these issues, the use of PPD has been extensively studied in crude oils and less in lubricants. Still their behaviors remain the same in any type of oils.<sup>10,216,224,226–229</sup>

### ***3.1.2. PPD function and mechanisms of action***

Pour point depressant, i.e. wax crystal modifiers or wax crystallization inhibitors, are polymeric additives that have similar chemical structure to the wax that is crystallizing.<sup>216,217</sup> Their role is to interact with the wax crystal to decrease their growth and thus decrease their

impact on viscosity. Consequently, they are added to decrease the pour point and allow the oil to flow at lower temperature. Depending on the type of oil, pour point depression of up to 30 °C can be achieved by PPD addition, although a lowering of the pour point by approximately 10 – 17 °C is more common.<sup>4</sup> The mechanism of pour point depression is still not fully understood.<sup>216,219,230</sup> However, it has been shown that PPD can impede crystal growth by a combination of interactions between polymeric PPD and paraffin, that involve nucleation, adsorption, co-crystallization and solubility.<sup>216,226–228,231,232</sup>

At temperatures well above the cloud point, some PPD can self-assemble into micelle like aggregates exhibiting a crystalline core and soluble hairy brushes surrounding the core. This self-assembly creates a larger number of partially shielded nuclei which reduces the supersaturation and facilitates the formation of more abundant smaller wax crystals.<sup>216,226,232,233</sup>

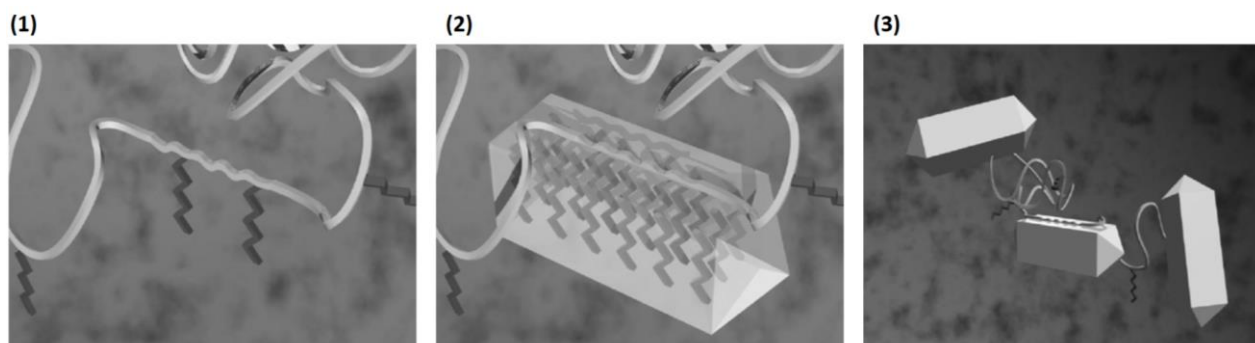


Figure I-31: (1) Schematic representation of a PPD, (2) PPD co-crystallization with a needle-like crystal structure and (3) PPD prevention of a gel network formation<sup>10</sup>

At temperatures near or below the cloud point, many PPD can co-crystallize with wax molecules or adsorb on the growing surface of wax crystals, see Figure I-32 (2). Due to their similar composition, i.e. most often long alkyl chains, PPD occupy the position of wax molecules on the crystal lattice. Meanwhile, it creates a steric hindrance on the crystal that can interfere the growth and aggregation of wax crystals. As illustrated in Figure I-32 (3), the PPD can interact favourably with wax crystals and dispersed them in the oil phase through steric hindrance and electrostatic repulsion avoiding agglomeration and decreasing the difficulty of the oil to flow and consequently the pour point.<sup>10,216,230,233,234</sup> It has been shown by means of microscopy or XRD that the PPD addition also induces a change in crystal morphology.<sup>216,235,236</sup> For instance, Yin *et al.*<sup>236</sup> observed a transition from orthorhombic to hexagonal lattice.

### 3.2. Main pour point depressant chemical structures

The first PPD developed were alkylated naphthalenes. Other small molecules are still used such as tetra paraffin phenol-based compounds. However, nowadays, polymeric PPD remain the most commercially viable option.<sup>6,10</sup> Most common pour point depressants present a polymeric comb structure with long alkyl side chains (> 12 carbons) and a polar portion. Polar moieties can be ester, vinyl acetate or maleic anhydride groups.<sup>10,216,226</sup> Semi-crystalline copolymers such as ethylene vinyl acetate copolymers (EVAs) and OCPs have been also developed.<sup>10,216,218</sup>

#### 3.2.1. Poly(alkylmethacrylate) comb polymers (PAMAs)

Poly(acrylate)s or poly(alkylmethacrylate)s were the first polymeric PPDs commercialized. Nowadays, they are the predominant polymeric family of PPDs. PAMAs are also largely used as viscosity modifiers; their chemistry has been detailed in the previous section. A schematic structure of a PAMA comb PPD is illustrated in Figure I-33.

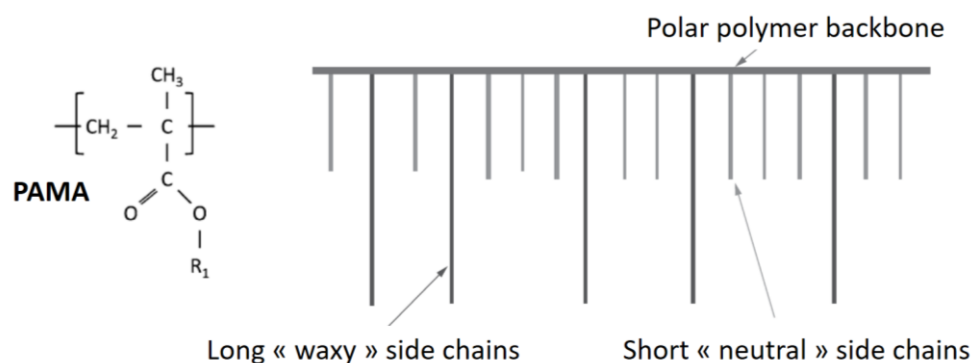


Figure I-32: Schematic illustration of a PAMA comb pour point depressant<sup>10</sup>

The PAMA side chains are usually a mixture of alkyl groups with a carbon range between 1 to 20. Consequently, some side chains are long enough (> 12 carbons) to co-crystallize at low temperature. The shorter side chains serve as inert diluent and spacers between long alkyl chains<sup>10,90,217,237,238</sup> Moreover, the composition of PAMAs have to be adapted to the base oil. The co-crystallization is enhanced when the PAMAs long waxy chains present a similar structure to the paraffin wax, leading to a higher pour point depression. It was shown that PAMAs with alkyl groups between 10 and 14 carbons are effective depressants for oils containing mainly short-chain paraffins. Conversely, PAMAs with long alkyl chains, i.e. between 16 and 20 carbons, are more adapted for oils with long paraffin chains.<sup>10,219,239</sup> For

instance, Nasser and coll.<sup>218</sup> showed that the PP depression was increased by increasing the alkyl chain length of acrylate based copolymers, see Figure I-34 (1).

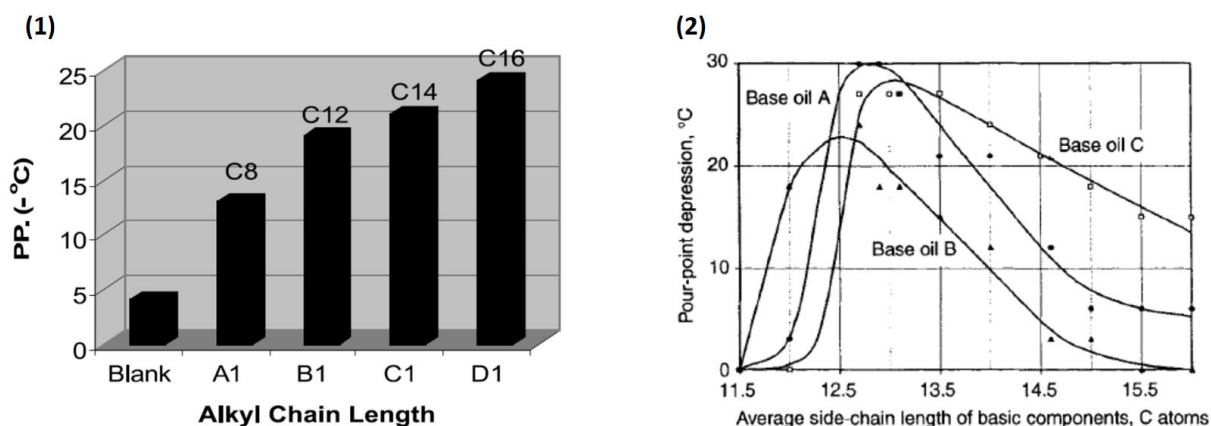


Figure I-33: Effect of the alkyl chain length on pour point depression of (1) acrylate based copolymers added at 0.25wt.% in mineral base oil<sup>218</sup> and (2)PAMA in three different mineral oils<sup>219</sup>

Florea *et al.*<sup>219</sup> also investigated the effect of PAMAs side chain length on PPD effectiveness on three different mineral base oils. As illustrated in Figure I-34 (2), it appears that it was mainly related to the type of base oil. It was concluded that the alkyl chain length has to be longer if the original pour point of the oil is higher. Yin *et al.*<sup>236</sup> showed that PAMAs addition in waxy crude oil permit a decrease of 10 °C of the pour point. A decrease of 27 °C was observed when an alkyl naphthalene copolymer was added in the same oil.

Some copolymers based on acrylates were also synthesized. For instance, Nasser and coll.<sup>218</sup> copolymerized maleic anhydride and vinyl acetate with various acrylate monomers. It was found that the polymer efficiency as PPD in a mineral base oil increased with both the concentration decrease (from 3 wt.% to 0.25 wt.%) and the copolymer molecular weight. A higher PPD was generally noticed with maleic anhydride copolymers than with vinyl acetate ones (between 3 °C and 15 °C lower depending on the acrylate chain length). Ren *et al.*<sup>240</sup> also investigated alkyl methacrylate-maleic anhydride copolymers as PPDs in diesel fuel.

As illustrated in Figure I-35, Dong *et al.*<sup>241</sup> synthesized methacrylate-maleic anhydride copolymers, P(MA-MAn) and derivatives by FRP. Aromatic derivatives, see Figure I-35 (4) showed the best effectiveness with a decrease of the PP about 19 °C. The authors explained this feature by the compatibility of benzene ring with asphaltenes and aromatic compounds in crude oil. It appears also that the short alkyl chains enhance the PPD effectiveness in crude oil.

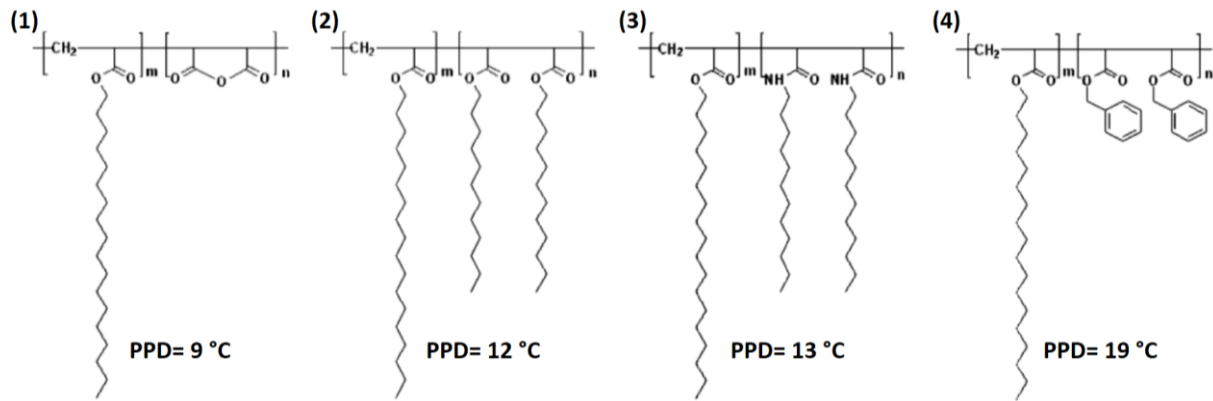


Figure I-34: Structure of PPDs added at 500 ppm in crude oil and their pour point depression effectiveness as relative values to the original oil PP (1) octadecyl acrylate-maleic anhydride copolymer and derivatives with (2) ester side chain, (3) amide side chain and (4) benzyl ester side chain<sup>241</sup>

Guo *et al.*<sup>241</sup> and El Gamal *et al.*<sup>229</sup> showed similar results with amide derivatives P(MA-MAN), both in highly paraffinic oil. The authors also observed that a Group I oil pour point was decreased from -9 °C to -33 °C by a styrene-acrylate copolymer addition at 0.5 wt.%.<sup>242</sup> Zhang *et al.*<sup>232</sup> developed a PPD based on the amidation of a terpolymer containing octadecyl acrylate, maleic anhydride and vinyl acetate units. As illustrated in Figure I-36, the PPD effect increases with the concentration and the PPD addition allows a high decrease of the oil viscosity at low temperature.

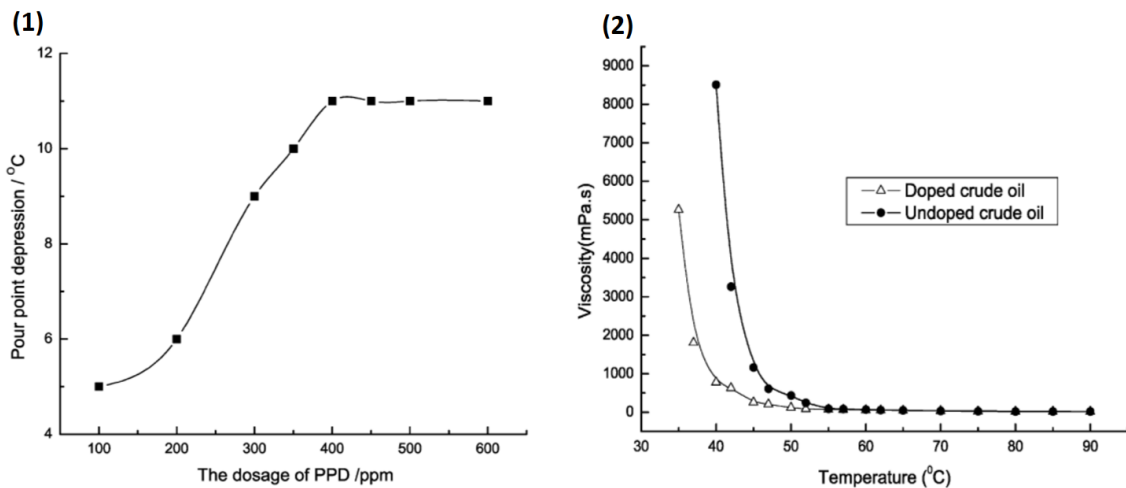


Figure I-35 : (1) Effect of the concentration on the pour point depression of crude oil and (2) influence of a PPD added at 400 ppm on the crude oil viscosity<sup>232</sup>

### 3.2.2. Other polymers

Semi-crystalline polymers, such as ethylene vinyl acetate copolymers (EVA) and ethylene/butene copolymers (OCPs) are also used as PPD.

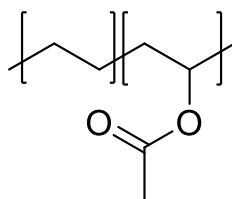
EVA copolymers

Figure I-36: EVA copolymer

EVA copolymers are obtained by copolymerization of vinyl acetate with ethylene see Figure I-37. Lucas *et al.*<sup>243</sup> studied the impact of EVA molecular weight on its pour point depression effectiveness in octacosane, a model oil. The authors conclude that a  $M_n > 10 \text{ kg.mol}^{-1}$  was required to ensure a PPD effect. For instance, when added at 1000 ppm in oil, EVA with  $M_n = 2600 \text{ g.mol}^{-1}$  decreased the pour point from  $+4 \text{ }^\circ\text{C}$  to  $-4 \text{ }^\circ\text{C}$  while a  $PP < -30 \text{ }^\circ\text{C}$  was obtained with EVA of  $M_n = 19\,300 \text{ g.mol}^{-1}$ . The authors<sup>244,245</sup> also studied the effect of vinyl acetate content in the copolymer on its PPD effectiveness in crude oil. EVA 20, with 20% of vinyl acetate achieved the best performance as PPD with concentration  $\leq 500 \text{ ppm}$  while EVA 30 and 40 exhibit a similar behavior for  $500 \text{ ppm} \leq c \leq 5000 \text{ ppm}$ , i.e. a pour point depression above  $26 \text{ }^\circ\text{C}$ . The authors explained that EVA co-crystallizes with the waxy paraffin, modifying their crystals. The loss of efficiency of EVA 20 at high concentration was attributed to precipitation of the pure copolymer in solution. On the other hand, EVA 80 did not show any PPD effect because of a lack of crystallinity. Based on molecular simulation, Wu *et al.*<sup>246</sup> deduced that side chain introduced by propylene moieties facilitated the affinity between EVA and paraffinic waxes. Ridzuan and coll.<sup>234</sup> compared P(MA-MAn) with EVA in octacosane and observed that the presence of carbonyl group in EVA plays a significant role to inhibit the wax formation.

OCPs copolymers

OCP copolymers are largely used as thickeners in lubricants but they are more barely used as PPD. Still, OCPs with appropriate ethylene content can self-assemble into micelles at low temperature with a crystalline core and amorphous brushes. The formed micelles may interact with paraffin waxes through nucleation effect and co-crystallization, resulting in more abundant smaller wax crystals. It has been shown<sup>230,233,247</sup> that OCPs PPD efficiency is governed by the crystalline degree, i.e. the amount of ethylene in the copolymer. Radulescu and coll.<sup>230,233</sup> identified two mechanisms of poly(ethylene-butylene) copolymer – paraffin

interaction. On one hand, copolymer co-crystallizes with paraffin. On the other hand, polymer aggregates at low temperature act as template for paraffin crystallization.

### 3.3. Summary and outlook

To conclude, the use of pour point depressants permits to increase the range of temperature in which the lubricant can be used by decreasing the oil pour point. PPD mainly acts by co-crystallization with the waxy crystals. Thanks to the amorphous part of PPD polymer, the crystal growth is limited and crystals are dispersed in solution, retarding the gel network formation. Efficient PPD should contain long alkyl chains as well as amorphous moieties such as PAMA comb polymers or EVA semi-crystalline copolymers. No specific  $M_w$  requirements were highlighted in literature but it appears that the polymer backbone should be long enough to ensure proper crystal dispersion. The additive concentration may be adapted for each system tested. Alike viscosity modifiers, future PPDs will have to be more environmentally friendly. The use of biodegradable and non-toxic compounds, such as bio-based polymers could be a promising option for further PPD development.

## 4. Bio-based viscosity control additives for lubricants

---

A lot of emphasis have been put recently on environmentally friendly lubricants. As already mentioned in the introduction, an annual growth of about 6% is expected for the market bio-based lubricants by 2025.<sup>19,20</sup> Bio-based oils such as vegetable oils and derivatives could represent an excellent substitute to mineral base oils in the near future.

### 4.1. Strategies to enhance bio-based part in lubricants

There are several ways to enhance the fraction of bio-based ingredients in lubricants formulation. First, it is possible to blend mineral or synthetic base oils with vegetable oils.<sup>39</sup> For instance, Durak<sup>248</sup> observed that, blended with rapeseed oil, the friction coefficient of a mineral oil was considerably reduced. Pop and coll.<sup>249</sup> blended corn oil with synthetic esters and observed pour point of  $-39$  °C and thermal-oxidative stability of 350 °C.

Inversely, petroleum-based additives can be used to improve the properties of vegetable oils.<sup>38,39</sup> For instance, Chiu *et al.*<sup>250</sup> patented lubricant formulations with transesterified triglyceride based oil blended with a synthetic ester and an OCP viscosity modifier. Quinchia and coll.<sup>251</sup> evaluated both EVA and HSD viscosity modifiers in high oleic sunflower oil (HOSO). HSD copolymers were also used as VM in sesame oil.<sup>252</sup> Erhan *et al.*<sup>253</sup> evaluated the effect of a PAMA PPD on cold flow behavior of vegetable oils. It appeared that PAMA PPD decreased the pour point of HOSO and canola oil of about 12 °C and 15 °C, respectively. The last strategy is to design fully bio-based lubricants in which tailor-made bio-based additives are added either to mineral or to bio-based oils. Many bio-based compounds were designed as additives for lubricants; they are briefly reviewed below. Special emphasize is paid on bio-based viscosity modifiers and pour point depressants.

## 4.2. Short overview of bio-based additives

Bio-based additives for lubricants can be obtained from different resources. For instance, Jain *et al.*<sup>254</sup> recently developed multifunctional additives from poultry chicken feather derivatives. Added in pentaerythritol tetraoleate, a polyol, it increased the oil oxidative stability by a factor 1.5. This additive was also found to be a good anticorrosive agent. Saga *et al.*<sup>255</sup> prepared an antioxidant additive for vegetable oils from microcrystalline cellulose. Polysaccharide as lubricant antioxidant was also synthesized from chitosan conjugated with gallic acid.<sup>256</sup>

However, most of the bio-based additives developed so far are based on vegetable oils and their derivatives.<sup>50</sup> For instance, mixtures of unsaturated fatty acids such as oleic, linoleic, and linolenic acids, are commonly used for the formulations of friction modifiers.<sup>38,257</sup> It was shown that fatty acids may form chemical bonds with metal oxide surfaces.<sup>79,258,259</sup> Fatty amines are also used as friction modifiers in engine oils.<sup>260,261</sup> Hydroxy thio-ether derivatives of vegetable oils were also used as sustainable antiwear and friction reducer additives for lubricants. They were prepared by epoxidation of soybean oil followed by an organic thiol addition.<sup>262,263</sup> It was shown that the incorporation of sulfur introduces polar functionalities in the molecule which improved the adsorption of the compound on metal surfaces. Wang *et al.*<sup>264</sup> described natural garlic oil, composed of a mixture of organosulfur compounds, as high performance extreme pressure (EP) additive for lubricating oil including PAO, synthetic esters and vegetable oils.

### 4.3. Bio-based viscosity modifiers

#### 4.3.1. Bio-based viscosity modifiers for petroleum-based oils

Some bio-based viscosity modifiers have been designed to enhance the bio-based part of mineral and synthetic oils. For instance, Unilever<sup>191,265</sup> patented polyesters based on dimeric fatty acid as viscosity index improvers for synthetic lubricants. Ghosh *et al.* largely worked on vegetable oil based VM for mineral oils. The authors<sup>266</sup> homopolymerized sunflower oil (SFO) and soybean oil (SBO) using benzoyl peroxide as initiator under microwave heating. SBO had a better thickening efficiency than SFO in base oil, i.e. the viscosity is increased of about 5.7% with SBO against 1.1% with SFO ( $c = 2000$  ppm in both cases). As a result, a higher Viscosity Index was obtained with SBO. SBO was then copolymerized with 10 wt.% of methyl acrylate, 1-decene and styrene respectively, see Figure I-38 (1).<sup>267</sup> The so-formed homo and copolymers were tested at 5 wt.% in mineral oil. The homopolymer of SBO showed good VM activity with an increase of the base oil VI from 80 to 227. The incorporation of 10 wt.% styrene and 1-decene to SBO enhances the VI values up to 240 and 242, respectively. Copolymer of SBO with methyl acrylate showed a VI of 138.

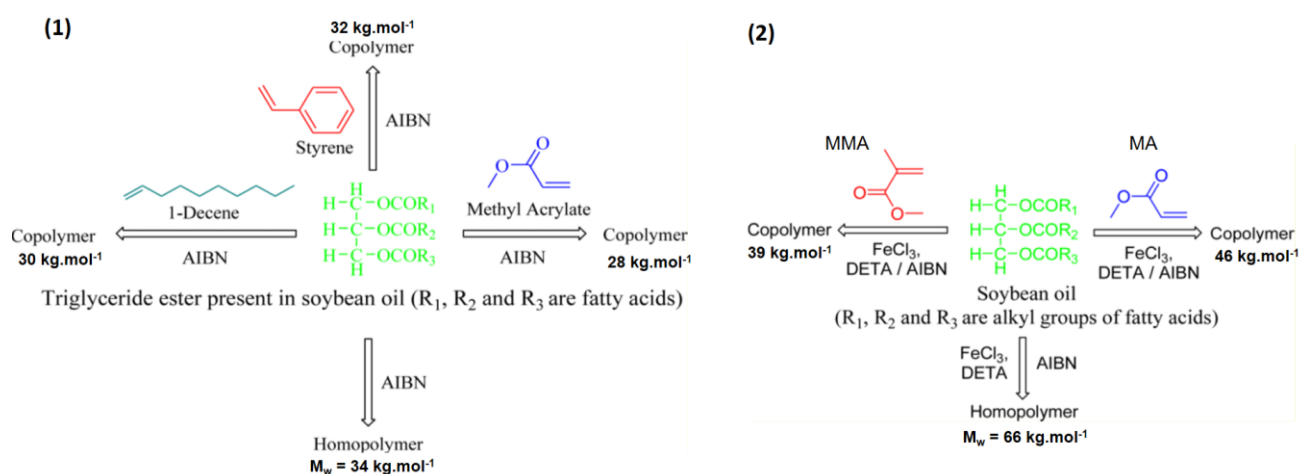


Figure I-37: (1) Soy bean oil (SBO) modification by FRP<sup>267</sup> and (2) SBO modification by ATRP<sup>268</sup>

As illustrated in Figure I-38 (2), Ghosh *et al.*<sup>268</sup> also homopolymerized and copolymerized SBO with methyl acrylate (MA) and methyl methacrylate (MMA) at 10 wt.% using ATRP. Added at 5 wt.% in mineral base oil, the homo-SBO increased the VI from 150 to 220. The VI was raised up to 239 with SBO-MA and to 262 with SBO-MMA copolymers, showing that incorporation of acrylate moiety enhances the VI effect. More recently, the authors<sup>269</sup> synthesized homopolymers of castor oil and partially bio-based copolymers with dodecyl acrylate (DA), see Figure I-39. The best VI value was obtained with the copolymers having the highest

molecular weight, independently of the copolymer composition. In all the above-mentioned studies, Ghosh *et al.* claimed that the synthesized polymers follow a coil expansion by increasing the temperature. However, they did not perform any analysis to confirm their hypothesis.

(1)

Polymers	% of monomers		Average molecular weights		
	DA	CO	$M_n$	$M_w$	PDI
P-1	100	0	17824	24588	1.38
P-2	95	5	8848	13515	1.53
P-3	90	10	35170	44644	1.27
P-4	85	15	15671	31312	1.99
P-5	80	20	16535	24538	1.48
P-6	75	25	8972	14700	1.64
P-7	0	100	7928	10022	1.26

(2)

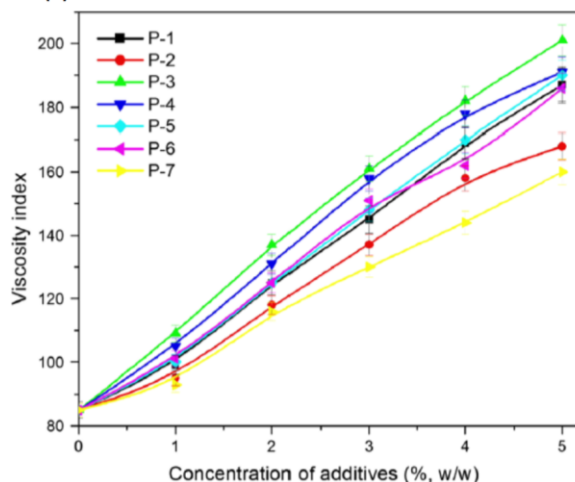


Figure I-38: (1) Polymers with different DA incorporation and their relative molecular weights and (2) variation of viscosity index of base oil blended with so-formed polymers at different concentration<sup>269</sup>

In the same frame, Nasser and coll.<sup>270</sup> copolymerized jojoba oil with alpha-olefins and vinyl acetate or vinyl pyrrolidone to design eco-friendly terpolymer viscosity modifiers using FRP, see Figure I-40. Polymers, with  $M_w$  around 30 kg.mol<sup>-1</sup>, were tested as VM in a mineral oil. Irrespectively of the concentration, terpolymers based on vinyl acetate showed a higher Viscosity Index improvement as compared to vinyl pyrrolidone analogues. The authors claimed this is due to the presence of five membered ring vinyl pyrrolidone which causes steric hindrance and limit the polymer mobility in solution.

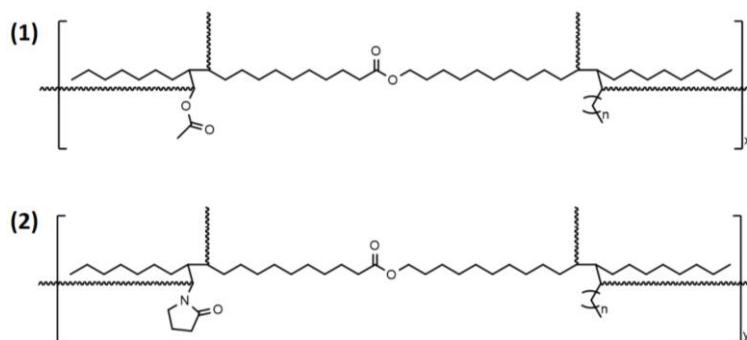
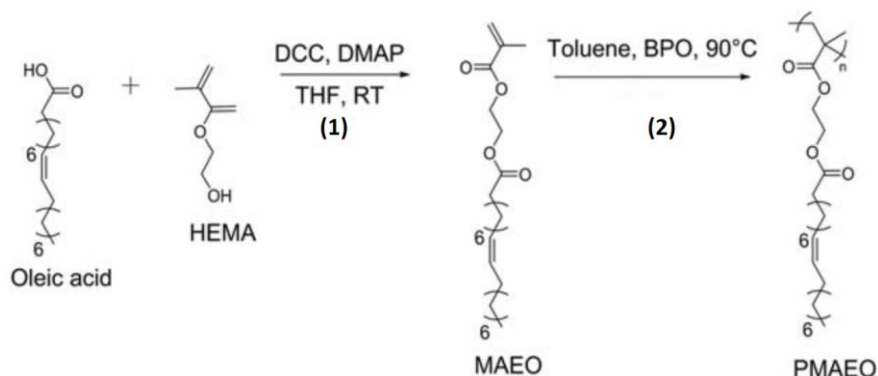


Figure I-39: (1) (Vinyl acetate-jojoba-olefin) terpolymer and (2) (Vinyl pyrrolidone-jojoba-olefin) terpolymer syntheses<sup>269</sup>

Recently, Lomège and coll.<sup>271</sup> developed bio-based poly(alkylmethacrylate)s for an evaluation as viscosity modifiers. As illustrated in Scheme I-1, 2-(methacryloyloxy)ethyl oleate (MAEO) was synthesized by Steglich esterification condensation of oleic acid and 2-hydroxyethyl

methacrylate (HEMA). Then, the corresponding polymer PMAEO was obtained by FRP with  $M_n = 45 \text{ kg}\cdot\text{mol}^{-1}$  and a dispersity of 3.6. An increase of the relative viscosity with the temperature was observed when the PMAEO was blended with mineral oil. The authors suggested that the mechanism engaged was the polymer coil expansion upon temperature increase.



Scheme I-1 : (1) Synthesis of MAEO by Steglich esterification of oleic acid and (2) synthesis of PMAEO by FRP<sup>271</sup>

Following the same methodology, methacrylate monomers were also prepared with other fatty acids including oleic, palmitic, myristic and lauric acids with different chain lengths.<sup>272</sup> The monomers were then polymerized by RAFT providing molecular weight around  $60 \text{ kg}\cdot\text{mol}^{-1}$ . The obtained polymers were then blended at 3 wt.% in a mineral oil. As illustrated in Figure I-41 (1), the longer the alkyl chain of the monomer, the larger the viscosity of the blend of polymer and mineral oil (both at 40 °C and 100 °C), and the better the viscosity modifier. PMAEO was also synthesized by telomerization in order to control its molecular weight and evaluate the influence of  $M_w$ . The series of PMAEO were blended at 3 wt.% in mineral oil. As illustrated in Figure I-41 (2), the highest the molecular weight, the largest the impact on relative viscosity. In addition, higher relative viscosities were observed at 100 °C than at 40 °C. The authors suggested then a VII effect and a coil expansion mechanism.

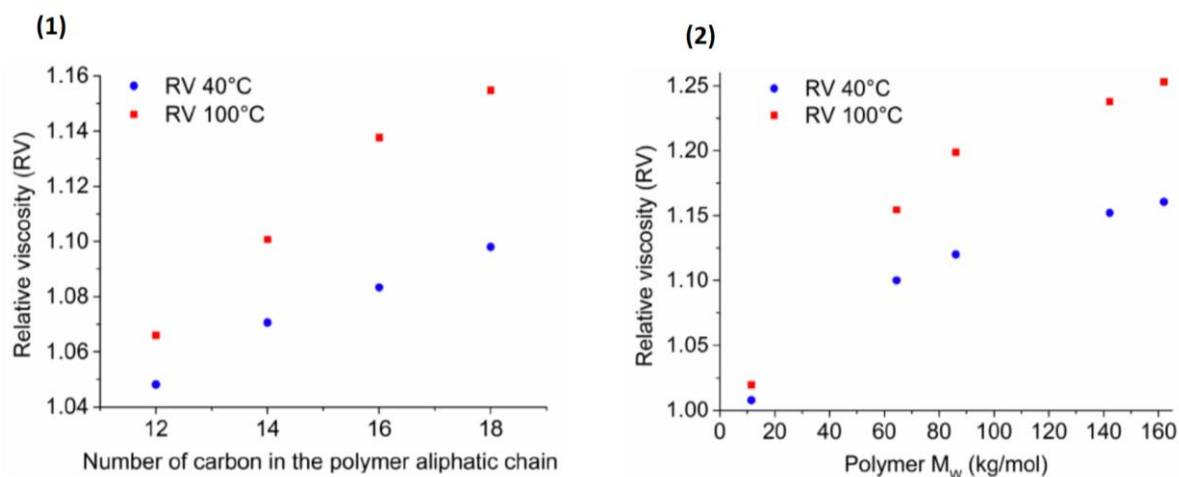


Figure I-40: Evaluation of the relative viscosity of a blend of mineral oil with bio-based PAMA at 40°C and 100°C as a function of (1) number of carbon in the polymer aliphatic chain and (2) polymer molecular weight<sup>272</sup>

#### 4.3.2. Viscosity modifiers for fully bio-based lubricants

Some bio-based VMs are already commercialized. For instance, *BASF*<sup>273</sup> developed oxyalkylated polyglycerol. These polyglycerol derivatives were described as efficient thickeners for water-based lubricants. *Function Products*<sup>274</sup> developed a range of thickeners dedicated to vegetable oils and synthetic esters. *ELM*<sup>275</sup> announced a new line of bio-based viscosity modifiers under the trademark Optibase®. These additives are made of a mixture of vegetable oils such as high oleic canola, soybean, sunflower or castor oil. The company claimed that their products are stable on a very large range of shear rates. *Croda*<sup>276</sup> also developed polyol esters that can be used as viscosity modifiers and commercialized under the trademark Priolube.

Ethyl cellulose (EC) was evaluated as viscosity modifier for vegetable oils.<sup>277,278</sup> It was compared to a non-toxic petroleum based VM: ethyl vinyl acetate copolymer (EVA) in two vegetable oils: castor oil (CO), and high oleic sunflower oil (HOSO). Added at 1 wt.% in castor oil, EC does not have a VM effect. However, in HOSO at the same concentration, EC increased the VI from 257 up to 314 while EVA added at 4 wt.% in the same oil decreased the VI to 218.

Gallegos *et al.*<sup>279,280</sup> blended high-oleic sunflower oil and castor oil with estolides obtained from both oleic and ricinoleic acids. Using acidic catalysts such as sulfuric acid, fatty acids were oligomerized with a maximum  $M_w$  of 2800 g.mol<sup>-1</sup>. Once blended at 50 wt.% with vegetable oils, estolides exhibited a thickening effect and significantly reduced wear. Lomège and coll.<sup>271</sup> also evaluated PMAEO as VM in bio-based oil. Despite a thickening effect, the relative viscosity

of the oil remained stable with temperature. This may be related to the similarity of chemical structure between triglycerides contained in vegetable oil and fatty esters contained in the polymer. This similarity may result in the oil being a good solvent of the polymer, preventing the coil expansion.

#### 4.4. Bio-based pour point depressant

##### 4.4.1. Bio-based PPD for petroleum-based oils

Many of the bio-based VMs were also evaluated as PPD. For instance, the polymerized sunflower oil and soybean oils developed by Ghosh *et al.*<sup>266</sup> decreased the pour point of a mineral base oil, from -3 °C to -18 °C and -12 °C, respectively, when added at 5000 ppm. Soybean oil (SBO) copolymerized with acrylate show better PPD properties in mineral oil when compared to SBO copolymerized with 1-decene or styrene.<sup>267</sup> The authors claimed that this is due to the polar nature of acrylate moieties. Soybean oil copolymerized with methyl acrylate and methyl methacrylate, see Figure I-38 (2), were also evaluated as pour point depressants. Once again, acrylate incorporation in SBO polymer enhanced its PPD effect in mineral oils.<sup>268</sup> Finally, the authors<sup>269</sup> showed that the higher the percentage of acrylate in castor oil-dodecyl acrylate copolymers, the better the PPD efficiency in mineral base oil, see table in Figure I-39 (1). Images of the different solutions were performed, as illustrated in Figure I-42.

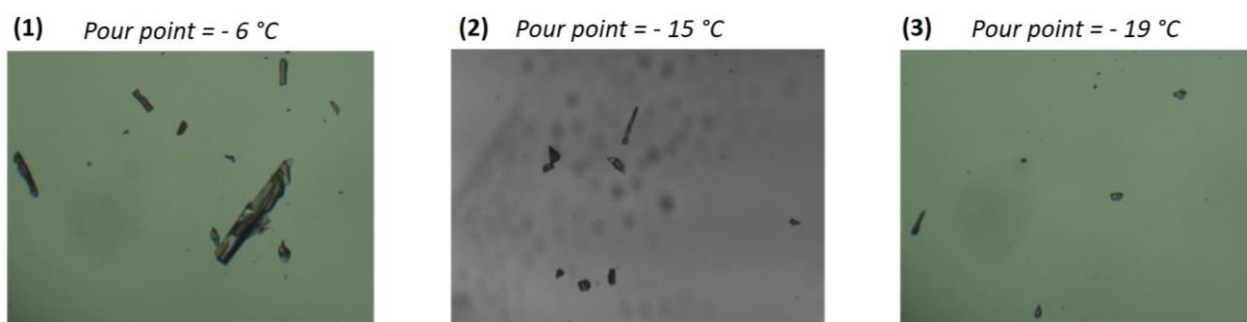


Figure I-41: Micrograph images of (1) mineral oil (MO) at - 6°C; (2) MO + 4 wt.% P-6 at -15 °C (3) MO + 4 wt.% P-2 at -19 °C<sup>269</sup>

A significant wax crystal modification was observed due to the addition of the copolymer with 5 wt.% of castor oil and 95wt.% of dodecyl acrylate (P-2) in mineral oil, in accordance with pour point depression. Nasser *et al.*<sup>270</sup> compared the PPD effectiveness of their terpolymers prepared from (jojoba: vinyl acetate:  $\alpha$ -olefins) and (jojoba: vinyl pyrrolidone:  $\alpha$ -olefins), see

Figure I-40. The terpolymer based on vinyl acetate shows the best performances with pour point depression in mineral oil of - 12 °C, against -6 °C for the terpolymer based on vinyl pyrrolidone.

#### **4.4.2. PPD for fully bio-based lubricants**

Lubricants based on vegetable oils tend to crystallize at relatively high temperature due to the crystallization of saturated fatty acids chains.<sup>281</sup> Chemical modification of vegetable oils led to a decrease of their pour point. Still, pour point depressant addition is required. PPD action has been described for biodiesel.<sup>282,283</sup> For instance, ozonized vegetable oils were evaluated as cold flow improvers in biodiesel.<sup>284</sup> No significant pour point depression was observed for soybean, sunflower and rapeseed based biodiesel. However, the palm oil biodiesel pour point was reduced of about 12 °C. The authors noticed that ozonized oil was a more effective PPD when it was prepared from the same vegetable oil as the biodiesel.

To the best of our knowledge, bio-based PPD designed for bio-lubricants have been scarcely described. For instance, ethyl cellulose has been tested as PPD. An addition of 1 wt.% in HOSO results in a pour point decrease of about 3 °C.<sup>285</sup> However, no positive effect was noticed when EC was added in castor oil.<sup>278</sup> Diesters<sup>286,287</sup> were also synthesized and evaluated as PPD in vegetable oil. No reduction of PP was reported in both studies. Biresaw *et al.*<sup>288</sup> added a butane-1-thiol in unsaturated canola oil, corn oil and castor-lauric 2-ethylhexyl ester estolide. The resulting products were added in corn oil and synthetic PAO for concentration ranging from 2 wt.% to 13.6 wt.%. No PP depression was observed for both oils.

## Conclusion

---

Lubricants are used as protective film between two surfaces in movement. Nowadays, lubricants are composed of a base oil and numerous additives. The base oil is mainly mineral but can be synthetic or bio-based. The additives are mandatory to reach the lubricant properties for modern equipment. The most common are dispersants and detergents, viscosity modifiers, oxidation inhibitors, anti-wear agents, corrosion inhibitors, foam inhibitors and pour point depressants. All the mentioned additives were shortly introduced here. However, this study mainly focuses on viscosity modifiers and pour point depressants.

The functions of a viscosity modifiers are to thicken the oil and to impact the oil V-T behavior, while resisting to the shear stress. Viscosity Index is a value set-up to evaluate the oil V-T behavior and the impact of a VM on the latter. However, the use of this value is controversial because it also takes into account the global thickening efficiency of a VM additive. For that reason, it is also required to evaluate both the relative viscosity as a function of the temperature and the  $Q$  value to properly evaluate the VM impact on an oil V-T relationship. Nowadays, olefin copolymers (OCPs), poly(alkylmethacrylate)s (PAMAs) and hydrogenated styrene diene copolymers (HSD) represent the main polymers used as viscosity modifiers. It has been shown that OCPs act mainly as thickeners, without impacting the oil V-T behavior. On the other hand, PAMAs appeared to impact oil V-T relationship by coil expansion. Some block or grafted copolymers such as HSD can also impact positively the oil V-T behavior through association – dissociation. Finally, it has been shown that polymer-solvent interaction could also impact oil V-T behavior.

Pour point depressants are added in lubricant oils in order to decrease the temperature at which the oil becomes too viscous to flow, i.e. the pour point. Usually, the waxy compounds of the oil start to crystallize at low temperature, creating a gel network. PPDs are polymeric compounds comprising most of the time an amorphous part and a crystalline part / long alkyl chains. The latter co-crystallize with wax at low temperature and amorphous part limited the crystal growth and the gel network formation. As a result, the oil pour point is decreased. PPDs are mostly comb polymers with some long alkyl side chains, such as PAMAs or semi-crystalline polymers such as EVA copolymers.

From several years, efficient viscosity modifiers and pour point depressants have been developed. However, environmental concerns lead to considerer the use of biodegradable and non-toxic lubricants instead of petroleum based ones. Some improvements have been done with the use of biodegradable synthetic esters or vegetable oil derivatives base oil as well as bio-based additives development. Some bio-based polymers from oils and fatty acids showed good viscosity modifier efficiency, especially on improving the Viscosity Index. Moreover, some of these VM present also promising PPD properties in oils.

## References

---

- 1 K. C. Ludema, *Friction, wear, lubrication*, CRC Press, 1996.
- 2 J. Ayel, *Lubrifiants; Techniques de l'ingénieur*, 1996, vol. 33.
- 3 S. Q. a Rizvi, *A Comprehensive Review of Lubricant Chemistry, Technology, Selection and Design*, ASTM International, 2009.
- 4 D. M. Pirro, M. Webster and E. Daschner, *Lubrication Fundamentals, Third edition*, CRC Press, 2016.
- 5 J. Ayel, *Lubrifiants - Propriétés et caractéristiques; Techniques de l'Ingénieur*, 1996.
- 6 R. M. Mortier, M. F. Fox and S. T. Orszulik, *Chemistry and Technology of Lubricants*, Springer, 2010.
- 7 L. R. Rudnick, *Synthetics, Mineral Oils, and Bio-Based Lubricants - Second edition*, CRC Press., 2013.
- 8 T. Mang and W. Dresel, in *Ullmann's Encyclopedia of Industrial Chemistry*, Wiley, 2007, pp. 1–850.
- 9 N. S. Ahmed and A. M. Nassar, *Tribol. Lubr. Lubr.*, 2011, 301–315.
- 10 L. R. Rudnick, *Lubricant Additives: Chemistry and Applications*, Taylor and Francis, 2017.
- 11 Fuchs group, Evolve magazine, <https://www.fuchs.com/group/magazine/en/topics/detail-view/do-disruptions-damage-durability-1/>.
- 12 P. Nagendramma and S. Kaul, *Renew. Sustain. Energy Rev.*, 2012, **16**, 764–774.
- 13 J. P. Davim, *Ecotribology*, Springer, 2016.
- 14 S. Shylesh, A. A. Gokhale, C. R. Ho and A. T. Bell, *Acc. Chem. Res.*, 2017, **50**, 2589–2597.
- 15 N. K. Myshkin and I. G. Goryacheva, *J. Frict. Wear*, 2016, **37**, 513–516.
- 16 V. W. Wong and S. C. Tung, *Friction*, 2016, **4**, 1–28.
- 17 H. M. Mobarak, E. Niza Mohamad, H. H. Masjuki, M. A. Kalam, K. A. H. Al Mahmud, M. Habibullah and A. M. Ashraful, *Renew. Sustain. Energy Rev.*, 2014, **33**, 34–43.
- 18 Grand Review Research, Synthetic Lubricants Forecasts To 2024, <https://www.grandviewresearch.com/industry-analysis/synthetic-lubricants-market>.
- 19 Research Crystal Market, Biolubricants Market: Growth Opportunity Analysis 2025, <https://www.utilitydive.com/press-release/20180614-biolubricants-market-key-manufactures-industry-scenario-and-the-growth-op/>.
- 20 Report Buyer, Bio-Lubricant Market - Global Forecast to 2022, <https://www.reportbuyer.com/product/4090177/bio-lubricant-market-by-base-oil-type-application-end-use-global-forecast-to-2022.html>.
- 21 P. Nancarrow and H. Mohammed, *ChemBioEng Rev.*, 2017, **4**, 106–119.
- 22 L. R. Rudnick and R. L. Shubkin, *Synthetic lubricants and high-performance functional fluids*, 1999.
- 23 G. Totten, S. Westbrook and R. Shah, *Fuels and lubricants handbook: technology, properties, performance, and testing*, ASTM Inter., 2003.
- 24 American Petroleum Institute, *Engine Oil Licensing and Certification System*, 2012.
- 25 S. Korcek and R. K. Jensen, *Tribol. Trans.*, 1976, **19**, 83–94.
- 26 ASTMInternational D2270-10, in *Annual Book of ASTM Standards*, 2015.
- 27 R. J. Prince and A. Sequeira, in *Lubricant base oils and wax processing-*, 1994.
- 28 J. E. Anderson, B. R. Kim, S. Mueller and T. Lofton, *Crit. Rev. Environ. Sci. Technol.*, 2003, **33**, 73–109.
- 29 S. M. Hsu, *Tribol. Int.*, 2004, **37**, 553–559.
- 30 D. C. Kramer, J. N. Ziemer, M. T. Cheng, C. E. Fry, R. N. Reynolds, B. K. Lok, M. L. Sztenderowicz and R. R. Krug, *NLGI Annu. Meet.*, 1999, 1–17.
- 31 <https://www.yubase.com/eng/index.html>.
- 32 R. L. Shubkin, M. S. Baylerian and A. R. Maler, *Ind. Eng. Chem. Prod. Res. Dev.*, 1980, **19**, 15–19.
- 33 A. Onopchenko, B. L. Cupples and A. N. Kresge, *Ind. Eng. Chem. Prod. Res. Dev.*, 1983, **22**, 182–191.
- 34 G. S. Kapur, A. S. Sarpal, R. Sarin, S. K. Jain, S. P. Srivastava and A. K. Bhatnagar, *J. Synth. Lubr.*, 1998, **15**, 177–191.
- 35 F. W. Sullivan, V. Voorhees, A. W. Neeley and R. V. Shankland, *Ind. Eng. Chem.*, 1931, **23**, 604–611.

- 36 J. Ayel, *Lubrifiants - Constitution; Techniques de l'Ingénieur*, 1997.
- 37 G. Karmakar, P. Ghosh and B. Sharma, *Lubricants*, 2017, **5**, 44.
- 38 G. Biresaw and B. K. Sharma, *Environmentally friendly and biobased lubricants*, Taylor and Francis, 2017.
- 39 J. C. J. Bart, E. Gucciardi and S. Cavallaro, *Biolubricants: Science and technology*, Woodhead P., 2013.
- 40 S. Z. Erhan, B. K. Sharma, Z. Liu and A. Adhvaryu, *J. Agric. Food Chem.*, 2008, **56**, 8919–8925.
- 41 M. K. Nizam and H. A. A. Bari, *Natl. Conf. Postgrad. Res. Malaysia*, 2009, 123–127.
- 42 J. Salimon, B. Abdullah, R. M. Yusop and N. Salih, *Chem. Cent. J.*, 2014, **8**, 16.
- 43 S. Z. Erhan and S. Asadauskas, *Ind. Crops Prod.*, 2000, **11**, 277–282.
- 44 T. A. Isbell, M. R. Edgcomb and B. A. Lowery, *Ind. Crops Prod.*, 2001, **13**, 11–20.
- 45 S. M. Erhan, R. Kleiman and T. A. Isbell, *J. Am. Oil Chem. Soc.*, 1993, **70**, 461–465.
- 46 B. Testud, D. Pintori, E. Grau, D. Taton and H. Cramail, *Green Chem.*, 2017, **19**, 259–269.
- 47 N. B. Samarth and P. a Mahanwar, *Open J. Org. Polym. Mater.*, 2015, **5**, 1–22.
- 48 Y. Gerbig, S. I. U. Ahmed, F. A. Gerbig and H. Haefke, *J. Synth. Lubr.*, 2004, **21**, 177–191.
- 49 J. Salimon, N. Salih and E. Yousif, *Eur. J. Lipid Sci. Technol.*, 2010, **112**, 519–530.
- 50 G. Karmakar, P. Ghosh and B. Sharma, *Lubricants*, 2017, **5**, 44.
- 51 B. K. Sharma, K. M. Doll and S. Z. Erhan, *Green Chem.*, 2007, **9**, 469–474.
- 52 Z. Liu, B. Sharma, S. Erhan, A. Biswas, R. Wang and T. Schuman, *Thermochim. Acta*, 2015, **601**, 9–16.
- 53 S. Gryglewicz, W. Piechocki and G. Gryglewicz, *Bioresour. Technol.*, 2003, **87**, 35–39.
- 54 H. A. Hamid, R. Yunus, U. Rashid, T. S. Y. Choong and A. H. Al-Muhtaseb, *Chem. Eng. J.*, 2012, **200–202**, 532–540.
- 55 Oleon-Lubricant, <http://www.oleon.com/market/lubricants>.
- 56 S. Li, L. Bouzidi and S. S. Narine, *Ind. Eng. Chem. Res.*, 2014, **53**, 20044–20055.
- 57 L. Raghunanan and S. S. Narine, *ACS Sustain. Chem. Eng.*, 2016, **4**, 693–700.
- 58 L. Raghunanan and S. S. Narine, *ACS Sustain. Chem. Eng.*, 2016, **4**, 686–692.
- 59 S. C. Cermak, K. B. Brandon and T. A. Isbell, *Ind. Crops Prod.*, 2006, **23**, 54–64.
- 60 S. C. Cermak, J. W. Bredsguard, B. L. John, J. S. McCalvin, T. Thompson, K. N. Isbell, K. a. Feken, T. a. Isbell and R. E. Murray, *Ind. Crops Prod.*, 2013, **46**, 386–391.
- 61 J. Bredsguard, J. Forest and T. Thompson, *Lubricant compositions comprising estolide base oils; US 8,287,754 B1*, 2012.
- 62 Y. M. Shashidhara and S. R. Jayaram, *Tribol. Int.*, 2010, **43**, 1073–1081.
- 63 J. Ayel, *Lubrifiants - Additifs à action physique ou physiologique; Techniques de l'Ingénieur*, 2002.
- 64 J. Ayel, *Lubrifiants - Additifs à action chimique; Techniques de l'Ingénieur*, 2001.
- 65 Frost and Sullivan, *Strategic Analysis of the Global Lubricant Additives Market*, 2014.
- 66 GrandViewResearch, *Lubricant Additives Market*, <https://www.grandviewresearch.com/industry-analysis/lubricant-additives-market>.
- 67 S. Al-Malaika, A. Marogi and G. Scott, *J. Appl. Polym. Sci.*, 1987, **33**, 1455–1471.
- 68 H. H. Abou El Naga and A. E. M. Salem, *Wear*, 1984, **96**, 267–283.
- 69 L. R. Rudnick, R. P. Buchanan and F. Medina, *J. Synth. Lubr.*, 2006, **23**, 11–26.
- 70 H. T. Ryan, *Ind. Lubr. Tribol.*, 1999, **51**, 287–293.
- 71 K. U. Ingold, *Chem. Rev.*, 1961, **61**, 563–589.
- 72 M. J. Covitch, B. K. Humphrey and D. E. Ripple, in *SAE Technical paper series*, 1985.
- 73 D. R. Lachowicz and K. L. Kreuz, *J. Org. Chem.*, 1967, **32**, 3885–3888.
- 74 K. Ryu, *Bioresour. Technol.*, 2010, **101**, S78–S82.
- 75 Y. Chevalier, B. Fixari, S. Brunel, E. Marie and P. De Guio, *Polym. Int.*, 2004, **53**, 475–483.
- 76 J. Mansot, M. Hallouis and J. Martin, *Colloids Surfaces A Physicochem. Eng. Asp.*, 1993, **71**, 123–134.
- 77 J. Mansot, M. Hallouis and J. Martin, *Colloids Surfaces A Physicochem. Eng. Asp.*, 1993, **75**, 25–31.

- 78 C. M. Allen and E. Drauglis, *Wear*, 1969, **14**, 363–384.
- 79 R. R. Sahoo and S. K. Biswas, *J. Colloid Interface Sci.*, 2009, **333**, 707–718.
- 80 Z. Tang and S. Li, *Curr. Opin. Solid State Mater. Sci.*, 2014, **18**, 119–139.
- 81 M. Masuko, H. Sato, A. Suzuki and O. Kurosawa, *Tribol. Int.*, 2008, **41**, 1097–1102.
- 82 E. S. Forbes, *Tribology*, 1970, **3**, 145–152.
- 83 R. C. Coy and R. B. Jones, *ASLE Trans.*, 1981, **24**, 77–90.
- 84 P. C. Hamblin, U. Kristen and D. Chasan, *Lubr. Sci.*, 1990, **2**, 287–318.
- 85 W. Grabowski, *Efficient diesel fuel antifoams of low silicon content; US 5542960*, 1996.
- 86 J. Carey, A. Galiano-Roth and G. Dudley, *Alkylated naphthalene base stock lubricant formulations ; US 8,716.201 B2*, 2014.
- 87 B. P. Binks, C. A. Davies, P. D. I. Fletcher and E. L. Sharp, *Colloids Surfaces A Physicochem. Eng. Asp.*, 2010, **360**, 198–204.
- 88 A. L. Fameau and A. Saint-Jalmes, *Adv. Colloid Interface Sci.*, 2017, **247**, 454–464.
- 89 L. T. Shearer and W. W. Akers, *J. Phys. Chem.*, 1958, **62**, 1269–1270.
- 90 W. L. Van Horne, *Ind. Eng. Chem.*, 1949, **41**, 952–959.
- 91 M. J. Souza De Carvalho, P. Rudolf Seidl, C. R. Pereira Belchior and J. Ricardo Sodr, *Tribol. Int.*, 2010, **43**, 2298–2302.
- 92 T. W. Selby, *ASLE Trans.*, 1958, **1**, 68–81.
- 93 A. Martini, U. S. Ramasamy and M. Len, *Tribol. Lett.*, 2018, **66**, 58.
- 94 T. Stöhr, B. Eisenberg and M. Müller, *SAE Int. J. Fuels Lubr.*, 2008, **1**, 2008-01–2462.
- 95 P. J. Flory, *Principles of polymer chemistry, Volume 1*, Cornell University Press, Ithaca, New-York, Cornell Un., 1953.
- 96 A. Einstein, *Ann. Phys.*, 1911, **339**, 591–592.
- 97 M. L. Huggins, *J. Am. Chem. Soc.*, 1942, **64**, 2716–2718.
- 98 H. M. Kwaambwa, J. W. Goodwin, R. W. Hughes and P. A. Reynolds, *Colloids Surfaces A Physicochem. Eng. Asp.*, 2007, **294**, 14–19.
- 99 A. Sen and I. D. Rubin, *Macromolecules*, 1990, **23**, 2519–2524.
- 100 S. G. Weissberg, R. Simha and S. Rothman, *J. Res. Natl. EurEau Stand.* 1951.
- 101 C. Neveu and F. Huby, *Lubr. Sci.*, 1988, **1**, 27–49.
- 102 R. P. Wool, *Macromolecules*, 1993, **26**, 1564–1569.
- 103 D. . Schulz and J. Glass, in *ACS Symposium series*, 1991, p. 345.
- 104 M. J. Covitch, *J. Test. Eval.*, 2017, **46**, 20150242.
- 105 J. Zakarian, *SAE Int. J. Fuels Lubr.*, 2012, **5**, 2012-01–1671.
- 106 J. Zakarian, M. E. Webb and B. Hunter, *SAE Int.*, 2015, 1–6.
- 107 H. G. Müller, *Tribol. Int.*, 1978, **11**, 189–192.
- 108 P. Cusseau, N. Bouscharain, L. Martinie, D. Philippon, P. Vergne and F. Briand, *Tribol. Trans.*, 2017, **0**, 1–11.
- 109 M. J. Covitch and K. J. Trickett, *Adv. Chem. Eng. Sci.*, 2015, **5**, 134–151.
- 110 M. T. Savoji, D. Zhao, R. J. Muisener, K. Schimossek, K. Schoeller, T. P. Lodge and M. A. Hillmyer, *Ind. Eng. Chem. Res.*, 2018, **57**, 1840–1850.
- 111 H. Singh and I. B. Gulati, *Wear*, 1987, **118**, 33–56.
- 112 J. Holtzinger, J. Green, G. Lamb, D. Atkinson and H. Spikes, *Tribol. Trans.*, 2012, **55**, 631–639.
- 113 M. Mortier, *Tribotest*, 1996, **2**, 329–349.
- 114 M. J. Covitch, J. Weiss and I. M. Kreutzer, *Lubr. Sci.*, 1999, **11**, 337–364.
- 115 W. J. Bartz, *Lubr. Sci.*, 2000, **12**, 215–237.
- 116 T. W. Selby, in *SAE Technical paper series*, 1993.
- 117 M. J. Covitch, *SAE Tech. Pap. Ser.*, 1998, 14–30.

- 118 J. L. Zakin and D. L. Hunston, *J. Appl. Polym. Sci.*, 1978, **22**, 1763–1766.
- 119 M. T. Devlin, T. Hammock and T. C. Jao, *Lubr. Sci.*, 2002, **14**, 169–184.
- 120 J. Wang, Z. Ye and S. Zhu, *Ind. Eng. Chem. Res.*, 2007, **46**, 1174–1178.
- 121 Y. Suzuki, J. Mitsui, M. Shiomi, H. Fukuchi and H. Okamura, in *SAE Technical paper series*, 1995.
- 122 L. Xue, U. S. Agarwal and P. J. Lemstra, *Macromolecules*, 2005, **38**, 8825–8832.
- 123 S. Morgan, Z. Ye, R. Subramanian and S. Zhu, *Polym. Eng. Sci.*, 2010, **50**, 911–918.
- 124 K. Marsden, *Lubr. Sci.*, 1989, **1**, 265–280.
- 125 J. C. W. Chien and D. He, *J. Polym. Sci. Part A Polym. Chem.*, 1991, **29**, 1585–1593.
- 126 N. J. Mark J. Struglinski, Bridgewater, *Oleaginous compositions containing novel ethylene alpha-olefin polymer Viscosity Index improver additive; US ,151,204*, 1992, vol. 96.
- 127 D. J. Arriola, *Science (80-. )*, 2006, **312**, 714–719.
- 128 I. K. L. Walton, L. Jackson, T. X. Us, M. M. Hughes, Y. W. Cheung, L. Jackson, T. X. Us and G. L. Rath, *Viscosity Index Improver for lubricant compositions; US 7,662,881 B2*, 2010.
- 129 R. Eckert, *Hydrogenated star-shaped polymer; US 4,116,917*, 1978.
- 130 I. C. Liou, R. C. C. Tsiang, J. Wu, J. S. Liou and H. C. Sheu, *J. Appl. Polym. Sci.*, 2002, **83**, 1911–1918.
- 131 P. Ravishankar, *Olefinic copolymer compositions for viscosity modification of motor oil ; US 2012/0015854 A1*, 2012.
- 132 S. Ikeda, *Viscosity modifier for lubricating oils, additive composition for lubricating oils, and lubricating oil composition ; US 9,045,574 B2*, US, 2015.
- 133 E. Kresge, *Ethylene polymer useful as a lubricating oil viscosity modifier E-25 ; US 4,666,619*, US, 1987.
- 134 Z. Dong and Z. Ye, *Polym. Chem.*, 2012, **3**, 286–301.
- 135 I. D. Rubin and A. Sen, *J. Appl. Polym. Sci.*, 1990, **40**, 523–530.
- 136 I. D. Rubin and M. M. Kapuscinski, *J. Appl. Polym. Sci.*, 1993, **49**, 111–115.
- 137 G. Ver Strate, C. Cozewith and S. Ju, *Macromolecules*, 1988, **21**, 3360–3371.
- 138 R. W. M. Wardle, R. C. Coy, P. M. Cann and H. A. Spikes, *Lubr. Sci.*, 1990, **3**, 45–62.
- 139 J. Hall, *Ethylene, C3-16 monoolefin polymer containing 0.02%-0.6% by weight vinyl norbornene bound in the polymer having improved cold flow ; US 4,156,767*, 1979.
- 140 L. J. Fetters, A. D. Kiss, D. S. Pearson, G. F. Quack and F. J. Vitus, *Macromolecules*, 1993, **26**, 647–654.
- 141 J. W. Robinson, Y. Zhou, J. Qu, J. T. Bays and L. Cosimbescu, *React. Funct. Polym.*, 2016, **109**, 52–55.
- 142 S. Roos, J. M. Bollinger, M. Scherer and B. Eisenberg, *Method for preparation of a composition that contains polymer ester compounds with long chain alkyl residues and use of this composition; US 6,403,746 B1*, 2002.
- 143 S. Schmidt, P. Callais, N. Macy and O. Guerrett, *Controlled radical acrylic copolymer thickeners; US 7,691,797 B2*, 2013.
- 144 D. Visger, M. Davies and D. Price, *Star polymers and compositions thereof ; EP 1 833 868 B1*, 2013.
- 145 J. Johnson and B. Schober, *Loose core star polymers and lubricating composition thereof; US 2015/0183915 A1*, 2015.
- 146 A. Dardin, M. Mueller and B. Eisenberg, *Lubricating oil composition with good frictional properties ; US 8,288,327 B2*, 2012.
- 147 L. Cosimbescu, J. W. Robinson, Y. Zhou and J. Qu, *RSC Adv.*, 2016, **6**, 86259–86268.
- 148 J. W. Robinson, Y. Zhou, J. Qu, R. Erck and L. Cosimbescu, *J. Appl. Polym. Sci.*, 2016, **133**, 1–11.
- 149 J. Fan, M. Müller, T. Stöhr and H. A. Spikes, *Tribol. Lett.*, 2007, **28**, 287–298.
- 150 L. Cosimbescu, J. W. Robinson and J. P. Page, *Ind. Eng. Chem. Res.*, 2018, 1–28.
- 151 C. Mary, D. Philippon, L. Lafarge, D. Laurent, F. Rondelez, S. Bair and P. Vergne, *Tribol. Lett.*, 2013, **52**, 357–369.
- 152 L. Cosimbescu, A. Vellore, U. S. Ramasamy, S. Burgess and A. Martini, *Eur. Polym. J.*, 2018, **104**, 39–44.
- 153 T. H. N. Nguyen, R. Nicolay, R. Iovine and P. Iliopoulos, *Lubricating compositions comprising thermoassociative and exchangeable copolymers ; US 2017/0009176 A1*, 2017.

- 154 R. Nicolay, T. H. N. Nguyen, R. Iovine and G. Descroix, *Compositions of thermoassociative additives with controlled association and lubricant composition containing them* ; US2018/0023028 A1, 2018.
- 155 G. Holden and R. Milkovich, *Block polymers of monovinyl aromatic hydrocarbons and conjugated dienes* ; US 3,265,765, 1966.
- 156 W. Anderson, *Block copolymers as viscosity index improvers for lubricating oils* ; US 3,763,044, 1973.
- 157 L. J. Fetters and L.-K. Bi, *Star polymers and process for the preparation thereof* ; US 3,985,830, 1976.
- 158 W. Abraham, M. Covitch and M. Galic, *Aromatic diblock copolymers for lubricant and concentrate compositions and methods thereof* ; US 2006/0052255A1, 2006.
- 159 R. Jones and C. Moberly, *Hydrogenated polybutadiene and process for producing same*; US 2,864,809, 1958.
- 160 D. Breslow and A. Matlack, *Hydrogenation of unsaturated hydrocarbons* ; US 3,113,986, 1963.
- 161 R. J. A. Eckert and D. F. Covey, *Lubr. Sci.*, 1988, **1**, 65–80.
- 162 S. Ayano and S. Yabe, *Polym. J.*, 1970, **1**, 706–715.
- 163 C. Huang and L. Breon, *Viscosity improver compositions providing improved low temperature characteristics to lubricating oil* ; US 2006/0211586 A1, 2006.
- 164 A. Paula, P. Almeida, A. Paula, L. Rodrigues, C. D. Ávila, C. Erbetta, R. G. De Sousa, R. Fernando, D. S. Freitas, M. Elisa and S. Ribeiro, 2014, 1085–1093.
- 165 Y. Tsunashima, *Macromolecules*, 1990, **23**, 2963–2969.
- 166 Y. Tsunashima, M. Hirata and Y. Kawamata, *Macromol. Symp.*, 1990, **23**, 1089–1096.
- 167 F. M. B. Coutinho and S. C. S. Teixeira, *Polym. Test.*, 1993, **12**, 415–422.
- 168 S. H. Choi, T. P. Lodge and F. S. Bates, *Phys. Rev. Lett.*, 2010, **104**, 1–4.
- 169 S. H. Choi, F. S. Bates and T. P. Lodge, *Macromolecules*, 2011, **44**, 3594–3604.
- 170 T. Kiovsy, *Star-shaped dispersant viscosity index improver* ; US 4,077,893, 1978.
- 171 M. Martin, *Dispersant-VI improver product*; US 4,427,834, 1984.
- 172 L. Willner, J. J. D. Richter, J. Roovers, L. Z, I. Festkorperforschung and F. J. Gmbh, *Macromolecules*, 1994, 3821–3829.
- 173 B. J. Bauer, L. J. Fetters, W. W. Graesslev, N. Hadjichristidis and G. F. Quack, *Macromolecules*, 1989, **22**, 2337–2347.
- 174 A. Jukić, L. J. Tomašek and Z. Janović, *Lubr. Sci.*, 2005, **17**, 431–449.
- 175 A. Jukić, F. Faraguna, I. Franjić and S. Kuzmić, *J. Ind. Eng. Chem.*, 2017, **56**, 270–276.
- 176 T. Stohr, B. Eisenberg and M. Muller, *Oil soluble comb polyesters*; EP 1 899 393 B1, 2012.
- 177 S. Takigawa, N. Teranishi, T. Nomura, T. Suzuki and K. Sakai, *Polymer composition useful as viscosity index improver* ; US 5,026,496, 1991.
- 178 B. Eisenberg, T. Stohr, D. Janssen and M. Stihulka, *Use of comb polymers as antifatigue additives* ; US 2011/0306533 A1, 2011.
- 179 B. Eisenberg and T. Stohr, *Transmission oil formulation for reducing fuel consumption* ; US 2016/0097.017 A1, 2016.
- 180 T. Stohr, D. Janssen, J. Schnabel, B. Eisenberg, H. Goerlitzer and M. Mueller, *Use of comb polymers for reducing fuel composition* ; US 9,783,630 B2, 2017.
- 181 H. Zorn and W. Rosinsky, *Production of high quality lubricating oils*; US 2,106,232, 1938.
- 182 M. Otto and M. Mueller-Cunradi, *High molecule weight iso-olefine polymer and process of producing the same* ; US 2,130,507, 1938.
- 183 B. Wilson, *Ind. Lubr. Tribol.*, 1994, **46**, 3–6.
- 184 L. Coleman, *Lubricant containing nitrogen-containing ester*; US 3,702,300, 1972.
- 185 J. Jarrin, M. Robine, G. Parc and F. Dawans, *Copolymer compositions usable as additives for lubrication oils*, 1988.
- 186 T.-Y. Wang, R. C.-C. Tsiang, J.-S. Liou, J. Wu and H.-C. Sheu, *J. Appl. Polym. Sci.*, 2001, **79**, 1838–1846.
- 187 A. Jukic, E. Vidovic and Z. Janovic, *Chem. Technol. Fuels Oils*, 2007, **43**, 386–394.
- 188 A. Jukić, M. Rogošić and E. Vidović, *Polym. Plast. Technol. Eng.*, 2009, **49**, 74–77.

- 189 J. Elliott, T. Davis, B and S. Norman, *Polyester lubricant additives, their preparation and compositions containing them* ; US 4,070,370, 1978.
- 190 M. Salomon and R. Lange, *Sulfur-containing polymeric polyesters and additive concentrates and lubricating oils containing same* ; US 4,909,952, 1990.
- 191 D. Kenbeek, R. Pouline and G. Van der Wall, *Polyester Viscosity Index improver* ; US 5,314,634, 1994.
- 192 S. Kitahara, S. Yutaka, J. Igarashi, S. Hasegawa and M. Miyamoto, *Oil-soluble polyester, additive for lubricating oil, and lubricating oil composition* ; US 5,723,417, 1998.
- 193 L. Cosimbescu, *Modified thermoresponsive hyperbranched polymers for improved viscosity and enhanced lubricity of engine oils*, 2016.
- 194 J. W. Robinson, Y. Zhou, P. Bhattacharya, R. Erck, J. Qu, J. T. Bays and L. Cosimbescu, *Sci. Rep.*, 2016, **6**, 1–10.
- 195 L. Cosimbescu and J. W. Robinson, *Branched polymers as viscosity and/or friction modifiers for lubricants*; US 2016/0046885 A1, 2016.
- 196 B. M. Tande, N. J. Wagner, M. E. Mackay, C. J. Hawker and M. Jeong, *Macromolecules*, 2001, **34**, 8580–8585.
- 197 P. Bhattacharya, U. S. Ramasamy, S. Krueger, J. W. Robinson, B. J. Tarasevich, A. Martini and L. Cosimbescu, *Ind. Eng. Chem. Res.*, 2016, **55**, 12983–12990.
- 198 D. LaRiviere, A. F. A. Asfour, A. Hage and J. Z. Gao, *Lubr. Sci.*, 2000, **12**, 133–143.
- 199 U. S. Ramasamy, S. Lichter and A. Martini, *Tribol. Lett.*, 2016, **62**, 1–7.
- 200 M. Rubinstein and A. Dobrynin, *Trends Polym. Sci.*, 1997, **5**, 181–186.
- 201 Z. Tuzar and P. Kratochvil, *Adv. Colloid Interface Sci.*, 1976, **6**, 201–232.
- 202 R. Longworth and H. Morawetz, *J. Polym. Sci.*, 1958, **21**, 307–319.
- 203 W. Mandema, H. Zeldenrust and C. A. Emeis, *Die Makromol. Chemie Banner*, 1979, **180**, 1521–1538.
- 204 J. S. Higgins, J. V Dawkins, G. G. Maghami and S. A. Shakir, *Polymer (Guildf.)*, 1986, **27**, 931–936.
- 205 J. S. Higgins, S. Blake, P. E. Tomlins, E. Staplest, J. Penfold and J. V Dawkins, *Polymer (Guildf.)*, 1988, **29**, 1968–1978.
- 206 C. Price, J. D. G. Mcadam, T. P. Lally and D. Woods, *Polymer (Guildf.)*, 1974, **15**, 13–17.
- 207 C. Price and D. Woods, *Polymer (Guildf.)*, 1974, **15**, 389–392.
- 208 W. Mandema, H. Zeldenrust and C. A. Emeis, *Die Makromol. Chemie Banner*, 1979, **180**, 2163–2174.
- 209 T. P. Lodge, J. Bang, S. Jain, J. S. Pedersen and Z. Li, *Macromolecules*, 2006, **39**, 1199–1208.
- 210 S. Choi, F. S. Bates and T. P. Lodge, *J. Phys. Chem.*, 2009, **113**, 13840–13848.
- 211 S. Choi, F. S. Bates and T. P. Lodge, *Macromolecules*, 2014, **47**, 7978–7986.
- 212 P. Bezot, B. Elmakoudi, B. Constans, D. Faure and P. Hoornaert, *J. Appl. Polym. Sci.*, 1994, **51**, 1715–1725.
- 213 P. E. Rouse, *J. Chem. Phys.*, 1953, **21**, 1272–1280.
- 214 R. G. Larson, *J. Rheol. (N. Y. N. Y.)*, 2005, **49**, 1–70.
- 215 M. Len, U. S. Ramasamy, S. Lichter and A. Martini, *Tribol. Lett.*, 2018, **66**, 5.
- 216 F. Yang, Y. Zhao, J. Sjöblom, C. Li and K. G. Paso, *J. Dispers. Sci. Technol.*, 2015, **36**, 213–225.
- 217 G. Gavlin, E. A. Swire and S. P. Jones, *Ind. Eng. Chem.*, 1953, **45**, 2327–2335.
- 218 N. S. Ahmed, A. M. Nassar, R. M. Nasser, A. F. Khatlab and A.-A. A. Abdel-Azim, *Pet. Sci. Technol.*, 2008, **26**, 1390–1402.
- 219 M. Florea, D. Catrinoiu, P. Luca and S. Balliu, *Lubr. Sci.*, 1999, **12**, 31–44.
- 220 E. Vignati, R. Piazza, R. F. G. Visintin, R. Lapasin, P. D’Antona and T. P. Lockhart, *J. Phys. Condens. Matter*, 2005, **17**, S3651–S3660.
- 221 Annual Book of ASTM Standards, *ASTM Standard D2500-11, Test Method for Cloud Point of Petroleum Products*, 2016.
- 222 B. Jia and J. Zhang, *Ind. Eng. Chem. Res.*, 2012, **51**, 10977–10982.
- 223 C. Chang, D. V. Boger and Q. D. Nguyen, *Ind. Eng. Chem. Res.*, 1998, **37**, 1551–1559.

- 224 H. P. Roenningsen, B. Bjoerndal, A. Baltzer Hansen and W. Batsberg Pedersen, *Energy & Fuels*, 1991, **5**, 895–908.
- 225 J. Xu, S. Xing, H. Qian, S. Chen, X. Wei, R. Zhang, L. Li and X. Guo, *Fuel*, 2013, **103**, 600–605.
- 226 T. Liu, L. Fang, X. Liu and X. Zhang, *Fuel*, 2015, **143**, 448–454.
- 227 I. M. El-Gamal and A. M. Al-Sabbagh, *Fuel*, 1996, **75**, 743–750.
- 228 J. A. P. Coutinho, C. Dauphin and J. L. Daridon, *Fuel*, 2000, **79**, 607–616.
- 229 I. M. El-Gamal, T. T. Khidr and F. M. Ghuiba, *Fuel*, 1998, **77**, 375–385.
- 230 A. Radulescu, D. Schwahn, J. Stellbrink, E. Kentzinger, M. Heiderich, D. Richter and L. J. Fetters, *Macromolecules*, 2006, **39**, 6142–6151.
- 231 A. M. Atta, H. I. Al-Shafy and E. A. Ismail, *J. Dispers. Sci. Technol.*, 2011, **32**, 1296–1305.
- 232 L. Fang, X. Zhang, J. Ma and B. Zhang, *Ind. Eng. Chem. Res.*, 2012, **51**, 11605–11612.
- 233 A. Radulescu, D. Schwahn, M. Monkenbusch, L. J. Fetters and D. Richter, *J. Polym. Sci. Part B Polym. Phys.*, 2004, **42**, 3113–3132.
- 234 N. Ridzuan, F. Adam, Z. Yaacob and P. Ump, *Spe*, 2014, 1–9.
- 235 S. Yi and J. Zhang, *Energy and Fuels*, 2011, **25**, 1686–1696.
- 236 W. Chen, Z. Zhao and C. Yin, *Fuel*, 2010, **89**, 1127–1132.
- 237 W. Böttcher and H. Jost, *SAE Tech. Pap. Ser.*, 1991.
- 238 P. Ghosh and M. Das, *J. Pet. Sci. Eng.*, 2014, **119**, 79–84.
- 239 A. . Kuzmic, M. Radosevic, G. Bogdanic, V. Srica and R. Vukovic, *Fuel*, 2008, **87**, 2943–2950.
- 240 Y. Song, S. Han and T. Ren, *Pet. Sci. Technol.*, 2010, **28**, 860–867.
- 241 Y. Wu, G. Ni, F. Yang, C. Li and G. Dong, *Energy & Fuels*, 2012, **26**, 995–1001.
- 242 F. Faraguna, K. Kraguljac, E. Vidović and A. Jukić, *Tribol. Trans.*, 2017, **60**, 1063–1069.
- 243 A. L. de C. Machado and E. F. Lucas, *Pet. Sci. Technol.*, 1999, **17**, 1029–1041.
- 244 A. L. . Machado, E. F. Lucas and G. González, *J. Pet. Sci. Eng.*, 2001, **32**, 159–165.
- 245 L. M. S. L. Oliveira, R. C. P. Nunes, I. C. Melo, Y. L. L. Ribeiro, L. G. Reis, J. C. M. Dias, R. C. L. Guimarães and E. F. Lucas, *Fuel Process. Technol.*, 2016, **149**, 268–274.
- 246 C. Wu, J. L. Zhang, W. Li and N. Wu, *Fuel*, 2005, **84**, 2039–2047.
- 247 H. S. Ashbaugh, A. Radulescu, R. K. Prud'homme, D. Schwahn, D. Richter and L. J. Fetters, *Macromolecules*, 2002, **35**, 7044–7053.
- 248 E. Durak, *Ind. Lubr. Tribol.*, 2004, **56**, 23–37.
- 249 L. Pop, C. Puşcaş, G. Bandur, G. Vlase and R. Nuţiu, *IAOCS, J. Am. Oil Chem. Soc.*, 2008, **85**, 71–76.
- 250 I.-C. Chiu, S. Gonsel and P. Lacey, *Environmentally friendly lubricants ; US 2003/0186824A1*, 2003.
- 251 L. A. Quinchia, M. A. Delgado, C. Valencia, J. M. Franco and C. Gallegos, *Environ. Sci. Technol.*, 2009, **43**, 2060–2065.
- 252 S. Sabarinath, K. Prabhakaran Nair, P. Rajendrakumar and P. Parameswaran, *Proc. Inst. Mech. Eng. Part J J. Eng. Tribol.*, 2018, **232**, 427–436.
- 253 S. Asadauskas and S. Z. Erhan, *J. Am. Oil Chem. Soc.*, 1999, **76**, 313–316.
- 254 P. P. Latha, R. K. Singh, A. Kukrety, R. C. Saxena, M. Bhatt and S. L. Jain, *ACS Sustain. Chem. Eng.*, 2016, **4**, 999–1005.
- 255 L. C. Saga, E.-O. Rukke, K. H. Liland, B. Kirkhus, B. Egelanddal, J. Karlsen and J. Volden, *J. Am. Oil Chem. Soc.*, 2011, **88**, 1883–1895.
- 256 W. Pasanphan, G. R. Buettner and S. Chirachanchai, *Carbohydr. Res.*, 2010, **345**, 132–140.
- 257 M. A. Maleque, H. H. Masjuki and S. M. Sapuan, *Ind. Lubr. Tribol.*, 2003, **55**, 137–143.
- 258 D. H. Wheeler, D. Potente and H. Wittcoff, *J. Am. Oil Chem. Soc.*, 1971, **48**, 125–128.
- 259 S. M. Lundgren, K. Persson, G. Mueller, B. Kronberg, J. Clarke, M. Chtaib and P. M. Claesson, *Langmuir*, 2007, **23**, 10598–10602.
- 260 A. Biswas, B. K. Sharma, J. L. Willett, S. Z. Erhan and H. N. Cheng, *Energy Environ. Sci.*, 2008, **1**, 639.
- 261 S. Yan, S. O. Salley and K. Y. Simon Ng, *Appl. Catal. A Gen.*, 2009, **353**, 203–212.

- 262 B. K. Sharma, A. Adhvaryu and S. Z. Erhan, *J. Agric. Food Chem.*, 2006, **54**, 9866–9872.
- 263 B. K. Sharma, A. Adhvaryu and S. Z. Erhan, *Tribol. Int.*, 2009, **42**, 353–358.
- 264 W. Li, C. Jiang, M. Chao and X. Wang, *ACS Sustain. Chem. Eng.*, 2014, **2**, 798–803.
- 265 R. Poulina and G. van der Waal, *Polyester viscosity index improvers ; EP 0335013 B1*, 1988.
- 266 G. Karmakar and P. Ghosh, *ACS Sustain. Chem. Eng.*, 2013, **1**, 1364–1370.
- 267 G. Karmakar and P. Ghosh, *ACS Sustain. Chem. Eng.*, 2015, **3**, 19–25.
- 268 G. Karmakar and P. Ghosh, *ACS Sustain. Chem. Eng.*, 2016, **4**, 775–781.
- 269 P. Ghosh, M. Hoque and G. Karmakar, *Polym. Bull.*, 2018, **75**, 501–514.
- 270 R. Nasser, N. Ahmed and A. Nassar, *Pet. coil*, 2016, **58**, 687–694.
- 271 J. Lomège, C. Negrell, J.-J. Robin, V. Lapinte and S. Caillol, *Polym. Eng. Sci.*, , DOI:10.1002/pen.24896.
- 272 J. Lomège, C. Negrell, J.-J. Robin, V. Lapinte and S. Caillol, *Green Mater.*, 2018, 1–11.
- 273 W. Langdon, *Oxyalkylated polyglycerols and water-based lubricants prepared therefrom; US 4,265,774*, 1981.
- 274 Functional products inc., *Additives for Biobased Products*, 2012.
- 275 ELM, *Optibase*, 2015.
- 276 [https://www.crodalubricants.com/en-gb/products-and-applications/product-finder/product/162/Priolube\\_1\\_3986](https://www.crodalubricants.com/en-gb/products-and-applications/product-finder/product/162/Priolube_1_3986).
- 277 L. a. Quinchia, M. a. Delgado, T. Reddyhoff, C. Gallegos and H. a. Spikes, *Tribol. Int.*, 2014, **69**, 110–117.
- 278 M. A. Delgado, L. A. Quinchia, H. A. Spikes and C. Gallegos, *J. Clean. Prod.*, 2017, **151**, 1–9.
- 279 L. a. García-Zapateiro, J. M. Franco, C. Valencia, M. a. Delgado and C. Gallegos, *J. Ind. Eng. Chem.*, 2013, **19**, 1289–1298.
- 280 L. A. García-Zapateiro, J. M. Franco, C. Valencia, M. A. Delgado, C. Gallegos and M. V. Ruiz-Méndez, *Eur. J. Lipid Sci. Technol.*, 2013, **115**, 1173–1182.
- 281 K. Sato, *Chem. Eng. Sci.*, 2001, **56**, 2255–2265.
- 282 R. D. Lanjekar and D. Deshmukh, *Renew. Sustain. Energy Rev.*, 2016, **54**, 1401–1411.
- 283 P. Lv, Y. Cheng, L. Yang, Z. Yuan, H. Li and W. Luo, *Fuel Process. Technol.*, 2013, **110**, 61–64.
- 284 N. U. Soriano, V. P. Migo and M. Matsumura, *Fuel*, 2006, **85**, 25–31.
- 285 L. A. Quinchia, M. A. Delgado, J. M. Franco, H. A. Spikes and C. Gallegos, *Ind. Crops Prod.*, 2012, **37**, 383–388.
- 286 A. Serdari, E. Lois and S. Stournas, *Ind. Eng. Chem.*, 1999, 3543–3548.
- 287 G. Knothe, R. O. Dunn, M. W. Shockley and M. O. Bagby, *JAOCs, J. Am. Oil Chem. Soc.*, 2000, **77**, 865–871.
- 288 G. Biresaw, G. B. Bantchev and S. C. Cermak, *Tribol. Lett.*, 2011, **43**, 17–32.



## Chapter II:

*Poly(methyl ricinoleate) as bio-based viscosity modifier: synthesis optimization and characterization*

## Table of content

Introduction.....	89
1. Poly(methyl ricinoleate): State of the art.....	90
1.1. From castor oil to methyl ester ricinoleate .....	90
1.2. Methyl ester ricinoleate as a monomer for polyesters .....	92
2. Poly(methyl ricinoleate) synthesis optimization.....	95
2.1. Monomer purity.....	95
2.2. Screening of catalyst and temperature .....	96
2.3. Polymerization kinetic .....	100
2.4. Magnetic versus mechanical stirring .....	101
2.5. Conclusion: polymerization by transesterification optimization .....	102
3. PRic characterization.....	103
3.1. Chemical structure.....	103
3.1.1. <i>Poly(methyl ricinoleate)</i> .....	103
3.1.2. <i>Poly(methyl-12-hydroxystearate)</i> .....	106
3.2. Molecular weights determination .....	107
3.3. Thermal properties .....	109
3.3.1. <i>Degradation temperature</i> .....	109
3.3.2. <i>Thermo-mechanical properties</i> .....	110
4. Melt poly(methyl ricinoleate) rheological behavior .....	112
4.1. Dynamic mechanical analysis .....	113
4.1.1. <i>Linear domain</i> .....	113
4.1.2. <i>Complex viscosity as function of angular frequency, Time-temperature superposition (TTS)</i> .....	114
4.2. Viscosity determination by creep tests .....	118
4.3. Viscosity as a function of molecular weights.....	120
5. PRic and PHS behavior in solution .....	122
5.1. Preliminary study .....	122
5.1.1. <i>Choice of the mineral and organic base oils</i> .....	122
5.1.2. <i>Choice of the commercial additives</i> .....	126
5.1.3. <i>Determination of the appropriate additive concentration</i> .....	127

5.2. Effect of the PRic and PHS on oil viscosity.....	129
5.2.1. <i>Solubility on oils depending on the molecular weights</i> .....	129
5.2.2. <i>Effect on oil viscosity: towards thickening agents</i> .....	130
5.3. Conclusion.....	133
Conclusion .....	134
References.....	135
Experimental .....	137
Appendix.....	138



## Introduction

---

Some bio-based viscosity control additives have been developed but this field is still in its infancy. The bio-sourced base oils are more developed and some vegetable oils derivatives appeared to have promising properties as lubricants, particularly estolides. Indeed, these fatty acid-based oligomers exhibit natural high viscosity, oxidation resistance and good stability with respect to the temperature. With a proper molecular weight, they could also be considered as polymeric additives such as viscosity modifiers. This PhD study focused on a particular estolide, namely poly(methyl ricinoleate), (PRic). PRic is obtained by polycondensation of methyl ricinoleate, a fatty acid methyl ester extracted from castor oil. It is a fully amorphous polymer, with a comb structure and thus appears to be a good candidate as potential viscosity modifier for lubricant. A short literature review will be given on this particular bio-based polyester, in the first section of this chapter.

As far as we could find in literature data, polyricinoleate has been barely described as additive for lubricant. Kelly and Hayes claimed the use of PRic oligomer as an environmentally-friendly lubricant.<sup>1</sup> Gallegos and coll. found that addition of ricinoleic estolide at the concentration of 50 wt.% in castor oil increases significantly the VI from 111 up to 135.<sup>2</sup> However, to the best of our knowledge, no additional study about the use of PRic as viscosity modifier was reported.

In this chapter, the conditions to achieve high molecular weight PRic will be first addressed as it is known that high molecular weight polymers are generally required to be efficient viscosity modifiers. A series of poly(methyl ricinoleate)s and their saturated equivalents, poly(hydroxy-12-stearate)s (PHS) from hydrogenated methyl ricinoleate, of different molecular weights were prepared to evaluate the impact of  $M_w$  on the rheological behavior. Finally, both saturated and unsaturated polyesters were tested as viscosity modifiers in organic and mineral lubricant base oils.

# 1. Poly(methyl ricinoleate): State of the art

## 1.1. From castor oil to methyl ester ricinoleate

As it was already discussed in the previous chapter, the global concern over environmental pollution has led to a growing interest in the use of renewable resources in both lubricants and polymer fields. The abundant availability and relatively low cost of vegetable oils make them one of the most important sustainable resources for the chemical and polymer industries.<sup>3-6</sup>

Vegetable oils are composed of different triglycerides resulting from the esterification of glycerol with three fatty acids (FA) with varied structures. Fatty acids account for 95% of the total weight of triglycerides and the most common structures are schematically represented in Figure II-1.<sup>4</sup> Although fatty acid pattern varies between crops, location, growth conditions and seasons, fatty acid content is characteristic of each plant oil.<sup>4</sup>

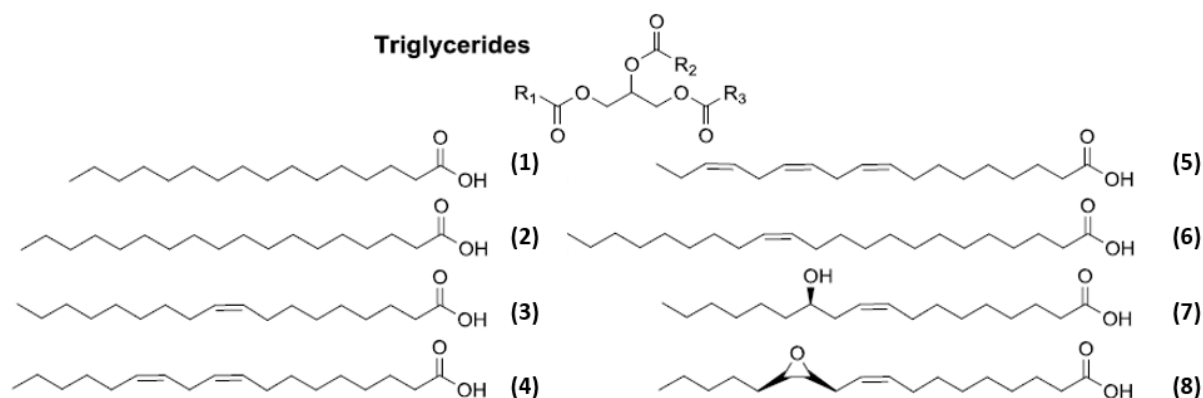


Figure II-1: Chemical structure of triglycerides and common FA found in vegetable oils: (1) palmitic acid, (2) stearic acid, (3) oleic acid, (4) linoleic acid, (5) linolenic acid, (6) erucic acid, (7) ricinoleic acid, (8) vernolic acid<sup>4</sup>

Thanks to the natural presence of reactive functions, such as hydroxyl or double bonds, vegetable oils have been used as starting materials for bio-based polymer thermoplastics and thermosets, using raw oils or functionalized triglycerides as monomers. However, the correlation between the polymer structure and its properties is hardly feasible due to the variation of fatty acids structure in triglycerides.<sup>4-6</sup> In the light of this, fatty acids and fatty acid methyl esters (FAMES) can be recovered from triglycerides respectively by saponification and transesterification with methanol in such a purity that they can be used as building blocks for the synthesis of well-defined thermoplastic polymers with controlled properties.<sup>5,7</sup>

Nowadays, 80% of vegetable oils are produced for food and feed purposes but some, like castor and linseed oils, are almost solely used for industrial applications.<sup>3,8,9</sup> Raw castor seeds, from *Ricinus communis* of the family of Euphorbiaceae, contain toxic compound such as ricin, ricinine and an allergen leading the oil to be classified as non-edible. Nevertheless, within a proper purification, it appears to be safe and biocompatible.<sup>7,10-13</sup>

Castor oil is a viscous, pale yellow, non-volatile and non-drying oil. In 2016-2017, 700 ktons have been produced all around the world.<sup>13</sup> India is currently the world's largest exporter of castor oil with more than 70% of the total volume, followed by China, Brazil and Thailand. It has attracted much attention in recent years for the preparation of functional materials and green polymers thanks to its particular composition. Actually, castor oil is one of the few naturally occurring triglycerides that approaches being a pure compound with up to 90% of ricinoleic acid, i.e. (R)-12-hydroxy-9Z-octadecenoic acid, and its chemical composition remains relatively constant regardless to the grown condition (Table II-1).<sup>7,11-13</sup>

Table II-1: Castor oil composition<sup>7</sup>

Fatty acid	Molecular formula	Percentage [%]
Palmitic	C <sub>16</sub> H <sub>32</sub> O <sub>2</sub>	0.8 – 1.1
Stearic	C <sub>18</sub> H <sub>36</sub> O <sub>2</sub>	0.7 – 1.0
Oleic	C <sub>18</sub> H <sub>34</sub> O <sub>2</sub>	2.2 – 3.3
Linoleic	C <sub>18</sub> H <sub>32</sub> O <sub>2</sub>	4.1 – 4.7
Linolenic	C <sub>18</sub> H <sub>30</sub> O <sub>2</sub>	0.5 – 0.7
Ricinoleic	C <sub>18</sub> H <sub>34</sub> O <sub>3</sub>	87.7 – 90.4

This high content of ricinoleic acid makes castor oil unique and highly valuable compared to other vegetable oils. It can be recovered from triglycerides to its acidic form by saponification or to an ester by methanolysis.<sup>7,13</sup> The natural presence of a hydroxyl group, a carbon-carbon double bond and a carboxyl or ester terminal function in this particular fatty acid offers a large palette of reaction sites for the preparation of many derivatives; some examples being illustrated in Figure II-2.<sup>4,7,11,14</sup>

Methyl ricinoleate is frequently derivatized by hydrogenation, leading to several compounds such as methyl-12-hydroxystearate.<sup>13</sup> The dehydration, while the hydroxyl group and one of its hydrogen atoms are removed, yields the formation of a regioisomeric second double bond, depending of the dehydration conditions.<sup>7</sup> The methyl ricinoleate pyrolysis leads to the

formation of heptaldehyde and methyl-10-undecenoate, the latter being precursor to PA-11.<sup>7</sup> Capryl alcohol and sebacic acid are formed by ricinoleic acid hydrolysis.

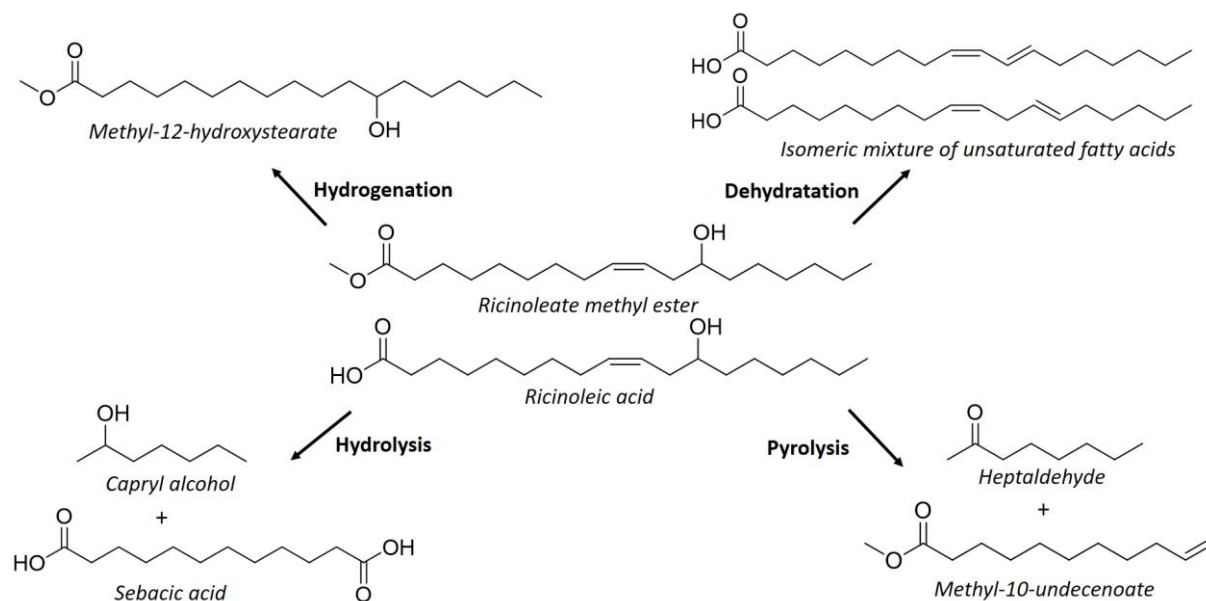


Figure II-2: Examples of methyl ricinoleate and ricinoleic acid derivatized<sup>10,15</sup>

In addition of these major chemical modifications, other reactions can be performed, such as reduction, amidation or halogenation of the acid or ester group, epoxidation, sulfation or thiol-ene reaction on the double bond, alkoxylation, esterification, urethane formation on the alcohol group etc. Moreover, methyl ricinoleate by its natural multifunctionality represents a high interest as a renewable monomer which can be readily polymerized.<sup>7,10,13–15</sup>

## 1.2. Methyl ester ricinoleate as a monomer for polyesters

Methyl ricinoleate and its derivatives are used as precursors for the synthesis of several types of polymers. One of the most relevant industrial success is the synthesis of PA-11 and PA-6,10, fully bio-sourced polyamides.<sup>5,15,16</sup> In addition, methyl ricinoleate derivatives are used as precursors for other types of polymers such as polyurethanes<sup>17</sup>, polyhydroxyurethanes<sup>18</sup>, polyethers<sup>19</sup> or polyanhydrides<sup>20</sup>. However, unmodified methyl ricinoleate or ricinoleic acid are almost exclusively used for the synthesis of bio-based polyesters.<sup>7,11</sup> Castor oil fatty acids and esters have been described in literature as comonomers for numerous polyester syntheses but their homopolymerization by self-condensation is more rarely reported.<sup>11,21,22</sup>

Both methyl ricinoleate and ricinoleic acid were used as monomers leading respectively to poly(methyl ricinoleate) and poly(ricinoleic acid), so called PRic with an ester or an acid moiety at the chain end, respectively. This self-condensation can be performed using organometallic, organic or enzymatic catalysis. PRic is already a commercial polymer, produced by ITERG for instance.

Domb and coll.<sup>23</sup> developed macrolactones from ricinoleic acid. First, ricinoleic acid lactones were synthesized with dicyclohexylcarbodiimide and (dimethylamino)pyridine as coupling agent. After purification, the lactones were polymerized by ring-opening in the presence of Y(OiPr), Sn(Oct)<sub>2</sub> or Me<sub>3</sub>SiONa. Only oligomers were obtained. A maximum M<sub>n</sub> of 3250 g.mol<sup>-1</sup> was reached with Yttrium isopropoxide as catalyst. Gallegos and coll.<sup>2</sup> performed ricinoleic acid estolides by polycondensation in the presence of sulfuric or perchloric acid. A mixture of poly(ricinoleic acid), unreacted fatty acids and some other undesired products were obtained with molecular weight around 3000 g.mol<sup>-1</sup>. These polymers demonstrated interesting properties when blended with vegetable oil at high concentration; from 15 wt.% up to 50 wt.%; the viscosity was increased and the crystallization process was delayed, yielding to better low-temperature properties. Cramail et al.<sup>24</sup> developed poly(ricinoleic acid) using Ti(OiPr)<sub>4</sub> as catalyst. Polymers with molecular weight of 11 kg.mol<sup>-1</sup> were obtained and used as precursors for copolymerization with lactic acid. All these syntheses led to relatively low molecular weight, i.e. a maximum of 11 kg.mol<sup>-1</sup> was reached.

Polyricinoleic acid has been also synthesized from acid ricinoleate using lipase CAL-B as biocatalyst.<sup>1</sup> The synthesis was performed in bulk for several months and led to mixtures with 57% monomer, dimer and tetramer. This mixture was then condensed with polyol in order to obtain star polymers with molecular weights of 5 kg.mol<sup>-1</sup> in average. The product formed exhibits Viscosity Index up to 155 and a low melting temperature below -7.5 °C suggesting their use as lubricant.<sup>1</sup> Matsumura and coll.<sup>25-29</sup> described the polycondensation of ricinoleic acid and methyl ricinoleate using an enzymatic catalyst. Firstly<sup>26,27</sup>, the highest molecular weight poly(methyl ricinoleate) with M<sub>w</sub> of 100 kg.mol<sup>-1</sup> was obtained using methyl ricinoleate as monomer and 150 wt.% of immobilized lipase from *Pseudomonas cepacia* (IM-CA) as catalyst. The synthesis was performed during seven days at 80 °C in bulk in the presence of molecular sieves 4 Å. After purification, the product was an amorphous viscous liquid at room temperature with a T<sub>g</sub> of -75 °C and revealed to be biodegradable. The internal double bonds

were then used to crosslink the polymer with peroxides. The same authors<sup>25</sup> performed the polycondensation of methyl 12-hydroxystearate, obtained from hydrogenation of methyl ricinoleate. After 4 days reaction at 90 °C in toluene with 50 wt.% of IM-CA, a polyester of 118 kg.mol<sup>-1</sup> was obtained. The latter polyester showed a crystallization at -40 °C and a good biodegradability. Matsumura and coll.<sup>28</sup> then improved the synthesis by increasing the reaction temperature up to 120 °C and by removing the solvent. In these bulk conditions, poly(methyl 12-hydroxystearate) with  $M_w$  of 232 kg.mol<sup>-1</sup> was obtained after 5 days. Finally, the same group<sup>29</sup> used also lipase catalyst to epoxidize methyl ricinoleate with H<sub>2</sub>O<sub>2</sub> followed by an enzymatic catalysed polycondensation as illustrated in Figure II-3.

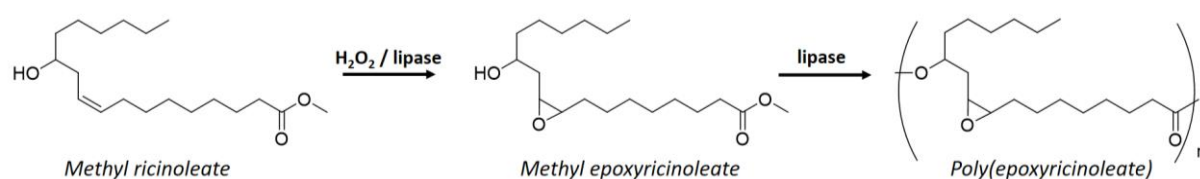


Figure II-3: Enzymatic synthesis of high molecular weight polyepoxyricinoleate<sup>28</sup>

The polyepoxyricinoleate reached molecular weight up to 272 kg.mol<sup>-1</sup> after five days at 80 °C using 100 wt.% of lipase PS-IM. The so-formed polymer was then cross-linked and evaluated as a biodegradable film.

To conclude this section, poly(methyl ricinoleate) was synthesized by ring-opening polymerization after chemical modification of ricinoleic acid to lactone. Only oligomers were formed using this method. Matsumura and coll.<sup>26,30</sup> described the enzymatic-catalyzed synthesis of high molecular weights amorphous poly(methyl ricinoleate) (200 kg.mol<sup>-1</sup>), well-soluble in apolar solvent. However, these systems required a large amount of expensive enzyme, with a minimum content of 50 wt.% with respect to the monomer, very long reaction times and the use of solvents.

Gallegos and coll.<sup>2</sup> performed low molecular weight poly(methyl ricinoleate)s. Once blended at 50 wt.% with vegetable oils, poly(methyl ricinoleate) has an excellent miscibility with oils and exhibits a thickening effect. An increase of PRic molecular weight should enhance this effect and allow its use at lower concentration. Its miscibility with vegetable oils such as apolar solvent could bring a compatibility with lubricant base oil. In addition, it is biodegradable<sup>11</sup> which is in accordance with the environmental requirement for bio-lubricants. As a result, high molecular weight poly(methyl ricinoleate) could be a promising bio-based viscosity modifier.

## 2. Poly(methyl ricinoleate) synthesis optimization

It has been mentioned in the previous chapter that high molecular weight is a key feature of viscosity modifiers to reach desirable thickening efficiency. Consequently, high molecular weight poly(methyl ricinoleate) is needed. Methyl ricinoleate as well as ricinoleic acid can be used as precursor to polyricinoleate. Nevertheless, the methyl ricinoleate polymerization sub-product is methanol while it is water in the case of ricinoleic acid. Methanol being more volatile than water, it is generally easier to remove it during the polymerization reaction in order to shift the equilibrium towards higher conversion. For this reason, methyl ricinoleate was selected as precursor to PRic.

In this scope, the polycondensation reaction conditions of methyl ricinoleate were investigated to achieve high molecular weight polymers (Figure II-4). First of all, methyl ricinoleate was dried overnight at 70 °C under dynamic vacuum to remove water and potential solvent and volatile impurity traces. After the addition of catalyst, a ramp of temperature was applied from 20 °C to 140 °C to let oligomerization to occur and avoid the possible monomer degradation. The polymerization temperature was then applied and maintained for 21 hours under magnetic stirring.



Figure II-4: Reaction overview of methyl ricinoleate polycondensation by transesterification

Different polymerization conditions were evaluated by varying the monomer purity, the type of catalysts and the temperature. The reaction duration was also investigated and a mechanical mode of stirring was then used to increase final polymer molecular weight.

### 2.1. Monomer purity

Methyl ricinoleate with two grades of purity (purity of 96% GC from ITERG and purity of 99%+ from Nu-check Prep) were polymerized at 180°C with 1 wt.% titanium (IV) isopropoxide ( $\text{Ti}(\text{O}i\text{Pr})_4$ ) as catalyst for a given reaction duration of 8 hours. Two other polymerizations were

performed at 220°C with 0.1 wt.% of Ti(O*i*Pr)<sub>4</sub> as catalyst during 24 hours. Results are reported in Table II-2.

Table II-2: Effect of the monomer purity on the polytransesterification

Entry	Purity	Catalyst	wt.% <sup>1</sup>	T (°C) <sup>2</sup>	Duration (h)	M <sub>n</sub> (g.mol <sup>-1</sup> ) <sup>3</sup>	M <sub>w</sub> (g.mol <sup>-1</sup> ) <sup>3</sup>	Đ <sup>3</sup>
P1	96%	Ti(O <i>i</i> Pr) <sub>4</sub>	1	180	8	5000	9000	1.8
P2	99%					8000	15000	1.9
P1-bis	96%	Ti(O <i>i</i> Pr) <sub>4</sub>	0.1	220	24	7200	14300	2
P2-bis	99%					9000	29000	3.2

**Reaction conditions: 8 hours reaction, bulky solution under vacuum**

**1 Catalyst concentration as weight percentage with respect to the monomer**

**2 Temperature of the last stage of polymerization**

**3 Obtained by SEC in THF – PS calibration**

As can be seen from Table II-2 (P1 vs P2) and as could be expected, the purity of the monomer is a crucial parameter to achieve high M<sub>w</sub> poly(ricinoleate). Independently of the reaction conditions, M<sub>w</sub> of P2 > M<sub>w</sub> of P1. Impurities present in methyl ricinoleate with a purity of 96% GC are mainly other fatty acids from the methanolysis of castor oil. Such derivatives could react as by-products such as end-capping agent during the polytransesterification and thus prevent the polymer growth. Consequently, methyl ricinoleate with a purity of 96% GC can be used for the synthesis of PRic oligomers while high purity monomer is required to obtain higher molecular weight poly(methyl ricinoleate)s.

## 2.2. Screening of catalyst and temperature

In order to determine the best catalytic system for the methyl ricinoleate transesterification, a scope of different commercially available catalysts was selected: an organic base, 1,5,7-triazabicyclo[4.4.0]dec-5-ene (TBD) and metallic catalysts including zinc acetate (Zn(OAc)<sub>2</sub>), sodium methoxide (NaOMe), titanium (IV) isopropoxide (Ti(O*i*Pr)<sub>4</sub>) (see Figure II-5). The latter catalysts are all well described as transesterification catalysts in literature.<sup>31-33</sup> Following the literature, the enzymatic route has been dismissed because of the drawbacks already discussed, i.e. the use of a minimum of 50 wt.% of an expensive enzyme and the long reaction times.<sup>26,28</sup>

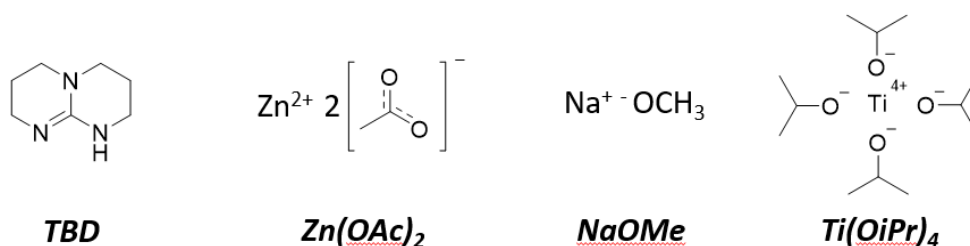


Figure II-5: Transesterification catalysts tested for methyl ricinoleate polycondensation

Catalyst concentrations of 0.1 wt.%, 1 wt.% and 5 wt.% were tested. For each catalyst concentration, three temperatures were screened: 140 °C, 180 °C and 220 °C. As all the polycondensations were performed in bulk, the crude polymers formed were analyzed by size exclusion chromatography (SEC) without any further purification. Polymerization data are reported in Table II-3.

Table II-3: Preliminary investigations of the polytransesterification of methyl ricinoleate

Entry	Catalyst	Amount (wt.%)	Temperature <sup>1</sup> (°C)	M <sub>n</sub> (g.mol <sup>-1</sup> ) <sup>2</sup>	M <sub>w</sub> (g.mol <sup>-1</sup> ) <sup>2</sup>	Đ <sup>2</sup>
P3	TBD	0.1	140	No polymer		
P4	TBD	1	140	1200	1300	1.1
P5	TBD	5	140	2500	5000	2
P6		0.1	140	No polymer		
P7	Zn(OAc) <sub>2</sub>	0.1	180	1700	3600	2
P8		0.1	220	2100	6300	3
P9		1	140	1600	2400	1.5
P10	Zn(OAc) <sub>2</sub>	1	180	5900	23600	4
P11		1	220	3400	7480	2.2
P12		0.1	140	8600	28400	3.3
P13	NaOMe	0.1	180	11800	34200	2.9
P14		0.1	220	1100	1300	1.2
P15		1	140	8500	11000	3.3
P16	NaOMe	1	180	16200	40100	2.5
P17		1	220	1700	2500	1.5
P18		0.1	140	No polymer		
P19	Ti(OiPr) <sub>4</sub>	0.1	180	3200	5400	1.7
P20		0.1	220	9000	29000	3.2
P21		1	140	15000	28500	1.4
P22	Ti(OiPr) <sub>4</sub>	1	180	13300	61000	4.6
P23		1	220	13300	51000	3.8
P24	Ti(OiPr) <sub>4</sub>	5	180	3100	8100	2.6

**Reaction conditions: 24 hours reaction, in melt under vacuum**

**1 Temperature of the last stage of polymerization**

**2 Obtained by SEC in THF – PS calibration**

Firstly, all the polymerizations performed at 140 °C led to low molecular weight poly(methyl ricinoleate)s. Except the case of P21 performed with Ti(OiPr)<sub>4</sub>, M<sub>n</sub> < 10 000 g.mol<sup>-1</sup> were obtained. As expressed in Table II-3 (P3 to P5 entries), polymerization of methyl ricinoleate in

the presence of TBD was not very efficient whatever the catalyst concentration used. In this peculiar case, the main reason of the poor monomer reactivity was attributed to the too low temperature (140 °C), value that could not be increased because of catalyst degradation/sublimation above this temperature.

As far as organometallic catalysts are concerned, the activity of the catalyst tested increases in the order  $Zn \ll Na < Ti$ . Independently of the other conditions, such as temperature or catalyst concentration,  $Zn(OAc)_2$  has a poor activity as catalyst, leading to PRic with  $M_n < 6000 \text{ g}\cdot\text{mol}^{-1}$ . NaOMe was widely described in oleochemistry for the transesterification of crude vegetable oils<sup>34,35</sup> but much less for transesterification polymerization.<sup>33,36</sup> Surprisingly, it appears to have a high catalytic activity, as produces PRic with  $M_n$  up to 16 000  $\text{g}\cdot\text{mol}^{-1}$  (P16) with lower dispersity than the PRics obtained with  $Ti(OiPr)_4$  (P22), e.g.  $\mathcal{D} = 2.5$  and  $\mathcal{D} = 4.6$ , respectively. Sodium methoxide appeared to be a promising catalyst for PRic synthesis.

Nevertheless, the highest  $M_w$  was obtained with  $Ti(OiPr)_4$  (P22,  $M_w = 61\,000 \text{ g}\cdot\text{mol}^{-1}$ ) at 180°C. According to literature, for the case of transesterification with hydroxyl-ester interchange reaction,  $Ti(OiPr)_4$  was largely described as a very efficient catalyst leading to high molecular weight polymers.<sup>31,33,37-43</sup> Investigations were performed on step-growth polymers such as poly(ethylene naphthalate)<sup>36</sup>, poly(ethylene terephthalate) (PET)<sup>33,39</sup> and, more recently, on linear bio-based polyesters<sup>31,38,41</sup>. Despite that kinetic studies in the melt are difficult and that reaction mechanisms not yet fully understood, the polymerization of methyl ricinoleate by transesterification may take place as displayed in Figure II-6.  $Ti(OiPr)_4$  acts as a Lewis acid to initiate the condensation reaction. According to this electrophilic mechanism, the ester group is first activated by coordination with the metal species. By this coordination, the electron density of the carbonyl atom becomes lower which facilitates the nucleophilic addition of the hydroxyl group from the alcohol.<sup>33,39,40</sup>

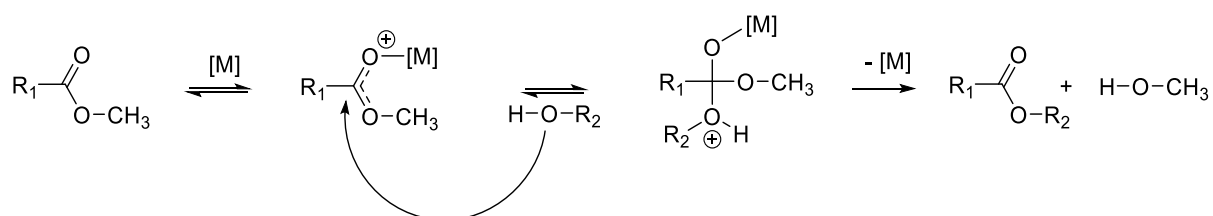


Figure II-6: Proposed mechanism of transesterification polymerization activated by a titanium catalyst. [M]=  $Ti(OiPr)_4$

Surprisingly, high polymerization temperature (220 °C) did not permit to achieve PRic with higher molecular weight. This is particularly true in the case of NaOMe catalysed-polymerization where a drop of molecular weight from  $M_n = 16\,200\text{ g.mol}^{-1}$  (P16) to  $M_n = 1\,700\text{ g.mol}^{-1}$  (P17) was observed. Similar trend was observed for  $\text{Zn(OAc)}_2$  catalysed-polymerization. However, the molecular weight obtained with  $\text{Ti(OiPr)}_4$  are similar, same  $M_n$  of  $13\,300\text{ g.mol}^{-1}$  between syntheses performed at 180 °C (P22) and 220 °C (P23). Therefore, the loss of reactivity at 220 °C could be attributed to the NaOMe and  $\text{Zn(OAc)}_2$  thermal deactivation. In the case of  $\text{Ti(OiPr)}_4$ , which is more stable with temperature, it could be expected that higher PRic molecular weight would have been obtained at 220°C than at 180°C. The molecular weight stagnation could not be due to polymer thermal decomposition. Indeed, as it will be detailed in the next section, PRic starts to degrade above 300 °C. It is then supposed that competitive reactions such as interchains transesterification could be more favoured at 220 °C than 180 °C.

As reported in Table II-3, the use of 1 wt.% of catalyst instead of 0.1 wt.% led to higher molecular weight polymers. It has been largely described in literature that catalyst concentration has a strong effect on transesterification polymerization.<sup>31,36,38-40</sup> Therefore, the effect of  $\text{Ti(OiPr)}_4$  catalyst concentration on the PRic synthesis was investigated. The conditions of 180 °C in bulk for 24 hours reaction time with a loading of  $\text{Ti(OiPr)}_4$  range from 0.1 to 5wt%.  $M_w$  reaches a maximum of  $61\,000\text{ g.mol}^{-1}$  with 1 wt.% of  $\text{Ti(OiPr)}_4$ . At the concentration of 5 wt.%, the PRic  $M_w$  decreases significantly down to  $8\,100\text{ g.mol}^{-1}$ . This phenomenon has been previously described by Gamlen and coll.<sup>39</sup> in the case of PET synthesis. It was found that the catalyst which enhances the propagation to a greater extent also catalyzes the polymer interchain transesterification efficiently. Beyond the optimal concentration, there is a competition between the end group sites; responsible of the chain growth; and the ester functions along the polymer backbone allowing chain scission. Gross and co-workers<sup>38</sup> showed the same phenomenon in the case of the polycondensation of hydroxytetradecanoic acid as well as Testud et al.<sup>32</sup> in the case of hyperbranched biobased polyesters synthesis.

To conclude this part, PRic syntheses were performed in order to improve the molecular weight. At 140 °C, mostly oligomers are obtained. The highest  $M_w$  (61 000 g.mol<sup>-1</sup>) were reached at 180 °C in the presence of Ti(O*i*Pr)<sub>4</sub>, which revealed to be the best catalyst tested. Regarding the amount of catalyst, a concentration of 1 wt.% was selected as the appropriate concentration to permit catalytic activity while to limit reaction chain transfer. As a conclusion, a temperature of 180°C and a Ti(O*i*Pr)<sub>4</sub> concentration of 1 wt.% was found as the most suitable conditions to achieve PRic with molecular weight up above 60 000 g.mol<sup>-1</sup>.

### 2.3. Polymerization kinetics

All the previous polymerizations were compared for a duration of 24 hours but, as transesterification polymerization is a slow process, an optimization of this parameter is required. To that purpose, a kinetic study was monitored by SEC analyses of aliquots.  $M_n$  and  $M_w$  as a function of the reaction time are plotted in Figure II-7 (1).

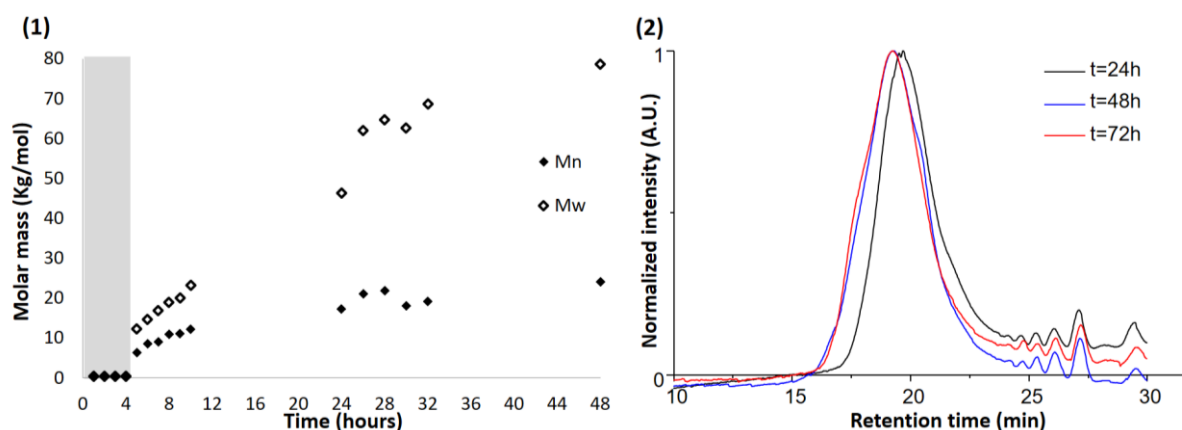


Figure II-7: P25 polymerization (1wt.% Ti(O*i*Pr)<sub>4</sub>, 180 °C, in the melt) .(1) Kinetic study followed by SEC in THF using PS calibration, the grey zone is the oligomerization state. (2) SEC traces of 24, 48 and 72 hours duration

After the first 3 hours, the steady temperature of 180°C was applied. The polymerization starts after 4 hours, with the temperature increase. During the first 24 hours reaction time,  $M_n$  and  $M_w$  increase similarly, with a constant dispersity around 1.8. Then  $M_n$  reaches a plateau while  $M_w$  continues to increase together with the dispersity to reach  $M_n = 24 \text{ kg.mol}^{-1}$ ,  $M_w = 75 \text{ kg.mol}^{-1}$  and  $\mathcal{D} = 3.5$ . As the dispersity increases with the reaction time, it is supposed that secondary reaction could occur such as chain transfer. SEC was performed on aliquots at  $t = 24 \text{ h}$ ,  $t = 48 \text{ h}$  and  $t = 72 \text{ h}$ ; SEC traces are illustrated in Figure II-7 (2). It appears that molecular

weights remain similar between 48h and 72 hours of reaction. As a result, 48 hours reaction is determined as the optimized reaction time.

## 2.4. Magnetic versus mechanical stirring

One major issue in bulk polycondensation is the high viscosity of the polymerization media. No longer after the oligomeric stage, the magnetic stirrer was most often blocked impeding an efficient stirring leading to a stagnation of the reactive function conversion and  $M_n$  values, see Figure II-7 (1).

As a result, magnetic stirring was replaced by a mechanical stirring at 200 rpm. The set-up is shown in Figure II-8 (1). The PRic molecular weights obtained by mechanical stirring (P26) were compared to the ones obtained by magnetic stirring (P25). The corresponding SEC traces are represented in Figure II-8 (2). As shown in Table II-4, higher  $M_n$  and  $M_w$  values were obtained using mechanical stirring, i.e. 36 400  $\text{g}\cdot\text{mol}^{-1}$  for P26 instead of 24 000  $\text{g}\cdot\text{mol}^{-1}$  for P25. In addition, the dispersity increases from 3.2 up to 4.6 and  $M_w$  increases up to 168 000  $\text{g}\cdot\text{mol}^{-1}$ . This result attests a better monomeric diffusion in the mixture and a proper contact between reactive functions. Short oligomeric peaks observed in the SEC traces for P26 suggest the appearance of some PRic cyclization leading to low molecular weight cyclic polymers. Once again, the dispersity increase suggests that secondary reaction occurred, such as chain transfer reaction. Indeed, polymerizations performed following P26 reaction conditions, i.e. the optimized conditions, led sometimes to an insoluble PRic fraction in usual solvent.

Table II-4: Influence of the mode of stirring on the PRic molecular weights obtained by polycondensation

Entry	Mode of stirring	$M_n$ ( $\text{g}\cdot\text{mol}^{-1}$ ) <sup>1</sup>	$M_w$ ( $\text{g}\cdot\text{mol}^{-1}$ ) <sup>1</sup>	$\mathcal{D}$ <sup>1</sup>
P25	Magnetic	24 000	78 600	3.2
P26	Mechanical	36 400	168 400	4.6

**Reaction conditions: 48 hours reaction, 180°C, 1wt.% of  $\text{Ti}(\text{OiPr})_4$  bulky solution under vacuum, 200 rpm**  
**1 Obtained by SEC in THF – PS calibration**

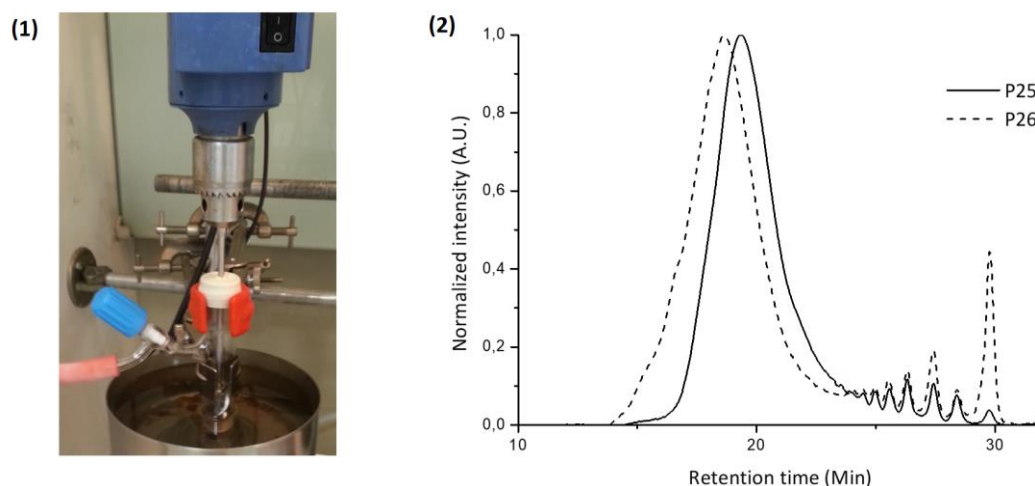


Figure II-8: (1) Mechanical stirring set-up and (2) SEC traces of P25 in solid line and P26 in dashed line, performed in THF

## 2.5. Conclusion: polymerization by transesterification optimization

As the transesterification reaction is really specific to the monomer considered, reaction conditions parameters were optimized. A methyl ricinoleate with a purity of 99% GC is required to obtain high molecular weight PRic.  $\text{Ti}(\text{O}i\text{Pr})_4$  appeared to have a high catalytic activity. In order to enhance polymerization while limiting the secondary reactions, the amount of 1 wt.% of  $\text{Ti}(\text{O}i\text{Pr})_4$  as catalyst and a reacting temperature of 180 °C were selected. Finally, a mechanical stirring was used to force the monomer diffusion in highly viscous media. The mechanical mode of stirring and the longest reaction time, i.e. 48 hours, increase the PRic  $M_w$  above 160  $\text{kg}\cdot\text{mol}^{-1}$  as well as the dispersity (i.e.  $\bar{D} = 4.6$  for optimized reaction conditions of P26). This dispersity increase suggests the occurrence of side reactions.

Still, polymerization optimization led to PRic  $M_w$  above 160  $\text{kg}\cdot\text{mol}^{-1}$ . Such molecular weights are in the range of the ones obtained by enzymatic route.<sup>26</sup> PRic with a large range of  $M_w$  can thus be designed in order to be evaluated as viscosity modifiers and methyl ricinoleate derivatives such as methyl 12-hydroxystearate could also be polymerized using the optimized reaction conditions.

### 3. PRic characterization

---

Two kinds of bio-based polyesters, i.e. poly(methyl ricinoleate) (PRic) and poly(methyl-12 hydroxystearate) (PHS) were synthesized using the optimized reaction conditions. These two polyesters, schematically represented in Figure II-9, discriminate only by the presence of a *cis*-double bond between the C9 and C10 carbons in the case of PRic.

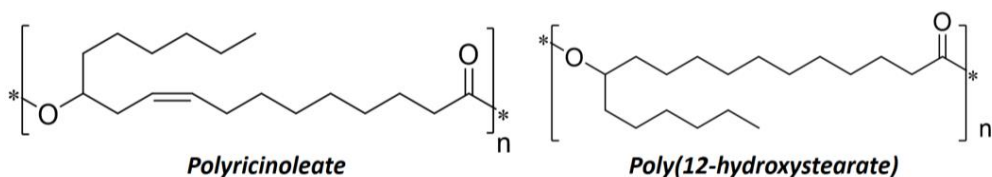


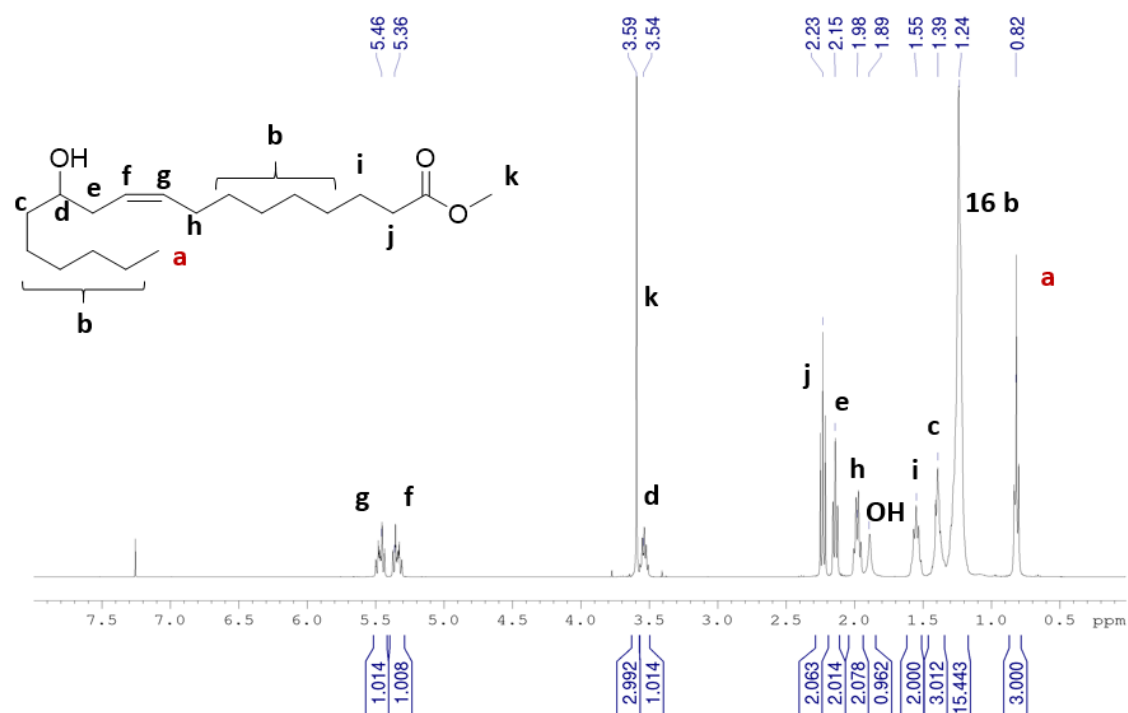
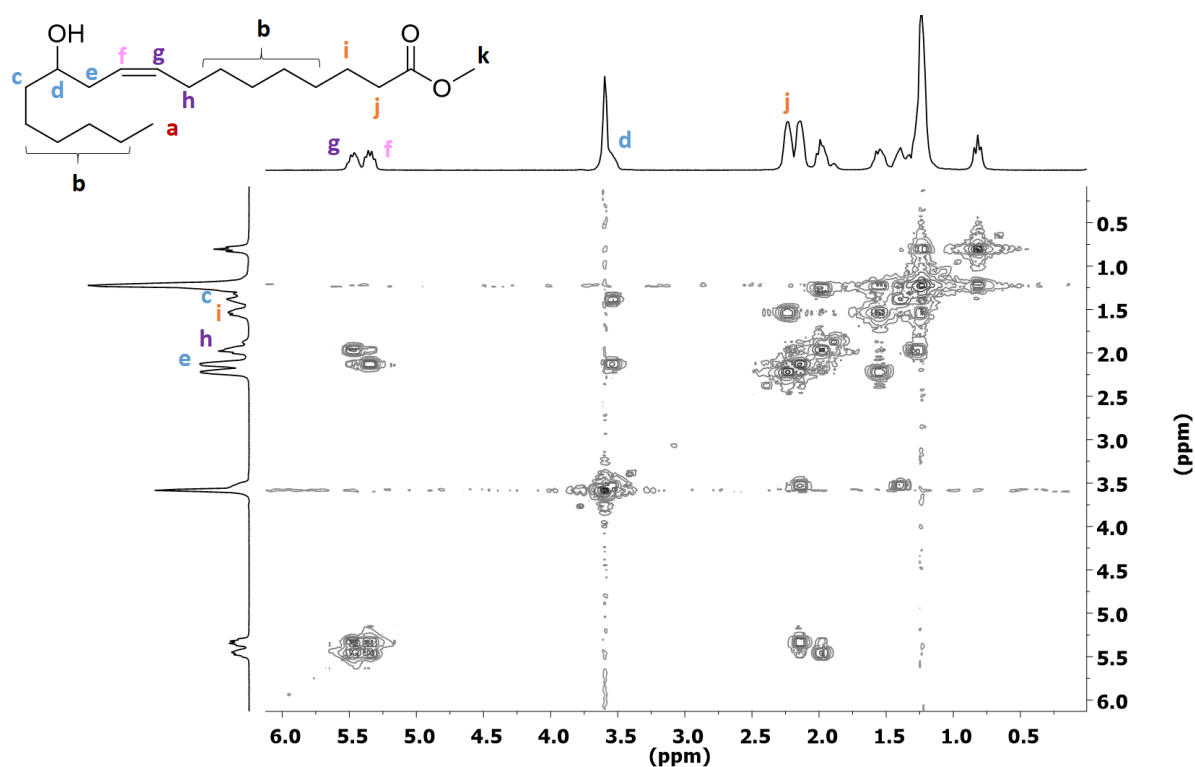
Figure II-9: PRic and PHS chemical structure

The chemical structure of these two polyesters have been characterized by  $^1\text{H}$  NMR. The effect of the polymer molecular weight on the thermal and rheological features was also investigated.

#### 3.1. Chemical structure

##### 3.1.1. Poly(methyl ricinoleate)

First of all, methyl ricinoleate was characterized by  $^1\text{H}$  NMR as well as a dimensional NMR technique  $^1\text{H}$ - $^1\text{H}$  COSY. As illustrated in Figure II-10, the NMR spectrum was fully assigned and the structure of methyl ricinoleate confirmed, with the help of  $^1\text{H}$ - $^1\text{H}$  COSY NMR, spectra are displayed in Figure II-11.

Figure II-10:  $^1\text{H}$  NMR spectra of methyl ricinoleate in  $\text{CDCl}_3$ Figure II-11:  $^1\text{H}$ - $^1\text{H}$  COSY NMR spectra of methyl ricinoleate

Poly(methyl ricinoleate) (P26) was analyzed by  $^1\text{H}$  NMR and its spectrum compared to the one of methyl ricinoleate. The two spectra are displayed in Figure II-12. The peak at 0.82 ppm, representative of the methyl protons of the fatty acid, is used as reference. The

polycondensation is confirmed by the disappearance of the characteristic methoxy peak at 3.59 ppm and the shift of the peak corresponding to the proton in  $\alpha$  position of the OH group from 3.50 ppm to 4.88 ppm. In addition, there is a small shift of the protons in  $\beta$  position of the OH group, from 1.40 ppm to 1.55 ppm and 2.15 ppm to 2.26 ppm. These assignments are also confirmed by  $^1\text{H}$ - $^1\text{H}$  COSY NMR (Figure II-13).

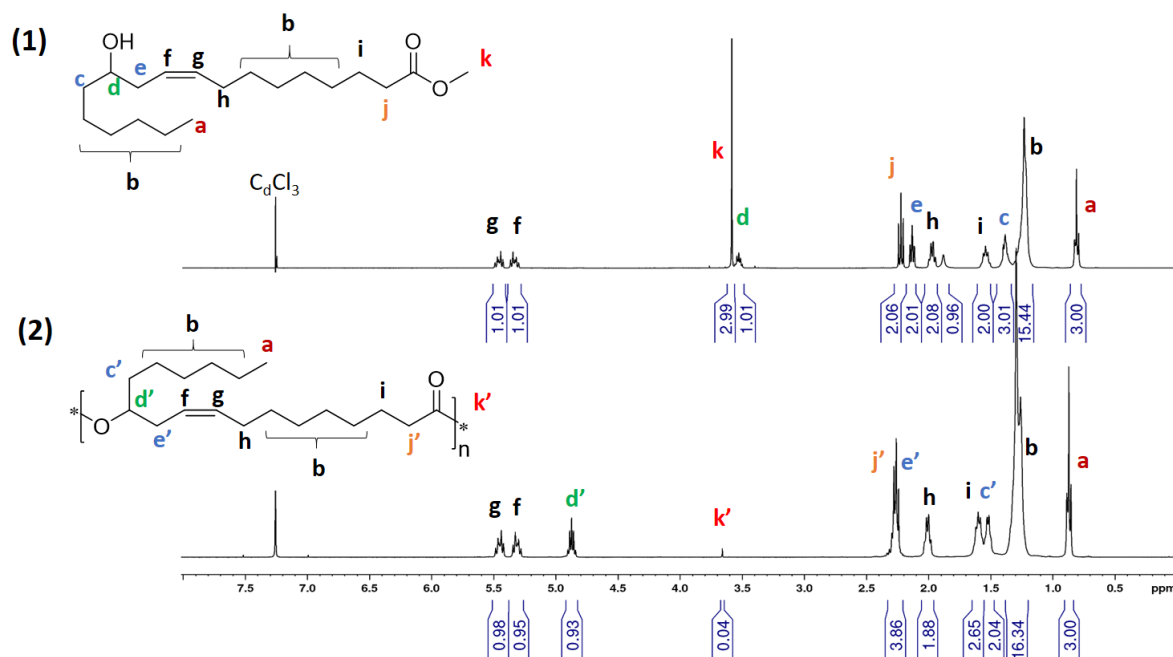


Figure II-12:  $^1\text{H}$  NMR spectra in  $\text{CDCl}_3$  of (1) methyl ricinoleate monomer and (2) poly(methyl ricinoleate), P26

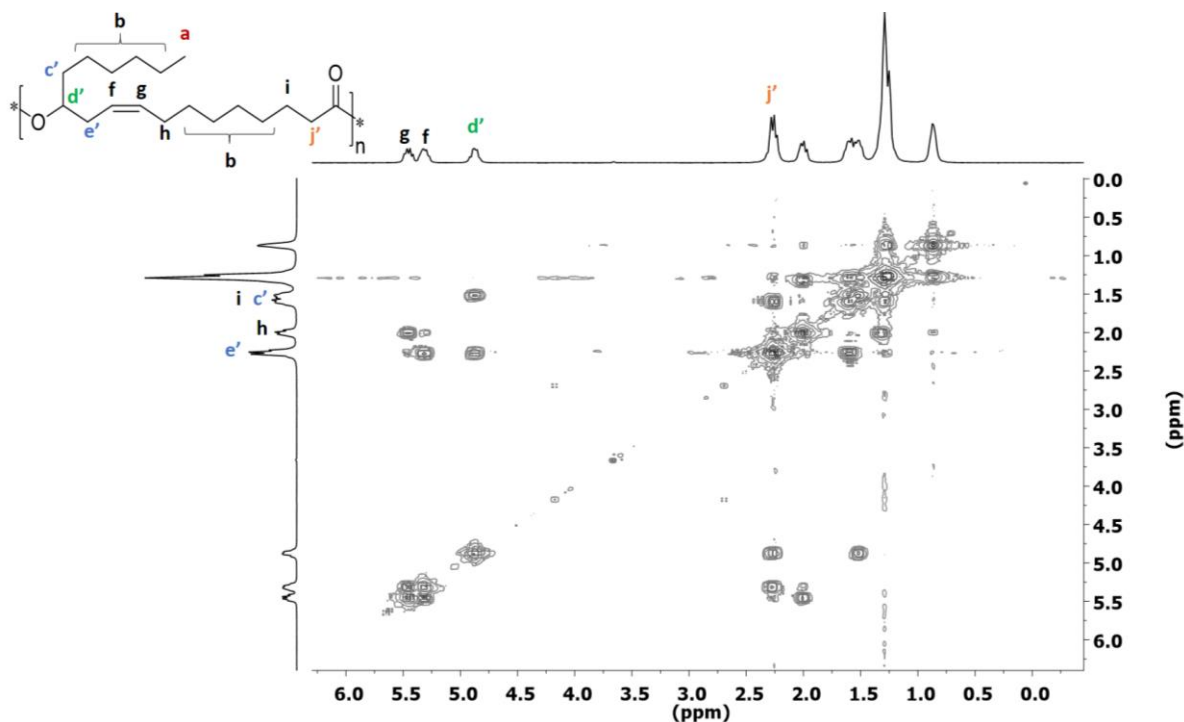


Figure II-13:  $^1\text{H}$ - $^1\text{H}$  COSY NMR spectrum of poly(methyl ricinoleate) P26

### 3.1.2. Poly(methyl-12-hydroxystearate)

The methyl-12-hydroxystearate monomer (MHS) and its corresponding polymer, PHS, were analysed by  $^1\text{H}$  NMR and  $^1\text{H}$ - $^1\text{H}$  COSY NMR; spectra are displayed in Figure II-14 and Figure II-15. The methyl protons of the fatty acid at the chain end, with a signal at 0.8 ppm, were used as reference. As they are correlated with the proton in  $\alpha$  of the OH group, see Figure II-15, the protons  $\text{H}_e$  and  $\text{H}_c$  in  $\beta$  position of the alcohol group are assigned to the signal at 1.4 ppm. The protons in  $\alpha$  and  $\beta$  positions of the ester group are assigned at 2.26 ppm and 1.6 ppm respectively by using the  $^1\text{H}$ - $^1\text{H}$  COSY technique. The characteristic peak of  $\text{H}_d$ , in  $\alpha$  of the OH group, shifts from 3.5 to 4.8 ppm during the polymerization. The methyl ester protons appear at the characteristic position of 3.6 ppm for the monomer and disappear after polymerization.

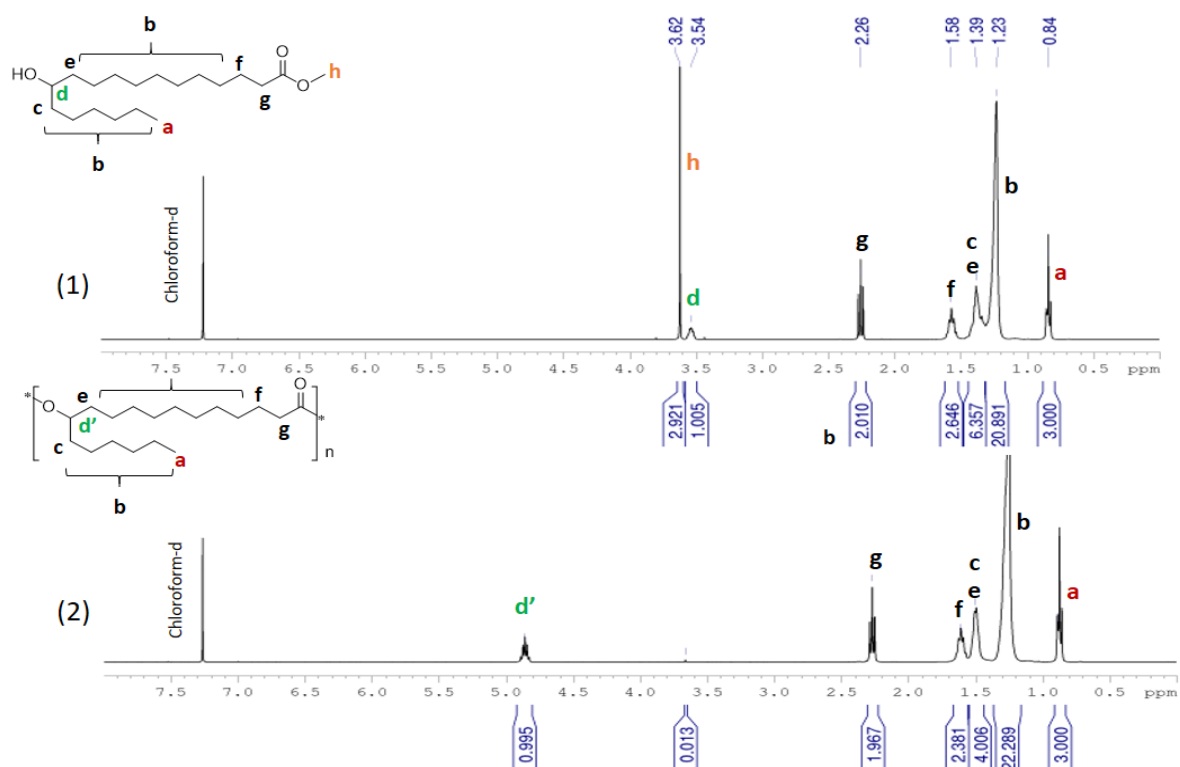


Figure II-14:  $^1\text{H}$  NMR spectra in  $\text{CDCl}_3$  of (1) MHS monomer and (2) PHS

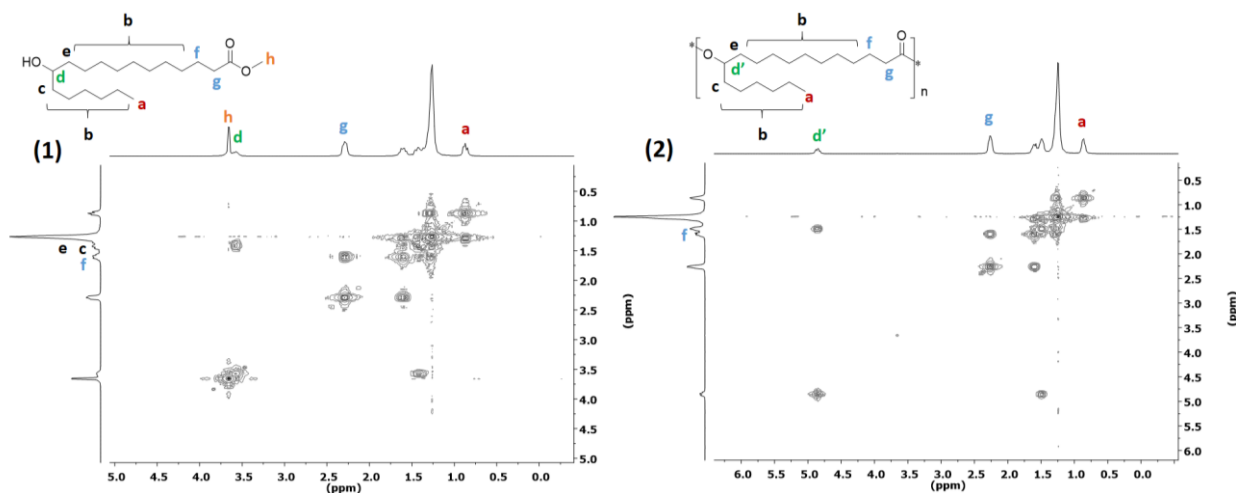


Figure II-15:  $^1\text{H}$ - $^1\text{H}$  COSY NMR spectra in  $\text{CDCl}_3$  of (1) MHS monomer and (2) PHS polymer

### 3.2. Molecular weights determination

Several PRic and PHS of different molecular weights were prepared. The SEC traces of this series of polyesters are displayed in Figure II-16 and their molecular weights reported in Table II-5. In order to ensure the molecular weight obtained by SEC using PS calibration,  $dn/dc$  values have been determined experimentally and used for molecular weight calculations. In addition,  $M_n$  values were also determined by  $^1\text{H}$  NMR.

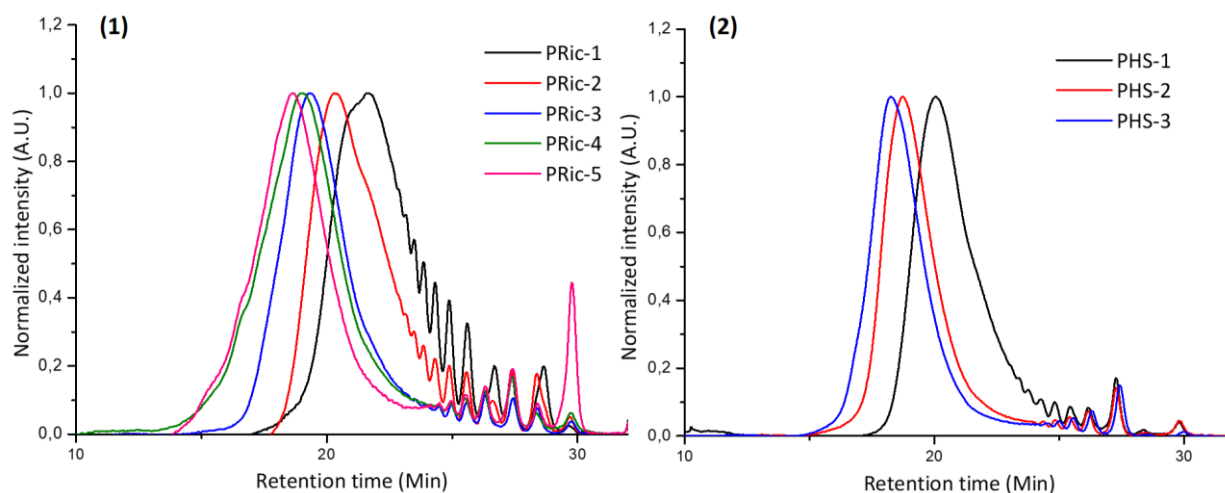


Figure II-16: SEC traces of (1) Poly(methyl ricinoleate) and (2) Poly(hydroxystearate). Measurements performed in THF

Following the polycondensation equation established by Carothers, it is possible to use  $^1\text{H}$  NMR to determine the reactive function conversion,  $p$ , the degree of polymerization  $DP_n$  and the molecular weight  $M_n$  of the obtained polymer:

$$p = \frac{I_{OCH_3 t=0} - I_{OCH_3 t=final}}{I_{OCH_3 t=0}} \quad (II-1)$$

$$DP_n = \frac{1}{1-p} \quad (II-2)$$

$$M_n = DP_n \times M_0 \quad (II-3)$$

As methyl ricinoleate is an AB monomer, the stoichiometry is always equal to  $r = 1$ .  $p$  represents the degree of reactive functions conversion,  $I_{OCH_3 t=0}$  the integration of the methyl ester peak at 3.6 ppm of the monomer and  $I_{OCH_3 t=final}$  the same integration but at the end of the polymerization.  $DP_n$  is the degree of polymerization,  $M_0$  the monomer unit molecular weight and  $M_n$  the final polymer molecular weight. The values for the further studied polyesters are expressed in Table II-5.

Table II-5: Conversion and molecular weights of PRic and PHS with different molecular weights

Entry	Time (h)	$P^1$	$DP_n^1$	$M_n^1$ (g.mol <sup>-1</sup> )	$M_n^2$ (g.mol <sup>-1</sup> )	$M_w^2$ (g.mol <sup>-1</sup> )	$\bar{D}^2$	dn/dc	$M_n^3$ (g.mol <sup>-1</sup> )	$M_w^3$ (g.mol <sup>-1</sup> )	$\bar{D}^3$
PRic-1 <sup>a</sup>	6	0.894	9.4	3000	5100	9200	1.8	0.0812	4000	6100	1.5
PRic-2 <sup>a</sup>	8	0.902	10.2	3200	8800	12900	1.5	0.0812	7200	10600	1.5
PRic-3 <sup>a</sup>	24	0.977	45	12400	15700	45400	2.9	0.0813	18200	32200	1.7
PRic-4 <sup>a</sup>	48	0.984	63	19800	25200	56800	2.3	0.0813	21700	47100	2.2
PRic-5 <sup>b</sup>	48	0.991	110	34000	36300	168400	4.6	0.0813	28100	131500	4.6
PHS-1 <sup>a</sup>	8	0.960	25	7700	9600	18400	1.9	0.0676	8100	17500	2.1
PHS-2 <sup>a</sup>	48	0.990	100	30200	25600	63000	2.4	0.0702	24000	68100	2.4
PHS-3 <sup>b</sup>	48	0.996	225	60000	35600	113400	3.1	0.0705	28500	78400	2.5

**Reaction conditions: 180°C, 1wt.% of Ti(OiPr)<sub>4</sub> in the melt under vacuum, 200 rpm**

**a: Magnetic stirring and b: mechanical stirring**

**1 Obtained by <sup>1</sup>H NMR using OCH<sub>3</sub> peak at 3.6 ppm for calculation**

**2 Obtained by SEC in THF – PS calibration**

**3 Obtained by SEC in THF – triple detection, dn/dc values used for calculation**

All the dn/dc values obtained are similar, independently of the molecular weight of the polyester. Depending on the reaction time and the mode of stirring, several degrees of polymerization are obtained, from  $DP_n = 9$  for PRic-1 up to  $DP_n = 110$  for PRic-5.  $M_n$  values determined by <sup>1</sup>H NMR are in agreement with  $M_n$  values obtained by SEC analysis. An exception is noticed in the case of PHS-3:  $M_n$  predicted by Carothers equation is doubled the one obtained by SEC. This is maybe due to the secondary reactions occurring for high conversion such as cyclisation. Interestingly, the molecular weights determined using PS calibration are very close to the ones obtained by universal calibration using dn/dc values. As a general trend, all the polyester molecular weight values correlate, whatever the method of determination, confirming that PS calibration gives accurate molecular weight values. As a result, all the methods previously mentioned can be used to determine PRic and PHS

molecular weight. Still, in order to be as precise as possible, molecular weight obtained by SEC using true  $dn/dc$  values will be considered in the following.

### 3.3. Thermal properties

#### 3.3.1. Degradation temperature

The thermal stability of the PRic and PHS were investigated by TGA analyses, under a nitrogen stream at a heating rate of  $10^{\circ}\text{C min}^{-1}$ . The polymer degradation temperatures at 5 wt.% are reported in Table II-6. TGA traces are displayed in Figure II-17.

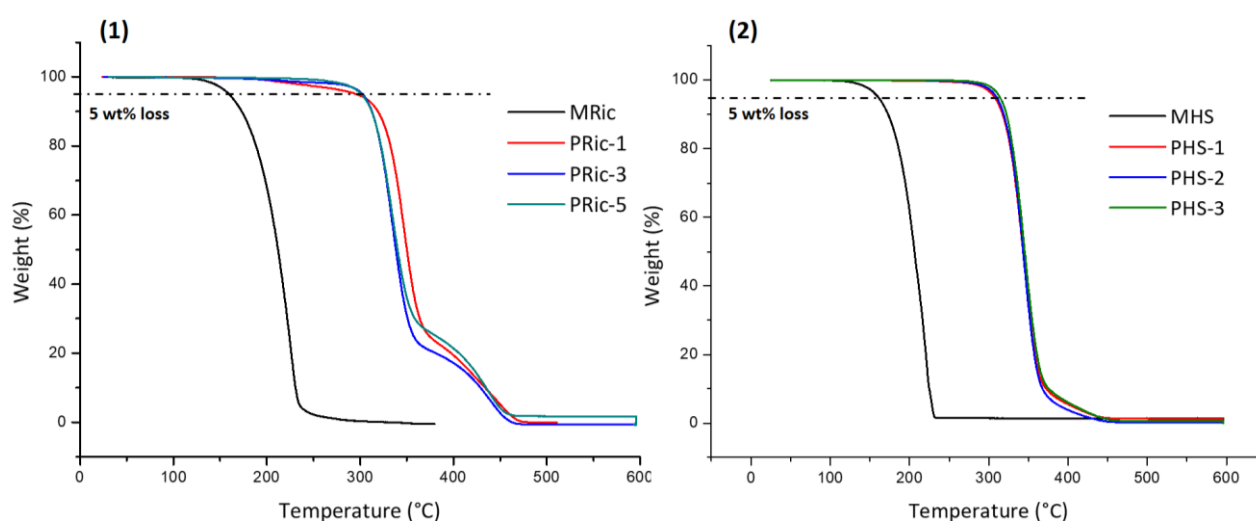


Figure II-17: Weight loss as a function of temperature for (1) Methyl ricinoleate monomer and its corresponding PRic with different molecular weights and (2) Methyl-12-hydroxystearate monomer and its corresponding PHS with different molecular weights

Table II-6: Thermal behavior of PRic and PHS determined by TGA

Entry	Mw <sup>1</sup> (g.mol <sup>-1</sup> )	$\bar{D}^1$	Td <sub>5%</sub> <sup>2</sup> (°C)	T <sub>max</sub> <sup>3</sup> (°C)	Weight residue (%)
PRic-1	6100	1.5	296	347	1.2
PRic-3	32200	1.7	303	303	0.2
PRic-5	131500	4.6	300	334	0.6
PHS-1	17500	2.1	307	343	0.8
PHS-2	68100	2.4	309	344	0.6
PHS-3	78400	2.5	314	345	1.7

**1** Obtained by SEC in THF – triple detection,  $dn/dc$  values using for calculation  
**2** Temperature for 5 wt % degradation- Obtained by TGA  
**3** Temperature at the maximum of degradation – Obtained by TGA

Both monomers begin to degrade at  $160^{\circ}\text{C}$  while the thermal stability of the polymer is higher, with a start of the degradation above  $300^{\circ}\text{C}$  for all the polymers. No influence of the polyester molecular weight on degradation is noticed. Moreover, all polyesters present negligible

residues (less than 2%). As a conclusion, all these bio-based polyesters exhibit good thermal stabilities in accordance with the petroleum based aliphatic polyesters.

### 3.3.2. Thermo-mechanical properties

All these polyesters were analyzed by DSC; traces of which are displayed in Figure II-18. The glass transition temperature,  $T_g$ , the crystallization temperature,  $T_{cris}$ , the melting temperature,  $T_{melt}$  and corresponding enthalpies were recorded after second heating scan at a rate of  $10^\circ\text{C min}^{-1}$ . All the results are reported in Table II-7.

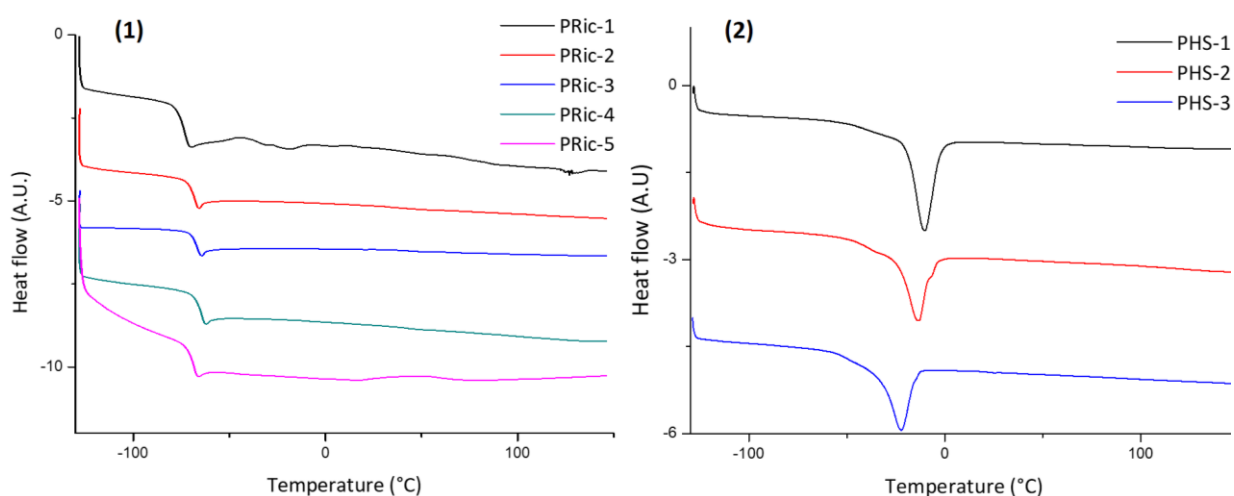


Figure II-18: DSC traces of (1) PRic with different molecular weights and (2) PHS with different molecular weights. Second heating cycle at a rate of  $10^\circ\text{C min}^{-1}$

Table II-7: Thermal behavior of PRic and PHS determined by DSC

Entry	$M_n^1$ ( $\text{g}\cdot\text{mol}^{-1}$ )	$M_w^1$ ( $\text{g}\cdot\text{mol}^{-1}$ )	$\bar{D}^1$	$T_g^2$ ( $^\circ\text{C}$ )	$T_{melt}^2$ ( $^\circ\text{C}$ )	$\Delta H_m^2$ ( $\text{J/g}$ )	$T_{cris}^2$ ( $^\circ\text{C}$ )	$\Delta H_c^2$ ( $\text{J/g}$ )
MRic	-	-	-	-	-7	79	-41	28
PRic-1	4000	6100	1.5	-77	-	-	-	-
PRic-2	7200	10600	1.5	-71	-	-	-	-
PRic-3	18200	32200	1.7	-69	-	-	-	-
PRic-4	21700	47100	2.2	-68	-	-	-	-
PRic-5	28100	131500	4.6	-68	-	-	-	-
MHS	-	-	-	-	54	235	47	201
PHS-1	8100	17500	2.1	-37	-20	30	-31	30
PHS-2	24000	68100	2.4	-44	-22	22	-33	29
PHS-3	28500	78400	2.5	-41	-22	27	-34	25

**1** Obtained by SEC in THF – triple detection,  $dn/dc$  values using for calculation

**2** Obtained by DSC- Second heating cycle at a rate of  $10^\circ\text{C min}^{-1}$

As already discussed, the internal unsaturation (cis configuration) in PRic leads to a completely amorphous state. In the opposite, poly(12-hydroxystearate) shows a semi-crystalline behavior

with a melting temperature about -20 °C. Despite the presence of pendant alkyl chains, the linear nature of saturated methyl-12-hydroxystearate backbone provides chain packing leading to a better organization of the polyester chains, allowing the crystallization. All the PHSs have a  $T_g$  around -40 °C, confirming their semi-crystalline nature. However, no effect of the molecular weight on the thermal behavior of PHS was noticed.

It was analyzed that  $T_g$  values follow the Fox-Flory equation (II-4) with respect to molecular weights (Figure II-19).<sup>44</sup>

$$T_g = T_{g,\infty} - \frac{K}{M_n} \quad (\text{II-4})$$

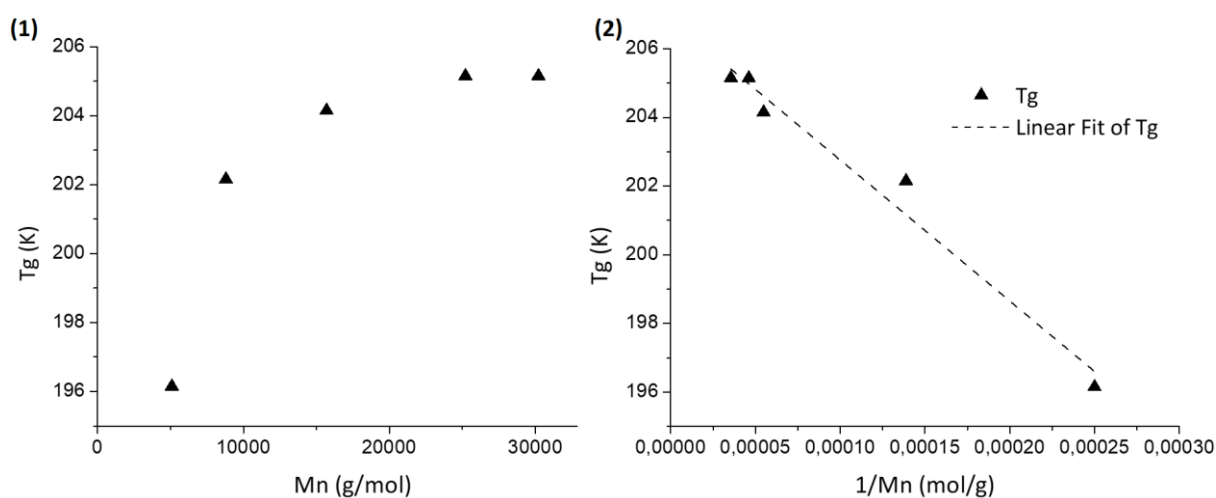


Figure II-19: PRic glass transition temperature as a function of (1) PRic molecular weight ( $M_n$ ) and (2)  $1/M_n$

In this equation,  $T_{g,\infty}$  is the maximum glass transition temperature that can be reached at a theoretical infinite molecular weight and  $K$  is an empirical parameter that is related to the polymer sample free volume. As displayed in Figure II-19, PRic samples followed the Fox-Flory equation with the following parameters  $T_{g,\infty} = -66$  °C and  $K = 4.1 \cdot 10^4$  g.mol<sup>-1</sup>. Concerning PHS, as the  $T_g$  cannot be determined precisely because of its crystalline behavior,  $T_{g,\infty}$  and  $K$  have not been calculated.

## 4. Melt poly(methyl ricinoleate) rheological behavior

As could be anticipated, the physical macroscopic aspects of PRic vary with the molecular weight. Indeed, PRic-1 with  $M_w = 6\,100\text{ g}\cdot\text{mol}^{-1}$  behaves as a viscous liquid while PRic-5 ( $M_w = 131\,000\text{ g}\cdot\text{mol}^{-1}$ ) does not flow at short time scale and look alike a gummy solid. This macroscopic observation suggests a strong effect of the molecular weight on the rheological properties of poly(methyl ricinoleate), especially on their melt viscosity. The aim is then to determine if the PRic is entangled or not regarding to its molecular weight.

As it was established by Fox and Flory in 1951, the viscosity of a polymer is strongly related to its molecular weight. This relationship varies depending on the polymer in entangled or not, according to equation (II-5) and (II-6)

$$\log \eta_0 = \log Mw + A \text{ for } M < M_c \quad (\text{II-5})$$

$$\log \eta_0 = 3,4 \log Mw + B \text{ for } M > M_c \quad (\text{II-6})$$

where  $\eta_0$  is the Newtonian steady-state shear viscosity and  $M_c$  the critical molecular weight of entanglement.  $A$  and  $B$  are empirical constants dependent on the nature of the polymer and the temperature. This relationship is schematically represented in Figure II-20. This relationship was empirically described by Fox and Flory for polystyrene and polyisobutylene.<sup>45,46</sup> It has been extended to all the polymer melts and theoretically interpreted by Bueche.<sup>47</sup> Some studies reported that, the slope of the plot for  $M_w > M_c$ , i.e. 3.4, was not absolute and can vary from 3.3 up to 3.7.<sup>48-50</sup>

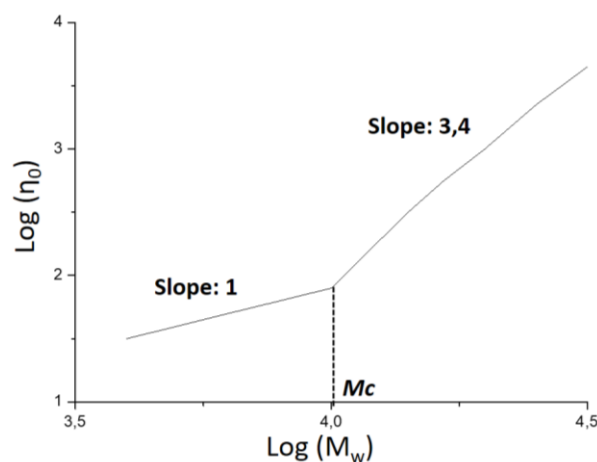


Figure II-20: Theoretical complex viscosity of a polymer as a function of its molecular weight in logarithmic scale

Consequently, this study aims at expressing the viscosity of poly(methyl ricinoleate)s as a function of their molecular weight. It could thus be possible to determine the potential PRic entanglement. To do so, dynamic mechanical analyses were performed, the aim being to measure complex viscosity  $\eta^*$ . According to Cox- Merz<sup>51</sup> rule, the dependence of the steady state shear viscosity on the shear rate is equal to the dependence of the complex viscosity as a function of the frequency. Therefore, the evaluation of complex viscosity at low frequency range, i.e. where it could reach a constant value, give information about the value of steady state shear Newtonian viscosity,  $\eta_0$ .

PRic, with molecular weights similar to those characterized in the previous sections but obtained from different batches, were used in this study. Their characteristics are reported in Table II-8. This rheological study was not performed on PHS because of their semi-crystalline nature.

## 4.1. Dynamic mechanical analysis

### 4.1.1. Linear domain

First, the linear domain of the poly(methyl ricinoleate), was evaluated at 20°C, at an angular frequency  $\omega = 10 \text{ rad.s}^{-1}$ , with  $\gamma$  varying from 0.1 to 100%. The plots of  $\eta^*$  as a function of  $\gamma$  are illustrated in Figure II-21. The resulting values of the complex viscosity are reported in Table II-8.

Table II-8: Molecular weight and bulk complex viscosity at 20 °C and 10 rad s<sup>-1</sup> of a series of PRics

Entry	$M_n^1$ (g.mol <sup>-1</sup> )	$M_w^1$ (g.mol <sup>-1</sup> )	$\bar{D}^1$	$\eta^*$ 20°C 10 rad.s <sup>-1</sup> (Pa.s)
PRic-6	3 000	5 000	1.1	20.5
PRic-7	8 000	18 000	1.7	170
PRic-8	11 000	31 000	2.2	460
PRic-9	15 000	92 000	6.1	820
PRic-10	28 000	131 500	4.6	3500

*1 Obtained by SEC in THF – triple detection, dn/dc values used for calculation*  
*2 Obtained by rheometry measurements at 20 °C, 10 rad.s<sup>-1</sup>*

For these measurements, the value of the angular frequency (e.g.  $\omega = 10 \text{ rad.s}^{-1}$ ) was arbitrarily chosen. For all the samples, the linear domain is extended until almost 100%. As expected, the complex viscosity increases with  $M_w$ , the higher the  $M_w$  value, the higher  $\eta^*$  at 20 °C.

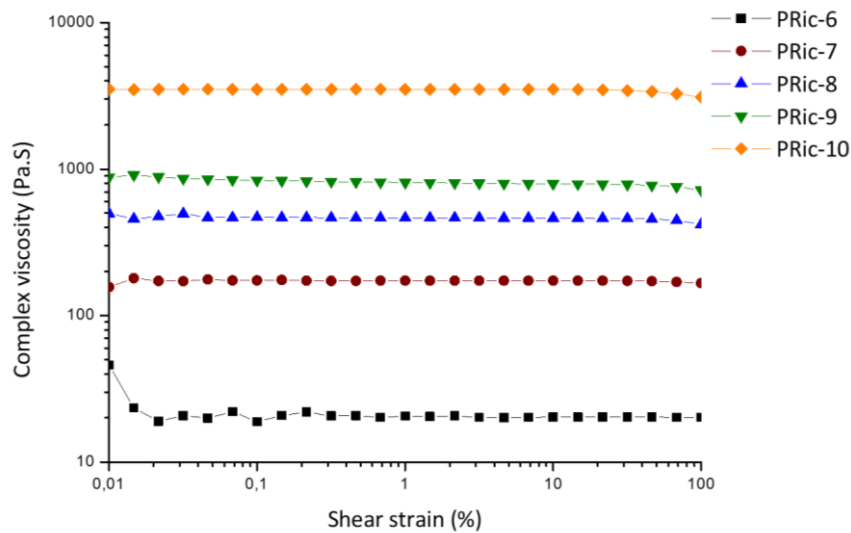


Figure II-21: Complex viscosity as a function of shear strain for a series of PRics with various  $M_w$ . Performed at 20 °C with an angular frequency of 10 rad  $s^{-1}$

#### 4.1.2. Complex viscosity as function of angular frequency, Time-temperature superposition (TTS)

To determine the frequency range in which the complex viscosity is constant, rheological properties of the PRics were evaluated under dynamic frequency sweep at different temperatures, and the time-temperature superposition (TTS) principle was applied. The TTS was established for the first time by Andrews and Tobolsky<sup>52</sup> and was rationalized by William, Landel and Ferry leading to the WLF equation.<sup>53</sup> This model, related to a macroscopic motion of a bulk material, is based on the equation (II-7):

$$\log(a_T) = \frac{-C_1(T-T_{Ref})}{C_2+(T-T_{Ref})} \quad (II-7)$$

$a_T$  corresponds to an horizontal translation factor (i.e. a ratio of characteristic time or frequency at two different temperatures,  $T_{ref}$  and  $T$ ),  $C_1$  and  $C_2$  are positive constants that depend on the material and the reference temperature  $T_{Ref}$ . This equation is usually valid in the range of temperature between  $T_g$  and  $T_g + 100$  °C.

For higher temperature, the local motion of polymer chains is considered instead of macroscopic motion. In that case, the shift factors normally follow an Andrade law<sup>54</sup> according to equation (II-8).

$$\ln(a_T) = \frac{E_a}{R} \left( \frac{1}{T} - \frac{1}{T_{Ref}} \right) \quad (II-8)$$

where  $E_a$  is the activation energy and  $R$  the universal gas constant. By using Andrade law, it is possible to determine the empirical activation energy of the system and to calculate the shift factor for a larger range of temperatures than those tested experimentally. Then, the viscosities could be estimated at any temperatures.

The storage modulus,  $G'$ , and loss modulus,  $G''$ , as a function of  $\omega$  were measured at various temperatures. Based on these, a master curve was established and translation factors were measured.

The first aim of this study is to determine a frequency range in which the complex viscosity is Newtonian. For the measurements, a shear strain,  $\gamma = 1\%$ , was applied and a frequency sweep from  $100 \text{ rad}\cdot\text{s}^{-1}$  down to  $0.1 \text{ rad}\cdot\text{s}^{-1}$  was performed at  $-30^\circ\text{C}$ ,  $-20^\circ\text{C}$ ,  $-10^\circ\text{C}$ ,  $0^\circ\text{C}$  and  $20^\circ\text{C}$ , all above PRic  $T_g$ . The master curves, obtained *via* the shift of the data at different temperatures are plotted in Figure II-22.

The reference temperature was fixed at  $-20^\circ\text{C}$  for all the samples. Translation factors  $a_T$  follow the Andrade law with  $E_a \approx 50 \text{ kJ}\cdot\text{mol}^{-1}$ , as illustrated in Figure II-A-1 in Appendix. Values are reported in the Table II-A-1 in Appendix.

As displayed in Figure II-22, the PRic-6 behaves as a viscoelastic fluid with a terminal zone visible at low frequency in which  $G' \approx f(\omega^2)$  and  $G'' \approx f(\omega)$ . This polymer is apparently not entangled as no crossover is observed between  $G'$  and  $G''$  curves in the frequency range investigated. In the case of PRic-7, with  $M_w = 18 \text{ kg}\cdot\text{mol}^{-1}$ , surprisingly, no terminal zone is observed meaning that the chains were still not completely relaxed at low frequencies. Still, the loss modulus remained higher than the storage modulus for the all range of frequency used in this study, i.e.  $0.003 < \omega < 294 \text{ rad}\cdot\text{s}^{-1}$ . That suggests an absence of entanglement. The PRic-8 behaves as a viscoelastic fluid with a terminal zone which is not completely reached at low frequencies suggesting the presence of non-relaxed chains. For  $\omega > 50 \text{ rad}\cdot\text{s}^{-1}$ , the storage modulus is higher than the loss modulus and seems to reach a plateau around  $10^5 - 10^6 \text{ Pa}$ . These are manifestly signs of entanglements.

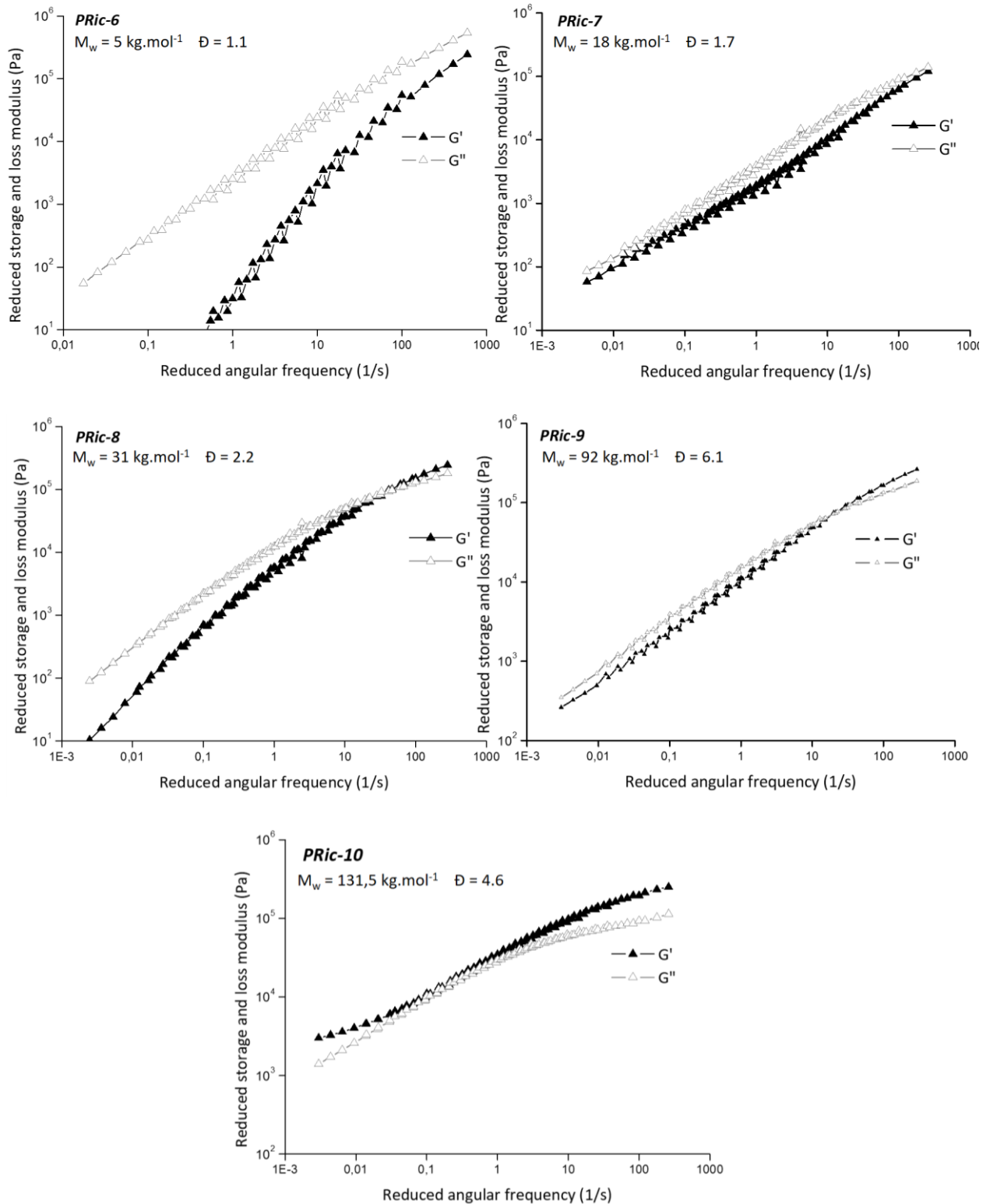


Figure II-22: Master curves at -20 °C of PRic samples. Reduced storage and loss modulus are expressed versus the reduced angular frequency

The behavior of PRic-9 is difficult to analyze. Such as PRic-7, at low frequencies,  $G'$  and  $G''$  seem to have a similar slope and no terminal zone is observed. This behavior may be due to the high dispersity ( $\bar{D} = 6.1$ ) of the polymer and consequently a very broad distribution of

relaxation times. Still, the cross point between the loss and the storage modulus at  $\omega = 20$   $\text{rad}\cdot\text{s}^{-1}$  conjures up an entanglement. In the case of PRic-10,  $G'$  tends to a plateau at high frequencies, suggesting chain entanglements. By examining the moduli on the whole frequency range, it is noteworthy that  $G' > G''$  independently of  $\omega$ . Moreover,  $G'$  reaches a plateau at low frequencies. Overall, these two peculiarities suggest that PRic-10 is partially cross-linked. This is in accordance with the presence of an insoluble gel fraction when PRic-10 is introduced in usual solvents. One possible explanation for these observations lies in the presence of the multifunctional  $\text{Ti}(\text{O}/\text{Pr})_4$  catalyst that may partially interact with the chain end functions and acts as a crosslinking agent. Because PRic-10 has the highest molecular weight of all the polyricinoleate tested in this study, this phenomenon could be more pronounced and results in a rheological behavior that suggests a partially cross-linked system. Globally, from these measurements, it is clear that the poly(methyl ricinoleate) properties are strongly dependent on their molecular weights.

The complex viscosity can thus be calculated with the data obtained from the dynamic shear measurements according to equation (II-9):<sup>54</sup>

$$|\eta^*| = \frac{|G^*|}{\omega} = \frac{\sqrt{(G')^2 + (G'')^2}}{\omega} \quad (\text{II-9})$$

where the elastic modulus  $G'$  and the loss modulus  $G''$  are given as a function of the angular frequency  $\omega$ .

Combining this relationship and the TTS principle, the complex viscosity of the series of PRics were expressed as a function of angular frequency, with  $0,003 < \omega < 294$   $\text{rad}\cdot\text{s}^{-1}$  at  $-20$  °C. Results are plotted in Figure II-23.

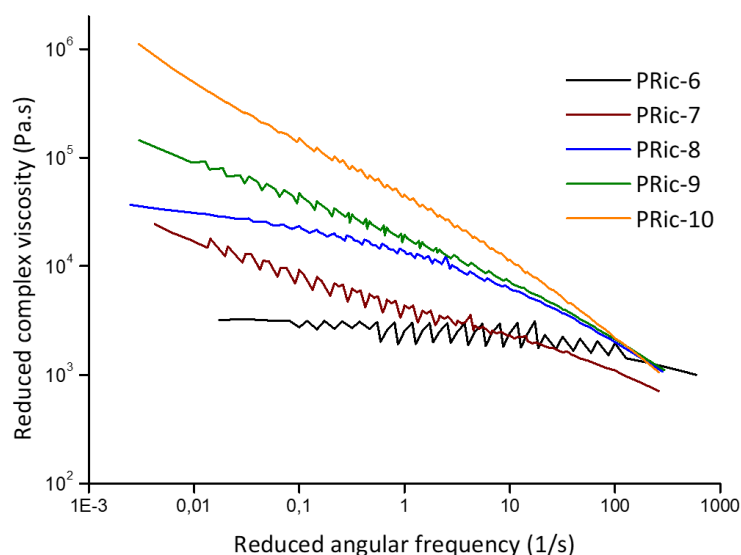


Figure II-23: Poly(methyl ricinoleate) reduced complex viscosity versus the reduced angular frequency obtained from TTS at  $-20\text{ }^{\circ}\text{C}$  as reference temperature, 1% shear strain

Master curves of complex viscosity was established at  $-20\text{ }^{\circ}\text{C}$  as the reference temperature. It appears clearly that for most of the poly(methyl ricinoleate)s tested, no viscosity plateau is observed at low frequencies, with the noticeable exceptions of PRic-6 and PRic-8. In these two cases, viscosity plateau is observed for  $\omega < 1\text{ rad}\cdot\text{s}^{-1}$  in the case of PRic-6 and  $\omega < 0.1\text{ rad}\cdot\text{s}^{-1}$  in the case of PRic-8 allowing determination of a Newtonian viscosity:

$$\text{PRic-6: } \eta^{*}_{-20\text{ }^{\circ}\text{C}} = 3010 \pm 230\text{ Pa}\cdot\text{s}$$

$$\text{PRic-8: } \eta^{*}_{-20\text{ }^{\circ}\text{C}} = 34900 \pm 1500\text{ Pa}\cdot\text{s}$$

For the other PRic samples, the viscosity was not stable with the frequency in the range of frequencies and temperatures tested. Newtonian viscosities were then determined using creep experiments.

## 4.2. Viscosity determination by creep tests

Creep experiment consists in applying a shear stress on the polymer sample and measuring the resulting shear strain as a function of the time. In the case of viscoelastic sample, after a certain time, a linear evolution of shear strain is obtained, defining a constant shear rate. The viscosity is obtained by the ratio of shear stress to the shear rate. A series of creep tests was performed on PRic-7, PRic-9 and PRic-10, an example is represented in Figure II-A-2 (see Appendix). Shear stresses of 1 Pa, 3 Pa, 5 Pa, 10 Pa, 30 Pa, 50 Pa, 100 Pa, 150 Pa and 200 Pa were successively applied to the sample. The viscosities obtained were plotted versus the

shear rate in order to evaluate the range of shear rate where the viscosity can be considered as Newtonian, see Figure II-24. It has to be noted that for some systems, higher temperatures were necessary to obtain stabilization of the shear rate during creep experiment in a reasonable time: 20°C was thus used for PRic-7, 200 °C for PRic-9 and 150°C for PRic-10.

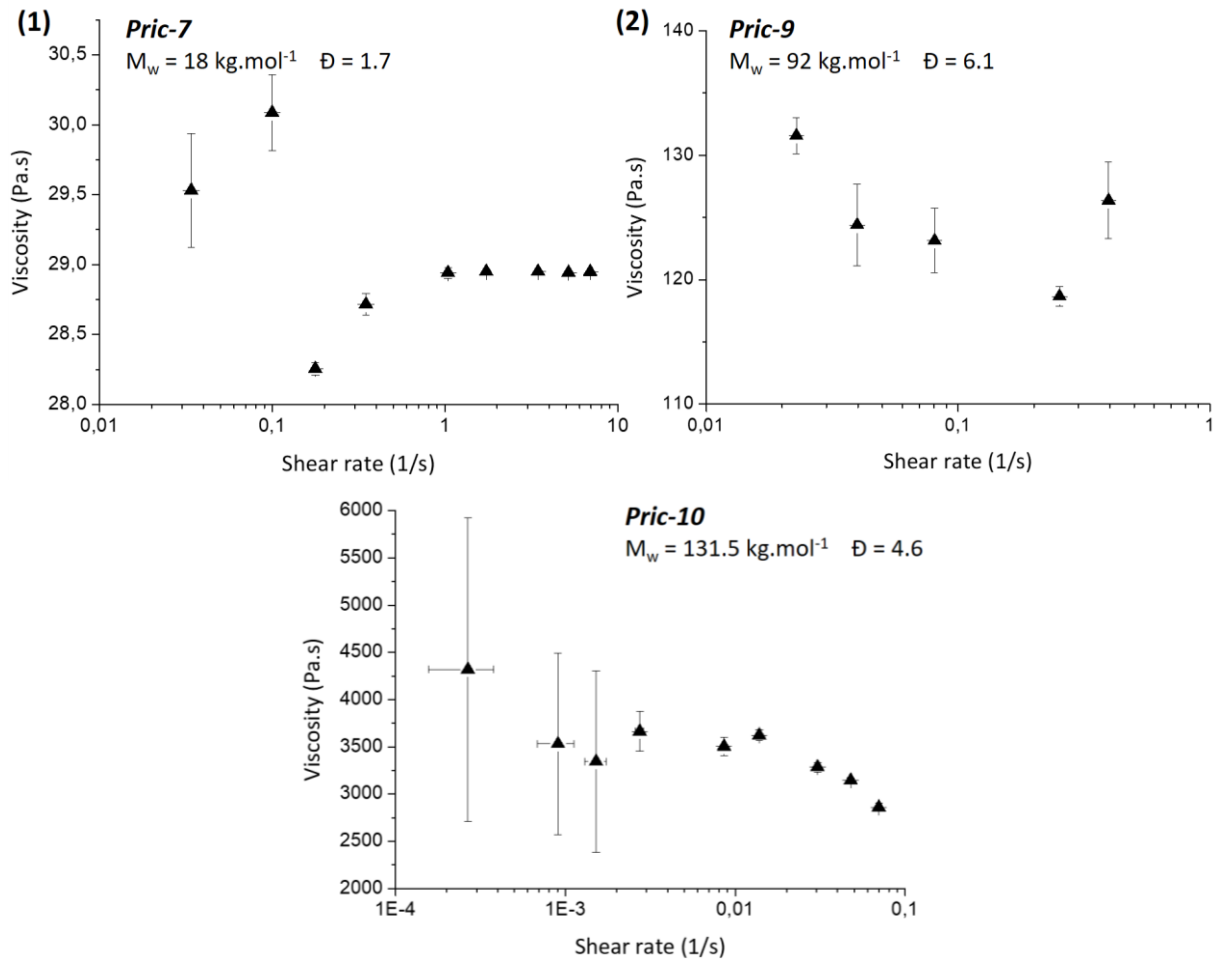


Figure II-24: Viscosity versus shear rate obtained by creep measurements. (1) PRic-7 performed at 20 °C, (2) PRic-9 performed at 200 °C and (3) PRic-10 performed at 150 °C

Except at low shear stress, such as 1 Pa and 3 Pa, the PRic viscosities were stable regarding to the shear rate. Unfortunately, error bars are larger in the case of PRic-9. In the case of PRic-10, the viscosity is stable for shear rate below 0.05 s<sup>-1</sup>. Viscosities obtained above this shear rate are not considered being in Newtonian regime. By using the creep measurements, the following viscosities were obtained:

$$\text{PRic-7: } \eta^*_{20^\circ\text{C}} = 28.81 \pm 0.028 \text{ Pa.s}$$

$$\text{PRic-9: } \eta^*_{200^\circ\text{C}} = 124.82 \pm 2.23 \text{ Pa.s}$$

$$\text{PRic-10: } \eta^*_{150^\circ\text{C}} = 3518 \pm 103 \text{ Pa.s}$$

### 4.3. Viscosity as a function of molecular weights

Newtonian viscosities of each PRic tested were determined at different temperatures. In order to compare them and to be able to express the viscosity as a function of the molecular weight, all the viscosities have to be obtained at the same temperature, i.e. 20 °C.

In the dynamic study, PRic-6 and PRic-8 viscosity appeared to be Newtonian at low frequency. The Newtonian viscosity was then determined at -20°C, the reference temperature of the TTS. The translation factor  $a_T$  is correlated to the melt polymer viscosity.<sup>54</sup> This relationship is defined according to equation (II-10)

$$a_T = \frac{\eta_T}{\eta_{T_{Ref}}} \quad (\text{II-10})$$

As the shift factor was determined empirically by the time-temperature superposition (see Table II-A-1 in Appendix), and knowing the viscosity of a polymer at the reference temperature of -20°C, it is possible to determine its viscosity at 20 °C. As a result, PRic-6 and PRic-8 viscosities at 20 °C were determined as:

$$\text{PRic-6: } \eta^*_{20^\circ\text{C}} = 6.87 \pm 0,53 \text{ Pa.s}$$

$$\text{PRic-8: } \eta^*_{20^\circ\text{C}} = 872 \pm 3,7 \text{ Pa.s}$$

For the other systems, values of Newtonian viscosities were determined by creep experiments, at different temperatures. In the case of PRic-7, the Newtonian viscosity was obtained directly at 20 °C:

$$\text{PRic-7: } \eta^*_{20^\circ\text{C}} = 28.81 \pm 0.028 \text{ Pa.s}$$

For PRic-9 and PRic-10, Newtonian viscosity was determined at 200°C and 150 °C respectively. Then, it has been recalculated at 20 °C using the same principle and using the Andrade Law determined with TTS.

However, the first TTS were realized with a reference temperature of -20 °C, far below the temperature at which the creep experiments were performed. This can lead to an important error regarding to the extrapolated translation factors and then, the final viscosity values. As a result, another series of dynamic measurements were performed from 20°C to 100°C on PRic-9 and PRic-10 with  $T_{Ref} = 80$  °C allowing the determination of translation factors  $a_T$  closer

to the creep experiments temperatures, limiting then errors in calculation. The master curves are displayed in Figure II-A-3 and the obtained translation factors  $a_T$  are reported in Table II-A-2 in Appendix. PRic-9 and PRic-10 Newtonian viscosities at 20°C were then calculated:

$$\text{PRic-9: } \eta^*_{200^\circ\text{C}} = 124.82 \pm 2.23 \text{ Pa.s} \quad \text{and} \quad \eta^*_{20^\circ\text{C}} = 260\,400 \pm 6\,440 \text{ Pa.s}$$

$$\text{PRic-10: } \eta^*_{150^\circ\text{C}} = 3518 \pm 103 \text{ Pa.s} \quad \text{and} \quad \eta^*_{20^\circ\text{C}} = 853\,000 \pm 82\,200 \text{ Pa.s}$$

Newtonian viscosities are then reported in Table II-9 and plotted as a function of  $M_w$  in Figure II-25.

Table II-9: Molecular weight and melt viscosity at 20 °C at 10 rad s<sup>-1</sup> and a low shear rate of a set of PRics

Entry	$M_n^1$ (g.mol <sup>-1</sup> )	$M_w^1$ (g.mol <sup>-1</sup> )	$\bar{D}^1$	$\eta_0$ 20°C (Pa.s) <sup>3</sup>
PRic-6	3 000	5 000	1.1	6.87 ± 0.53
PRic-7	8 000	18 000	1.7	28.81 ± 0.028
PRic-8	11 000	31 000	2.2	872 ± 3.7
PRic-9	15 000	92 000	6.1	2.60*10 <sup>5</sup> ± 6.4*10 <sup>3</sup>
PRic-10	28 000	131 500	4.6	8.53*10 <sup>5</sup> ± 8.2*10 <sup>4</sup>

*1 Obtained by SEC in THF – triple detection, dn/dc values used for calculation*  
*2 Obtained by rheometry at 20°C, 10 rad.s<sup>-1</sup> - 3 Determined in Newtonian conditions*

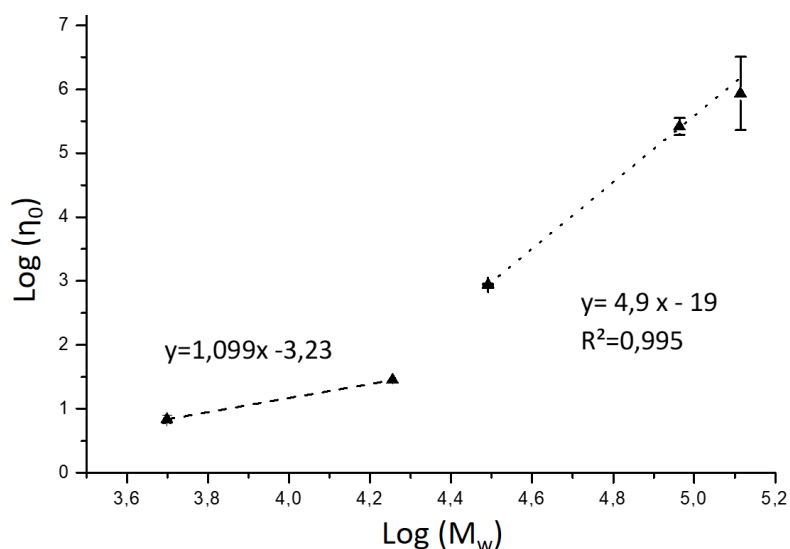


Figure II-25: Logarithmic viscosity versus logarithmic molecular weights for PRic samples at 20°C

As illustrated in Figure II-25, a slope rupture is clearly observed for  $\text{Log}(M_w) \approx 4.3$  corresponding to molecular weight around  $M_w = 25\,000 \text{ g.mol}^{-1}$ . For  $M_w < 25\,000 \text{ g.mol}^{-1}$ , a slope of 1 is obtained, confirming that the chains are disentangled (PRic-6 and PRic-7). For  $M_w > 25\,000 \text{ g.mol}^{-1}$ , a slope around 4.9 is obtained. This is superior to the value usually reported in the literature for entangled polymer chains, i.e. 3.4. However, the slope rupture is in

accordance with a transition from disentangled to entangled chains for PRic of  $M_w = 25\ 000\ \text{g}\cdot\text{mol}^{-1}$ . The discrepancy between the experimental slope value and the one predicted by the literature remains unexplained. The large dispersity of PRic-9 ( $\mathcal{D} = 6.1$ ) and PRic-10 ( $\mathcal{D} = 4.6$ ) could explain a slight difference between the experimental and the given value of 3.4. Indeed, it is known that dispersity has an impact on the rheological behavior of the polymer chains and, consequently, on the sample viscosity.<sup>55,56</sup> However, as reported in literature, this effect implies only variation from 3.3 to 3.7. There is also probably an impact of the pendant alkyl segments along the polymer backbone (comb-like structure).<sup>56,57</sup>

To conclude, dynamic mechanical analyses and creep experiments allowed the determination of a Newtonian viscosity for all the PRic tested. It appeared that the PRic rheological behavior in bulk is strongly related to its molecular weight, with an entanglement observed for PRic with  $M_w > 25\ \text{kg}\cdot\text{mol}^{-1}$ .

## 5. PRic and PHS behavior in solution

---

Poly(ricinoleate) and poly(12-hydroxystearate) were obtained with relatively high molecular weights compared to previous systems described in literature.<sup>1,2,26</sup> As reported in the first section, the latter can be interesting candidates as oil additives. In order to evaluate their ability to be used as viscosity modifiers, these bio-based polyesters have been studied in solution, using commercially available organic and mineral oil lubricant not containing any other additives, i.e. base oil, and compared to commercial Viscosity Index improvers (VII).

### 5.1. Preliminary study

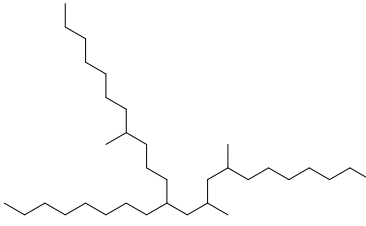
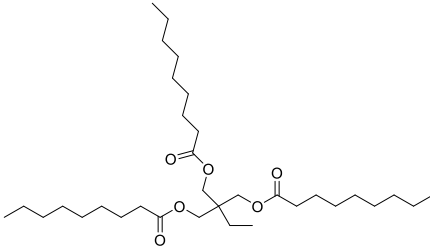
#### 5.1.1. Choice of the mineral and organic base oils

Currently, mineral oils are predominantly used as lubricants. They are classified in three groups depending on their composition and properties. Oils from group III present currently the best properties for lubricant applications with, for instance, Viscosity Index above 120.<sup>58</sup> For this reason, a Group III mineral oil was selected as base oil for this study: Yubase 4+, provided by Total. It is mostly used in automotive field as gasoline engine oil.<sup>59</sup> On the other

hand, in order to set-up a fully bio-based system, an organic base oil from Group V was also selected: Radialube 7368, from Oleon. This biodegradable oil is used in marine, automotive or hydraulic fluids fields.<sup>60</sup>

These two selected oils varied a lot in terms of structure, density, Viscosity Index (VI) and Pour Point (PP). All these characteristics are reported in Table II-10. The values were determined experimentally by densimetry-viscometry for density and viscosity measurements and rheological measurements for the pour point. All the data are in good accordance with literature data, given in brackets in the Table II-10. The molecular weights were determined by SEC using PS calibration. As both oils are low molecular weight compounds, molecular weight data obtained by SEC are approximated values.

Table II-10: Oils' characteristics, determined experimentally or from literature [in brackets]

Base oil	Yubase 4+	Radialube 7368
		
Density <sup>1</sup>	0.8226 [0.825]	0.941 [0.945]
Molecular weight (g.mol <sup>-1</sup> ) <sup>2</sup>	600	750 [512.8]
Flash point (°C)	[220]	[235]
$\eta$ at 40°C (mm <sup>2</sup> .s <sup>-1</sup> ) <sup>1</sup>	18,6	20,4
$\eta$ at 100°C (mm <sup>2</sup> .s <sup>-1</sup> ) <sup>1</sup>	4.3 [4.1]	4.6 [4.5]
VI	128	152
Pour Point (°C) <sup>3</sup>	-15 [-17]	[<-40]

**1- Obtained using a densimeter-viscosimeter**  
**2- Obtained by SEC in THF, PS calibration**  
**3- Obtained using a rheometer with a temperature ramp of 1°C.min<sup>-1</sup> (cone plate 1mm,  $\phi$ = 50 mm)**

The Radialube 7368 chemical structure was confirmed by <sup>1</sup>H NMR analysis. The spectrum is displayed in Figure II-26. The protons H<sub>c</sub> at 4ppm are characteristic of a CH<sub>2</sub> in  $\alpha$  of ester bonds. The two protons H<sub>b</sub> at 1.45 ppm confirmed the trimethylolpropane structure. Regarding to the CH<sub>2</sub> integration, the alkyl chains contain 8 carbons.

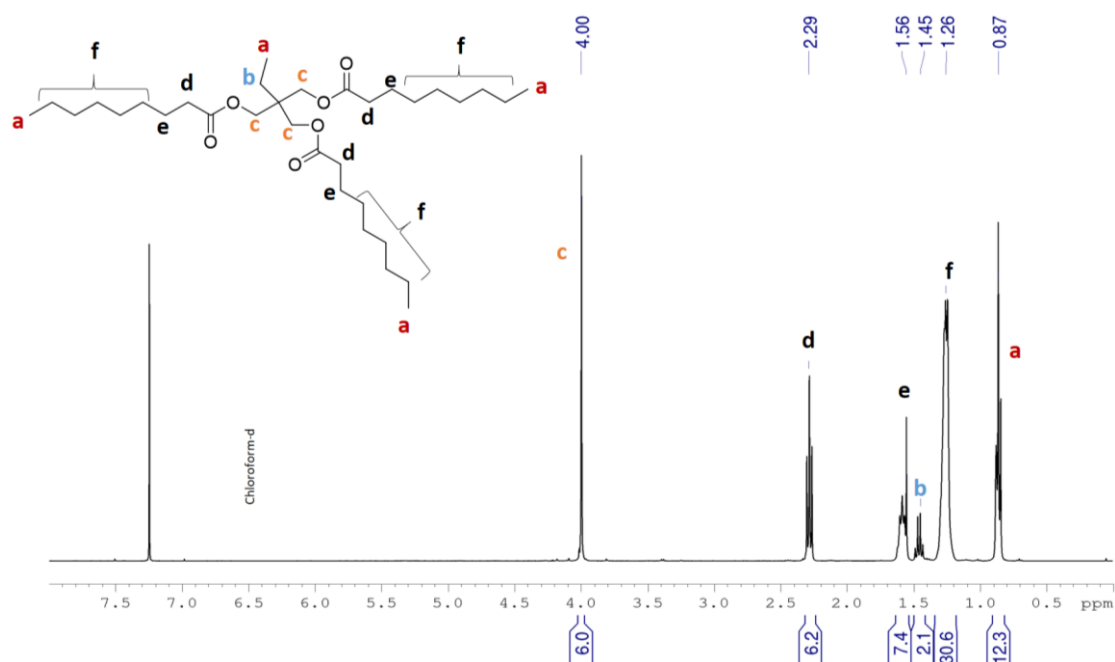


Figure II-26:  $^1\text{H}$  NMR spectrum in  $\text{CDCl}_3$  of Radialube 7368

The case of Yubase 4+ is a bit different as its chemical structure is not given in literature. A  $^1\text{H}$  NMR analysis was thus performed. The  $^1\text{H}$  NMR spectrum (Figure II-27 (1)) does not show any peaks of aromatic carbons confirming a fully aliphatic structure, with signals of methyl group at 0.8 ppm and of aliphatic  $\text{CH}_2$  at 1.28 ppm. The integrals ratio between  $\text{CH}_3$  and  $\text{CH}_2$  peaks, i.e. 1 : 4, does not correspond to a proper linear structure but rather as a branched one, which is correlated with the viscosity values observed at  $40^\circ\text{C}$ , close to data observed for the branched structure of Radialube 7268. In order to confirm the structure of Yubase 4+, a DEPT-135  $^{13}\text{C}$  NMR was performed (Figure II-27 (2)). All the carbon peaks appear between 0 and 40 ppm, in agreement with a fully aliphatic structure. According to literature<sup>61</sup>,  $\text{CH}_3$  peaks appear mostly in the range of 0-30 ppm while  $\text{CH}$  peaks are in the 20-40 ppm area, confirming that Yubase 4+ oil is composed of branched aliphatic chains. Regarding to the  $\text{CH}_3$  peaks, it appeared that side chains are mostly methyl groups (1B1) and alkyl chains with more than 4 carbons (1Bn with  $n > 4$ ). Only few ethyl groups (1B2) and no propyl groups (1B3) were observed. As a result, an hypothetical schematic structure is displayed in Table II-10.

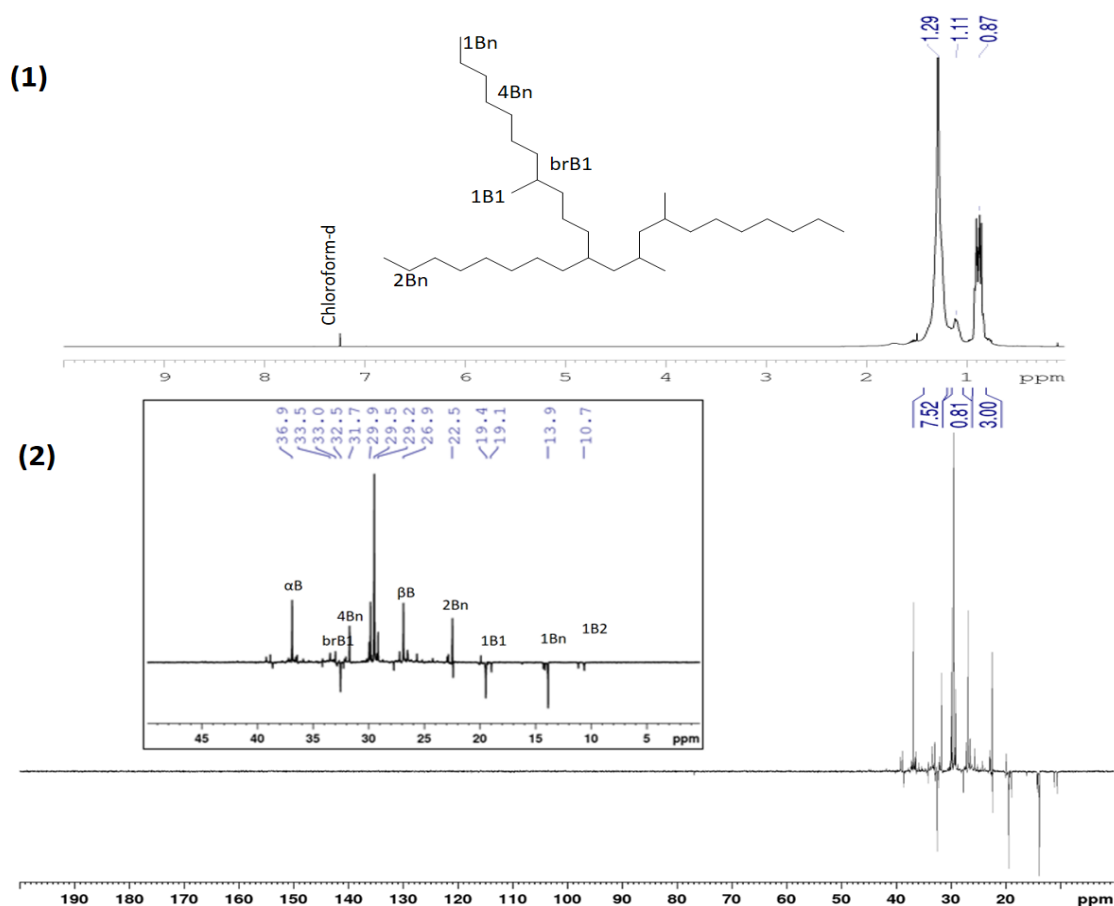


Figure II-27: (1)  $^1\text{H}$  NMR spectra of Yubase (2) DEPT-135  $^{13}\text{C}$  NMR spectra of Yubase 4+ and zoom between 0 and 40 ppm

The viscosity of the oils with respect to the temperature was thus investigated. Density, dynamic viscosity and kinematic viscosity were measured at a range of temperatures from 20 °C to 100 °C three times each. Yubase 4+ and Radialube 7368 kinematic viscosities as a function of the temperature are displayed in Figure II-28. The average of three measurements is represented with the error bars. The oils display a similar behavior with a dramatic decrease of the viscosity with temperature. For instance, Radialube 7368 kinematic viscosity dropped from 45.5  $\text{mm}^2.\text{s}^{-1}$  at 20 °C to 4.67  $\text{mm}^2.\text{s}^{-1}$  at 100 °C. Yubase 4+ viscosity decreases from 41.8 to 4.34  $\text{mm}^2.\text{s}^{-1}$  for the same temperatures. A good reproducibility is observed with a maximum standard deviation of 0.03 for 20 °C for both oils. The standard deviation is in the range of 0.001 to 0.005 for Radialube 7368 and 0.008 to 0.02 for Yubase 4+ for the other temperatures.

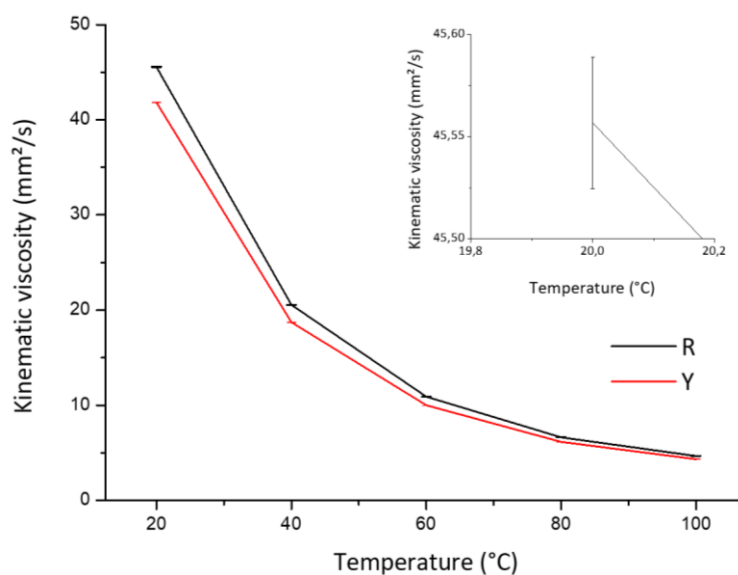


Figure II-28: Viscosity behavior as a function of the temperature for Radialube 7368 (in black) and Yubase 4+ (in red) and a zoom on the standard deviation at 20 °C for Radialube 7368

To conclude, the two selected oils, Radialube 7368 and Yubase 4+ have been fully characterized. They display a different nature, organic and mineral respectively, but a similar viscosity behavior regarding to the temperature. Viscosity measurements show a good repeatability with a maximum standard deviation of 0.03.

### 5.1.2. Choice of the commercial additives

Once the two oils characterized, a commercial viscosity modifier was selected in order to compare with the bio-based PRic and PHS. A polyester from Croda, Priolube 3986 was chosen. The latter is used as Extreme Pressure enhancing additive, lubricity additive, thickening agent and as Viscosity Index improver.<sup>62</sup> This additive was also analysed by SEC using PS calibration. SEC trace is illustrated in Figure II-29 and values of  $M_n = 6\,400\text{ g}\cdot\text{mol}^{-1}$ ,  $M_w = 16\,800\text{ g}\cdot\text{mol}^{-1}$  and  $\bar{D} = 2.6$  were obtained.

Priolube 3986 was added in Radialube 7368 and Yubase 4+ at 3 wt.%. The mixture was heated at 100°C overnight and cooled down to room temperature. Priolube 3986 was found only soluble in the organic base oil, Radialube 7368. In order to have also a comparison in mineral oil, another commercial additive was selected: Viscoplex 10-250. This poly(alkylmethacrylate) with  $M_w = 40\,000\text{ g}\cdot\text{mol}^{-1}$  is commercialized by Evonik, as a shear stable Viscosity Index improver.

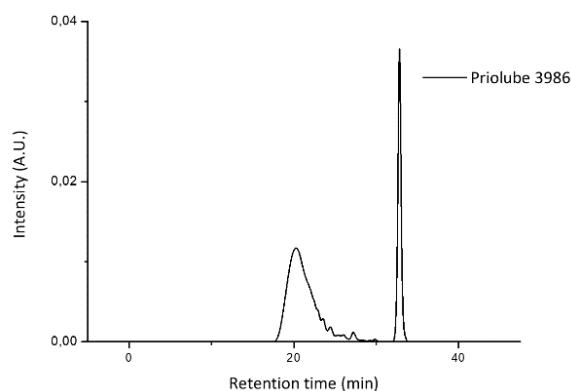


Figure II-29: SEC trace of Priolube 3986 (PS calibration)

### 5.1.3. Determination of the appropriate additive concentration

The concentration of additive in solution has a strong impact on the viscosity. Indeed, Priolube 3986 was added in Radialube 7368 at concentrations from 0,05 wt.% to 10 wt.% and the solutions analysed by viscometry. The experiments were performed from 20 °C to 100°C in order to estimate the impact of the additive on the oil viscosity with temperature. The density, dynamic viscosity and kinematic viscosity were measured and reported in Table II-A-3 in Appendix.

The relative viscosity values, Viscosity Index and Q values of the blend of Radialube 7368 with Priolube 3986 (**P**) are reported in Table II-11. The relative viscosity as a function of the temperature is plotted in Figure II-30 (1). Viscosity Indexes were calculated for each concentration of Priolube 3986 in Radialube 7368 and expressed as a function of the concentration in Figure II-30 (2). Finally, the relative viscosity against the concentration at 40 °C and 100 °C is plotted in Figure II-30 (3).

Table II-11 : Relative viscosity as a function of the temperature, VI and Q values of Radialube 7369 (R) blended with Priolube 3986 (P)

	T (°C)	0.05 wt.% P	0.5 wt.% P	1 wt.% P	3 wt.% P	5 wt.% P	10 wt.% P
$\eta_{rel}$	20	1.011	1.070	1.134	1.361	1.740	1.909
	40	1.002	1.060	1.112	1.323	1.650	1.793
	60	1.005	1.058	1.106	1.309	1.590	1.730
	80	1.007	1.056	1.102	1.299	1.553	1.689
	100	1.005	1.051	1.094	1.280	1.517	1.646
VI	R=152	153	157	161	175	178	185
Q		1.960	0.837	0.836	0.867	0.796	0.815

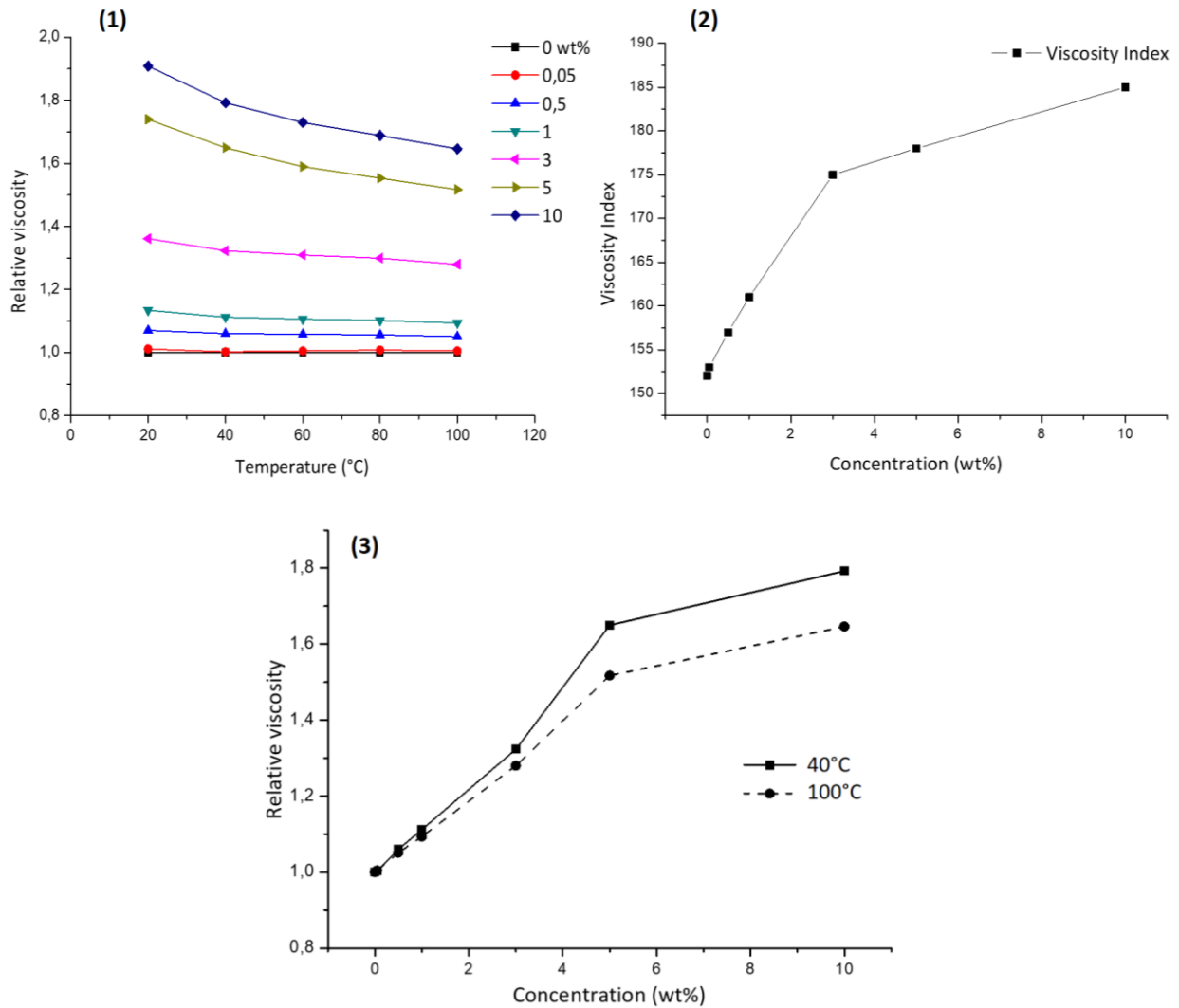


Figure II-30: (1) Relative viscosity of Radialube 7368 with Priolube 3986 added at several concentrations; (2) Viscosity Index as a function of Priolube 3986 concentration in Radialube 7368 and (3) relative viscosity as a function of the Priolube concentration in R, at 40 °C (solid line) and 100°C (dashed line)

As expected, the highest the additive concentration, the highest the relative viscosity, see Figure II-30 (1). The Priolube 3986 has a thickening effect on the oil with, for instance, an increase of the relative viscosity up to 1.9 at 20 °C for the sample with 10 wt.% of additive. This behavior corresponds to an increase of the kinematic viscosity from 45 to 87 mm<sup>2</sup>.s<sup>-1</sup>. However, the relative viscosity decreases with the temperature. This phenomenon is more representative at the highest concentration. For instance, a reduction from 1.9 at 20 °C to 1.65 at 100 °C is observed when 10 wt.% of Priolube 3986 is added.

Despite this behavior, the Viscosity Index increases by increasing the additive concentration, see Figure II-30 (2). For instance, a VI of 185 is obtained at 10 wt.% of additive despite a decrease of the relative viscosity of 0.15 between 40 °C and 100 °C. At only 3 wt.%, with a VI of 175, the decrease of relative viscosity is only about 0.04. The concentration plays a major

role in the modification of the oil viscosity, as illustrated in Figure II-30 (3). The highest the concentration, the highest the relative viscosity and the VI. Nevertheless, the VI appears to increase linearly with the concentration of additive up to 5 wt.%. Above this value, the impact of additional additive decreases drastically.

As reported in Table II-11,  $Q < 1$  for all the concentration. As a result, the addition of Priolube 3986 in the organic oil does not have a positive impact on the oil V-T behavior, it is a thickener. The highest Q value, i.e. 0.866, is obtained with a concentration of 3 wt.%. Moreover, Priolube 3968 added at 3 wt.% has a significant impact on relative viscosity (1.28 at 100 °C) as well as on the VI (+13 related to base oil VI). Consequently, the concentration of 3 wt.% was chosen for the rest of the study.

## **5.2. Effect of the PRic and PHS on oil viscosity**

All the so-formed PRic and PHS presented previously were tested as additives at a concentration of 3 wt.% in the two oils, Yubase 4+ and Radialube 7368. Their solubility in these oils were first investigated then the effect of their addition on the oil viscosity studied.

### ***5.2.1. Solubility on oils depending on the molecular weights***

PRic and PHS were added in the mineral and organic base oils at the concentration of 3 wt.%. The mixture was heated at 100 °C overnight under stirring to promote the solubilisation and then cooled down without stirring at room temperature during 24 hours. The solubility at this concentration was determined by visual appearance and tested at 20°C in the viscometer. It is worth noting that an inhomogeneous solution leads to unreproducible viscosity results. The solubility of PRic and PHS in the two oils are reported in Table II-12.

The higher molecular weight poly(methyl ricinoleate), such as PRic-4 and PRic-5 are not soluble in the two oils. This loss of solubility depends on the nature of the base oil. Indeed, PRic-3 is still soluble in Radialube while not in Yubase. Surprisingly, poly(hydroxystearate) is perfectly soluble in both base oils, independently of the molecular weight.

Table II-12 : Solubility of PRic and PHS in Radialube 3986 and Yubase 4+

Entry	$M_n^1$ (g.mol <sup>-1</sup> )	$M_w^1$ (g.mol <sup>-1</sup> )	$\bar{D}^1$	Solubility in R	Solubility in Y
PRic-1	4 000	6 100	1.5	Yes	Yes
PRic-2	7 200	10 600	1.5	Yes	Yes
PRic-3	18 200	32 200	1.7	Yes	No
PRic-4	21 700	47 100	2.2	No	No
PRic-5	28 100	131 500	4.6	No	No
PHS-1	8 100	17 500	2.1	Yes	Yes
PHS-2	24 000	68 100	2.4	Yes	Yes
PHS-3	28 500	78 400	2.5	Yes	Yes

**1 Obtained by SEC in THF – triple detection, dn/dc values used for calculation**

### 5.2.2. Effect on oil viscosity: towards thickening agents

The two oils, Radialube 7368 and Yubase 4+, containing PRic or PHS as additive were analyzed by viscometry. The kinematic viscosity of the mixtures was measured from 20 °C to 100°C allowing determining the relative viscosity and the Viscosity Indexes.

#### *Effect of bio-based polyesters in Radialube 7368*

All the density, dynamic and kinematic viscosity values are reported in Table II-A-4, see Appendix. The relative viscosity, Viscosity Index and Q values are reported in Table II-13.

Table II-13: Relative viscosity depending on the temperature, VI and values of Radialube 7369 with 3 wt.% of additives

	Ref	Pric-1	Pric-2	Pric-3	PHS-1	PHS-2	PHS-3	
$M_w$ (g.mol <sup>-1</sup> )	16 800	61 00	10 600	32 200	17 500	68 100	78 400	
$\eta_{rel}$	20 °C	1.36	1.13	1.37	1.55	1.46	2.06	2.32
	40 °C	1.32	1.11	1.33	1.49	1.40	1.96	2.19
	60 °C	1.31	1.10	1.30	1.44	1.38	1.90	2.14
	80 °C	1.30	1.10	1.29	1.42	1.37	1.86	2.10
	100 °C	1.28	1.09	1.27	1.40	1.34	1.81	2.05
VI	R=152	<b>175</b>	<b>163</b>	<b>172</b>	<b>175</b>	<b>176</b>	<b>195</b>	<b>204</b>
Q		<b>0.87</b>	<b>0.90</b>	<b>0.83</b>	<b>0.81</b>	<b>0.84</b>	<b>0.85</b>	<b>0.88</b>

The most significant impact on the relative viscosity is related to the polymer molecular weight. The highest the molecular weight, the highest the relative viscosity. The PHS-3 with a molecular weight around 80 kg.mol<sup>-1</sup> shows the best thickening properties with an increase of the kinematic viscosity from 43 mm<sup>2</sup>.s<sup>-1</sup> to 100 mm<sup>2</sup>.s<sup>-1</sup> at 20 °C. As it was previously observed, the addition of a polymer in Radialube 7368 induced a decrease of the relative viscosity with the temperature. This phenomenon is displayed in Figure II-31 (1) and confirmed with  $Q < 1$ . The same behavior is observed for all the polyesters tested, independently of their chemical composition and molecular weight. Despite that, the Viscosity Index is significantly increased by the addition of a polymer additive in the oil (see Figure II-31 (2)). Even the blend with the

lowest molecular weight PRic led to a significant VI increase from 152 to 163. A maximum of VI = 204 is obtained for the oil blended with PHS-3. As expected, the highest the polyester molecular weight, the highest the Viscosity Index increase, compared to the Radialube 7368 alone.

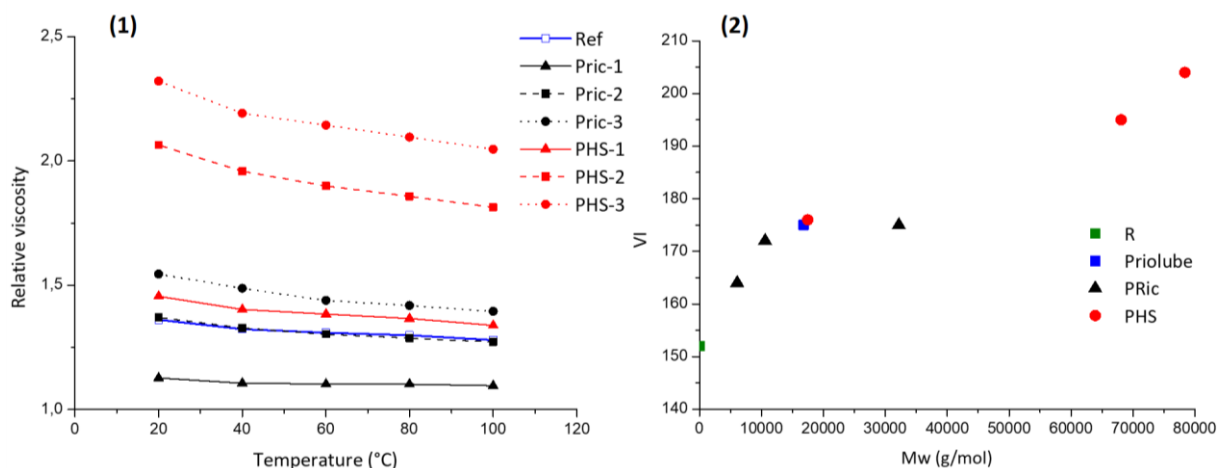


Figure II-31: Effect of polyesters, added at 3 wt.% in Radialube: (1) Relative viscosity as a function of the temperature and (2) VI as a function of Mw, the reference of the Priolube 3986

In Radialube 7386, the prepared bio-based polyesters show good thickening properties, especially for the highest molecular weight (PHS-3). A significant effect on the VI is observed, with an increase from 152 to 204 in the best case. Results can be compared with the commercial additives: PHS presents better thickening properties than Priolube 9386 for the same concentration in oil.

#### Effect of bio-based polyesters in Yubase 4+

The same study was realized in the mineral oil. All the viscosity measurements are reported in the Table II-A-5 in Appendix. As the Priolube 3986 is not soluble in Yubase, Viscoplex 10-250 (VP) was used as a reference. Polymers were added at 3 wt.% in oil, their impact on the relative viscosity and Viscosity Index are listed in Table II-14.

Table II-14: Relative viscosity as a function of temperature, VI and Q values of Yubase 4+ with 3 wt.% additives

		VP	Pric-1	Pric-2	PHS-1	PHS-2	PHS-3
$M_w$ (g.mol <sup>-1</sup> )		40 000	6 100	10 600	17 500	68 100	78 400
$\eta_{rel}$ (mm <sup>2</sup> .s <sup>-1</sup> )	20°C	n.d	1.076	1.205	1.314	1.730	1.931
	40°C	1.21	1.093	1.188	1.312	1.769	1.957
	60°C	n.d	1.083	1.185	1.286	1.743	1.970
	80°C	n.d	1.061	1.218	1.272	1.745	1.966
	100°C	1.17	1.064	1.187	1.267	1.731	1.896
VI	Y=145	163	147	172	171	205	209
Q		0.84	0.69	0.99	0.85	0.93	0.94

As it was already observed in Radialube 7368 (**R**), the increase of the relative viscosity is related to the polyester molecular weights. Only low molecular weights PRic are soluble in Yubase 4+ (**Y**), consequently their impact on relative viscosity is less significant than PHS in oil. As illustrated in Figure II-32 (1), the relative viscosity remains quite stable independently of the temperature. The decrease of relative viscosity with temperature is lower in Yubase 4+ than in Radialube 7368. This effect is enhanced with high molecular weight polyesters. For instance, PHS-3 blended with **R** has a Q factor of 0.88 while Q factor = 0.94 for PHS-3 blended in **Y**. For PRic-2, Q = 0.83 in **R** and Q = 0.99 in **Y**. The thickening effect is lower in mineral than in organic oil but the viscosity is more stable with respect to the temperature. This behavior may be due to a lower polymer solubility in mineral than in organic oil.

As illustrated in Figure II-32 (2), the Viscosity Index improvement is mainly due to the molecular weight of the polymer blended with Yubase 4+. PHS-2 and PHS-3 increased significantly the Yubase 4+ viscosity, independently of the temperature, and consequently a high increase of the Viscosity Index, with values up to 209. The relative viscosity remains more stable in Yubase 4+ than in Radialube 7368 regarding to the temperature change. As a result, VI is better improved in **Y** than in **R**. For instance, **Y** VI increases from 145 to 209 while **R** VI goes from 152 to 204 with 3 wt.% of PHS-3 in both cases.

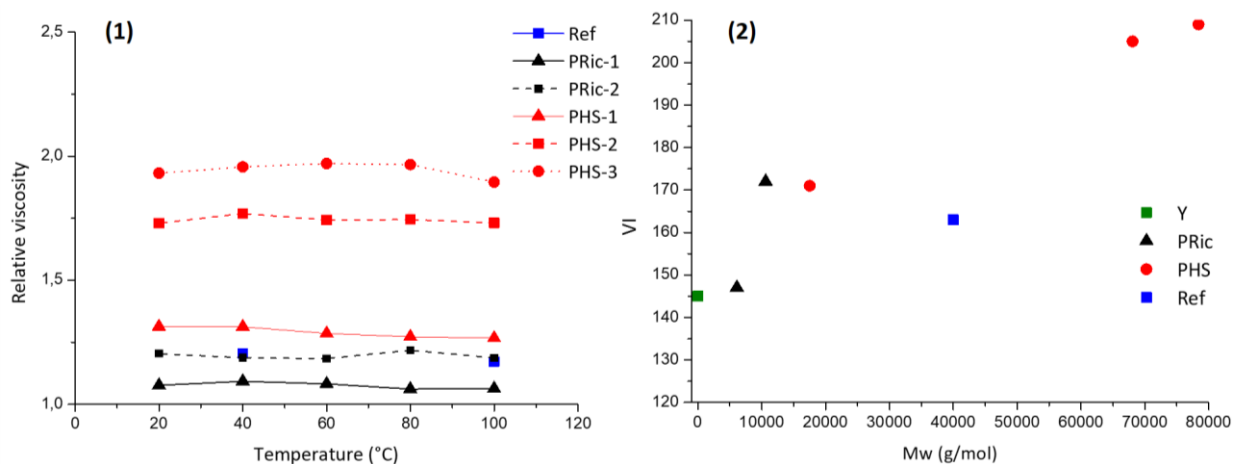


Figure II-32: Effect of polyesters blended at 3 wt.% in Yubase: (1) Relative viscosity depending on the temperature and (2) Viscosity Index as a function of polyester molecular weights, ref is Viscoplex 10-250

### 5.3. Conclusion

In order to evaluate PRic and PHS properties in solution, two oils were selected: Radialube 7386 as an organic oil and Yubase 4+ as a mineral one. Two commercial additives were tested in solution in comparison to the bio-based polyesters. The concentration of 3 wt.% of additive in oil was selected as the appropriate concentration according to the specification requirements.

Both poly(methyl ricinoleate) and poly(hydroxyl-12-stearate) were evaluated as viscosity modifiers in organic and mineral oils. The solubility in the oils of PRic was found limited by its molecular weights. As expected, a better solubility in organic than in mineral oil was observed. The oil viscosity increases by adding the polyesters at the concentration of 3 wt.%. The highest the polymer molecular weights, the highest its thickening effect, leading to a VI increase. PHS-3 presented the best properties in both oils with an increase of the VI from 152 to 204 in Radialube 7368 and from 145 to 209 in Yubase 4+. The relative viscosity tended to decrease with the temperature in the case of **R** but remained almost stable with **Y**. Finally, the polymer  $M_w$  is a key parameter to reach a significant thickening effect.

## Conclusion

---

The polycondensation of methyl ricinoleate was performed using  $\text{Ti}(\text{OiPr})_4$  as a catalyst. After optimization of the synthesis conditions, poly(methyl ricinoleate) was obtained by transesterification with molecular weights above  $130 \text{ kg}\cdot\text{mol}^{-1}$ . Both poly(methyl ricinoleate) and its saturated homologous poly(hydroxy-12-stearate) can be obtained in one step by direct polycondensation without any purification, which make them interesting candidates for industrial applications.

PRic and PHS exhibit a thermal stability above  $300 \text{ }^\circ\text{C}$ . PRic is a fully amorphous polymer with glass transition temperature around  $-70 \text{ }^\circ\text{C}$ . PHS presents a crystallinity with a melting point around  $-25 \text{ }^\circ\text{C}$ .

Poly(methyl ricinoleate) rheological behavior was evaluated as a function of its molecular weight. It appears that, for low  $M_w$ , PRic behaves as a viscous material. Above  $M_w = 25 \text{ kg}\cdot\text{mol}^{-1}$ , its melt viscosity increases drastically due to the presence of chain entanglements.

Finally, PRic and PHS were tested as viscosity modifiers. A preliminary study on a commercial additive allowed for determining the appropriate concentration of 3 wt.% for maximizing the thickening effect of the polymers added while remaining in low concentration regarding to the literature. Contrary to PHS, high molecular weight PRic are not soluble in the organic or mineral oils. Only PRic with  $M_w \leq 10 \text{ kg}\cdot\text{mol}^{-1}$  and  $M_w \leq 32 \text{ kg}\cdot\text{mol}^{-1}$  could be tested in mineral and organic oil, respectively. Both PRic and PHS have a thickening effect in oil. The highest the molecular weight, the highest the relative viscosity and, consequently the Viscosity Index. Indeed, when blended with a polymer additive, the base oil VI increases while its viscosity dependency to the temperature is not improved ( $Q < 1$ ). PRic and PHS show a good thickening efficiency but does not improve oil V-T behavior. Still, the VI could be improved from 145 to 210 in the best case.

In this study, the  $M_w$  increase of PRic and PHS led to get promising viscosity modifiers. A high thickening efficiency was reached. However, neither PRic nor PHS had a positive impact on oil V-T behavior. In order to target the other viscosity modifier applications, investigations on the chemical structure of the so-formed bio-based polyesters have to be performed. Such studies will be presented in the next chapter.

## References

---

- 1 A. R. Kelly and D. G. Hayes, *J. Appl. Polym. Sci.*, 2006, **101**, 1646–1656.
- 2 L. a. García-Zapateiro, J. M. Franco, C. Valencia, M. a. Delgado and C. Gallegos, *J. Ind. Eng. Chem.*, 2013, **19**, 1289–1298.
- 3 A. Gandini, *Green Chem.*, 2011, **13**, 1061.
- 4 A. Gandini, T. M. Lacerda, A. J. F. Carvalho and E. Trovatti, *Chem. Rev.*, 2016, **116**, 1637–1669.
- 5 L. Maisonneuve, T. Lebarbé, E. Grau and H. Cramail, *Polym. Chem.*, 2013, **4**, 5472.
- 6 N. B. Samarth and P. a Mahanwar, *Open J. Org. Polym. Mater.*, 2015, **5**, 1–22.
- 7 H. Mutlu and M. A. R. Meier, *Eur. J. Lipid Sci. Technol.*, 2010, **112**, 10–30.
- 8 A. Corma, S. Iborra and A. Velty, *Chem. Rev.*, 2007, **107**, 2411–2502.
- 9 U. Biermann, W. Friedt, S. Lang, W. Lühs, G. Machmüller, J. Metzger, Rüschen Klaas M, H. Schäfer and M. Schneider, *Angew. Chem. Int. Ed. Engl.*, 2000, **39**, 2206–2224.
- 10 F. C. Naughton, *J. Am. Oil Chem. Soc.*, 1974, **51**, 65–71.
- 11 K. R. Kunduru, A. Basu, M. Haim Zada and A. J. Domb, *Biomacromolecules*, 2015, **16**, 2572–2587.
- 12 G. Totaro, L. Cruciani, M. Vannini, G. Mazzola, D. Di Gioia, A. Celli and L. Sisti, *Eur. Polym. J.*, 2014, **56**, 174–184.
- 13 E. B. Mubofu, *Sustain. Chem. Process.*, 2016, **4**, 11.
- 14 D. S. Ogunniyi, *Bioresour. Technol.*, 2006, **97**, 1086–1091.
- 15 A. Gandini and T. M. Lacerda, *Polymers from Plant Oils*, Smithers., 2015.
- 16 P. F. H. Harmsen, M. M. Hackmann and H. L. Bos, *Biofuels, Bioprod. Biorefining*, 2014, **8**, 306–324.
- 17 D. V. Palaskar, A. Boyer, E. Cloutet, C. Alfos and H. Cramail, *Biomacromolecules*, 2010, **11**, 1202–1211.
- 18 L. Maisonneuve, A. S. More, S. Foltran, C. Alfos, F. Robert, Y. Landais, T. Tassaing, E. Grau and H. Cramail, *RSC Adv.*, 2014, **4**, 25795–25803.
- 19 S. Warwel, B. Wiege, E. Fehling and M. Kunz, *Eur. Polym. J.*, 2000, **36**, 2655–2663.
- 20 C. Lluch, G. Lligadas, J. C. Ronda, M. Galià and V. Cadiz, *Macromol. Rapid Commun.*, 2011, **32**, 1343–1351.
- 21 C. Vilela, A. F. Sousa, A. C. Fonseca, A. C. Serra, J. F. J. Coelho, C. S. R. Freire and A. J. D. Silvestre, *Polym. Chem.*, 2014, **5**, 3119–3141.
- 22 D. Teomim, A. Nyska and A. J. Domb, *J. Biomed. Mater. Res.*, 1999, **45**, 258–267.
- 23 R. Slivniak and A. J. Domb, *Macromolecules*, 2005, **38**, 5545–5553.
- 24 T. Lebarbé, E. Ibarboure, B. Gadenne, C. Alfos and H. Cramail, *Polym. Chem.*, 2013, **4**, 3357–3369.
- 25 H. Ebata, K. Toshima and S. Matsumura, *Macromol. Biosci.*, 2008, **8**, 38–45.
- 26 H. Ebata, K. Toshima and S. Matsumura, *Macromol. Biosci.*, 2007, **7**, 798–803.
- 27 H. Ebata, M. Yasuda, K. Toshima and S. Matsumura, *J. Oleo Sci.*, 2008, **57**, 315–320.
- 28 T. Kobayashi and S. Matsumura, *Polym. Degrad. Stab.*, 2011, **96**, 2071–2079.
- 29 A. Kazariya and S. Matsumura, *Polymers (Basel)*, 2012, **4**, 486–500.
- 30 T. Toyota, T. Banno, S. Nitta, M. Takinoue, T. Nomoto, Y. Natsume, S. Matsumura and M. Fujinami, *J. Oleo Sci.*, 2014, **63**, 1085–1098.
- 31 N. Kasmí, M. Majdoub, G. Papageorgiou, D. Achilias and D. Bikiaris, *Polymers (Basel)*, 2017, **9**, 607.
- 32 B. Testud, D. Pintori, E. Grau, D. Taton and H. Cramail, *Green Chem.*, 2017, **19**, 259–269.
- 33 M. E. Rogers and T. E. Long, *Synthetic Methods in Step-Growth Synthetic Methods in Step-Growth*, Wiley-Interscience, 2003.
- 34 A. Demirbas, *Energy Convers. Manag.*, 2008, **49**, 125–130.
- 35 U. Schuchardt, R. Sercheli and R. Matheus, *J. Braz. Chem. Soc.*, 1998, **9**, 199–210.
- 36 D. K. KIM and sang soon Park, *J. Polym. Sci. Part A Polym. Chem.*, 1994, **32**, 2873–2881.
- 37 J. Otera, *Chem. Rev.*, 1993, **93**, 1449–1470.

- 38 C. Liu, F. Liu, J. Cai, W. Xie, T. E. Long, S. R. Turner, A. Lyons and R. a Gross, *Biomacromolecules*, 2011, **12**, 3291–3298.
- 39 T. H. Shah, J. I. Bhatti, G. A. Gamlen and D. Dollimore, *Polymer (Guildf)*, 1984, **25**, 1333–1336.
- 40 J. Yang, S. Zhang, X. Liu and A. Cao, *Polym. Degrad. Stab.*, 2003, **81**, 1–7.
- 41 T. Lebarbé, E. Grau, B. Gadenne, C. Alfos and H. Cramail, *ACS Sustain. Chem. Eng.*, 2015, **3**, 283–292.
- 42 J. Liu, C. Kubis, R. Franke, R. Jackstell and M. Beller, *ACS Catal.*, 2016, **6**, 907–912.
- 43 H. Shirahama, Y. Kawaguchi, M. S. Aludin and H. Yasuda, *J. Appl. Polym. Sci.*, 2001, **80**, 340–347.
- 44 T. G. Fox and P. J. Flory, *J. Appl. Phys.*, 1950, **21**, 581–591.
- 45 T. G. Fox and P. J. Flory, *J. Phys. Chem.*, 1951, **55**, 221–234.
- 46 P. J. Fox, T. G; Flory, *J. Am. Chem. Soc.*, 1948, **70**, 2384–2395.
- 47 F. Bueche, *J. Chem. Phys.*, 1956, **25**, 599–600.
- 48 M. M. Cross, *Polymer (Guildf)*, 1970, **11**, 238–244.
- 49 R. H. Colby, L. J. Fetters and W. W. Graessley, *Macromolecules*, 1987, **20**, 2226–2237.
- 50 F. Bueche, *J. Chem. Phys.*, 1952, **20**, 1959–1964.
- 51 Cox and Merz, *J. Polym. Sci. Part A Gen. Pap.*, 1958, 619–622.
- 52 R. D. Andrewst and A. V Tobolsky, *J. Polym. Sci.*, 1950, **7**, 221–242.
- 53 M. L. Williams, R. F. Landel and J. D. Ferry, *J. Am. Chem. Soc.*, 1955, **77**, 3701–3707.
- 54 D. Van Krevelen and K. Nijenhuis, *Properties of Polymers*, Elsevier, 1992, vol. 16.
- 55 M. J. Struglinski and W. W. Graessley, *Macromolecules*, 1985, **18**, 2630–2643.
- 56 P. M. Wood-Adams, J. M. Dealy, A. W. DeGroot and O. D. Redwine, *Macromolecules*, 2000, **33**, 7489–7499.
- 57 R. G. Larson, *Macromolecules*, 2001, **34**, 4556–4571.
- 58 <http://www.machinerylubrication.com/Read/29113/base-oil-groups>.
- 59 <https://www.yubase.com/eng/index.html>.
- 60 <http://www.oleon.com/market/lubricants-and-performance-additives>.
- 61 G. B. Galland, R. F. de Souza, R. S. Mauler and F. F. Nunes, *Macromolecules*, 1999, **32**, 1620–1625.
- 62 [https://www.crodalubricants.com/en-gb/products-and-applications/product-finder/product/162/Priolube\\_1\\_3986](https://www.crodalubricants.com/en-gb/products-and-applications/product-finder/product/162/Priolube_1_3986).

## Experimental

---

### ***General procedure of polycondensation***

For the optimization of the reaction conditions, methyl ricinoleate (1 g, 3.125 mmol) polycondensation was performed in a 25 mL Schlenk under magnetic stirring at 200 rpm. After optimization of the reaction conditions, PRic and PHS were prepared from methyl ester ricinoleate and methyl-12-hydroxystearate, respectively, (1.5 g, 4.8 mmol) dried overnight under vacuum at 70 °C with mechanical stirring in 50 mL Schlenk flask at 200 rpm. The mixture was cooled at room temperature under static vacuum and a 5 wt.% solution of  $\text{Ti}(\text{O}i\text{Pr})_4$  in DCM (0.015 g of catalyst, 0.053 mmol, 1 wt.%) was added under nitrogen flow. The mixture was stirred at room temperature for 30 min under static nitrogen then put under vacuum and heated at 70 °C for 30min. Then the mixture was heated at 120 °C for one hour, 140 °C for another hour and 180 °C for 45 hours still under dynamic vacuum to remove the MeOH sub-product and mechanical stirring at 200 rpm. After 48 hours reaction, stirring was stopped, the highly viscous mixture was cooled to room temperature and the flask was opened to air in order to stop the reaction. No purification was performed on the final product.

### ***Rheological measurements***

Rheological measurements were monitored using an Anton Paar Physica MCR302 operating in the parallel plates geometry. The measurements were performed under nitrogen flow in the environmental chamber to avoid potential moisture effect. The temperature was controlled by Peltier device. The top plate has a diameter of 8 mm and the gap between plates was fixed at 1mm. Samples were loaded at room temperature. The sample was stabilized at the desirable temperature for 5 min before the measurement started.

Strain sweep measurements were performed from 0.01 to 100% with a constant shear frequency of 10  $\text{rad s}^{-1}$ . Dynamic frequency sweep was performed under oscillation at an angular frequency from 100  $\text{rad.s}^{-1}$  to 0.1  $\text{rad.s}^{-1}$  with a constant shear strain of 1%. Creep measurements were performed which shear stress of 1 Pa, 3 Pa, 5 Pa, 10 Pa, 30 Pa, 50 Pa, 100 Pa, 150 Pa and 200 Pa successively applied to the sample. For every shear stress, a constant shear rate was obtained within 1% of error for a minimum of 20 s before applying a new shear stress.

### ***Preparation of oil blended with additives***

Viscosity modifiers were added to the mineral and organic base oils at the concentration of 3 wt.%. The mixture was heated at 100 °C overnight under magnetic stirring to promote the solubilisation and then cooled down without stirring at room temperature during 24 hours. The solubility of the additive in the oil was evaluated macroscopically. Samples were degassed under vacuum and magnetic stirring for 30 minutes right before to be analysed by LOVIS 2000 densimeter-viscometer.

## **Appendix**

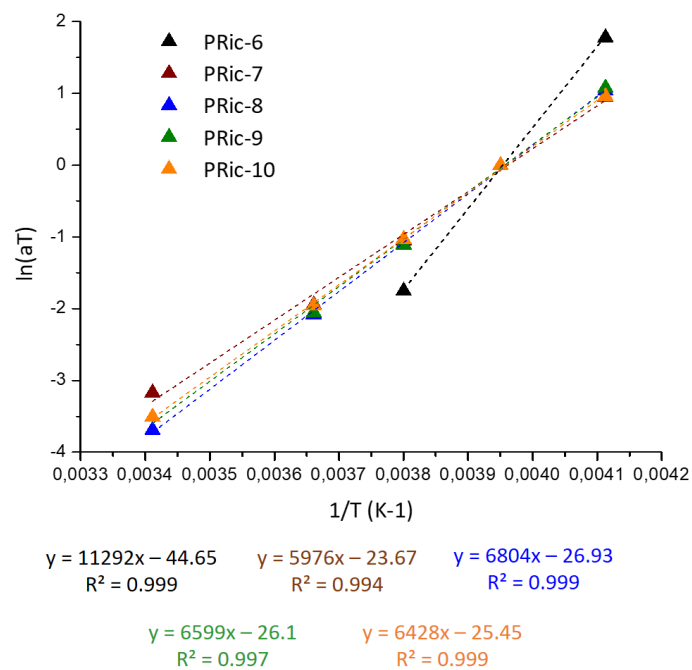


Figure II-A-1: Translation factor as a function of 1/T according to Andrade law

Table II-A-1: Translation factor obtained by TTS master curves, using WLF model and Arrhenius law for the five PRic tested

	T (°C)	-30	-20*	-10	0	20	Ea (kJ.mol <sup>-1</sup> )
PRic-6	$a_T$	5.911	1	0.173	-	-	93.72
	$a_{T\text{ calc}}$	6.256	1	0.184	0.038	0.002	
	%error	5.62	0	5.67	-	-	
PRic-7	$a_T$	2.592	1	0.350	0.143	0.042	49.57
	$a_{T\text{ calc}}$	2.634	1	0.408	0.178	0.040	
	%error	1.74	0	16.97	24.65	5.21	
PRic-8	$a_T$	2.832	1	0.328	0.125	0.025	56.63
	$a_{T\text{ calc}}$	3.028	1	0.359	0.139	0.025	
	%error	6.93	0	9.41	11.25	2.58	
PRic-9	$a_T$	2.937	1	0.332	0.128	0.030	54.80
	$a_{T\text{ calc}}$	2.921	1	0.371	0.148	0.029	
	%error	0.531	0	-11.767	-16.115	4.959	
PRic-10	$a_T$	2.612	1	0.356	0.141	0.030	53.47
	$a_{T\text{ calc}}$	2.846	1	0.380	0.155	0.031	
	%error	-8.957	0	-6.996	-10.430	-4.458	

\*: Reference temperature -  $a_{T\text{ calc}}$  are shift factors from computation using Arrhenius law

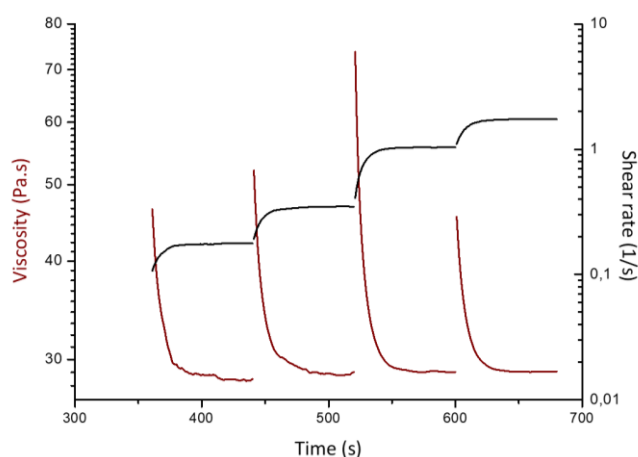


Figure II-A-2: Steady state creep test of PRic-7 at 20 °C. Applied shear stress of 5 Pa, 10 Pa, 30 Pa and 50 Pa successively

Table II-A-2: Translation factor obtained by TTS master curves at 80°C as reference, using WLF model and Arrhenius law for PRic-9 and PRic-10

	T (°C)	20	40	60	80*	100	150	200	Ea (kJ.mol <sup>-1</sup> )
PRic-9	$a_T$	30.457	8.497	2.687	1	0.413	-	-	43.90
	$a_{T\text{ calc}}$	30.365	8.415	2.721	1	0.409	-	0.015	
	%error	0.301	0.953	1.286	0	0.889	-	-	
PRic-10	$a_T$	21.480	5.387	2.294	1	0.450	-	-	42.98
	$a_{T\text{ calc}}$	20.061	6.498	2.410	1	0.456	0.089	-	
	%error	6.608	20.620	5.045	0	1.243	-	-	

\*: Reference temperature -  $a_{T\text{ calc}}$  are shift factors from computation using Arrhenius law

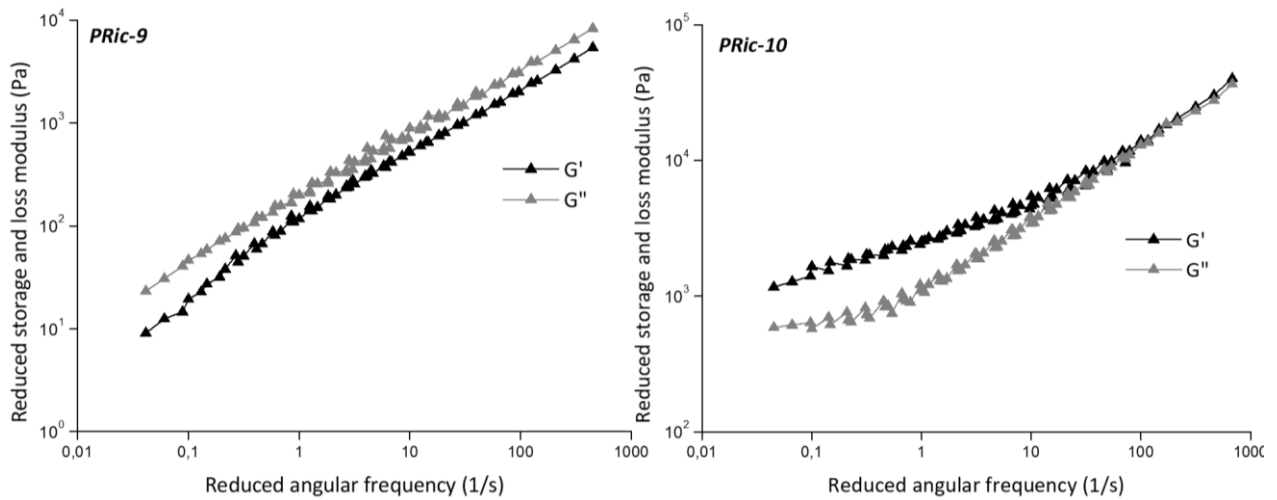


Figure II-A-3: Master curves at 80°C of PRic-9 and PRic-10 samples. Reduced storage and loss modulus are expressed versus the reduced angular frequency

Table II-A-3: Kinematic viscosity and Viscosity Index of Radialube 7368 doped with several concentration of Priolube 3986

	T (°C)	R	0,05wt.% P	0,5wt.% P	1wt.% P	3wt.% P	5wt.% P	10wt.% P
$\eta_{kin}$ ( $mm^2.s^{-1}$ )	20	45.57	46.04	48.75	51.68	62.01	79.27	86.96
	40	20.55	20.6	21.79	22.85	27.19	33.9	36.84
	60	10.91	10.96	11.54	12.06	14.28	17.34	18.87
	80	6.64	6.69	7.01	7.315	8.63	10.31	11.21
	100	4.67	4.694	4.91	5.11	5.98	7.09	7.69
<b>VI</b>		<b>152</b>	<b>153</b>	<b>157</b>	<b>161</b>	<b>175</b>	<b>178</b>	<b>185</b>

Table II-A-4: Radialube 7368 with 3wt.% additives. Density, dynamic and kinematic values at several temperatures

	Temperature	20°C	40°C	60°C	80°C	100°C
<b>Radialube</b>	<b>Density</b>	0.94	0.93	0.91	0.90	0.88
	$\eta_{dyn}$ (mPa.s-1)	42.91	19.05	9.96	5.96	4.13
	$\eta_{kin}$ (mPa.s-1)	45.56	20.55	10.91	6.64	4.67
<b>+3wt.% Priolube</b>	<b>Density</b>	0.9419	0.9275	0.9133	0.899	0.8865
	$\eta_{dyn}$ (mPa.s-1)	58.41	25.22	13.04	7.75	5.30
	$\eta_{kin}$ (mPa.s-1)	62.01	27.19	14.28	8.62	5.98
<b>+3wt.% PRic-1</b>	<b>Density</b>	0.9417	0.9273	0.913	0.8987	0.8848
	$\eta_{dyn}$ (mPa.s-1)	48.34	21.08	10.99	6.57	4.53
	$\eta_{kin}$ (mPa.s-1)	51.34	22.73	12.03	7.31	5.12
<b>+3wt.% PRic-2</b>	<b>Density</b>	0.9416	0.9276	0.9133	0.8991	0.8848
	$\eta_{dyn}$ (mPa.s-1)	58.82	25.31	12.98	7.68	5.26
	$\eta_{kin}$ (mPa.s-1)	62.45	27.29	14.21	8.54	5.94
<b>+3wt.% PRic-3</b>	<b>Density</b>	0.9416	0.9276	0.9133	0.8991	0.8848
	$\eta_{dyn}$ (mPa.s-1)	58.82	25.31	12.98	7.68	5.26
	$\eta_{kin}$ (mPa.s-1)	62.45	27.29	14.21	8.544	5.94

<b>+3wt.% PHS-1</b>	<b>Density</b>	0.9416	0.9272	0.9131	0.8988	0.8846
	$\eta_{\text{dyn}}$ (mPa.s-1)	62.45	26.72	13.78	8.15	5.53
	$\eta_{\text{kin}}$ (mPa.s-1)	66.32	28.82	15.1	9.07	6.25
<b>+3wt.% PHS-2</b>	<b>Density</b>	0.9415	0.9271	0.9128	0.8986	0.8845
	$\eta_{\text{dyn}}$ (mPa.s-1)	88.53	37.31	18.91	11.08	7.49
	$\eta_{\text{kin}}$ (mPa.s-1)	94.03	40.24	20.72	12.33	8.47
<b>+3wt.% PHS-3</b>	<b>Density</b>	0.9416	0.9272	0.9129	0.8987	0.8846
	$\eta_{\text{dyn}}$ (mPa.s-1)	99.51	41.77	21.35	12.5	8.46
	$\eta_{\text{kin}}$ (mPa.s-1)	105.7	45.05	23.38	13.91	9.56

Table II-A-5: Yubase 4+ with 3wt.% additives. Density, dynamic and kinematic values at several temperatures

	<b>Temperature</b>	<b>20°C</b>	<b>40°C</b>	<b>60°C</b>	<b>80°C</b>	<b>100°C</b>
<b>Yubase</b>	<b>Density</b>	0.8226	0.8099	0.7973	0.7846	0.7720
	$\eta_{\text{dyn}}$ (mPa.s-1)	34.41	15.16	7.97	4.82	3.35
	$\eta_{\text{kin}}$ (mPa.s-1)	41.82	18.71	9.99	6.14	4.34
<b>+3wt.% Viscoplex</b>	<b>Density</b>	-	-	-	-	-
	$\eta_{\text{dyn}}$ (mPa.s-1)	-	-	-	-	-
	$\eta_{\text{kin}}$ (mPa.s-1)	-	22.55	-	-	5.08
<b>+3wt.% PRic-1</b>	<b>Density</b>	0.8254	0.8127	0.8	0.7874	0.7748
	$\eta_{\text{dyn}}$ (mPa.s-1)	37.16	16.62	8.656	5.13	3.57
	$\eta_{\text{kin}}$ (mPa.s-1)	45.02	20.45	10.82	6.51	4.61
<b>+3wt.% PRic-2</b>	<b>Density</b>	0.8257	0.8129	0.8003	0.7876	0.7971
	$\eta_{\text{dyn}}$ (mPa.s-1)	41.59	18.07	9.473	5.89	4.10
	$\eta_{\text{kin}}$ (mPa.s-1)	50.38	22.23	11.84	7.48	5.15
<b>+3wt.% PHS-1</b>	<b>Density</b>	0.8255	0.8128	0.8001	0.7875	0.7749
	$\eta_{\text{dyn}}$ (mPa.s-1)	45.35	19.96	20.28	6.15	4.26
	$\eta_{\text{kin}}$ (mPa.s-1)	54.94	24.56	12.85	7.81	5.49
<b>+3wt.% PHS-2</b>	<b>Density</b>	0.8255	0.8128	0.8001	0.7875	0.7748
	$\eta_{\text{dyn}}$ (mPa.s-1)	59.72	26.9	13.94	8.44	5.82
	$\eta_{\text{kin}}$ (mPa.s-1)	72.34	33.1	17.42	10.71	7.51
<b>+3wt.% PHS-3</b>	<b>Density</b>	0.8256	0.8129	0.8003	0.7876	0.7971
	$\eta_{\text{dyn}}$ (mPa.s-1)	66.7	29.77	15.76	9.50	6.55
	$\eta_{\text{kin}}$ (mPa.s-1)	80.78	36.62	19.69	12.07	8.22



## Chapter 3:

*Structural modification of bio-based polyesters: from linear to comb polymers*

## Table of content

Introduction.....	145
1. From linear to comb bio-based polyesters .....	145
1.1. Synthesis of A-B monomers from renewable resources .....	146
1.1.1. 2-Mercaptoethanol addition on methyl-10-undecanoate .....	146
1.1.2. 2-Mercaptoethanol addition of methyl oleate.....	147
1.1.3. Dodecane-1-thiol addition on methyl ricinoleate.....	148
1.2. Polyesters synthesis by transesterification .....	150
1.3. Effect of the various architectures on polyester properties .....	155
1.3.1. Thermal properties .....	156
1.3.2. Polyesters behavior in base oil .....	158
1.4. Conclusion.....	161
2. Comb poly(9-alkyl 12-hydroxystearate)s with various dangling chains.....	162
2.1. Synthesis of comb poly(9-alkyl 12-hydroxystearate)s with various side chains .....	163
2.1.1. Methyl ricinoleate functionalization by thiol-ene addition .....	163
2.1.2. Polymerization of the functionalized monomers .....	164
2.2. Comb poly(9-alkyl 12-hydroxystearate)s thermal properties .....	167
2.3. Investigation of comb poly(9-alkyl 12-hydroxystearate)s as viscosity modifiers.....	168
2.3.1. Comb poly(9-alkyl 12-hydroxystearate)s behavior in organic oil.....	168
2.3.2. Comb poly(9-alkyl 12-hydroxystearate)s behavior in mineral oil .....	171
2.4. Investigation of comb poly(9-alkyl 12-hydroxystearate)s as pour point depressants	174
2.4.1. Evaluation of some comb poly(9-alkyl 12-hydroxystearate)s as potential PPD ...	174
2.4.2. Influence of the polymer concentration on oil pour point.....	175
2.4.3. Influence of the molecular weight on additive efficiency as PPD.....	177
2.4.4. Comb versus semi-crystalline polyesters .....	178
2.4.5. Comb poly(9-octadecyl 12-hydroxystearate) investigation as PPD in organic oil	180
Conclusion .....	181
References.....	183
Experimental .....	184
Appendix.....	188

## Introduction

---

In the previous chapter, polyricinoleate and poly(hydroxyl-12-stearate) were evaluated as promising thickeners but did not act as Viscosity Index improvers properties. Both polymers contain a pendant alkyl chain. Polymers with various architectures were described as viscosity modifiers and pour point depressants.<sup>1,2</sup> It was shown that linear polymers such as polyolefins have a high thickening efficiency while comb PAMAs have an impact on oil viscosity-temperature behavior by coil expansion.<sup>3-5</sup> Long alkyl chains in PAMAs also provide a good pour point depressant efficiency.<sup>6,7</sup> It could then be interesting to develop different polyricinoleate-based architectures in order to evaluate the architecture impact on modified PRic efficiency as viscosity modifiers.

As a result, the aim of this study is to investigate the effect of the polymer architecture on its properties in bulk and in solution. First, bio-based polyesters with various amounts of side alkyl chains; from linear to two pendant alkyl chains per repeating unit; will be described and evaluated as viscosity modifiers. Then, comb polyesters exhibiting different pending chains – in terms of size and nature- will be discussed and the impact of these architectures on the polymer properties in bulk and in solution investigated.

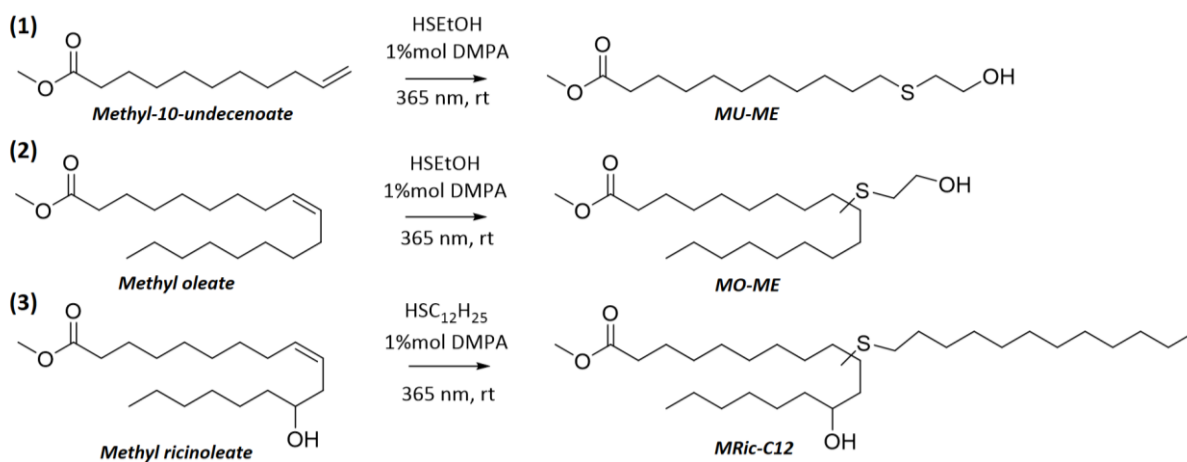
### 1. From linear to comb bio-based polyesters

---

In order to evaluate the effect of pendant alkyl chains on polyester properties, three bio-based polyesters were synthesized from renewable resources. The latter were designed in order to have a similar backbone as the one of PRic, with various amounts of pendant chains. To this purpose, thiol-ene click chemistry was performed on the bio-based precursors to design novel A-B monomer. A linear polyester was obtained from methyl-10-undecenoate, a polyester with one pendant alkyl chain was synthesized from methyl oleate and a polyester with two pendant alkyl chains was obtained from functionalized methyl ricinoleate. The properties of the so-formed polyesters were then evaluated in bulk and in solution.

## 1.1. Synthesis of A-B monomers from renewable resources

The three synthesized bio-based monomers are schematically presented in Scheme III-1.



Scheme III-1: Representation of bio-based precursors for further polyester syntheses and their functionalization by thiol-ene addition

In this study, as illustrated in Scheme III-1, 2-mercaptoethanol (ME) was added on methyl undecenoate (MU) and methyl oleate (MO) by thiol-ene click reaction in order to obtain self-condensable A-B type monomers with respectively a linear structure or one alkyl pendant chain. Then a dodecane thiol was added on methyl ricinoleate (MRic) to give a second pendant chain on the monomer backbone. All the reactions were performed without solvent, reactants being liquid at room temperature. Reactions were performed by photo-initiation using 2,2-dimethoxy-2-phenylacetophenone (DMPA) as photo-initiator at 1 mol.% under a UV lamp at 365 nm at 20 °C. Conversions were monitored by <sup>1</sup>H NMR spectroscopy.

### 1.1.1. 2-Mercaptoethanol addition on methyl-10-undecanoate

A mixture of methyl-10-undecanoate, mercaptoethanol used at 1 equivalent per double bond and photo-initiator was irradiated until the complete disappearance of the fatty ester double bond as proved by <sup>1</sup>H NMR analysis. The final monomer was obtained with a yield of 98%.

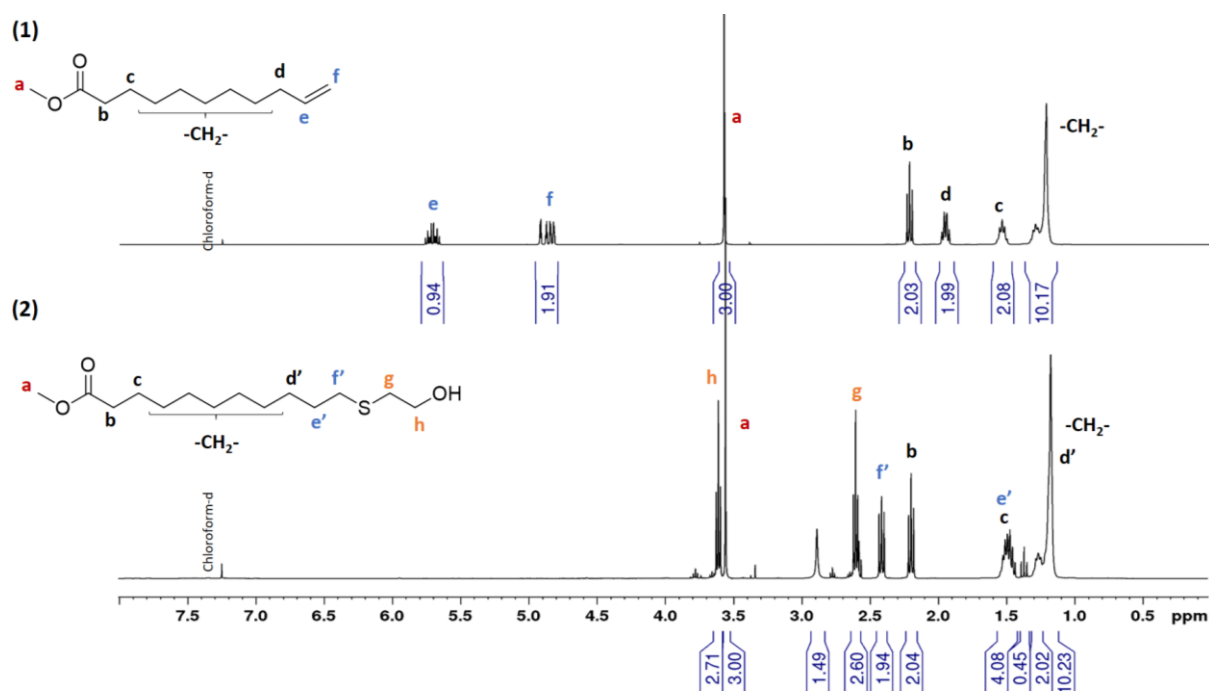


Figure III-1:  $^1\text{H}$  NMR spectra in  $\text{CDCl}_3$  of (1) methyl-10-undecanoate and (2) methyl-10-undecanoate functionalized by mercaptoethanol after 2 hours reaction

As displayed in Figure III-1, the fully disappearance of C=C peaks at 5.6 ppm and 4.8 ppm was observed after 2 hours reaction, demonstrating a complete conversion. Protons H<sub>e</sub> on carbon 10 shifted from 5.6 ppm to 1.6 ppm and integrated for 2 protons. Terminal protons H<sub>f</sub> shifted from 4.8 ppm to 2.4 ppm. This feature suggests that the thiol was added on the terminal carbon, in accordance with an anti-Markovnikov reaction.<sup>8</sup> As the photo-initiator concentration was negligible and the ME fully consumed, no purification was required. Nevertheless, 2-mercaptoethanol was added in slight excess. Indeed, both couples of protons at 2.55 ppm and 3.6 ppm integrated at 2.2 instead of 2. Consequently, the product was put under vacuum to eliminate the unreacted thiol.

To conclude, the methyl 11-(2-hydroxyethylthio) undecanoate (MU-ME), a linear AB-type monomer was prepared following click chemistry principle.<sup>9</sup> A complete conversion was performed within 2 hours at room temperature and no purification was required.

### 1.1.2. 2-Mercaptoethanol addition of methyl oleate

Methyl oleate (MO) contains an internal double bond on C9-C10. As the internal double bond is less reactive than terminal one, an excess of thiol was used for the addition reaction. According to literature<sup>10</sup>, 3 equivalents of 2-mercaptoethanol were added per double bond

with 1 mol.% DMPA. Monitored by  $^1\text{H}$  NMR spectroscopy, UV irradiation was stopped after 2 hours reaction. Unreacted ME was removed by washing the reaction mixture with water. The final yield is about 77%.  $^1\text{H}$  NMR spectra of unreacted MO and MO-ME are displayed in Figure III-2.

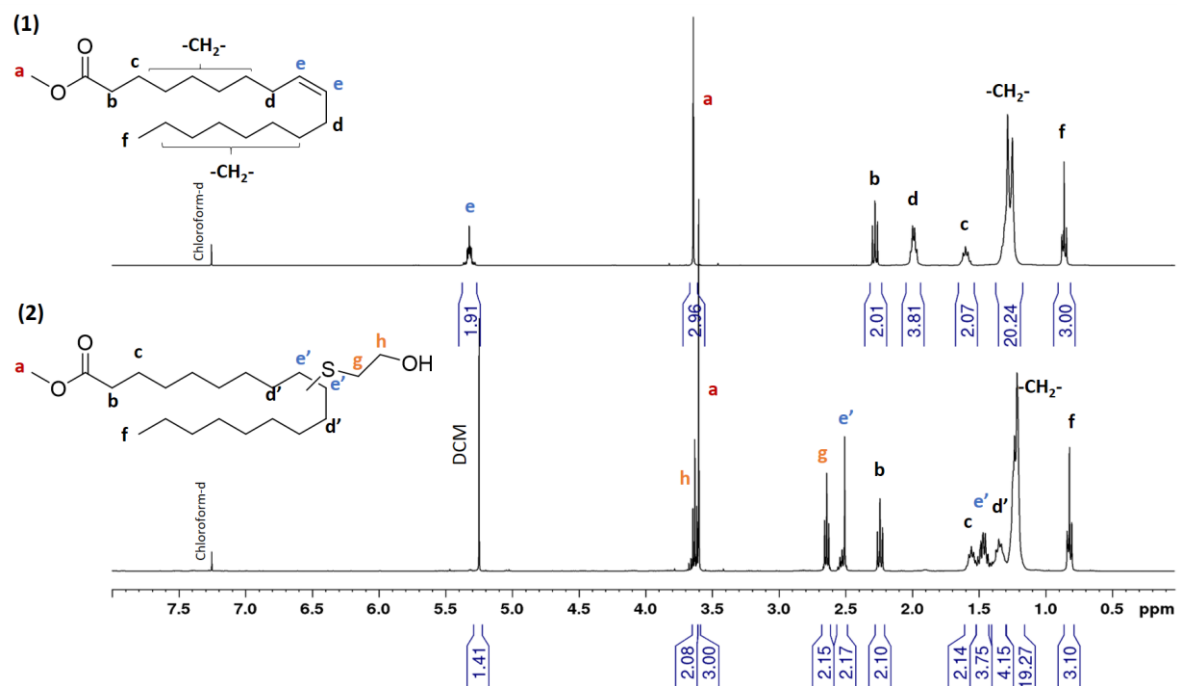


Figure III-2:  $^1\text{H}$  NMR spectra  $\text{CDCl}_3$  of (1)methyl oleate and (2)MO-ME methyl oleate functionalized with mercaptoethanol – DCM as remained solvent

A complete conversion of the double bond was observed by  $^1\text{H}$  NMR spectroscopy. The shift of protons  $\text{H}_d$  in  $\alpha$  of the double bond as well as the appearance of ME protons  $\text{H}_g$  and  $\text{H}_h$  at 2.6 ppm and 3.6 ppm respectively confirmed the thiol-addition. Regioselectivity of the thiol-ene reaction is not controlled thus the thiol group can be added on C9 as well as C10. After washing with water, a pure product was obtained, without any presence of unreacted mercaptoethanol. The methyl 10-(2-hydroxyethylthio) stearate (MO-ME) is then a AB monomer with one pendant chain.

### 1.1.3. Dodecane-1-thiol addition on methyl ricinoleate

In order to add a second alkyl pendant chain to methyl ricinoleate, dodecane thiol was selected. The thiol-ene addition occurred within the same conditions as described above. As illustrated in Figure III-3, a full conversion was obtained within three hours.

A conversion of the C=C bonds of 86% was reached within the first hour reaction then the reaction kinetics slowed down. Only 90% conversion was reached after 2 hours reaction and the complete conversion appeared after 3 hours. Because of the steric hindrance induced by the dodecyl- alkyl chain, the reaction is slower than the ones described before, for which a complete conversion was observed within 2 hours under irradiation.

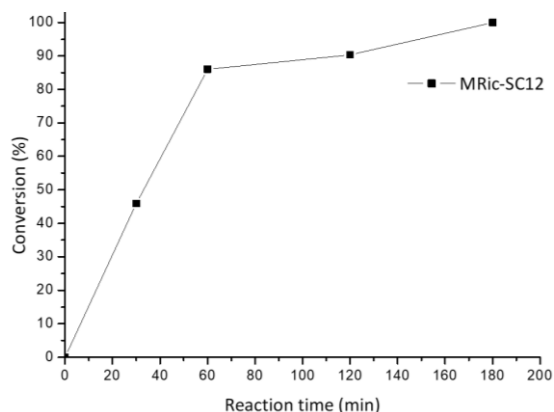


Figure III-3: Kinetics of the addition of dodecane thiol on methyl ricinoleate monitored by the C=C peak disappearance on  $^1\text{H}$  NMR spectrum

The mixture was purified by Flash chromatography to eliminate the unreacted dodecane thiol using cyclohexane/ethyl acetate solvent system. A yield of 67% was obtained.  $^1\text{H}$  NMR spectrum of the obtained product compared to the one of methyl ricinoleate is displayed in Figure III-4.

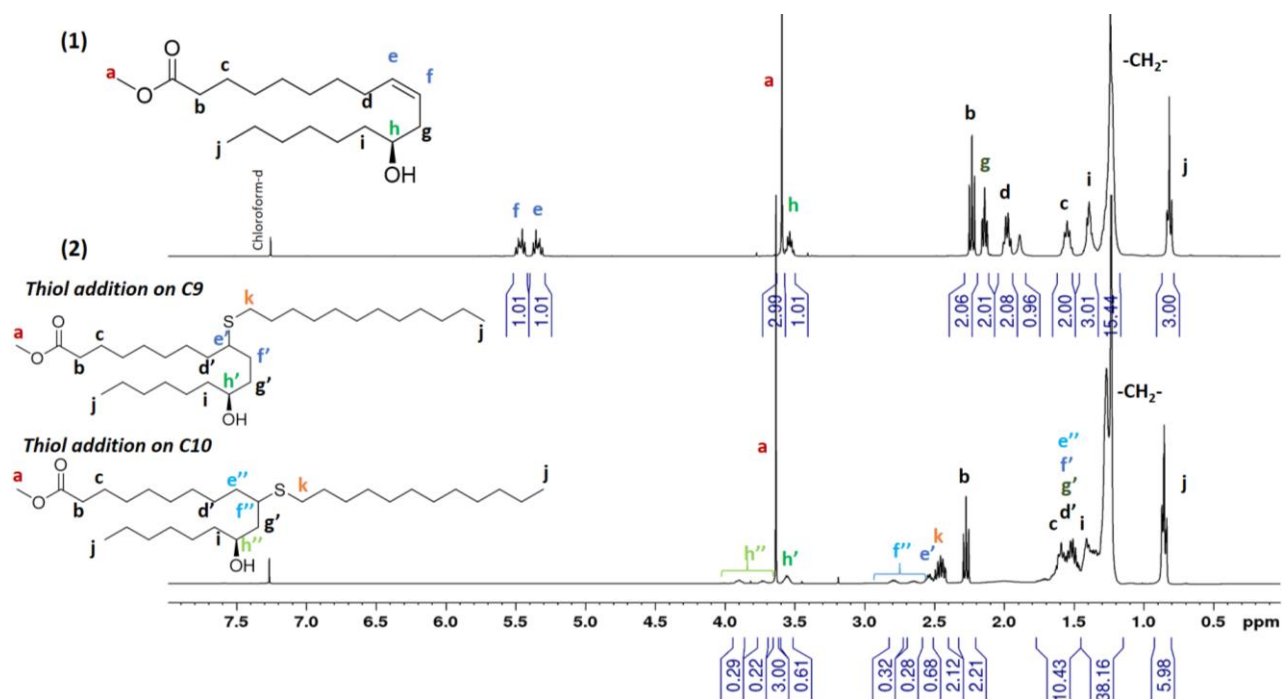


Figure III-4:  $^1\text{H}$  NMR spectra in  $\text{CDCl}_3$  of (1) methyl ricinoleate and (2) methyl 9-alkyl 12-hydroxystearate

The double bond peak at 5.4 – 5.6 ppm disappeared. There is a shift of protons H<sub>d</sub> and H<sub>g</sub> from 2.0 and 2.2 ppm, respectively, to the characteristic position of alkyl groups at 1.2 – 1.4 ppm. The appearance of the signal of protons in α of the thiol at 2.4 ppm confirms the addition of the 1-dodecane thiol on methyl ricinoleate.

The signal of the proton in α of the OH group, H<sub>h</sub>, appears in 3 peaks after the thiol addition, at 3.55 ppm, 3.7 ppm and 3.9 ppm. The peak at 3.55 ppm (H<sub>h'</sub>) is the same as H<sub>h</sub> proton peak of methyl ricinoleate, meaning that the proton environment was not affected by the reaction. The signal is consequently related to molecules in which the thiol addition has been done on the C9 of methyl ricinoleate. The proton on C9 H<sub>e'</sub> at 2.55 ppm has the same integration of 0.6; as a result, 60% of the thiol addition occurred on C9.

The two other peaks of H<sub>h''</sub> proton, at 3.7 and 3.9 ppm; with a total integration around 0.4; are related to molecules with a thiol added on C10, in a closest environment of the considered proton H<sub>h''</sub>. It is supposed that addition on C10 could be done on cis or trans position, leading to two different peaks of proton H<sub>h''</sub>. The same behavior is observed for the proton on C10, H<sub>g''</sub>. Its signal is also separated in two peaks at 2.7 and 2.9 ppm and integrate in total for 0.5. Then, 40% of the thiol was added on C10. As the thiol is added in majority on the C10, the prepared monomer was noted as methyl 9(10)-dodecyl 12-hydroxystearate or more simply methyl 9-dodecyl 12-hydroxystearate (MRic-C12).

To conclude this section, the three bio-based precursors were fully derivatized by thiol-ene addition. This click reaction was performed without any solvent, at room temperature and did not required complex purification. Three AB type monomers were thus obtained and readily prepared for polymerization by self-condensation.

## 1.2. Polyesters synthesis by transesterification

The A-B monomers previously synthesized were polymerized by transesterification. The reaction conditions optimized in the previous chapter were selected, i.e. in the melt with 1 wt.% of Ti(OiPr)<sub>4</sub> as catalyst, 48 hours reaction at 180 °C under vacuum under mechanical stirring. The polyesters were characterized by <sup>1</sup>H NMR spectroscopy, see Figure III-5. The linear polyester based on methyl 11-(2-hydroxyethylthio) undecanoate, i.e. Poly(MU-ME), was characterized after 24 hours reaction (see spectra (1)). Indeed, after 48 hours of reaction, the polyester formed was insoluble in usual solvents, avoiding its characterization.

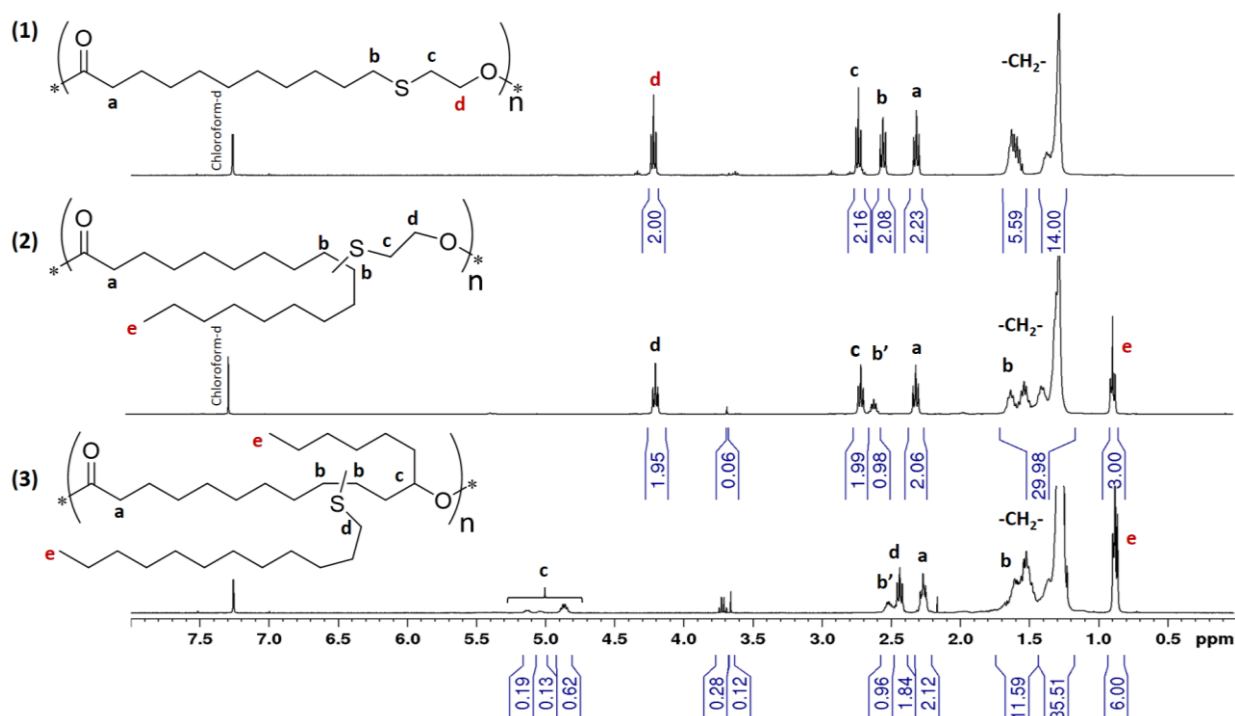


Figure III-5:  $^1\text{H}$  NMR spectra in  $\text{CDCl}_3$  of (1) poly(MU-ME), (2) poly(MO-ME) and (3) poly(Ric-C12) obtained by transesterification – Protons in red are used as reference for integration values – b' corresponds to the proton in  $\alpha$  position of the thiol group and b to the two protons in  $\beta$  position of the thiol group

The chemical structures of the bio-based polyesters obtained by transesterification were confirmed by  $^1\text{H}$  NMR analyses. The disappearance of the methyl peak characteristic of the ester group at 3.6 ppm proved that polymerization occurred. In the case of P(Ric-C12),  $\text{H}_c$  at 4.8 – 5.2 ppm is split in three peaks due to the dodecyl thiol addition both on C9 and C10 (in cis-trans conformations). These three bio-based polyesters present similar backbone structure, all with a thioether group while the amount of pendant chain varies from 0 to 2. The presence of pendant alkyl chains may impact the monomer reactivity and the polymer molecular weight. However, in order to properly evaluate the impact of the pendant chains on the polyester properties, the polyesters may have similar molecular weights. The kinetics of polymerization of the three prepared monomers were then studied and compared to the previously performed methyl ricinoleate polymerization.

The kinetics of polymerization were evaluated according to the reactive functions conversion and the polyester molecular weight variation. Aliquots were taken out from the reaction mixture at different times and analyzed readily by  $^1\text{H}$  NMR spectroscopy and SEC measurement using PS calibration. The reactive functions conversion was determined by the

disappearance of the methyl ester peak at 3.6 ppm. Reactive functions conversions and polyester molecular weights are plotted as a function of time in Figure III-6.

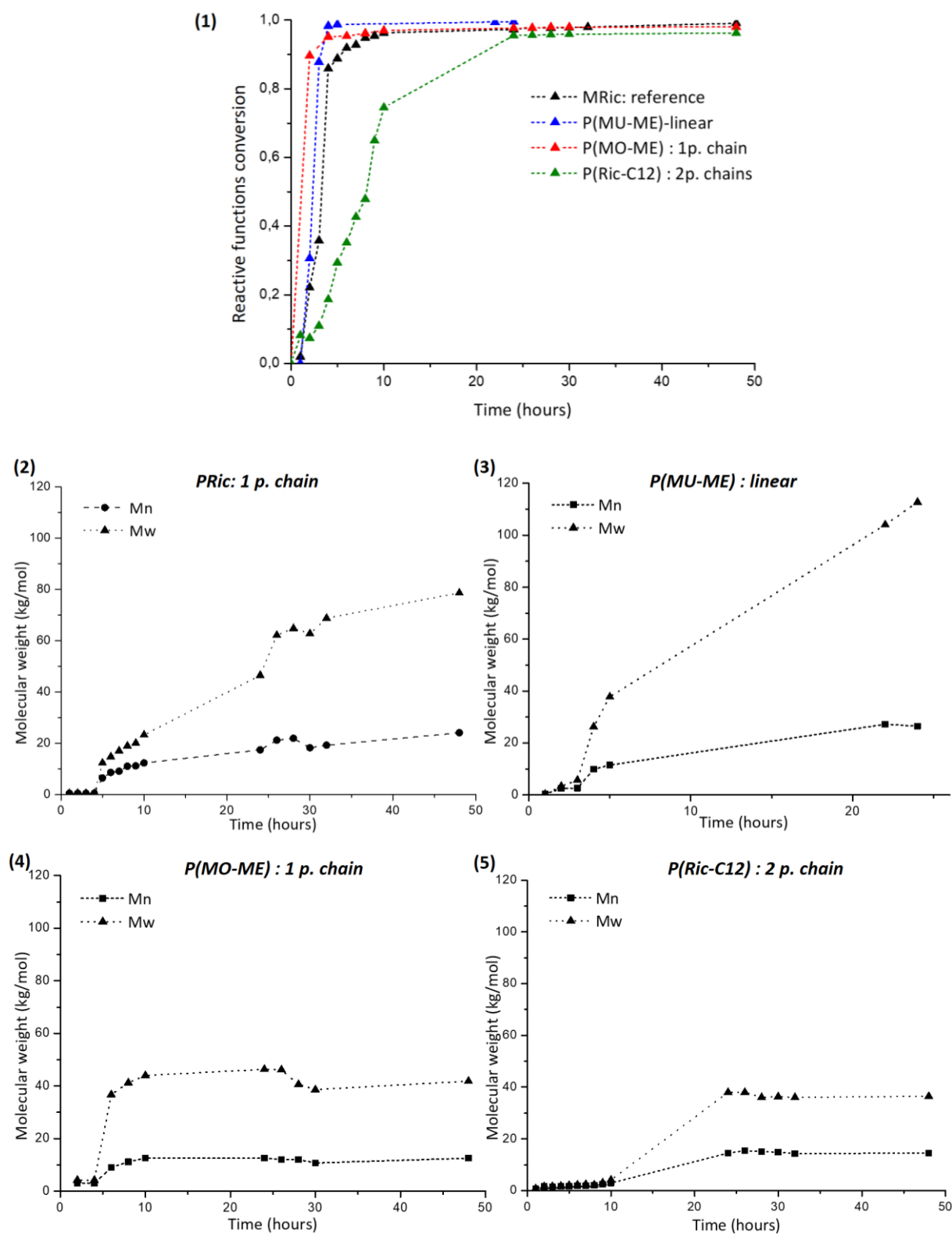


Figure III-6 : Kinetics of polymerization of the three considered monomers. (1) Reactive functions conversion versus time, monitored by  $^1\text{H}$  NMR spectroscopy in  $\text{CDCl}_3$ . (2) P(Ric) (3) P(MU-ME), (4) P(MO-ME), (5) P(MRic-C12) molecular weight variation as a function of time, measured by SEC analyses (PS calibration)

The polymerizations of MRic, MU-ME, MO-ME and Ric-C12 were realized in the same reaction conditions. As illustrated in Figure III-6, the monomer structure has a strong impact on the kinetics, both in terms of reactive functions conversion and molecular weight. These differences are due both from the nature of the alcohol reactive group and the presence of pendant chains.

Both monomers MU-ME and MO-ME bear a primary OH group due to mercaptoethanol addition. In these cases, more than 95% of functions reacted within the first 4 hours while 95% of conversion is obtained after 6 hours of reaction for the MRic. The conversion of methyl ricinoleate is slightly slower than MO-ME due to the lower reactivity of its secondary alcohol reactive group. As well-known, primary OH function is less substituted, so more reactive than secondary alcohol, allowing faster conversion. In the case of PRic-C12, the reactive functions conversion reached 95% only after 24 hours meaning that the presence of a second pendant chain slows down the polymerization because of steric hindrance.

For both P(MU-ME) and P(MO-ME), the conversion reached 95% after 4 hours then increased up to 0.994 for P(MU-ME) and 0.98 for P(MO-ME) after 24 hours. However, P(MU-ME) molecular weights keep increasing from  $M_w = 24\ 000\ \text{g}\cdot\text{mol}^{-1}$  at  $t = 5$  hours up to  $M_w = 165\ 000\ \text{g}\cdot\text{mol}^{-1}$  at  $t = 24$  hours.  $\bar{D}$  increased also to 4.4 while it is expected around 2. After this reaction time, the linear polyester became insoluble in usual solvent, suggesting even higher molecular weight and potential secondary reactions.

A different behavior was observed for P(MO-ME). For instance, its molecular weight reached a plateau after 6 hours reaction, i.e. at the same time reactive functions conversion stabilized. At  $t = 6$  hours reacting,  $M_w$  of  $37\ 000\ \text{g}\cdot\text{mol}^{-1}$  was reached and only increase to  $41\ 800\ \text{g}\cdot\text{mol}^{-1}$  after 48 hours. Moreover, the final P(MO-ME) molecular weight is in the same range of P(Ric-C12) ones, with  $M_w$  of  $41\ 800\ \text{g}\cdot\text{mol}^{-1}$  for P(MO-ME) and  $M_w$  of  $36\ 400\ \text{g}\cdot\text{mol}^{-1}$  for P(Ric-C12). As a result, it is supposed that the presence of pendant alkyl chains limits the polymer chain growth during polymerization. The PRic molecular weight did not reach a plateau such as P(MO-ME) and P(Ric-C12) and final  $M_w = 78\ 000\ \text{g}\cdot\text{mol}^{-1}$ . The polymer chain growth seems also limited by the presence of a thioether linkage in the monomeric repetitive unit.

To conclude, the difference of polymerization kinetics between the MO-ME monomer and the MRic can confirm that reactive functions conversion was faster with primary OH group instead

of secondary one. The reactive functions conversion is also affected by the amount of pendant chains, the more hindered the monomer, the lower the conversion. In addition, the molecular weight increase was affected by the presence of pendant alkyl chains. The synthesis of a linear polyester such as P(MU-ME) led to high molecular weight polyester, above  $M_w = 164\ 000\ \text{g.mol}^{-1}$  while the  $M_w$  values of comb polyesters reached a plateau around  $M_w$  of  $40\ 000\ \text{g.mol}^{-1}$ .

Once the kinetics of polymerization were investigated, the reaction conditions were adapted for each polymerization in order to synthesize the polyesters with similar molecular weights allowing proper comparison of their properties. Two ranges of molecular weights were then targeted:  $M_n = 15\ \text{kg.mol}^{-1}$  and  $M_n = 25\ \text{kg.mol}^{-1}$ . P(MU-ME), P(MO-ME), P(Ric-C12) as well as PRic and PHS were then obtained. PHS was also synthesized because it has a close structure to P(MO-ME) but without a thioether bond. Reactive functions conversion and molecular weight are depicted in Table III-1 and SEC traces are illustrated in Figure III-7.

Table III-1: Reactive functions conversion and polyester molecular weight

Entry	Time (h)	$P^1$	$DP^1$	$Mn^1\ (\text{g.mol}^{-1})$	$Mn^2\ (\text{g.mol}^{-1})$	$Mw^2\ (\text{g.mol}^{-1})$	$\bar{D}^2$
P(MU-ME) - 2 <sup>a</sup>	24	0.995	211	58 300	26 500	112 700	4.4
P(MO-ME) - 1 <sup>a</sup>	24	0.978	46	15 900	15 700	32 100	2
P(MO-ME) - 2 <sup>b</sup>	48	0.981	54	18 400	22 500	76 000	3.4
P(Ric-C12) - 1 <sup>a</sup>	24	0.962	27	13 000	14 500	36 400	2.5
P(Ric-C12) - 2 <sup>b</sup>	48	0.983	58	28 000	24 000	55 000	2.2
PRic - 2 <sup>a</sup>	48	0.984	63	19 800	25 200	56 800	2.3
PHS - 2 <sup>a</sup>	48	0.990	100	30 200	25 600	63 000	2.4

*Reaction conditions: 180°C, 1 wt.% of  $Ti(O_iPr)_4$  in the melt under vacuum, 200 rpm*  
*a: Magnetic stirring and b: mechanical stirring*  
*1 Obtained by  $^1H$  NMR using  $OCH_3$  peak at 3.6 ppm for calculation*  
*2 Obtained by SEC in THF – PS calibration*

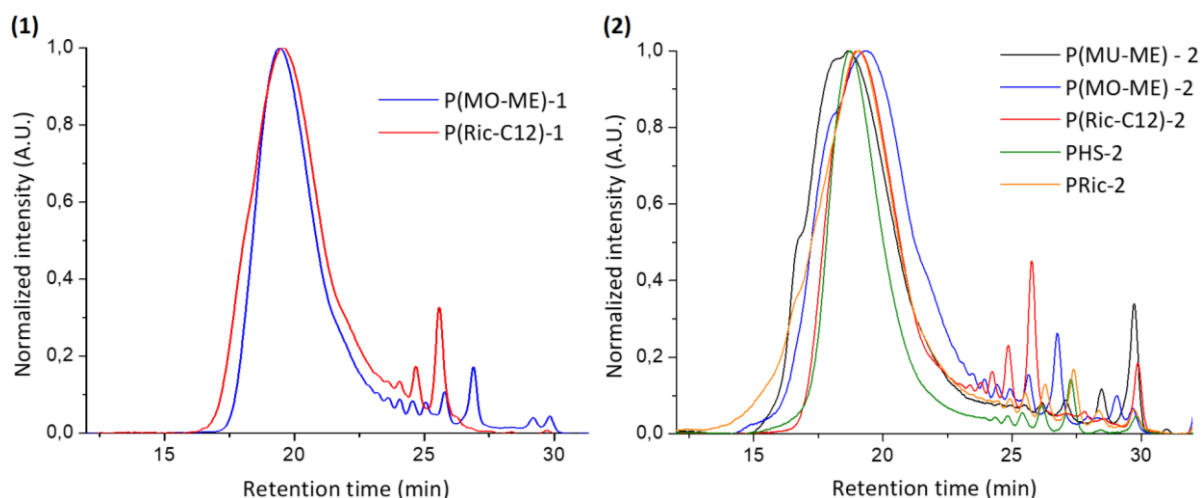


Figure III-7: SEC traces of (1) first series ( $M_n \approx 15 \text{ kg.mol}^{-1}$ ) and (2) second series ( $M_n \approx 25 \text{ kg.mol}^{-1}$ ) of polyesters, performed in THF (PS calibration)

All the polyesters were synthesized through transesterification method.  $M_n$  calculated from  $^1\text{H}$  NMR spectroscopy are in accordance with  $M_n$  obtained from SEC measurements. Regarding the kinetics of polymerization, P(MO-ME)-1 and P(Ric-C12)-1 were polymerized during 24 hours under magnetic stirring. Similar molecular weights were obtained, i.e.  $M_n = 15\,700 \text{ g.mol}^{-1}$  and  $M_w = 32\,100 \text{ g.mol}^{-1}$  for P(MO-ME)-1 and  $M_n = 14\,500 \text{ g.mol}^{-1}$  and  $M_w = 36\,400 \text{ g.mol}^{-1}$  for P(Ric-C12)-1. Due to the high reactivity of MU-ME, the P(MU-ME) molecular weight could not be well-controlled by reaction duration. As a result, a polymer with the targeted  $M_n = 15 \text{ kg.mol}^{-1}$  could not be obtained. P(MO-ME)-2 and P(Ric-C12)-2 obtained after 48 hours exhibited  $M_n$  values around  $25\,000 \text{ g.mol}^{-1}$  and were further compared.

In a nutshell, thanks to the kinetic study, two ranges of polyesters with different architectures but similar molecular weights were obtained. Their properties can be then further compared.

### 1.3. Effect of the various architectures on polyester properties

Polyesters with four different structures were compared. They are schematically illustrated in Figure III-8. As the PRic has an internal double bond, it will not be compared to the others polymers here. All have similar backbone structure with a different amount of pendant alkyl chains. P(MO-ME) and PHS contain both one pendant chain but differ by the presence of a thioether linkage in the backbone or not. They were synthesized in the same range of

molecular weight. Consequently, the impact of the pendant alkyl chain and the presence of a thioether function in the repeating unit on the polyester properties was evaluated.

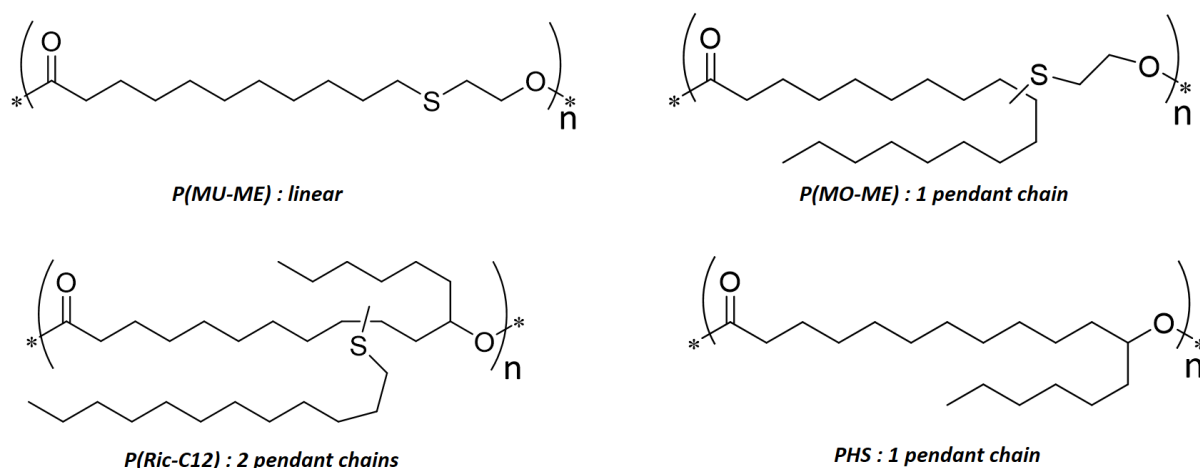


Figure III-8: Chemical structure of polyesters with different amounts of pendant alkyl chains

### 1.3.1. Thermal properties

Polyester thermal properties were evaluated in terms of thermal stability and thermo-mechanical behavior. Only the polyester in the range of  $M_n = 25 \text{ kg}\cdot\text{mol}^{-1}$  were considered in this study. The thermal stability was investigated by TGA under non-oxidative conditions at a heating rate of  $10 \text{ }^\circ\text{C}\cdot\text{min}^{-1}$ . The temperature corresponding to 5 wt.% of polymer degraded are reported in Table III-2. The thermo-mechanical properties of the polyesters were determined by DSC. The crystallization, melting and glass transition temperature were recorded from the first cooling and the second heating scan at a rate of  $10 \text{ }^\circ\text{C}\cdot\text{min}^{-1}$ . DSC thermograms are illustrated in Figure III-9 and thermal characteristic values are displayed in Table III-2.

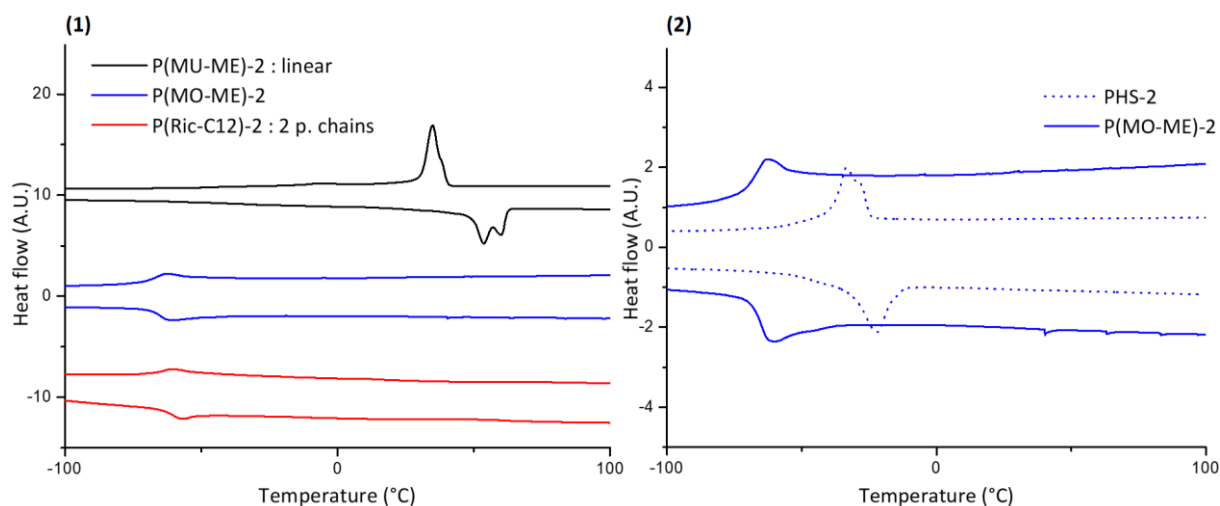


Figure III-9: DSC traces of (1) linear polyesters (in black), with one pendant alkyl chain (in blue) and two pendant alkyl chains (in red) and (2) polyester with one pendant alkyl chain, with and without thioether function in the backbone. Second heating cycle at a rate of  $10^{\circ}\text{C min}^{-1}$

Table III-2: Polyester molecular weight and thermal characteristic temperatures

Entry	$M_w^1$ ( $\text{g.mol}^{-1}$ )	$\bar{D}^1$	$T_{d5\%wt}^2$ ( $^{\circ}\text{C}$ )	$T_g^3$ ( $^{\circ}\text{C}$ )	$T_m^3$ ( $^{\circ}\text{C}$ )	$T_{cris}^3$ ( $^{\circ}\text{C}$ )
P(MU-ME) - 2	112 700	4.4	328	-33	53 (43 J/g)	35 (49 J/g)
P(MO-ME) - 2	76 000	3.4	318	-64	-	-
PHS - 2	63 000	2.4	309	-44	-22 (22 J/g)	-33 (29 J/g)
P(Ric-C12) - 2	55 000	2.2	310	-61	-	-

<sup>1</sup> Obtained by SEC in THF – PS calibration  
<sup>2</sup> Obtained by TGA with a heating ramp of  $10^{\circ}\text{C.min}^{-1}$   
<sup>3</sup> Obtained by DSC in the first cooling and second heating at  $10^{\circ}\text{C.min}^{-1}$

The polymer structure does not impact its thermal stability. The  $T_{5\text{ wt.}\%}$  were found between  $309^{\circ}\text{C}$  and  $328^{\circ}\text{C}$ . As a result, the polyester structure as well as the presence of a thioether function may not impact significantly the polyester thermal stability. In contrast, thermal behavior is impacted by the polymer architecture as well as its chemical composition. As expected, the linear polyester P(MU-ME) is semi-crystalline, with a melting temperature around  $50^{\circ}\text{C}$ . According to the literature<sup>11</sup>, the polyesters with long aliphatic chains have melting points above  $70^{\circ}\text{C}$ , for instance  $T_{mPE12} = 84^{\circ}\text{C}$ . Then, the presence of a thioether group, which has a good mobility, decreases the P(MU-ME) chain organization and thus its melting point. The grafting of one or two pendant chains should avoid the chain packing. As a result, P(MO-ME) and P(Ric-C12) are fully amorphous.

As illustrated in Figure III-9 (2), the thioether function has also an effect on the thermal behavior. Indeed, PHS, which has the same pendant alkyl chain as P(MO-ME) but no thioether

function in its backbone, is semi-crystalline with a melting point at -22 °C. The linear P(MU-ME) melts at 53 °C with an enthalpy about 40 J/g while PHS melts at -22°C with an enthalpy twice lower. Consequently, both the flexibility of the C-S-C linkage and the presence of pendant alkyl chains limit the chain packing thus leading to amorphous polymer.

Both P(MO-ME) and P(Ric-C12) have a particularly low glass transition temperature, with  $T_g = -64$  °C and  $T_g = -61$  °C respectively. These values are similar, meaning that the amount of pendant chains does not affect the glass transition temperature.

To conclude, the grafting of pendant chains by thiol-ene addition leads to amorphous polymers. No thermal behavior disparities are noticed between polyester with one or two pendant alkyl chains. However, both pendant alkyl chains and thioether functions in the polymer backbone have an impact on the polymer thermal behavior.

### 1.3.2. Polyesters behavior in base oil

The impact of the polyester architecture was also evaluated in solution. The polyesters were thus added at 3 wt.% in the organic base oil, Radialube 7368, and the mineral one, Yubase 4+. First, the polyester solubility in oil was determined. Then, the polymer addition on the base oil viscosity behavior was investigated.

#### 1.3.2.1. Polyesters solubility in base oil

The polymer was added in base oil, stirred at 100 °C for two hours in order to force the polymer dissolution in oil and then cooled down at room temperature during one day. Solubility tests were performed for the two series of polyesters. Results are sum-up in Table III-3.

Table III-3: Polyester solubility in Radialube 7368 and Yubase 4+

Entry	$M_w^1$ (g.mol <sup>-1</sup> )	$\bar{D}^1$	Solubility in R	Solubility in Y
P(MU-ME) - 2 <sup>a</sup>	112 700	4.4	No	No
P(MO-ME) - 1 <sup>a</sup>	32 100	2	Yes	No
P(MO-ME) - 2 <sup>b</sup>	76 000	3.4	Yes	No
PHS - 2 <sup>a</sup>	63 000	2.4	Yes	Yes
P(Ric-C12) - 1 <sup>a</sup>	36 400	2.5	Yes	Yes
P(Ric-C12) - 2 <sup>b</sup>	55 000	2.2	Yes	Yes

*1 Obtained by SEC in THF – using PS calibration  
Polymers added at 3wt.% in oil*

Both the pendant alkyl chain and the presence of thioether bond have an effect on the polyester solubility in base oil. For instance, the linear polyester P(MU-ME) is completely

insoluble in mineral and organic oils while polyesters with one or two pendant chains are soluble at least in organic oil. P(MU-ME) being a linear aliphatic semi-crystalline polyester, chain packing is strong, leading to intermolecular interactions which decrease the solubility in solvent such as oils. The insolubility of P(MU-ME) may be also due to its high molecular weight.

All the polymers with one or two pendant chains are soluble in organic oil. Surprisingly, P(MO-ME) is not soluble in mineral oil, contrary to PHS. This is not due to the polyester molecular weight as P(MO-ME)-1, with a lower  $M_w$  than PHS-2, is even not soluble. Consequently, the P(MO-ME) insolubility in Yubase 4+ was attributed to the thioether function in the polymer backbone. However, P(Ric-C12) remains soluble in mineral oil thanks to the presence of dodecyl pendant alkyl chains which bring some affinity between the oil and the polymer chain.

Except the case of linear P(MU-ME), the polyesters were soluble in the organic oil, thus their impact on the oil viscosity could be investigated. The presence of a C-S-C bond in the P(MO-ME) avoided its complete solubility in mineral oil. Consequently, only P(Ric-C12) and PHS were tested in Yubase 4+.

#### *1.3.2.2. Impact of polyester structures on oil viscosity*

The polyesters were solubilized in both organic and mineral oils to evaluate their impact on oil viscosity with respect to the temperature. The oils with 3 wt.% polyesters were analyzed using a densimeter-viscosimeter at several temperatures. The solution densities, dynamic viscosities and kinematic viscosities were measured from 20 °C to 100 °C. Values are reported in Table III-A-1 in Appendix. Then, the relative viscosity,  $\eta_{rel}$ , was evaluated as a function of temperature. The aim was to evaluate the efficiency of polyesters as thickeners as well as Viscosity Index improvers. In that sense, a comparison has been done with commercial additives already described in the previous chapter: Priolube 3986 in Radialube 7368 and Viscosplex 10-250 in Yubase 4+. Viscosity Index and Q factor were then calculated. Values are reported in Table III-4.

As displayed in Figure III-10, the relative viscosity decreased by increasing the temperature for all the polyesters tested in Radialube 7368. However, the relative viscosity remained stable when polymers were mixed with Yubase 4+. This behavior is also confirmed regarding to the Q values. For instance, Q values in organic oil are in the range of 0.81 – 0.88 while in mineral

oil, Q values are in the range of 0.95 – 1. As Q factor  $\leq 1$  in all cases, the polyesters can be considered as thickeners but not as VI improvers even though the VI is actually improved.

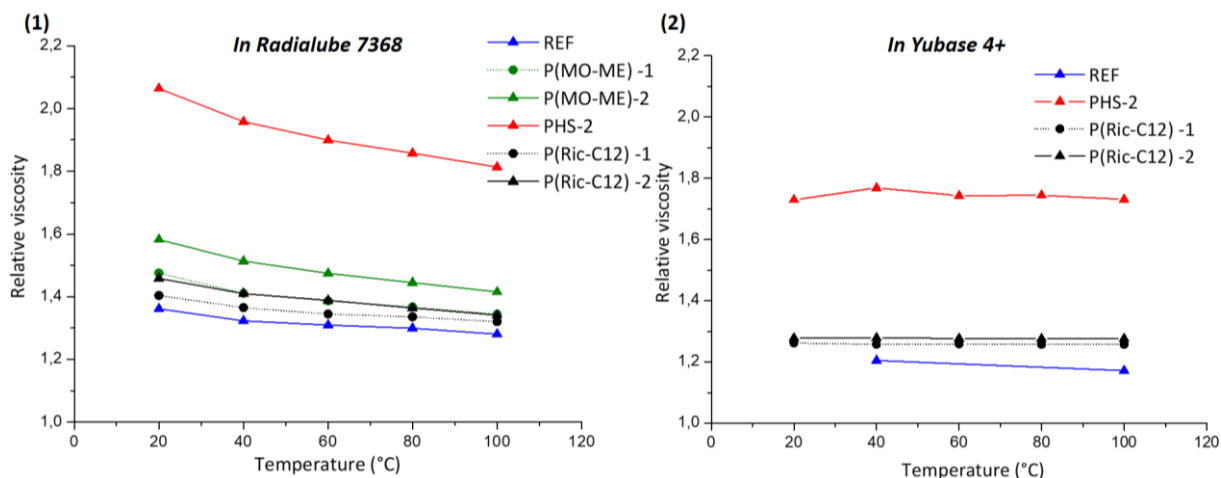


Figure III-10: Relative viscosity as a function of temperature for blends of polyester at 3 wt.% in (1) organic oil and (2) mineral oil

Table III-4: Relative viscosity depending on the temperature, Viscosity Index and Q factor of Radialube 7368 and Yubase 4+ with 3 wt.% of additives

Blended at 3 wt.% in Radialube								
	$M_w$ (g.mol <sup>-1</sup> )	Relative viscosity					VI	Q
		20 °C	40 °C	60 °C	80 °C	100 °C	152	
Priolube	16 800	1.36	1.32	1.31	1.30	1.28	175	0.87
P(MO-ME)-1	32 100	1.48	1.41	1.39	1.37	1.34	176	0.84
P(MO-ME)-2	76 000	1.58	1.51	1.47	1.44	1.42	176	0.81
PHS-2	63 000	2.06	1.96	1.90	1.86	1.81	195	0.85
P(Ric-C12)-1	36 400	1.40	1.36	1.34	1.34	1.32	178	0.88
P(Ric-C12)-2	55 000	1.46	1.41	1.39	1.36	1.34	175	0.83

Blended at 3 wt.% in Yubase								
	$M_w$ (g.mol <sup>-1</sup> )	Relative viscosity					VI	Q
		20 °C	40 °C	60 °C	80 °C	100 °C	145	
VP	40 000	-	1.21	-	-	1.17	163	0.84
PHS-2	63 000	1.73	1.77	1.74	1.74	1.73	205	0.95
P(Ric-C12)-1	36 400	1.26	1.26	1.26	1.26	1.26	181	1.00
P(Ric-C12)-2	55 000	1.28	1.28	1.28	1.28	1.28	182	1.00

The polymer behavior in solution is related to its composition. For instance, PHS and P(MO-ME) have similar structure, see Figure III-8. However, PHS-2, without thioether function impacts more the oil viscosity than P(MO-ME)-2, e.g.  $\eta_{rel 100^\circ C} = 1.81$  for PHS-2 blend while  $\eta_{rel 100^\circ C} = 1.42$  for P(MO-ME)-2 blend, both in Radialube 7368. This feature is not due to a molecular weight effect, as  $M_w_{PHS-2} < M_w_{P(MO-ME)-2}$ . As a result, the C-S-C linkage may bring some incompatibility with the oil, leading to a more collapsed coil in solution.

The polymer structure has also an impact on the polymer behavior in solution. For instance, when added in Radialube 7368, P(MO-ME) increases more the oil viscosity than P(Ric-C12) does, whatever their  $M_w$ . The addition of another pendant chain may lead to a more compact polymer in solution. It has been reported in literature <sup>2,3,12</sup> that side chains limit the polymer coil expansion leading to more compact structure in solution.

The impact of P(Ric-C12) on Yubase 4+ VI is higher than commercial VP for similar  $M_w$ , with VI = 181 compared to VI = 163, which may be due to the higher stability of the polyester regarding to the temperature ( $Q = 1$  for P(Ric-C12) while  $Q = 0.84$  for VP).

As a result, polyesters could be used as thickeners both in organic and mineral oils. The polyesters impact more the relative viscosity of organic oil than the one of mineral oil, feature explained by a better affinity with the organic than with the mineral oil. However, their thickening efficiency was stable regarding to the temperature in mineral oil while it decreased with temperature in organic oil. It appeared that the presence of sulfur atoms in the polyester backbone decreased the polymer impact on oil viscosity, whatever the temperature. Moreover, it was observed that the higher the amount of alkyl chains, the more compact the polymer in solution and the lower the thickening efficiency.

#### 1.4. Conclusion

In order to evaluate the impact of pendant chains on polyester properties, bio-based polyesters were synthesized with 0, 1 and 2 alkyl pendant chains in the repeating units. Precursors from renewable resources were functionalized by thiol-ene addition. The AB type monomers were then polymerized in bulk. Both the nature of the reactive alcohol and the presence of pendant chains influenced the kinetics of polymerization. As expected, the MU-ME linear monomer led to the fastest polymerization and the highest molecular weights.

A series of polyesters were synthesized in the same ranges of  $M_n$  in order to evaluate and compare their properties in bulk and in solution. It was shown that both the presence of C-S-C bonds in the backbone and the amount of pendant chains had an impact on thermal polyester behavior. For instance, the linear polyester is semi-crystalline. As expected, the addition of a pendant chain decreased the polyester crystallinity. The presence of alkyl pendant chains combined with the presence of thioether groups in the polyester backbone

led to amorphous polymers. No effect of the content of pendant chain on the glass transition temperature was observed.

The so-formed polyesters were added at 3 wt.% in organic and mineral oils. The linear P(MU-ME) is not soluble in both oils. The presence of thioether functions in the polymer backbone leads to a decrease of the polymer solubility in mineral oil; for instance, P(MO-ME) could not be tested in mineral oil. It was observed that both the thioether function and the presence of a second pendant alkyl chain decreased the polyester thickening efficiency. Both features could lead to a more compact polymeric coil in solution. Despite a decrease of the thickening efficiency, the design of comb polyesters should lead to shear stable viscosity modifiers. Unfortunately, this feature will not be tested in this project. In addition, the presence of thioether bonds could be interesting for lubricant applications because of the sulfur affinity with metal. As a result, the so-formed polyesters are promising thickeners compared to commercial additives tested and could be eventually also considered as multi-function additives thanks to the presence of thioether linkages.

## **2. Comb poly(9-alkyl 12-hydroxystearate)s with various dangling chains**

---

The aim of this section is to evaluate the impact of the nature and size of the pendant chain on the polyester thermal properties and behavior in solution. To this end, methyl ricinoleate was functionalized with various thiols including different linear alkyl groups, phenyl ethyl or 2-ethyl hexyl groups. The so-formed methyl 9-alkyl 12-hydroxystearates were then polymerized to yield comb poly(9-alkyl 12-hydroxystearate)s. The polyester thermal properties were evaluated and their efficiency as viscosity modifiers and pour point depressants in organic and mineral base oils were evaluated.

## 2.1. Synthesis of comb poly(9-alkyl 12-hydroxystearate)s with various side chains

### 2.1.1. Methyl ricinoleate functionalization by thiol-ene addition

Methyl ricinoleate (MRic) was functionalized with several thiols using the same methodology as described in section 1.1.3., see Figure III-11 (1). The thiols added as second pendant chain on methyl ricinoleate are illustrated in Figure III-11 (2).

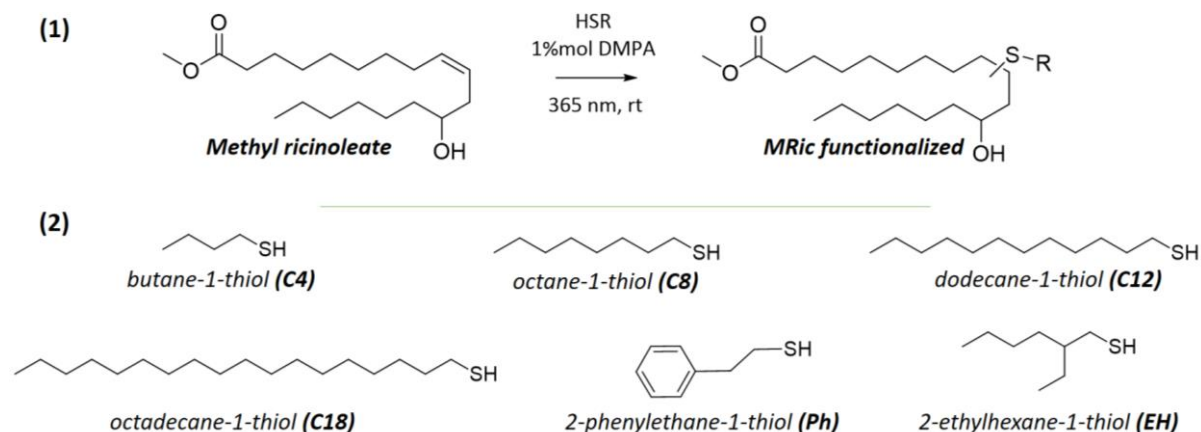


Figure III-11: (1) Methyl ricinoleate functionalization through thiol-ene addition (2) Thiol compounds added as pendant chain on methyl ricinoleate

The thiol-ene additions were monitored by  $^1\text{H}$  NMR and stopped after complete disappearance of the methyl ricinoleate double bonds. As octadecane-1-thiol is a solid at room temperature, a small amount of cyclohexane was added in the mixture to dissolve it. The other reactions were performed in bulk. In order to reach a complete conversion, 3 equivalents of thiol were used. The products were purified using Flash Chromatography. Results are reported in Table III-5.

Table III-5: Methyl ricinoleate functionalization by thiol-ene addition with various thiol compounds

Monomer	Reaction Time (h)	MR C=C conversion <sup>1</sup>	Ratio RS addition on MR C9 : C10 (%) <sup>1</sup>	Yield (%)
MRic-C4	1.5	100	40 : 60	84
MRic-C8	2	100	35 : 65	70
MRic-C12	3	100	30 : 70	67
MRic-C18	3	100	35 : 65	66
MRic-Ph	3	100	30 : 70	70
MRic-EH	4	100	30 : 70	62

**1 Obtained by  $^1\text{H}$  NMR**

The structures of the purified functionalized methyl ricinoleate were confirmed by  $^1\text{H}$  NMR, see an example in section 1.1.3, Figure III-4. The complete conversion of the MRic double bond

was reached depending on the thiol compound added. For instance, the complete conversion was observed within 1.5 hours of reaction in the case of butane-1-thiol addition, 3 hours with octadecane-1-thiol and 4 hours with 2-ethylhexyl-1-thiol. This difference of kinetics may be correlated to the steric hindrance of the thiol compound. The shorter the thiol alkyl chain, the easier the addition on methyl ricinoleate. In that sense, 2-ethylhexyl-1-thiol is more hindered due to its branched structure, leading to a slower addition on the monomer than butane thiol, for instance. In agreement with the previous observations in section 1.1.3, whatever the thiol nature, the thiol addition occurred mostly on the C10 (at 60% - 70%) than on C9 (30% - 40%) because of the presence of the hydroxyl function in  $\beta$  of the C9.

### 2.1.2. Polymerization of the functionalized monomers

The methyl 9-alkyl 12-hydroxystearate were polymerized by transesterification following the same reaction conditions as previously mentioned in section 1.2. The polyesters obtained are illustrated in Figure III-12.

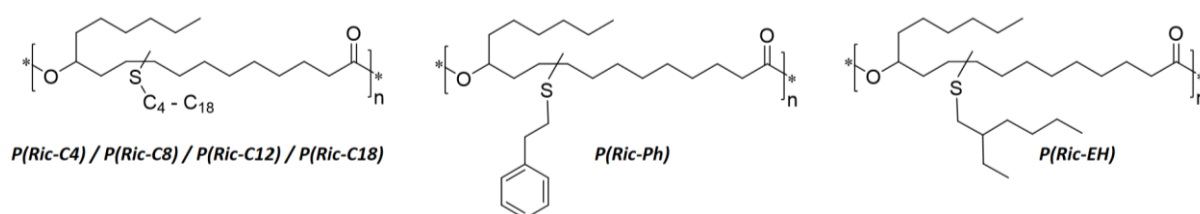


Figure III-12: Comb polyesters with various pendant chains

Two series of poly(9-alkyl 12-hydroxystearate) regarding to their molecular weights were synthesized. As it was observed in the previous chapter, the use of TBD as catalyst for polycondensation led to the synthesis of PRic with  $M_w$  about  $10 \text{ kg}\cdot\text{mol}^{-1}$ . As a result, TBD was selected as catalyst for the synthesis of the first series of poly(9-alkyl 12-hydroxystearate)s. In that case, the reaction mixture was stirred magnetically during 24 hours at  $140 \text{ }^\circ\text{C}$  with 5 wt.% of TBD. To reach higher molecular weights, the second series was obtained using a mechanical stirring during 48 hours at  $180 \text{ }^\circ\text{C}$ , and 1 wt.% of  $\text{Ti}(\text{O}i\text{Pr})_4$ . The molecular weights obtained for the two series of comb polyesters are reported in Table III-6. All the polyesters structures were confirmed by  $^1\text{H}$  NMR analyses, the spectra are displayed in Figure III-13. The decrease of the methoxy peak at 3.6 ppm as well as the position of the  $\text{H}_b$  peak in  $\alpha$  of the hydroxyl function

confirmed the polymerization. The H<sub>b</sub> peak is separated in three peaks because the thiol compound can be added on C9 (H<sub>b</sub> at 4.9 ppm) as well as on C10. The addition on C10 led to two different configurations due to the presence of the hydroxyl function in β position of C10 (H<sub>b</sub> at 5.05 ppm and 5.1 ppm).

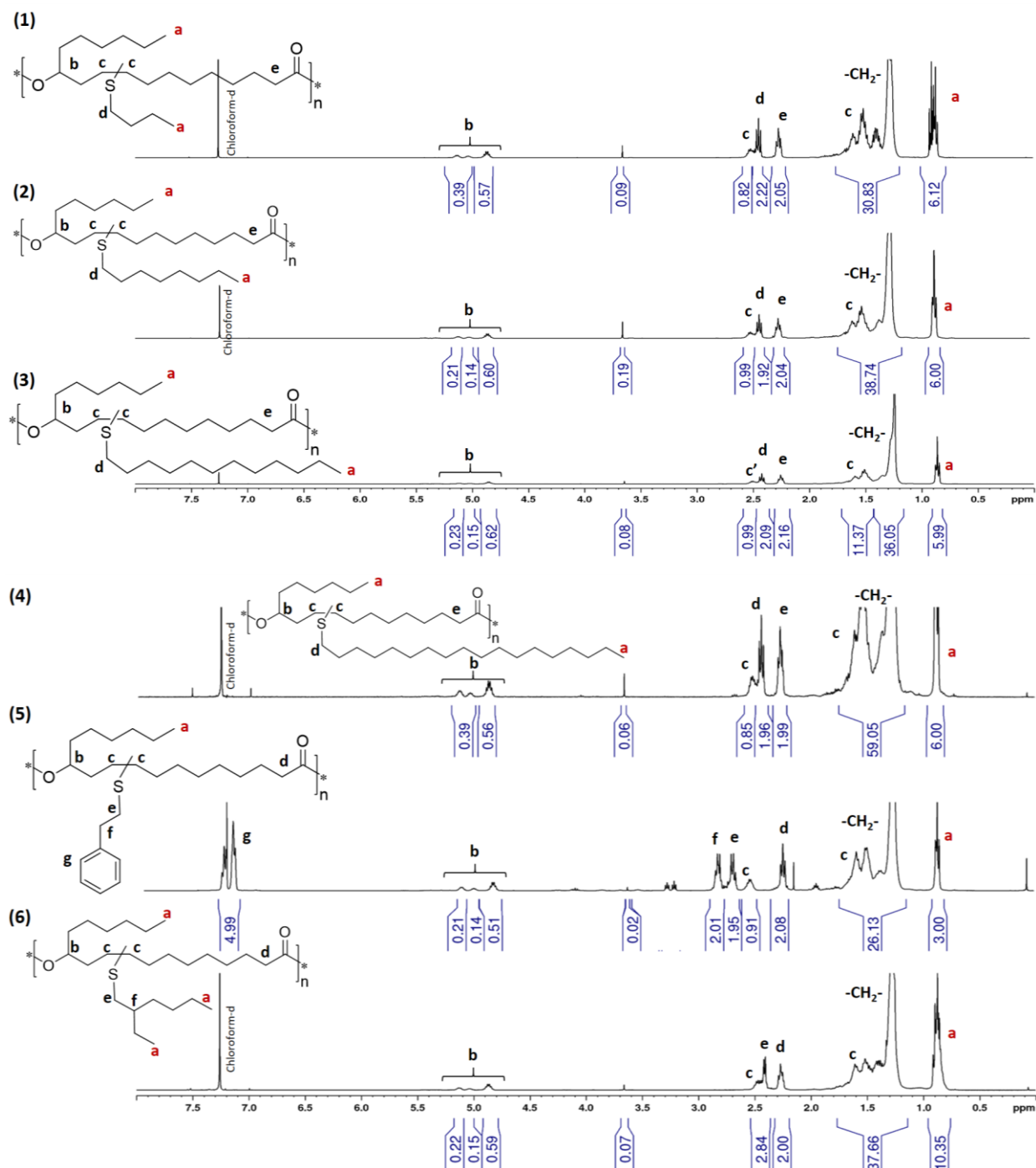


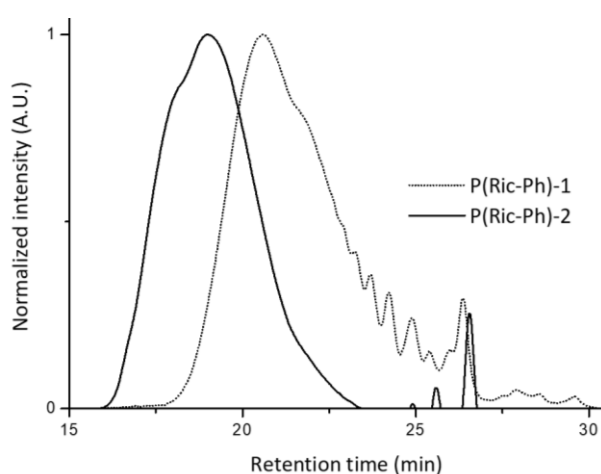
Figure III-13: <sup>1</sup>H NMR spectra of comb polyesters (1) P(Ric-C4) (2) P(Ric-C8) (3) P(Ric-C12) (4) P(Ric-C18) (5) P(Ric-Ph) (6) P(Ric-EH)

Table III-6: Functionalized methyl ricinoleate conversion and comb poly(9-alkyl 12-hydroxystearate) molecular weight

Entry	Time (h)	$P^1$	$DP^1$	$Mn^1$ (g/mol)	$Mn^2$ (g/mol)	$Mw^2$ (g/mol)	$\bar{D}^2$
PRic - 1 <sup>a</sup>	8	0.894	9.4	3 000	5 100	9 200	1.8
P(Ric-C4) - 1 <sup>a</sup>	8	0.947	19	6 400	2 600	6 400	2.4
P(Ric-C8) - 1 <sup>a</sup>	8	0.944	18	6 000	3 800	8 900	2.3
P(Ric-C12) - 1 <sup>a</sup>	8	0.925	13	4 500	2 400	5 000	2.1
P(Ric-C18) - 1 <sup>a</sup>	8	0.934	15	5 200	3 500	7 900	2.3
P(Ric-Ph) - 1 <sup>a</sup>	8	0.910	11	3 800	3 500	9 800	2.8
P(Ric-EH) - 1 <sup>a</sup>	8	0.945	18	6 300	7 000	21 000	3.1
PRic - 2 <sup>b</sup>	48	0.977	45	12 400	15 700	45 400	2.9
P(Ric-C4) - 2 <sup>b</sup>	48	0.972	35	12 100	20 300	44 600	2.2
P(Ric-C8) - 2 <sup>b</sup>	48	0.989	48	16 600	16 800	34 000	2.1
P(Ric-C12) - 2 <sup>b</sup>	48	0.962	27	13 000	14 500	36 400	2.5
P(Ric-C18) - 2 <sup>b</sup>	48	0.988	46	15 800	12 000	44 800	3
P(Ric-Ph) - 2 <sup>b</sup>	48	0.996	72	24 900	23 000	50 000	2.2
P(Ric-EH) - 2 <sup>b</sup>	48	0.983	60	20 500	20 400	41 300	2

**Reaction conditions: a: Magnetic stirring, 5 wt.% of TBD, 140 °C, in the melt under vacuum and b: mechanical stirring 1 wt.% of Ti(OiPr)<sub>4</sub>, 180 °C, in the melt under vacuum, 200 rpm**  
**1 Obtained by <sup>1</sup>H NMR using OCH<sub>3</sub> peak at 3.6 ppm for calculation**  
**2 Obtained by SEC in THF –PS calibration**

The transesterification occurred for each type of functionalized methyl ricinoleate. The two series are well distinct regarding to their molecular weight, examples are illustrated in Figure III-14. In average,  $M_w \approx 10 \text{ Kg.mol}^{-1}$  and  $M_w \approx 45 \text{ Kg.mol}^{-1}$  were obtained for the first and second series, respectively. Dispersity is around 2 for all the polyesters, in accord with polycondensation reaction. The  $M_n$  values obtained by <sup>1</sup>H NMR using equations established by Carothers are in accordance with the  $M_n$  obtained by SEC measurement.

Figure III-14: Examples of the SEC traces of P(Ric-Ph)-1,  $M_w = 9 800 \text{ g.mol}^{-1}$  and P(Ric-Ph)-2,  $M_w = 50 000 \text{ g.mol}^{-1}$ , performed in THF

## 2.2. Comb poly(9-alkyl 12-hydroxystearate) thermal properties

Comb poly(9-alkyl 12-hydroxystearate)s thermal properties were evaluated in terms of thermal stability and thermo-mechanical behavior for the two series of  $M_w$ . The thermal stability was investigated by TGA under non-oxidative conditions at a heating rate of  $10\text{ }^\circ\text{C}\cdot\text{min}^{-1}$ . The  $T_{d5wt\%}$  are reported in Table III-7. The thermal properties of the polyesters were determined by DSC. The crystallization, melting and glass transition temperatures were recorded from the first cooling and the second heating scan at a rate of  $10\text{ }^\circ\text{C}\cdot\text{min}^{-1}$ . DSC thermograms are illustrated in Figure III-15 and thermal characteristic values are reported in Table III-7 .

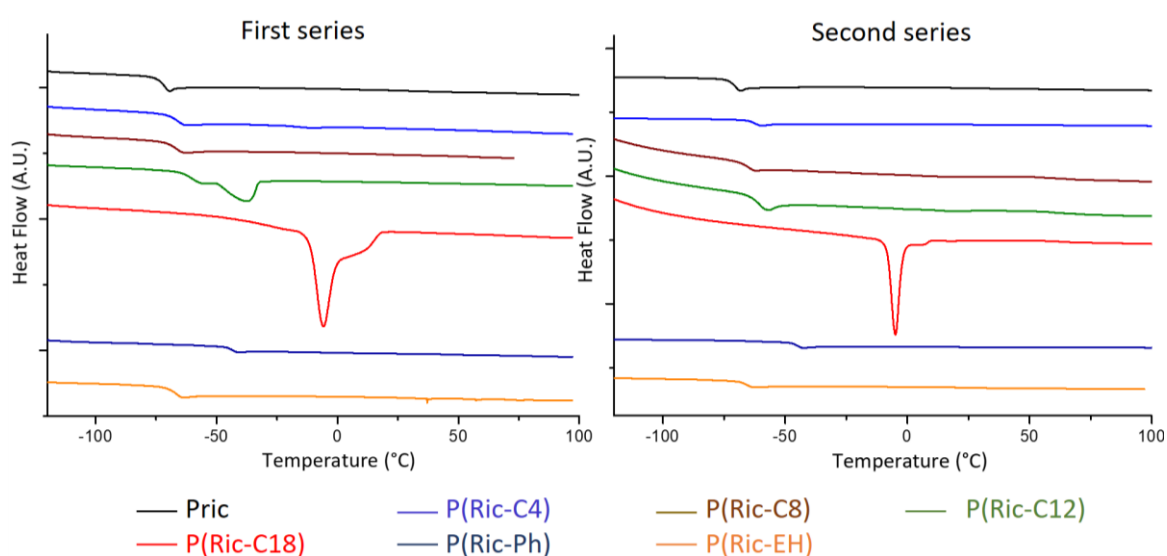


Figure III-15: DSC traces of two series of comb polyesters: first series with  $M_w = 10\text{ kg}\cdot\text{mol}^{-1}$  and second series with  $M_w = 45\text{ kg}\cdot\text{mol}^{-1}$

The  $T_{d5wt\%}$  of the polyesters determined by TGA are in the range  $296 - 307\text{ }^\circ\text{C}$ . No influence of the side chain nature on the polymer thermal stability is observed. Conversely and as expected, the side chain nature influences the thermo-mechanical properties of the comb polyesters. For instance, P(Ric) derivatives without additional side alkyl chains or with short side chains such as butyl-, phenyl ethyl- or 2-ethylhexyl- pendant chains are fully amorphous. Poly(9-alkyl 12-hydroxystearate)s with long alkyl side chains, such as dodecyl- and octadecyl- groups, are semi-crystalline with a melting temperature of  $-37\text{ }^\circ\text{C}$  and  $-5\text{ }^\circ\text{C}$ , respectively. The longest the side chain, the highest the polymer melting point and the highest the enthalpy of crystallization, i.e.  $46\text{ J/g}$  for P(Ric-C18)-1 versus  $11\text{ J/g}$  for P(Ric-C12)-1. The packing at low temperature of the long alkyl side chains generates crystallinity to the system. This

crystallization disappears in the case of high molecular weight PRic-C12, phenomenon that could be explained by the low chain mobility.

Table III-7: Molecular weight and thermal characteristic temperatures of comb poly(9-alkyl 12-hydroxystearate)s

Entry	$M_w^1$ (g.mol <sup>-1</sup> )	$\bar{D}^1$	$T_{5\%wt}^2$ (°C)	$T_g^3$ (°C)	$T_m^3$ (°C)	$T_{cris}^3$ (°C)
PRic - 1	9 200	1.8	296	-77	-	-
P(Ric-C4) - 1	6 400	2.4	307	-66	-	-
P(Ric-C8) - 1	8 900	2.3	306	-66	-	-
P(Ric-C12) - 1	5 000	2.1	305	-61	-37 (11 J/g)	-49 (18 J/g)
P(Ric-C18) - 1	7 900	2.3	306	-	-5 (46 J/g)	-12 (50 J/g)
P(Ric-Ph) - 1	9 800	2.8	307	-49	-	-
P(Ric-EH) - 1	21 000	3.1	306	-67	-	-
PRic - 2	45 400	2.9	303	-68	-	-
P(Ric-C4) - 2	44 600	2.2	306	-62	-	-
P(Ric-C8) - 2	34 000	2.1	306	-64	-	-
P(Ric-C12) - 2	36 400	2.5	311	-60	-	-
P(Ric-C18) - 2	44 800	3	312	-	-5 (42 J/g)	-12 (46 J/g)
P(Ric-Ph) - 2	50 000	2.2	306	-44	-	-
P(Ric-EH) - 2	41 300	2	306	-66	-	-

1 Obtained by SEC in THF – PS calibration  
 2 Obtained by TGA with a heating ramp of 10°C.min<sup>-1</sup>  
 3 Obtained by DSC in the first cooling and second heating at 10°C.min<sup>-1</sup>

As expected, the glass transition temperature ( $T_g$ ) is also influenced by the nature of the polymer pendant chains. An increase of the  $T_g$  with the side chain length is observed. For instance, the  $T_g$  of P(Ric-C4)-1 is about -66 °C while the one of P(Ric-C12)-1 is about -61 °C. Moreover, the  $T_g$  of P(Ric-Ph) increases due to the phenyl ethyl- pendant chains interactions. As a result, poly(9-phenyl ethyl 12-hydroxystearate)s has a  $T_g$  between 10 and 15 °C higher than those of other comb polyesters. The polyester glass transition is also affected by its molecular weight, e.g.  $T_g$  P(Ric-C4)-1 = -66 °C and  $T_g$  P(Ric-C4)-2 = -62 °C. This is due to the decrease of both the general chain mobility and the influence of chain end by increasing the polymer chain length.

## 2.3 Investigation of comb poly(9-alkyl 12-hydroxystearate)s as viscosity modifiers

### 2.3.1. Comb poly(9-alkyl 12-hydroxystearate)s behavior in organic oil

The comb poly(9-phenyl ethyl 12-hydroxystearate)s synthesized were added in Radialube 7368. The same dissolution protocol as described before was followed. All the poly(9-alkyl 12-hydroxystearate)s were soluble in this organic oil, irrespective to their molecular weight or

nature of their side chains. The variation with temperature of the viscosity of the oil with 3 wt.% of the comb polyesters was evaluated; results are illustrated in Figure III-16. Density, dynamic and kinematic values are reported in Table III-A-2 in Appendix. The relative viscosity, Viscosity Index and Q values are reported in Table III-8.

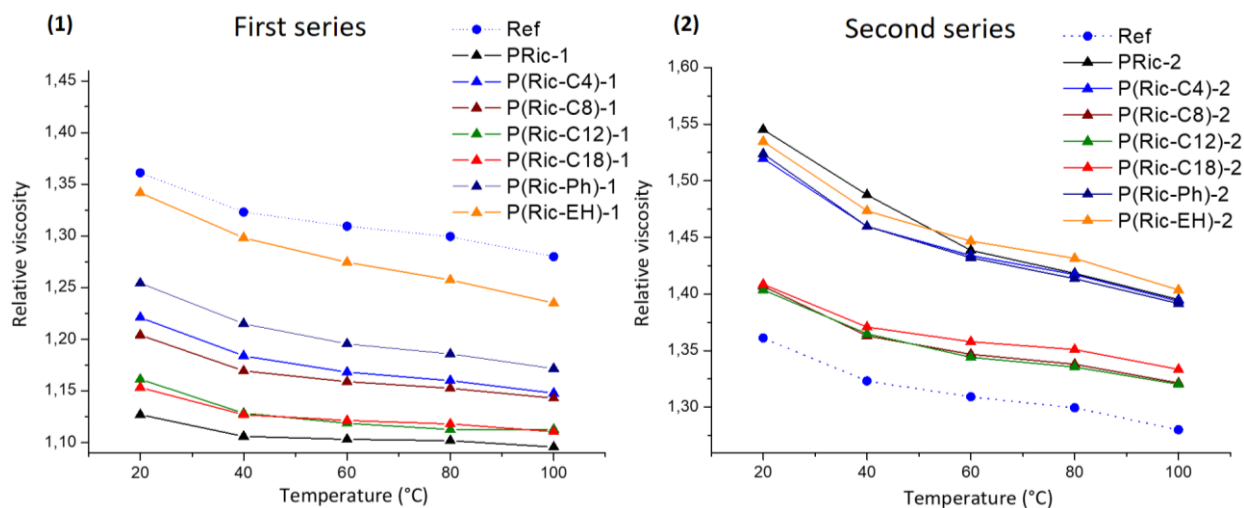


Figure III-16: Relative viscosity as a function of temperature for blends of comb polyester at 3 wt.% in organic oil. (1) Comb polyesters with  $M_w \approx 10 \text{ Kg.mol}^{-1}$  and (2) with  $M_w \approx 45 \text{ Kg.mol}^{-1}$ . The reference is the Priolube 9386

Table III-8: Relative viscosity with respect to temperature, Viscosity Index and Q factor of Radialube 7368 and with 3 wt.% of comb polyesters with  $M_w \approx 10 \text{ Kg.mol}^{-1}$  (first series) and  $M_w \approx 45 \text{ Kg.mol}^{-1}$  (second series)

First series $M_w \approx 10 \text{ Kg.mol}^{-1}$								
	$M_w$ ( $\text{g mol}^{-1}$ )	Relative viscosity					VI	Q
		20 °C	40 °C	60 °C	80 °C	100 °C	152	
Priolube	16 800	1.36	1.32	1.31	1.30	1.28	175	0.87
PRic - 1	9 200	1.127	1.106	1.103	1.102	1.10	164	0.90
P(Ric-C4) - 1	6 400	1.221	1.184	1.168	1.160	1.14	164	0.80
P(Ric-C8) - 1	8 900	1.204	1.169	1.159	1.153	1.14	166	0.85
P(Ric-C12) - 1	5 000	1.161	1.128	1.119	1.113	1.11	164	0.88
P(Ric-C18) - 1	7 900	1.153	1.127	1.121	1.118	1.11	164	0.87
P(Ric-Ph) - 1	9 800	1.254	1.215	1.196	1.186	1.17	161	0.80
P(Ric-EH) - 1	21 000	1.342	1.298	1.274	1.258	1.24	167	0.79

Second series $M_w \approx 45 \text{ Kg.mol}^{-1}$								
	$M_w$ ( $\text{g mol}^{-1}$ )	Relative viscosity					VI	Q
		20 °C	40 °C	60 °C	80 °C	100 °C	152	
Priolube	16 800	1.36	1.32	1.31	1.30	1.28	175	0.87
PRic - 2	45 400	1.545	1.488	1.439	1.418	1.395	175	0.81
P(Ric-C4) - 2	44 600	1.520	1.460	1.434	1.417	1.394	180	0.87
P(Ric-C8) - 2	34 000	1.407	1.363	1.347	1.338	1.321	179	0.89
P(Ric-C12) - 2	36 400	1.404	1.365	1.344	1.336	1.320	178	0.88
P(Ric-C18) - 2	44 800	1.409	1.371	1.358	1.351	1.333	181	0.89
P(Ric-Ph) - 2	50 000	1.524	1.460	1.432	1.414	1.392	179	0.85
P(Ric-EH) - 2	41 300	1.535	1.473	1.447	1.432	1.404	180	0.85

As a general trend, all the comb poly(9-alkyl 12-hydroxystearate)s thickened the organic oil. As expected, the second series of high molecular weight polyesters has a higher thickening efficiency in comparison to the first series. For instance, at 40 °C,  $\eta_{rel} = 1.18$  for oil mixed with P(Ric-C4)-1 and  $\eta_{rel} = 1.46$  for the blend with P(Ric-C4)-2. The addition of polyesters to the oil, whatever the polyester  $M_w$  or side chain nature, induced a decrease of the relative viscosity with the temperature. Q values are around 0.8 for all systems.

No clear influence of the polyester side chain was noticed on the relative viscosity as a function of the temperature. In order to evaluate the impact of the polyester pendant chain nature on its behavior in organic oil, the relative viscosity at 100 °C was expressed as a function of the polymer molecular weight, see Figure III-17 (1). In addition, the Viscosity Index and Q values with respect to the polyester pendant chain function is illustrated in Figure III-1 (2), for the two series of comb polyesters.

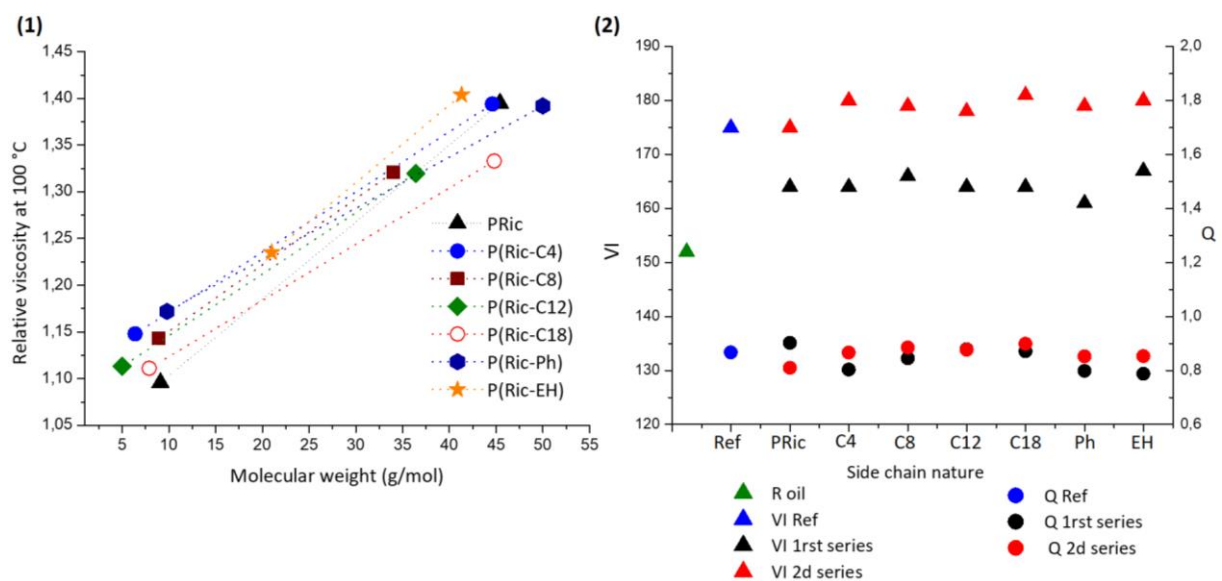


Figure III-17 : Radialube 7368 with 3 wt.% of comb polyesters (1) Relative viscosity at 100°C as a function of the polymer Mw. (2) VI and Q values as a function of the nature of the polyesters side chains

As it was already shown in Figure III-16, the highest the polyester molecular weight, the highest the thickening efficiency of the polymer. The impact of the polymer addition in organic oil is similar whatever the side chains. However, a small difference regarding to the alkyl side chain is noticed. Indeed, it appears that  $\eta_{rel} 100^\circ\text{C P(Ric-C18)} < \eta_{rel} 100^\circ\text{C P(Ric-C12)} < \eta_{rel} 100^\circ\text{C P(Ric-C8)} < \eta_{rel} 100^\circ\text{C P(Ric-C4)}$ , whatever the  $M_w$ . This behavior was already described for PAMAs viscosity modifiers.<sup>13</sup> Still, this effect is too low to have a proper impact on organic oil VI, which remains

stable whatever the pendant chain added to the PRic. Viscosity Index is about 165 for the first series of polyesters and about 180 for the second one. Conversely, the Q values remain stable whatever the polyester  $M_w$ , around 0.8. As a result, VI is improved by increasing the molecular weight of the poly(9-alkyl 12-hydroxystearate)s while this increase does not enhance the impact of polyester on oil V-T behavior. This drawback has been already described.<sup>14</sup> Despite the increase of VI values from 152 to 181 for the oil mixed with P(Ric-C18)-2, comb polyesters are not Viscosity Index improvers but can be used as thickeners in organic oil.

### 2.3.2. Comb poly(9-alkyl 12-hydroxystearate)s behavior in mineral oil

The comb poly(9-alkyl 12-hydroxystearate)s were also evaluated as viscosity modifiers in mineral oil, Yubase 4+. The blends of Yubase 4+ with the polymers were heated at 100 °C for two hours and cooled down to room temperature for one day. P(Ric-C4) and P(Ric-Ph) were not soluble in Yubase 4+, whatever their molecular weight. As expected, PRic-1 with  $M_w = 9\ 000\ \text{g}\cdot\text{mol}^{-1}$  was soluble while Pric-2 with  $M_w = 45\ 000\ \text{g}\cdot\text{mol}^{-1}$  was not. Branched and long pendant alkyl chains (> 8 carbons) are then required to ensure proper polyester solubility in mineral oil. The viscosity of the oil with 3 wt.% of soluble comb poly(9-alkyl 12-hydroxystearate)s added with temperature was evaluated, see Figure III-18. Density, dynamic and kinematic values are reported in Table III-A-3 in Appendix. The relative viscosity, Viscosity Index and Q values are reported in Table III-9.

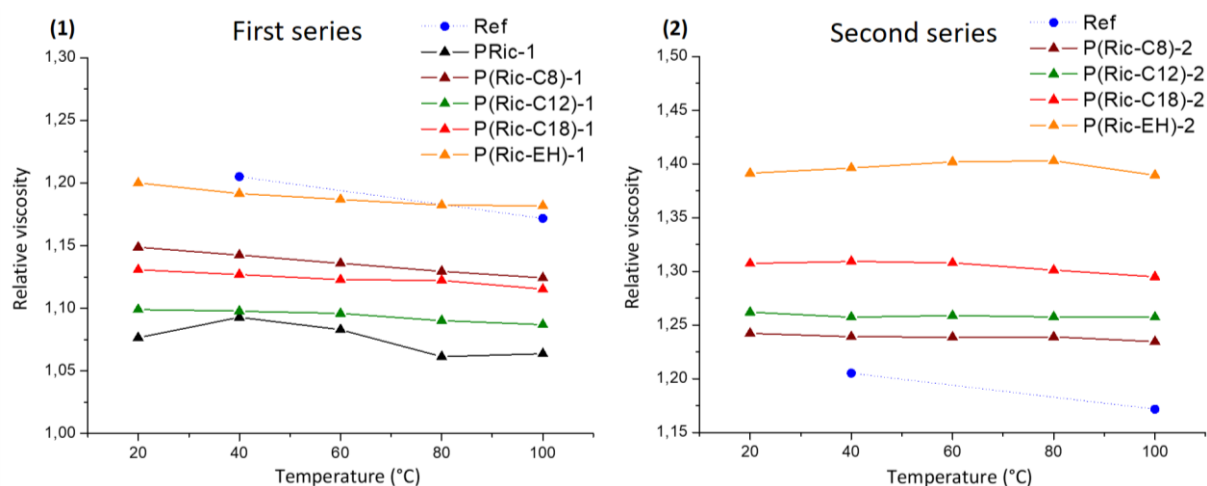


Figure III-18: Relative viscosity as a function of temperature for blends of comb polyester at 3 wt.% in mineral oil. (1) Comb polyesters with  $M_w \approx 10\ \text{Kg}\cdot\text{mol}^{-1}$  and (2) with  $M_w \approx 45\ \text{Kg}\cdot\text{mol}^{-1}$ , Ref is Viscoplex 10-250

In comparison to previous results in Radialube 7368, the relative viscosity remains stable over the temperature for all the systems evaluated. This stability is even increased by increasing

the polyester molecular weight. For instance, Q values for the first series are around 0.9 while reach almost 1 for the second series. Still, no improvement of the oil Viscosity-Temperature behavior was observed. Concerning the thickening efficiency of the comb poly(9-alkyl 12-hydroxystearate)s tested, it appeared for both series than P(Ric-EH) improved more the oil viscosity than other polyesters. For instance,  $\eta_{rel}$  of P(Ric-EH)-2 oil system is about 1.4 while the other relative viscosities are in the range 1.25 – 1.3. P(Ric-EH)-1 increased the Yubase 4+ viscosity similarly to the commercial additive VP even if its molecular weight is twice lower than the latter. As a result, P(Ric-EH) could be considered as a promising thickener for mineral base oil. Its thickening efficiency could be attributed to the branched structure of the side chain. Because of its architecture, the side chain may avoid backbone interactions and potential chain coil contraction, leading to a larger coil size in solution. In Figure III-18, the effect of side chain length is not clear as the viscosity appears mostly affected by the polyester molecular weight. For instance,  $\eta_{rel} P(Ric-C12)-1 < \eta_{rel} P(Ric-C18)-1 < \eta_{rel} P(Ric-C8)-1$  for the first series while  $\eta_{rel} P(Ric-C8)-2 < \eta_{rel} P(Ric-C12)-2 < \eta_{rel} P(Ric-C18)-2$  for the second series. In order to highlight the effect of the pendant chain nature on the poly(9-alkyl 12-hydroxystearate)s behavior in solution, the relative viscosity at 100°C was expressed as a function of the polymer molecular weight in Figure III-19 (1). The Viscosity Index and Q values were reported with respect to the side chain type in Figure III-19 (2).

Table III-9: Relative viscosity depending on the temperature, Viscosity Index and Q factor of Yubase 4+ and with 3 wt.% of comb polyesters with  $M_w \approx 10 \text{ kg.mol}^{-1}$  (first series) and  $M_w \approx 45 \text{ kg.mol}^{-1}$  (second series)

First series $M_w \approx 10 \text{ Kg.mol}^{-1}$								
	Mw (g.mol <sup>-1</sup> )	Relative viscosity					VI	Q
		20 °C	40 °C	60 °C	80 °C	100 °C	145	
VP	40 000	-	1.21	-	-	1.17	163	0.84
PRic - 1	9 200	1.076	1.093	1.083	1.061	1.064	147	0.69
P(Ric-C8) - 1	8 900	1.149	1.143	1.136	1.129	1.124	160	0.87
P(Ric-C12) - 1	5 000	1.099	1.098	1.096	1.090	1.087	156	0.89
P(Ric-C18) - 1	7 900	1.131	1.127	1.123	1.122	1.115	160	0.91
P(Ric-EH) - 1	21 000	1.200	1.192	1.187	1.182	1.182	170	0.95
Second series $M_w \approx 45 \text{ Kg.mol}^{-1}$								
	Mw (g.mol <sup>-1</sup> )	Relative viscosity					VI	Q
		20 °C	40 °C	60 °C	80 °C	100 °C	145	
VP	40 000	-	1.205	-	-	1.17	163	0.84
P(Ric-C8) - 2	34 000	1.242	1.239	1.239	1.239	1.235	177	0.98
P(Ric-C12) - 2	36 400	1.262	1.257	1.259	1.258	1.257	181	1.00
P(Ric-C18) - 2	44 800	1.307	1.309	1.308	1.301	1.295	181	0.95
P(Ric-EH) - 2	41 300	1.391	1.396	1.402	1.403	1.390	190	0.98

There is no influence of the alkyl pendant chain length on the polyester thickening efficiency in mineral oil. P(Ric-C8), P(Ric-C12) and P(Ric-C18) have similar impact on the oil viscosity at 100°C, whatever their molecular weight. Reversibly, as already shown in Figure III-18, P(Ric-EH) has a better thickening efficiency than the other polyesters, leading to a higher VI. It is also visible that non functionalized PRic has a lower impact on oil viscosity than the polyesters with a second alkyl side chain. This is explained by a lower solubility of PRic in Yubase 4+ than the other polymers.

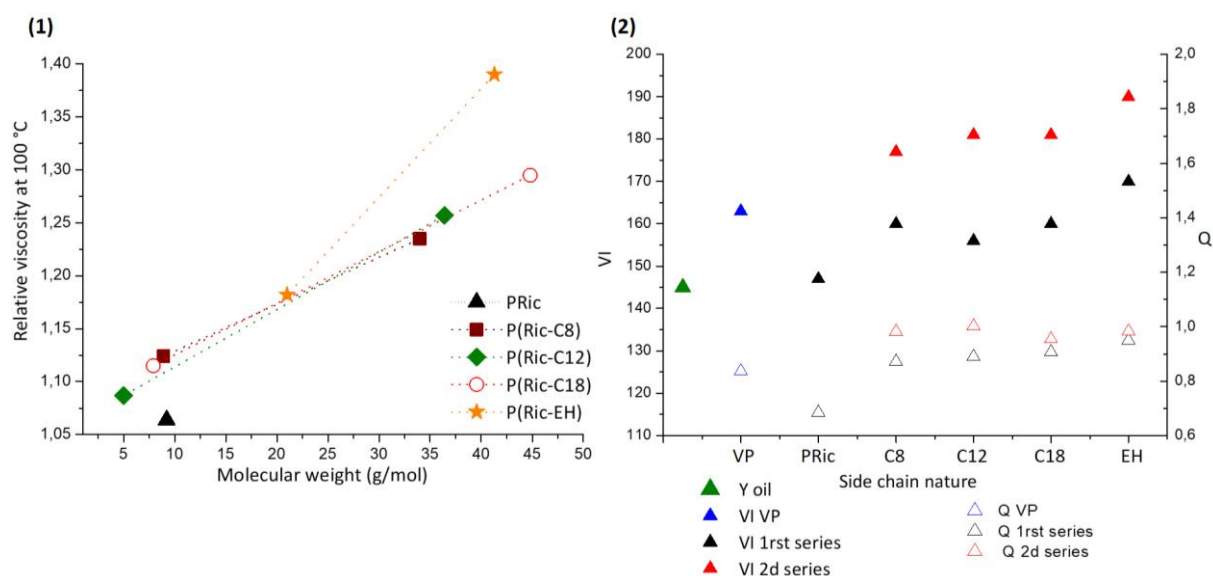


Figure III-19: Yubase 4+ with 3 wt.% of comb polyesters (1) Relative viscosity at 100 °C as a function of the polymer  $M_w$ . (2) VI and Q values as a function of the nature of the polyester side chains

To conclude, the comb polyesters synthesized could be used as thickeners both in organic and mineral oils. The side chain nature does not have a proper influence on the behavior of polyesters in organic oil. Their impact on Viscosity Index seems mainly related to the polymer molecular weight. Some comb poly(9-alkyl 12-hydroxystearate)s such as P(Ric-C4) and P(Ric-Ph) were not soluble in mineral oils. The poly(9-ethyl hexyl 12-hydroxystearate)s showed better thickening efficiency than the other polyesters with a Yubase 4+ VI improvement from 145 to 190 for instance. This feature is explained by the branched architecture of its side chain. As a result, it can be considered as a promising thickener for lubricant oils.

## 2.4. Investigation of comb poly(9-alkyl 12-hydroxystearate)s as pour point depressants

As it was mentioned in chapter I, at the pour point temperature, the waxy compounds of the oil crystallize and form a gel leading to an increase of the viscosity and a change from Newtonian to non-Newtonian behavior. This natural behavior at low temperature is an issue for lubricant applications because the oil stops to flow and cannot ensure its lubricating role.<sup>2,13</sup> For that reason, polymeric additives are added in oil to interact with the waxy compounds and decrease its pour point. Polymers currently used as pour point depressants are mostly semi-crystalline comb PAMAs and other copolymers such as some ethylene/propylene copolymers and ethyl vinyl acetate copolymers.<sup>1,7</sup> By their comb structure with aliphatic side chains, the comb poly(9-alkyl 12-hydroxystearate)s previously evaluated as viscosity modifiers could potentially have a pour point depression effect.

### 2.4.1. Evaluation of some comb poly(9-alkyl 12-hydroxystearate)s as potential PPD

Some comb poly(9-alkyl 12-hydroxystearate)s were thus evaluated as pour point depressants in mineral oil, their structures are illustrated in Figure III-207. The selected polyesters contain alkyl side chains and are soluble in mineral oil.

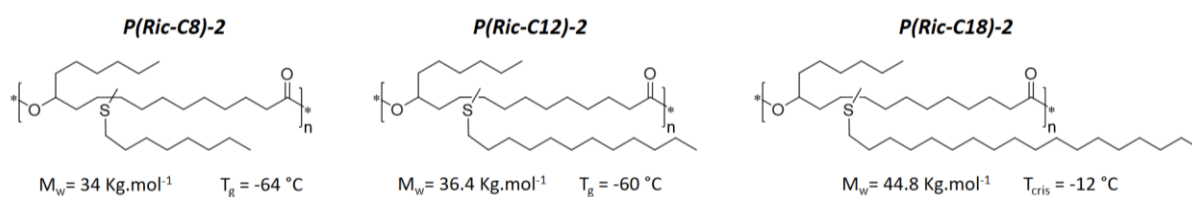


Figure III-207: Schematic representation of three comb poly(9-alkyl 12-hydroxystearate) with various pendant chain length

The three selected comb poly(9-alkyl 12-hydroxystearate)s have pendant alkyl chains from 8 to 18 carbons. P(Ric-C8) and P(Ric-C12) are amorphous with  $T_g = -64$  °C and  $-60$  °C, respectively, while P(Ric-C18) is semi-crystalline with a crystallization temperature of  $-12$  °C ( $T_m = -5$  °C). The so-formed polyesters were added at 0.1 wt.% in Yubase 4+. In order to estimate the impact of comb polyesters addition on cold temperature behavior of the oil, rheological measurements were performed under a ramp of temperature from 20 °C to  $-30$  °C at 1 °C.min<sup>-1</sup>. The variation of the oil viscosity against temperature is illustrated in Figure III-21.

A dramatic increase of the Yubase 4+ viscosity is observed at  $-14^{\circ}\text{C}$  which can be attributed to the oil pour point. This value is close to the oil pour point given in literature, i.e.  $-15^{\circ}\text{C}^{15}$ , which confirms that the rheological method performed to evaluate oil pour point is accurate.

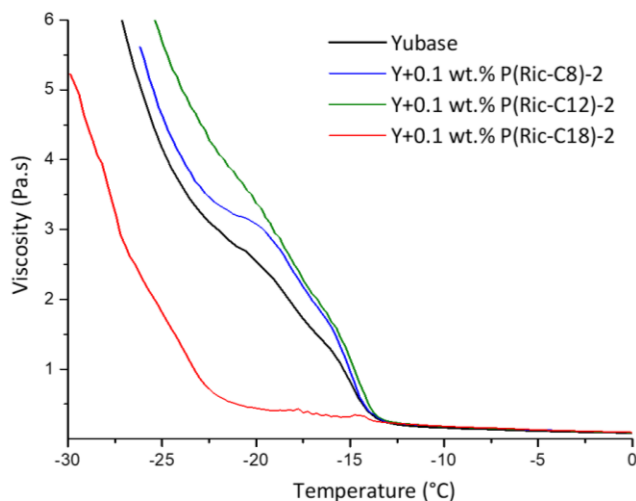


Figure III-21: Yubase and Yubase with comb polyesters added at 0.1 wt.% viscosities as a function of the temperature. Temperature ramp of  $1^{\circ}\text{C}\cdot\text{min}^{-1}$  from 20 to  $-30^{\circ}\text{C}$ .

As illustrated in Figure III-21, the two amorphous poly(9-alkyl 12-hydroxystearate)s, P(Ric-C8)-2 and P(Ric-C12)-2 impact in the same way the oil viscosity behavior at low temperature. In both cases, a dramatic increase of the oil viscosity is observed at the same temperature than the oil without additive, i.e.  $-14^{\circ}\text{C}$ . At lower temperature, the oil viscosity is increased by the addition of the polyesters. Conversely, P(Ric-C18)-2 in Yubase 4+ exhibit a PPD effect with a pour point depression from  $-14^{\circ}\text{C}$  to  $-23^{\circ}\text{C}$ . Moreover, the P(Ric-C18)-2 addition in oil induces a decrease of the oil viscosity at temperature below the pour point. This effect may be due to the semi-crystalline nature of the comb poly(9-octadecyl 12-hydroxystearate). Indeed, the polymer backbone is amorphous while the pendant chains crystallize in bulk at  $-12^{\circ}\text{C}$ . This temperature is close to the Yubase 4+ pour point. It is then supposed that the long alkyl chains co-crystallize with the waxy compounds in mineral oil while the amorphous backbone has a dispersant effect and limits the formation of a 3D gelled network.

#### **2.4.2. Influence of the polymer concentration on oil pour point**

The polymer concentration in oil is crucial to ensure a proper pour point depressant effect. As a result, P(Ric-C18)-2 was added in Yubase 4+ at various concentration, from 0.001 wt.% to 10 wt.% in order to estimate the impact of the concentration on oil behavior at low temperature.

The same temperature ramp from 20 to  $-30^{\circ}\text{C}$  at  $1^{\circ}\text{C}\cdot\text{min}^{-1}$  was applied; results are illustrated in Figure III-22.

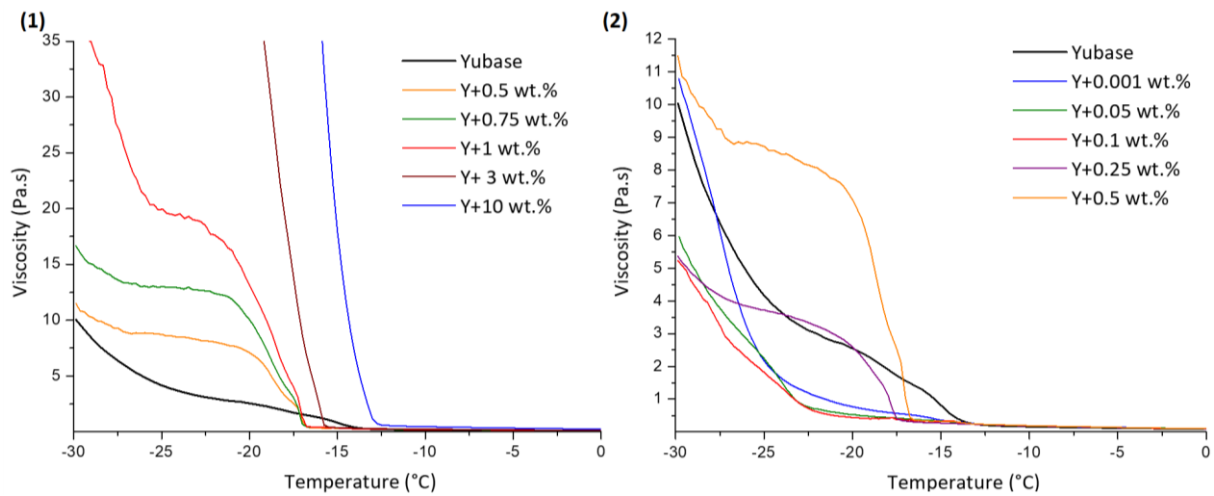


Figure III-22: Impact of the P(Ric-C18) concentration on the viscosity of Yubase 4+ as a function of the temperature. Temperature ramp of  $1^{\circ}\text{C}\cdot\text{min}^{-1}$ . (1) Concentrations from 0.5 wt.% to 10 wt.% (2) Concentrations from 0.001 wt.% to 0.5 wt.%

The impact of the P(Ric-C18) on the oil viscosity behavior at low temperature is strongly related to its concentration in solution. At the highest concentration, i.e. 10 wt.%, the increase of the viscosity appears at  $-12^{\circ}\text{C}$  which is the crystallization temperature of the polymer in bulk. It is then assumed that the polymer concentration is over  $C^*$ . As the polymer coils are in contact with each other, the polymer side chains crystallization occurs as in bulky condition leading to a general crystallization of the system and a drastic increase of the viscosity. In the case of P(Ric-C18) added at 3 wt.%,  $C$  is thus probably below  $C^*$ . The crystallization process is delayed at lower temperature because the polymer coils are not in contact with each other. But once the temperature decreased over the pour point, here  $-15.5^{\circ}\text{C}$ , the PPD concentration is still too high to permit a proper crystal dispersion, allowing the formation of a partial 3D network.

Another behavior is observed for the concentration in the range 1 wt.% - 0.25 wt.%. In these cases, the oil pour point is delayed from  $-14^{\circ}\text{C}$  to  $-17^{\circ}\text{C}$  due to the presence of P(Ric-C18) in solution. Between  $-17^{\circ}\text{C}$  and  $-25^{\circ}\text{C}$ , the presence of additive in solution leads to a higher viscosity than the oil itself. Below  $-25^{\circ}\text{C}$ , the viscosity reaches a plateau. The polymer side chains may thus interact with the waxy crystals at low temperature but the amount of polymers is still too high to ensure a proper dispersion of the wax in the oil. This could lead to

the formation of some aggregates in solution, and thus to the oil viscosity increase below the pour point.

The optimum concentration is in the range 0.05 – 0.1 wt.%. When P(Ric-C18) is added at this concentration range, the oil pour point is delayed to -23 °C and the viscosity increase is limited at lower temperature. It is then assumed that P(Ric-C18) are able to co-crystallize with the waxy compounds while the amorphous backbone enables a proper dispersion of the crystals in solution, limiting the viscosity increase in this temperature range evaluated, i.e. until -30 °C. Below this concentration, at 0.001 wt.% for instance, the co-crystallization may still happen and the pour point is slightly delayed but there is not enough polymer in solution to ensure a complete dispersion of the waxy compound. The increase of viscosity is delayed but not decreased.

It appeared in this study that the polymer concentration is crucial to ensure efficient pour point depression. The range 0.05 wt.% - 0.1 wt.% appeared to be the optimum concentration range for the system studied. Some hypotheses have been done about the behavior of the polymer at low temperature with respect to its concentration in solution. Still, some further characterizations should be performed, such as microscopy, to confirm or not these hypotheses.

### 2.4.3. Influence of the molecular weight on additive efficiency as PPD

The comb poly(9-octadecyl 12-hydroxystearate) appeared to be a promising pour point depressant. Added at 0.1 wt.% in mineral oil, it decreased the pour point from -14 °C to -23 °C. P(Ric-C18)-1 as well as the corresponding monomer, MRic-C18 was also evaluated as PPD at 0.1 wt.% in Yubase 4+. Their characteristics are reported in Table III-10. The oil viscosity with additives against temperature is displayed in Figure III-23.

Table III-10: Methyl ricinoleate and corresponding polymers branched with octadecyl- side chain molecular weight, thermal characteristic and pour point depression efficiency

Entry	M <sub>n</sub> <sup>1</sup> (g.mol <sup>-1</sup> )	M <sub>w</sub> <sup>1</sup> (g.mol <sup>-1</sup> )	Đ <sup>1</sup>	T <sub>g</sub> <sup>2</sup> (°C)	T <sub>m</sub> <sup>2</sup> (°C)	T <sub>cris</sub> <sup>2</sup> (°C)	PPD (°C)
MRic-C18	598	598	1	-	-1 (58 J/g)	-5 (65 J/g)	+2
P(Ric-C18) - 1	3 500	7 900	2.3	-	-5 (46 J/g)	-12 (50 J/g)	-11
P(Ric-C18) - 2	12 000	44 800	3	-	-5 (42 J/g)	-12 (46 J/g)	-9

<sup>1</sup> Obtained by SEC in THF – PS calibration

<sup>2</sup> Obtained by DSC in the first cooling and second heating at 10°C.min<sup>-1</sup>

The poly(9-octadecyl 12-hydroxystearate)s as well as the corresponding monomer are semi-crystalline. However, only the two polymers decreased the oil pour point when added in mineral oil. Conversely, the addition of methyl 9-octadecyl 12-hydroxystearate in oil lead to an increase of the oil pour point about 2 °C. This may be due to the crystallization temperature of this compound, i.e. -5 °C. As it crystallizes at higher temperature than the oil pour point, MRic-C18 could create nuclei which can enhance wax crystallization. Moreover, in that case, this small molecule does not contain a long amorphous backbone enabling to disperse the wax crystals. That could explain the viscosity increase of the system compared to the oil itself under the pour point. Machado et al.<sup>16</sup> already observed that a certain molecular weight had to be reached to observe a PPD effect in the case of EVA copolymers.

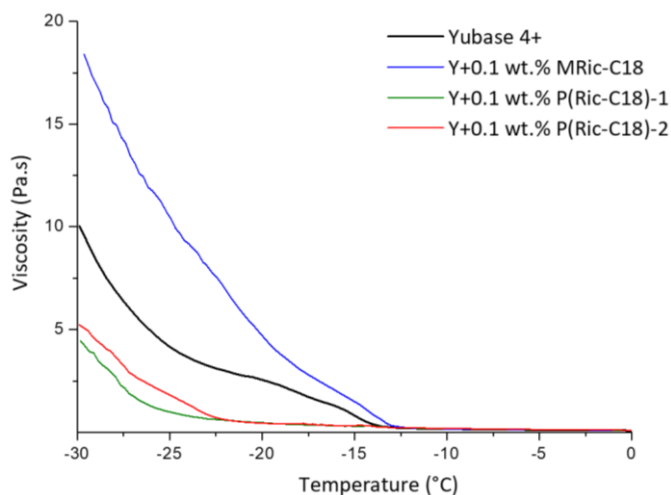


Figure III-23: Viscosity of Yubase 4+ with 0.1 wt.% of MRic-C18, P(Ric-C18)-1 and P(Ric-C18)-2 as a function of the temperature. Temperature ramp of 1°C.min<sup>-1</sup>.

The two P(Ric-C18)s decrease the Yubase 4+ viscosity at low temperature and decrease the pour point. The lower  $M_w$  P(Ric-C18)-1 has a greater PPD efficiency than P(Ric-C18)-2, with a pour point depression of 11°C and 9°C, respectively. Lower molecular weight polymer could thus facilitates the formation of more abundant smaller wax crystals, decreasing consequently the overall viscosity of the system and the pour point.

#### 2.4.4. Others semi-crystalline polyesters

It has been shown that both comb polymers with long alkyl chains and semi-crystalline linear polymers can be used as pour point depressants. In the previous section, polyhydroxystearate (PHS) was synthesized and appeared to be a promising thickener. This polyester, soluble in

mineral oil, is semi-crystalline by nature, with a crystallization temperature at  $-31\text{ }^{\circ}\text{C}$ . For this reason, it was also evaluated as pour point depressant and compared to P(Ric-C18)-1. Their structures are displayed in Figure III-24.

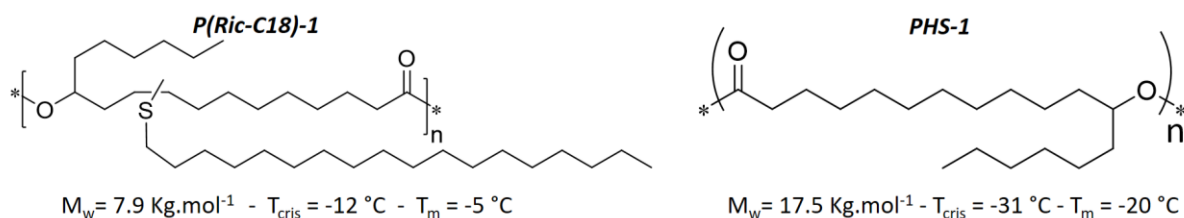


Figure III-24 : Illustration of a comb poly(9-octadecyl 12-hydroxystearate) P(Ric-C18) and the poly(12-hydroxystearate) (PHS) a semicrystalline polyester

The variation of the Yubase 4+ with 0.1 wt.% of these two additives against temperature between  $20\text{ }^{\circ}\text{C}$  and  $-30\text{ }^{\circ}\text{C}$  is displayed in Figure III-25.

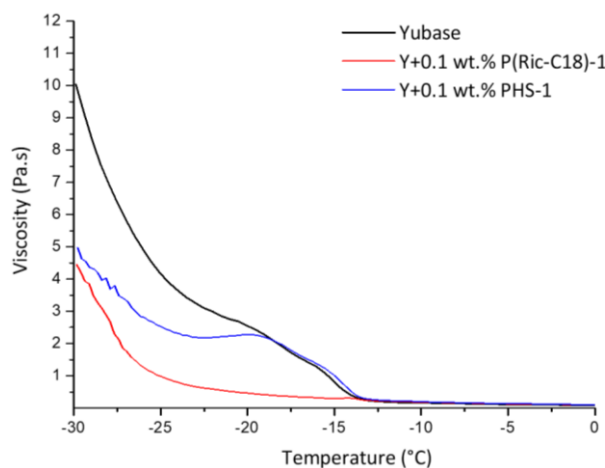


Figure III-25: Viscosity of Yubase 4+ with 0.1 wt.% of P(Ric-C18)-1 and PHS-1 as a function of the temperature. Temperature ramp of  $1\text{ }^{\circ}\text{C.min}^{-1}$  from  $20\text{ }^{\circ}\text{C}$  to  $-30\text{ }^{\circ}\text{C}$ .

The viscosity of Yubase 4+ increases drastically at  $-14\text{ }^{\circ}\text{C}$  with or without PHS addition. Consequently, no improvement of the oil pour point is noticed. However, the addition of PHS-1 in mineral oil impacts the viscosity of the oil when the temperature is below  $-20\text{ }^{\circ}\text{C}$ . It seems that when the polymer in solution starts to crystallize, the mixture viscosity reaches a plateau. As a result, PHS-1 does not have a PPD effect in Yubase 4+, compared to P(RIC-C18) but could be promising PPD for mineral oils with a lower pour point than Yubase 4+.

### 2.4.5. Comb poly(9-octadecyl 12-hydroxystearate) investigation as PPD in organic oil

As P(Ric-C18) appeared to be an efficient pour point depressant in mineral oil, its behavior as PPD was also evaluated in an organic oil. The organic oil used as viscosity modifier tests, Radialube 7368, has a pour point of -30 °C which is already a particularly low pour point. Therefore, P(Ric-C18) was added in High Oleic Sunflower Oil (HOSO) with a pour point of -14 °C. Three concentrations of additives were investigated: 0.05 wt.%, 0.1 wt.% and 0.5 wt.%. The solution viscosities regarding to the temperature are illustrated in Figure III-26. The temperature was decreased from 20 °C to -30 °C following a ramp of 1 °C.min<sup>-1</sup>.

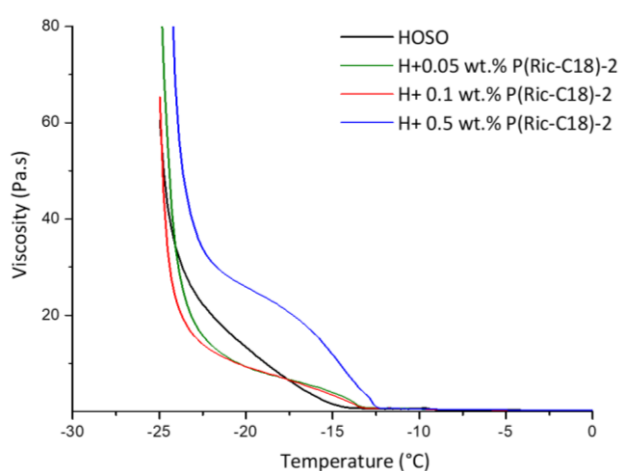


Figure III-26: Effect of P(Ric-C18) concentration on viscosity of HOSO as a function of the temperature. Temperature ramp of 1°C.min<sup>-1</sup> from 20 °C to -30 °C

In organic oil, no proper pour point depression was observed by adding P(Ric-C18). However, the polymer impacts the oil viscosity at low temperature. For instance, at 0.5 wt.% concentration of P(Ric-C18)-2, the viscosity of the system is higher than the oil viscosity and the pour point is about -12 °C, i.e. the crystallization temperature of the polymer is two degrees higher than the oil pour point. At lower concentration, the pour point appeared at -13 °C instead of -14 °C and the viscosity of the system is lower than the oil viscosity between -13 °C to -24 °C. It is assumed that the polymer side chains may not co-crystallize with the waxy compounds in oil (no pour point depression). However, polymer coils under -12 °C may act as numerous partially crystalline nuclei facilitating the formation of lower size waxy crystals, reducing the viscosity increase by increasing the temperature. Then, below -24 °C, the gelled network was formed leading to an exponential viscosity increase.

To conclude, comb polyesters can have a PPD effect only if the alkyl side chains are able to co-crystallize with the waxy compounds of the mineral oil. As a result, P(Ric-C18) is a promising PPD for mineral oil. The concentration of the polyester is a preponderant parameter of pour point depression. An optimum concentration of 0.1 wt.% was determined. The molecular weight of the polymer has also an impact on PPD efficiency. For instance, P(Ric-C18)-1 with  $M_w$  of 9 kg.mol<sup>-1</sup> decreases the Yubase 4+ pour point about 11 °C while the same polyester with  $M_w$  of 45 kg.mol<sup>-1</sup> decreased the oil pour point about 9 °C. It appeared also that a PPD effect is ensured when the polymer crystallization temperature is close to the oil pour point. Therefore, it is supposed that PHS-1 could be used as PPD for mineral oil with pour point around -20 °C. Unfortunately, the poly(9-octadecyl 12-hydroxystearate) did not show a proper efficiency in organic oil such as HOSO. As P(Ric-C18) is a promising PPD additive, further investigations should be performed such as microscopy or PPD measurement using ASTM D97 norm in order to compare the values with literature ones.<sup>17</sup>

## Conclusion

---

The aim of this chapter was to evaluate the impact of the polyester structure on its thermal properties and behavior in oil. First, bio-based polyesters were synthesized with 0, 1 and 2 alkyl pendant chains in the repeating unit. To do so, methyl undecenoate, methyl oleate and methyl ricinoleate were functionalized by thiol-ene addition to design AB type monomers then polymerized in bulk by polycondensation. Both the nature of the reactive alcohol and the presence of pendant chains influence the kinetics of polymerization. As expected, the most reactive monomer is the linear one exhibiting a primary OH function. It appeared that both the presence of a thioether linkage in the backbone and the amount of pendant alkyl side chains have an impact on the thermal polyester behavior. Polyesters with linear structure are not soluble in organic and mineral base oil. It was then observed that both the thioether function and the presence of a second pendant alkyl side chain decreases the polyester thickening efficiency. Both features could lead to a more compact polymeric coil in solution. Still, the so-formed polyesters are promising thickeners in comparison to commercial additives tested.

Secondly, comb poly(9-alkyl 12-hydroxystearate)s were synthesized with various pendant chains. In this case, methyl ricinoleate was derivatized by thiol-ene addition with various thiol compounds. The nature of the side chains does not influence the thermal stability of the comb polyesters. However, an effect was observed on the glass transition temperature; the longest the alkyl side chain, the highest the  $T_g$ . Moreover, poly(9-alkyl 12-hydroxystearate)s with additional long alkyl chains, such as octadecyl- group, are semi-crystalline. In organic oil, such comb poly(9-alkyl 12-hydroxystearate)s are soluble and no impact of the pendant chain nature was noticed on the polymer behavior in solution.

Conversely, short side chains such as butyl- and phenyl ethyl- groups avoid the polymer solubility in mineral oil. It appeared that poly(9-ethyl hexyl 12-hydroxystearate) exhibits a higher thickening efficiency than other comb polyesters. As a result, it could be considered as a promising thickener. Still, no positive influence of the polymers was observed on the oil V-T behavior, avoiding their possible use as Viscosity Index improvers. Comb polyesters were also evaluated as pour point depressants. P(Ric-C18) with a crystallization temperature at  $-12\text{ }^\circ\text{C}$  is an efficient PPD in mineral oil. A decrease of the pour point about  $11\text{ }^\circ\text{C}$  was obtained. Long alkyl side chains with a crystalline behavior is required to provide PPD effect. Both the concentration and the polymer molecular weight have an impact on PPD properties. This PPD efficiency was observed in mineral oil but not in organic one. Some further investigations are required to understand and confirm the mechanism of pour point depression.

To conclude this part, the polyester structure impacts its behavior in solution. Comb polyesters could be used both as thickeners (PRic-EH) and pour point depressants (PRic-C18). Still, investigations on the poly(9-alkyl 12-hydroxystearate)s chemical structure have to be performed in order to design Viscosity Index improvers.

## References

---

- 1 L. R. Rudnick, *Lubricant Additives: Chemistry and Applications*, Taylor and Francis, 2017.
- 2 R. M. Mortier, M. F. Fox and S. T. Orszulik, *Chemistry and Technology of Lubricants*, Springer, 2010.
- 3 J. Wang, Z. Ye and S. Zhu, *Ind. Eng. Chem. Res.*, 2007, **46**, 1174–1178.
- 4 M. J. Covitch and K. J. Trickett, *Adv. Chem. Eng. Sci.*, 2015, **5**, 134–151.
- 5 C. Mary, D. Philippon, L. Lafarge, D. Laurent, F. Rondelez, S. Bair and P. Vergne, *Tribol. Lett.*, 2013, **52**, 357–369.
- 6 W. L. Van Horne, *Ind. Eng. Chem.*, 1949, **41**, 952–959.
- 7 F. Yang, Y. Zhao, J. Sjöblom, C. Li and K. G. Paso, *J. Dispers. Sci. Technol.*, 2015, **36**, 213–225.
- 8 K. Griesbaum, *Angew. Chemie Int. Ed.*, 1970, **9**, 273.
- 9 H. C. Kolb, M. G. Finn and K. B. Sharpless, *Angew. Chemie - Int. Ed.*, 2001, **40**, 2004–2021.
- 10 M. Desroches, S. Caillol, V. Lapinte, R. Auvergne and B. Boutevin, *Macromolecules*, 2011, **44**, 2489–2500.
- 11 F. Stempfle, P. Ortmann and S. Mecking, *Chem. Rev.*, 2016, **116**, 4597–4641.
- 12 L. Cosimbescu, *Modified thermoresponsive hyperbranched polymers for improved viscosity and enhanced lubricity of engine oils*, 2016.
- 13 S. Q. a Rizvi, *A Comprehensive Review of Lubricant Chemistry, Technology, Selection and Design*, ASTM International, 2009.
- 14 M. J. Covitch, *J. Test. Eval.*, 2017, **46**, 20150242.
- 15 <https://www.yubase.com/eng/index.html>.
- 16 A. L. . Machado, E. F. Lucas and G. González, *J. Pet. Sci. Eng.*, 2001, **32**, 159–165.
- 17 ASTMInternational, 2015, 1–6.

## Experimental

---

### ***Monomer synthesis***

#### *Mercaptoethanol addition on methyl-10-undecanoate*

5 g of methyl undecenoate (25 mmol, 1eq.) were mixed with mercaptoethanol (1.97 g, 25 mmol, 1 eq.). DMPA was added to the mixture (0.064 g, 0.25 mmol, 0.01 eq.). Photochemical thiol-ene addition in a 50 mL round bottom flask with a magnetic stirring under UV irradiation. A Lightningcure spot light source L9588-06A from Hamamatsu and a filter A9616-05 wavelength 350 to 400nm was used as UV source. During reaction, the conversion of double bonds was monitored by  $^1\text{H}$  NMR spectroscopy (vinyl proton signals at 5.40 ppm). The irradiation was stopped once the double bond was no more detectable by NMR, i.e. after 2 hours reaction. The mixture was put under vacuum in order to remove potential traces of unreacted thiol. A yield of 98% was obtained.

#### *Mercaptoethanol addition of methyl oleate*

As an example, 8 g of methyl oleate (27 mmol, 1 eq.) were mixed with mercaptoethanol (6.3 g, 81 mmol, 3 eq.). DMPA was added to the mixture (0.07 g, 0.2 mmol, 0.01 eq.). Photochemical thiol-ene addition in a 100 mL round bottom flask with a magnetic stirring under UV irradiation. A Lightningcure spot light source L9588-06A from Hamamatsu and a filter A9616-05 wavelength 350 to 400nm was used as UV source. During the reaction, the conversion of double bonds was monitored by  $^1\text{H}$  NMR spectroscopy (vinyl proton signals at 5.40 ppm). The irradiation was stopped once the double bond was no more detectable by NMR, i.e. after 2 hours reaction.

After the reaction, 20 mL of dichloromethane were added to the mixture. The solution was then washed with 50 mL of water twice to remove the excess of mercaptoethanol. The solution was then washed twice with 50 mL of brine and dried by  $\text{MgSO}_4$ . The organic phase was filtered and the DCM was evaporate using a rotary evaporator. The product was then recovered with a yield of 77%.

### Methyl ricinoleate functionalization by thiol-ene addition

As a typical example, 10 g of methyl ester ricinoleate (32 mmol, 1 eq.) was mixed with 1-dodecanethiol (19.48 g, 96 mmol, 3 eq.), DMPA was added to the mixture (0.082 g, 0.32 mmol, 0.01 eq.). Photochemical thiol-ene reaction was performed in a 100 mL round bottom flask with a magnetic stirring under UV irradiation. A Lightningcure spot light source L9588-06A from Hamamatsu and a filter A9616-05 wavelength 350 to 400nm was used as UV source. During reaction, the conversion of double bonds was monitored by  $^1\text{H}$  spectroscopy (vinyl proton signals at 5.40 ppm). The irradiation was stopped once the double bond was no more detectable by  $^1\text{H}$  NMR.

After reaction, the viscous liquid was dissolved in 10 mL of dichloromethane (DCM) and the methyl ester ricinoleate with a thiol pendant group was purified by Flash column chromatography, using a gradient of cyclohexane (100 %) to ethyl acetate (100 %) eluent mixture. Product was recovered by solvent evaporation and dried overnight under vacuum (0.22 mBar) at 80 °C.

The same methodology was used for all the thiol-ene reaction performed on methyl ricinoleate, with a yield in the range of 62% - 84%. In the case of octadecane-1-thiol addition, 5 mL of cyclohexane were added to solubilize the solid thiol.

### **Procedure of polymerization**

#### Polyesters with various amounts of pendant chains

Polyesters were prepared from the previously synthesized AB monomers following the reaction conditions optimized in Chapter II. As an example, the methyl 9-dodecyl 12-hydroxystearate, MRic-C12, (1.5 g, 4.8 mmol) was dried overnight under vacuum at 70 °C with mechanical stirring in 50 mL Schlenk flask at 200 rpm. The mixture was cooled at room temperature under static vacuum and a 5 wt.% solution of  $\text{Ti}(\text{O}i\text{Pr})_4$  in DCM (0.015 g of catalyst, 0.053 mmol, 1 wt.%) was added under nitrogen flow. The mixture was stirred at room temperature for 30 min under static nitrogen then put under vacuum and heated at 70 °C for 30min. Then the mixture was heated at 120 °C for one hour, 140 °C for another hour and 180

°C for 45 hours still under dynamic vacuum to remove the MeOH sub-product and mechanical stirring at 200 rpm. After 48 hours reaction, stirring was stopped, the highly viscous mixture was cooled to room temperature and the flask was opened to air in order to stop the reaction. The synthesis of linear P(MU-ME) was performed during 24 hours. No purification was performed on the final product.

#### *Comb polyesters with various natures of side chains*

Two series of polyesters with different molecular weights were synthesized using two different methodologies.

For the first series, polyesters were prepared from the previously synthesized thioderivatized methyl ester ricinoleate (1.5 g, 4.8 mmol) dried overnight under vacuum at 70 °C with magnetic stirring in a 50 mL Schlenk flask. The mixture was cooled at room temperature under static vacuum and TBD (0.075 g, 0.054 mmol, 5 wt.%) was added under nitrogen flow. The mixture was stirred magnetically at 200 rpm at 120 °C under nitrogen flow for 2 hours then heated at 140 °C still under nitrogen. After 2 hours, the mixture was placed under vacuum for 20 hours at 140 °C. No purification was performed.

The second series was performed following the same protocol as described for polyesters with various amounts of pendant chains

#### ***Preparation of oil blended with additives and evaluation as viscosity modifiers***

The so-formed polyesters were added to the mineral and organic base oils at the concentration of 3 wt.%. The mixture was heated at 100 °C overnight under magnetic stirring to promote the solubilisation and then cooled down without stirring at room temperature during 24 hours. The solubility of the additive in the oil was evaluated macroscopically. Samples were degassed under vacuum and magnetic stirring for 30 minutes right before to be analysed by LOVIS 2000 densimeter-viscometer.

#### ***Evaluation of polyesters as pour point depressants***

Polyesters were added in oil and solubilized following the same methodology as described before. After the 24 hours cooling down, samples were analysed by rheological measurement.

The rheological measurements were monitored using an Anton Paar Physica MCR operating in the cone plan geometry. The measurements were performed under nitrogen flow in the environmental chamber to avoid potential moisture effect. The temperature was controlled by Peltier device. The top cone plate has a diameter of 50 mm with 1° angle and the gap between plates was fixed at 1mm. Samples were loaded at room temperature. The sample was stabilized at 20°C for 5min before the measurement started.

The viscosity was evaluated regarding to the temperature. A temperature ramp was applied from 20 °C to -30°C with a decrease rate of 1 °C.min<sup>-1</sup>. A constant shear frequency of 1 rad.s<sup>-1</sup> was applied during the measurement.

## Appendix

Table III-A-1: Radialube 7368 and Yubase 4+ with 3 wt.% additives. Density, dynamic and kinematic values at several temperatures

	Temperature	20°C	40°C	60°C	80°C	100°C
<b>Radialube 7368</b>	<b>Density</b>	0.9418	0.9274	0.9130	0.8988	0.8846
	$\eta_{\text{dyn}}$ (mPa.s-1)	42.91	19.05	9.96	5.96	4.13
	$\eta_{\text{kin}}$ (mPa.s-1)	45.56	20.55	10.91	6.64	4.67
<b>+3%wt Priolube</b>	<b>Density</b>	0.9419	0.9275	0.9133	0.899	0.8865
	$\eta_{\text{dyn}}$ (mPa.s-1)	58.41	25.22	13.04	7.75	5.30
	$\eta_{\text{kin}}$ (mPa.s-1)	62.01	27.19	14.28	8.63	5.98
<b>+3%wt P(MO-ME)-1</b>	<b>Density</b>	0.9431	0.9287	0.9144	0.9002	0.8861
	$\eta_{\text{dyn}}$ (mPa.s-1)	67.98	28.88	14.71	8.63	5.86
	$\eta_{\text{kin}}$ (mPa.s-1)	72.09	31.1	16.08	9.59	6.61
<b>+3%wt P(MO-ME)-2</b>	<b>Density</b>	0.943	0.9286	0.9143	0.9001	0.8859
	$\eta_{\text{dyn}}$ (mPa.s-1)	63.38	26.91	13.82	8.17	5.56
	$\eta_{\text{kin}}$ (mPa.s-1)	67.21	28.98	15.12	9.08	6.28
<b>+3%wt PHS-1</b>	<b>Density</b>	0.9415	0.9271	0.9128	0.8986	0.8845
	$\eta_{\text{dyn}}$ (mPa.s-1)	88.53	37.31	18.91	11.08	7.49
	$\eta_{\text{kin}}$ (mPa.s-1)	94.03	40.24	20.72	12.33	8.47
<b>+3%wt P(MR-C12)-1</b>	<b>Density</b>	0.9416	0.9272	0.913	0.8988	0.8846
	$\eta_{\text{dyn}}$ (mPa.s-1)	60.22	26.00	13.39	7.97	5.46
	$\eta_{\text{kin}}$ (mPa.s-1)	63.95	28.05	14.66	8.86	6.17
<b>+3%wt P(MR-C12)-2</b>	<b>Density</b>	0.9416	0.9272	0.9129	0.8987	0.8845
	$\eta_{\text{dyn}}$ (mPa.s-1)	62.56	26.86	13.82	8.14	5.54
	$\eta_{\text{kin}}$ (mPa.s-1)	66.44	28.97	15.14	9.05	6.27
	Temperature	20°C	40°C	60°C	80°C	100°C
<b>Yubase 4+</b>	<b>Density</b>	0.8226	0.8099	0.7973	0.7846	0.7720
	$\eta_{\text{dyn}}$ (mPa.s-1)	34.41	15.16	7.97	4.82	3.35
	$\eta_{\text{kin}}$ (mPa.s-1)	41.82	18.71	9.99	6.14	4.34
<b>+3%wt Viscoplex</b>	<b>Density</b>	-	-	-	-	-
	$\eta_{\text{dyn}}$ (mPa.s-1)	-	-	-	-	-
	$\eta_{\text{kin}}$ (mPa.s-1)	-	22.55	-	-	5.08
<b>+3%wt PHS-1</b>	<b>Density</b>	0.8255	0.8128	0.8001	0.7875	0.7748
	$\eta_{\text{dyn}}$ (mPa.s-1)	59.72	26.90	13.94	8.44	5.82
	$\eta_{\text{kin}}$ (mPa.s-1)	72.34	33.10	17.42	10.71	7.51
<b>+3%wt P(MR-C12)-1</b>	<b>Density</b>	0.8255	0.8128	0.8002	0.7876	0.7749
	$\eta_{\text{dyn}}$ (mPa.s-1)	43.57	19.63	10.06	6.08	4.23
	$\eta_{\text{kin}}$ (mPa.s-1)	52.78	23.53	12.58	7.72	5.45
<b>+3%wt P(MR-C12)-2</b>	<b>Density</b>	0.8255	0.8128	0.8001	0.7875	0.7748
	$\eta_{\text{dyn}}$ (mPa.s-1)	44.12	19.45	10.21	6.17	4.29
	$\eta_{\text{kin}}$ (mPa.s-1)	53.45	23.93	12.76	7.83	5.53

Table III-A-2: Radialube 7368 with 3 wt.% of comb polyesters. Density, dynamic and kinematic values at several temperatures

First series $M_w \approx 10 \text{ Kg.mol}^{-1}$						
	Temperature	20°C	40°C	60°C	80°C	100°C
Radialube 7368	Density	0.94	0.93	0.91	0.90	0.88
	$\eta_{\text{dyn}} \text{ (mPa.s-1)}$	42.91	19.05	9.96	5.96	4.13
	$\eta_{\text{kin}} \text{ (mPa.s-1)}$	45.56	20.55	10.91	6.64	4.67
+3%wt Priolube	Density	0.9419	0.9275	0.9133	0.899	0.8865
	$\eta_{\text{dyn}} \text{ (mPa.s-1)}$	58.41	25.22	13.04	7.75	5.30
	$\eta_{\text{kin}} \text{ (mPa.s-1)}$	62.01	27.19	14.28	8.625	5.98
+3%wt PRic-1	Density	0.9417	0.9273	0.913	0.8987	0.8848
	$\eta_{\text{dyn}} \text{ (mPa.s-1)}$	48.34	21.08	10.99	6.57	4.53
	$\eta_{\text{kin}} \text{ (mPa.s-1)}$	51.34	22.73	12.03	7.31	5.12
+3%wt P(Ric-C4)-1	Density	0.9424	0.928	0.9138	0.8995	0.8854
	$\eta_{\text{dyn}} \text{ (mPa.s-1)}$	52.43	22.58	11.64	6.93	4.75
	$\eta_{\text{kin}} \text{ (mPa.s-1)}$	55.63	24.33	12.74	7.70	5.36
+3%wt P(Ric-C8)-1	Density	0.9426	0.928	0.9139	0.9	0.8856
	$\eta_{\text{dyn}} \text{ (mPa.s-1)}$	51.7	22.3	11.55	6.88	4.73
	$\eta_{\text{kin}} \text{ (mPa.s-1)}$	54.85	24.03	12.64	7.65	5.34
+3%wt P(Ric-C12)-1	Density	0.9415	0.9271	0.9128	0.8986	0.8845
	$\eta_{\text{dyn}} \text{ (mPa.s-1)}$	49.81	21.5	11.13	6.64	4.56
	$\eta_{\text{kin}} \text{ (mPa.s-1)}$	52.9	23.19	12.2	7.385	5.20
+3%wt P(Ric-C18)-1	Density	0.9412	0.9267	0.9124	0.8982	0.884
	$\eta_{\text{dyn}} \text{ (mPa.s-1)}$	49.44	21.46	11.16	6.67	4.59
	$\eta_{\text{kin}} \text{ (mPa.s-1)}$	52.54	23.16	12.23	7.41	5.19
+3%wt P(Ric-Ph)-1	Density	0.9438	0.9294	0.9151	0.9009	0.8871
	$\eta_{\text{dyn}} \text{ (mPa.s-1)}$	53.92	23.2	11.94	7.09	4.86
	$\eta_{\text{kin}} \text{ (mPa.s-1)}$	57.14	24.97	13.04	7.87	5.47
+3%wt P(Ric-EH)-1	Density	0.9421	0.9277	0.9134	0.8992	0.885
	$\eta_{\text{dyn}} \text{ (mPa.s-1)}$	57.58	24.76	12.69	7.51	5.11
	$\eta_{\text{kin}} \text{ (mPa.s-1)}$	61.13	26.68	13.9	8.35	5.77
Second series $M_w \approx 45 \text{ Kg.mol}^{-1}$						
	Temperature	20°C	40°C	60°C	80°C	100°C
+3%wt PRic-2	Density	0.9416	0.9276	0.9133	0.8991	0.8848
	$\eta_{\text{dyn}} \text{ (mPa.s-1)}$	58.82	25.31	12.98	7.68	5.26
	$\eta_{\text{kin}} \text{ (mPa.s-1)}$	62.45	27.29	14.21	8.54	5.94
+3%wt P(Ric-C4)-2	Density	0.9424	0.928	0.9137	0.8995	0.8854
	$\eta_{\text{dyn}} \text{ (mPa.s-1)}$	65.24	27.84	14.29	8.46	5.76
	$\eta_{\text{kin}} \text{ (mPa.s-1)}$	69.23	30	15.64	9.41	6.51
+3%wt P(Ric-C8)-2	Density	0.9419	0.9276	0.9133	0.8991	0.8849
	$\eta_{\text{dyn}} \text{ (mPa.s-1)}$	60.37	25.98	13.42	7.99	5.46
	$\eta_{\text{kin}} \text{ (mPa.s-1)}$	64.09	28.01	14.69	8.88	6.17
+3%wt P(Ric-C12)-2	Density	0.9416	0.9272	0.913	0.8988	0.8846
	$\eta_{\text{dyn}} \text{ (mPa.s-1)}$	60.22	26	13.39	7.97	5.46
	$\eta_{\text{kin}} \text{ (mPa.s-1)}$	63.95	28.05	14.66	8.86	6.17
+3%wt P(Ric-C18)-2	Density	0.9411	0.9268	0.9125	0.8983	0.8844
	$\eta_{\text{dyn}} \text{ (mPa.s-1)}$	60.39	26.11	13.51	8.05	5.51
	$\eta_{\text{kin}} \text{ (mPa.s-1)}$	64.17	28.17	14.81	8.97	6.23
+3%wt P(Ric-Ph)-2	Density	0.9438	0.9295	0.9152	0.901	0.8868
	$\eta_{\text{dyn}} \text{ (mPa.s-1)}$	65.52	27.88	14.29	9.45	5.76

	$\eta_{kin}$ (mPa.s-1)	69.42	30	15.62	9.383	6.502
	<b>Density</b>	0.9421	0.9277	0.9134	0.8992	0.8850
<b>+3%wt P(Ric-EH)-2</b>	$\eta_{dyn}$ (mPa.s-1)	65.87	28.09	14.42	8.54	5.80
	$\eta_{kin}$ (mPa.s-1)	69.92	30.28	15.78	9.50	6.56

Table III-A-3: Yubase 4+ with 3 wt.% of comb polyesters. Density, dynamic and kinematic values at several temperatures

First series $M_w \approx 10 \text{ Kg.mol}^{-1}$						
	Temperature	20°C	40°C	60°C	80°C	100°C
<b>Yubase 4+</b>	<b>Density</b>	0.8226	0.8099	0.7973	0.7846	0.7720
	$\eta_{dyn}$ (mPa.s-1)	34.41	15.16	7.97	4.82	3.35
	$\eta_{kin}$ (mPa.s-1)	41.82	18.71	9.99	6.14	4.34
<b>+3%wt VP</b>	<b>Density</b>	-	-	-	-	-
	$\eta_{dyn}$ (mPa.s-1)	-	-	-	-	-
	$\eta_{kin}$ (mPa.s-1)	-	22.552	-	-	5.082
<b>+3%wt PRic-1</b>	<b>Density</b>	0.8254	0.8127	0.8	0.7874	0.7748
	$\eta_{dyn}$ (mPa.s-1)	37.16	16.62	8.656	5.13	3.57
	$\eta_{kin}$ (mPa.s-1)	45.02	20.45	10.82	6.51	4.61
<b>+3%wt P(Ric-C8)-1</b>	<b>Density</b>	0.8257	0.813	0.8003	0.7877	0.7751
	$\eta_{dyn}$ (mPa.s-1)	39.67	17.39	9.086	5.46	3.78
	$\eta_{kin}$ (mPa.s-1)	48.04	21.38	11.35	6.93	4.87
<b>+3%wt P(Ric-C12)-1</b>	<b>Density</b>	0.8255	0.8128	0.8001	0.7874	0.7748
	$\eta_{dyn}$ (mPa.s-1)	37.94	16.69	8.76	5.27	3.65
	$\eta_{kin}$ (mPa.s-1)	45.96	20.54	10.95	6.69	4.71
<b>+3%wt P(Ric-C18)-1</b>	<b>Density</b>	0.8252	0.8125	0.7998	0.7872	0.7745
	$\eta_{dyn}$ (mPa.s-1)	39.02	17.14	8.977	5.42	3.75
	$\eta_{kin}$ (mPa.s-1)	47.29	21.09	11.22	6.89	4.84
<b>+3%wt P(Ric-EH)-1</b>	<b>Density</b>	0.8257	0.8131	0.8004	0.7878	0.7751
	$\eta_{dyn}$ (mPa.s-1)	41.44	18.13	9.492	5.72	3.97
	$\eta_{kin}$ (mPa.s-1)	50.19	22.3	11.86	7.26	5.12
Second series $M_w \approx 45 \text{ Kg.mol}^{-1}$						
	Temperature	20°C	40°C	60°C	80°C	100°C
<b>+3%wt P(Ric-C8)-2</b>	<b>Density</b>	0.8257	0.813	0.8004	0.7877	0.7751
	$\eta_{dyn}$ (mPa.s-1)	42.9	18.86	9.907	5.99	4.151
	$\eta_{kin}$ (mPa.s-1)	51.96	23.19	12.38	7.60	5.35
<b>+3%wt P(Ric-C12)-2</b>	<b>Density</b>	0.8255	0.8128	0.8002	0.7876	0.7749
	$\eta_{dyn}$ (mPa.s-1)	43.57	19.63	10.06	6.08	4.23
	$\eta_{kin}$ (mPa.s-1)	52.78	23.53	12.58	7.72	5.45
<b>+3%wt P(Ric-C18)-2</b>	<b>Density</b>	0.825	0.8125	0.7998	0.7872	0.7752
	$\eta_{dyn}$ (mPa.s-1)	45.12	19.9	10.45	6.29	4.35
	$\eta_{kin}$ (mPa.s-1)	54.68	24.5	13.07	7.99	5.62
<b>+3%wt P(Ric-EH)-2</b>	<b>Density</b>	0.8259	0.8132	0.8006	0.7879	0.7753
	$\eta_{dyn}$ (mPa.s-1)	48.06	21.25	11.22	6.79	4.67
	$\eta_{kin}$ (mPa.s-1)	58.19	26.13	14.01	8.61	6.03

## Chapter 4:

*Comb copoly(9-alkyl 12-hydroxystearate)s: from thickeners towards Viscosity Index improvers*

## Table of content

Introduction.....	193
1. Comb copoly(9-phenyl ethyl 12-hydroxystearate- <i>r</i> -9-dodecyl 12-hydroxystearate)s P(Ric-Ph- <i>r</i> -Ric-C12).....	194
1.1. First series of comb P(Ric-Ph- <i>r</i> -Ric-C12)s with $M_w \approx 10 \text{ kg}\cdot\text{mol}^{-1}$ .....	195
1.1.1. Copolymers synthesis .....	195
1.1.2. Thermal properties .....	197
1.1.3. Solubility and behavior in mineral oil regarding to the temperature .....	199
1.1.4. Conclusion .....	200
1.2. Second series of comb copolyesters with $M_w > 50 \text{ kg}\cdot\text{mol}^{-1}$ .....	201
1.2.1. Copoly(9-alkyl 12-hydroxystearate)s synthesis .....	201
1.2.2. Behavior in oil with temperature .....	202
1.3. Conclusion.....	203
2. Variation of copolyesters pendant chain moieties .....	204
2.1. Copoly(9-alkyl 12-hydroxystearate)s synthesis and solubility in oil.....	205
2.1.1. Copolymers with phenyl ethyl pendant chains and various soluble pendant chains .....	205
2.1.2. Copolymers with butyl pendant chains and various soluble pendant chains .....	207
2.2. Copoly(9-alkyl 12-hydroxystearate)s behavior in Yubase 4+ with temperature .....	209
2.3. Conclusion.....	211
3. Study in model solvent: conformational behavior.....	212
3.1. Behavior of homo- and copoly(9-alkyl 12-hydroxystearate)s in dodecane with the temperature.....	213
3.2. Evolution of the intrinsic viscosity regarding to the temperature .....	215
3.2.1. Determination of the dilute regime .....	215
3.2.2. Intrinsic viscosity determination .....	217
3.3. Determination of the polymer size with respect to the temperature .....	219
Conclusion .....	221
References.....	223
Experimental .....	224
Appendix.....	226

## Introduction

Polyricinoleate, polyhydroxystearate and functionalized comb poly(9-alkyl 12-hydroxystearate)s, described in the previous chapters, are promising thickeners both in organic and mineral oils. However, no impact on the oil viscosity-temperature relationship was observed, excluding the potential of these biobased polyesters to be used as Viscosity Index improvers.

Based on literature, the polymers used as VII can affect the oil V-T behavior following two main mechanisms, both based on polymer solubility in oil. The first one, mostly described for PAMAs comb polymers, is the coil expansion.<sup>1-3</sup> At low temperature, the polymer coil is isolated in solution under a contracted conformation, alike in a bad solvent. By increasing the temperature, the polymer affinity with the solvent increases, thus, the polymer coil expands, counterbalancing the oil viscosity decreasing with temperature. The second mechanism is called the aggregation-disaggregation behavior.<sup>4-6</sup> It was observed for copolymers or grafted polymers such as Hydrogenated Styrene Diene copolymers and grafted OCP-PAMAs polymers. Generally, in such a case, the polymers contain an insoluble part and a soluble part against the solvent. The soluble part ensures the polymer solubility while the insoluble part tends to aggregate at low temperature. By increasing the temperature, the polymer solubility increases and the coils disaggregate progressively. The polymer effect on oil viscosity is then enhanced by the increasing amount of polymer chains swelled in solution. A schematic illustration of the two mechanisms is displayed in Figure IV-1.

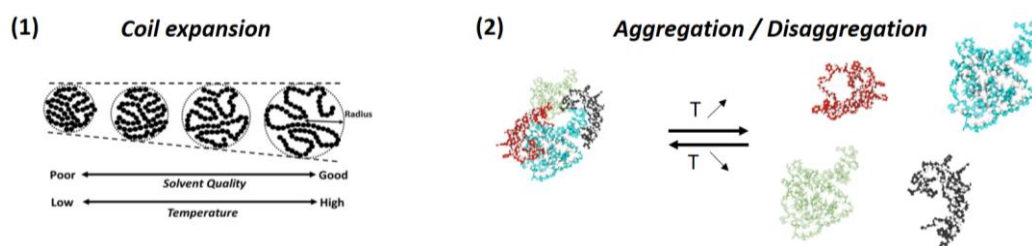


Figure IV-1: Illustration of two VII behaviors in solution (1) coil expansion and (2) aggregation / disaggregation<sup>7</sup>

In both cases, the impact of the polymer on oil V-T behavior is related to its solubility as a function of the temperature. Yet, it was observed in the previous chapter that the grafting of pendant alkyl chains on poly(9-alkyl 12-hydroxystearate), such as butyl or ethyl phenyl moieties, avoids its solubilisation in mineral oil. The idea was then to design copolymers based

on functionalized methyl ricinoleate bearing insoluble and soluble pendant chains, as depicted in Figure IV-2.

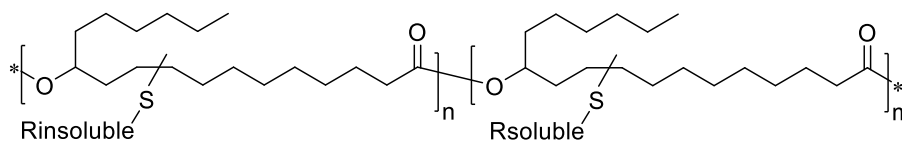


Figure IV-2: Schematic illustration of PRic copolymer with different pendant chains

First, copoly(9-alkyl 12-hydroxystearate)s containing dodecyl- and phenyl ethyl- pendant chains were synthesized and evaluated as viscosity modifiers. The impact of the alkyl chains on the performance of these polyesters as viscosity modifiers will be investigated. Finally, in order to understand how the copolymers behave in solution with temperature, a study will be performed in model solvents, i.e. the dodecane.

## 1. Comb copoly(9-phenyl ethyl 12-hydroxystearate-*r*-9-dodecyl 12-hydroxystearate)s P(Ric-Ph-*r*-Ric-C12)

As it was already observed in previous chapters, both the grafting of phenyl ethyl- and butyl- side chains on poly(9-alkyl 12-hydroxystearate) avoid its solubilisation in mineral oil. Conversely, poly(9-alkyl 12-hydroxystearate)s with long alkyl chains such as octyl-, dodecyl- or octadecyl-, as well as 2-ethyl hexyl moieties, are soluble in mineral oil. As a result, copoly(9-alkyl 12-hydroxystearate)s were synthesized with various ratios of insoluble / soluble pendant chains. Phenyl ethyl- group was selected as the insoluble side chain and dodecyl- as the soluble one, see Figure IV-3.

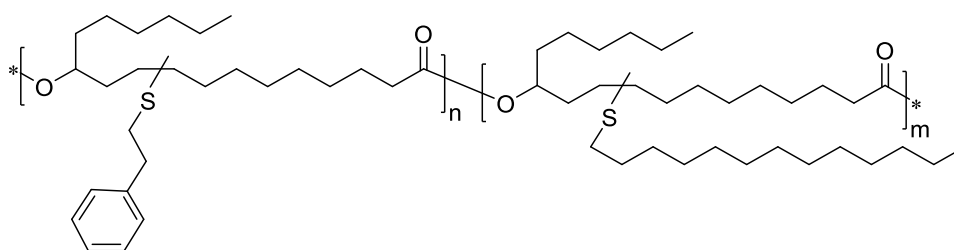


Figure IV-3: Schematic illustration of P(Ric-Ph-*r*-Ric-C12)

Two series of copolyesters were synthesized with two different molecular weights, i.e. with  $M_w = 10 \text{ kg.mol}^{-1}$  and  $M_w > 50 \text{ kg.mol}^{-1}$ . The first series was synthesized with phenyl ethyl ratio

from 0 to 100%. The copolyester solubility was then evaluated in mineral oil regarding to the phenyl ethyl ratio of dangling chains. Following the first series P(Ric-Ph-*r*-Ric-C12) solubility in mineral oil, the second series of P(Ric-Ph-*r*-Ric-C12) was synthesized with appropriate ratio of phenyl ethyl side chains.

## 1.1. First series of comb P(Ric-Ph-*r*-Ric-C12)s with $M_w \approx 10 \text{ kg.mol}^{-1}$

### 1.1.1. Copolymers synthesis

First, a series of random copolyesters P(Ric-Ph-*r*-Ric-C12) were synthesized by polycondensation. MRic-PH and MRic-C12 were added at different ratios, and copolymerized in bulk using 1 wt.% of  $\text{Ti}(\text{O}i\text{Pr})_4$  as catalyst during 8 hours. The copolyester structures were confirmed by  $^1\text{H}$  NMR spectroscopy. The  $^1\text{H}$  NMR spectrum of the P(Ric-C12<sub>0.5</sub>-*r*-Ric-Ph<sub>0.5</sub>), i.e. with 50 wt.% of MRic-Ph and 50 wt.% of MRic-C12, is given in Figure IV-4 as an example. The spectra of other copolyesters are illustrated in Figure IV-A-1 .

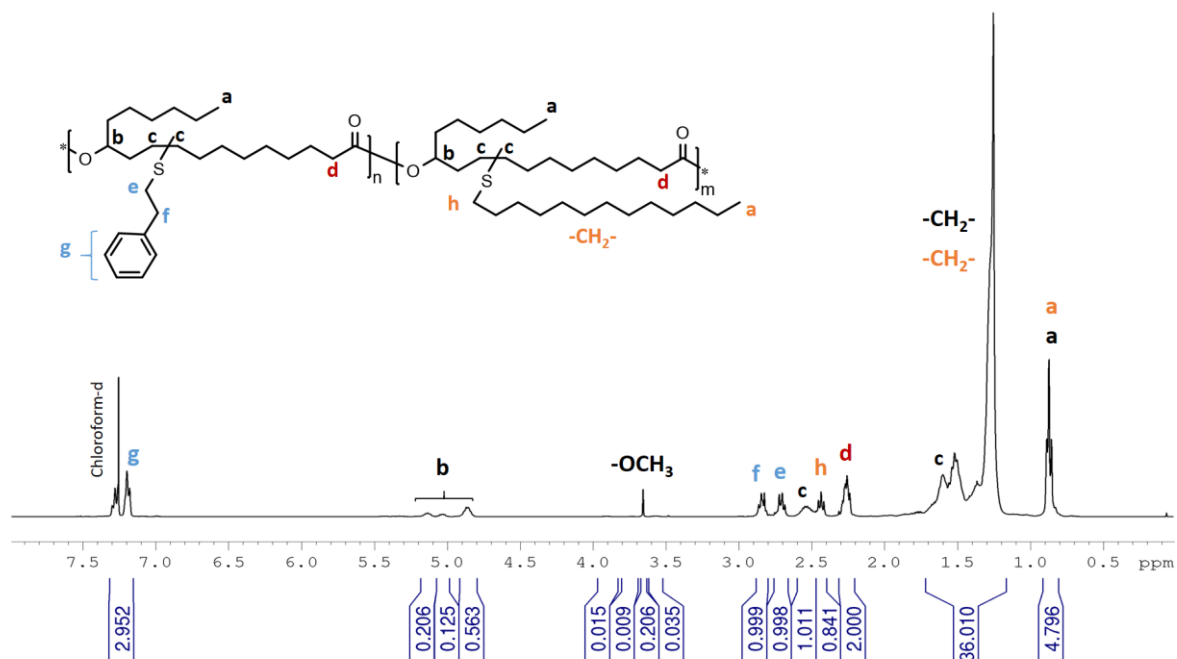


Figure IV-4:  $^1\text{H}$  NMR spectrum in  $\text{CDCl}_3$  of P(Ric-C12<sub>0.5</sub>-*r*-Ric-Ph<sub>0.5</sub>)

The amount of MRic-Ph and MRic-C12 for each copoly(9-alkyl 12-hydroxystearate) determined the ratio of pendant chains which were then reported in weight and molar percentages. These ratios were confirmed by  $^1\text{H}$  NMR analyses using the integration of protons H<sub>f</sub> and H<sub>h</sub> belonging to phenyl ethyl- and dodecyl- group, respectively. Using  $^1\text{H}$  NMR

spectroscopy, the degree of polymerization was determined following Carothers rules established for polycondensation. Calculations were based on the integration of the methyl ester end group at 3.6 ppm. Then, the copolyester molecular weights were determined by SEC analyses using PS calibration. Results are reported in Table IV-1.

Table IV-1: Ratio of pendant chains, reactive functions conversion and copoly(9-alkyl 12-hydroxystearate)s molecular weights

Entry	Ratio (wt.%)	Ratio (mol.%)	Ratio (mol.%) <sup>1</sup>	$P^2$	DPn <sup>2</sup>	M <sub>n</sub> <sup>2</sup> (g/mol)	M <sub>n</sub> <sup>3</sup> (g/mol)	M <sub>w</sub> <sup>3</sup> (g/mol)	Đ <sup>3</sup>
	Ph : C12	Ph : C12	Ph : C12						
#1	0 : 100	0 : 100	0 : 100	0.896	10	3 300	6 400	10 300	1.6
#2	25 : 75	28 : 72	29 : 71	0.829	6	2 000	3 000	6 500	2.2
#3	50 : 50	54 : 46	50 : 50	0.931	15	5 000	4 800	12 200	2.6
#4	75 : 25	77 : 22	74 : 26	0.891	9	3 200	4 100	9 100	2.2
#5	100 : 0	100 : 0	100 : 0	0.910	11	3 800	3 500	9 800	2.8

Reaction conditions: 180°C, 1wt.% of Ti(OiPr)<sub>4</sub> in the melt under vacuum, magnetic stirring, 8 hours

1 Obtained by <sup>1</sup>H NMR using H<sub>h</sub> peak at 2.4 ppm and H<sub>f</sub> peak at 2.9 ppm

2 Obtained by <sup>1</sup>H NMR using OCH<sub>3</sub> peak at 3.6 ppm for calculation

3 Obtained by SEC in THF – PS calibration

The ratios obtained from <sup>1</sup>H NMR analyses are in accordance with the ratio calculated from monomer feed. The conversion generally remains around 0.9 due to the short reaction time (i.e. 8 hours) and the low molecular weight targeted. The molecular weight obtained by <sup>1</sup>H NMR analyses are comparable to M<sub>n</sub> obtained by SEC. Comb copolyesters with similar M<sub>w</sub> around 10 kg.mol<sup>-1</sup> were obtained, in accordance with the molecular weight targeted. SEC traces are displayed in Figure IV-5.

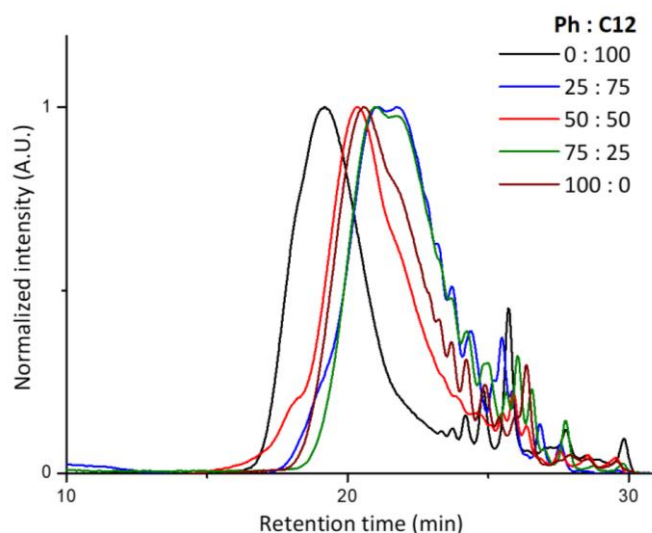


Figure IV-5: SEC traces of first series of copoly(9-alkyl 12-hydroxystearate)s with different ratios of phenyl ethyl and dodecyl pendant chains, M<sub>w</sub> = 10 kg.mol<sup>-1</sup>- Performed in THF

### 1.1.2. Thermal properties

It was shown in the previous chapter that the addition of pendant chains on poly(9-alkyl 12-hydroxystearate) did not impact its thermal stability. However, it influenced the polymer glass transition temperature. As a result, the thermal behavior of the prepared copolyesters was evaluated by DSC; traces are displayed in Figure IV-6. The glass transition temperature,  $T_g$ , the crystallization temperature,  $T_{cris}$ , the melting temperature,  $T_{melt}$  and corresponding enthalpies were recorded after second heating scan at a rate of  $10^\circ\text{C min}^{-1}$ . All the results are reported in Table IV-2.

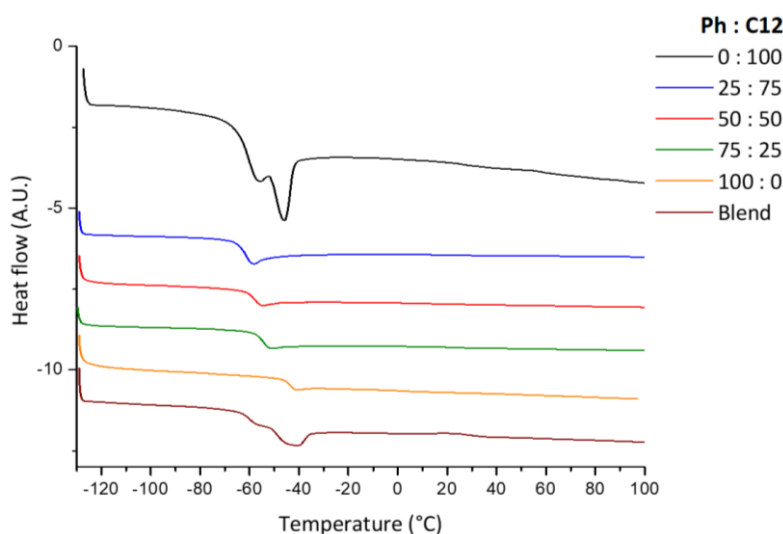


Figure IV-6: DSC traces of P(Ric-Ph-r-Ric-C12) with different ratios of phenyl ethyl and dodecyl pendant chains (Ph : C12) and a blend. Second heating cycle at a rate of  $10^\circ\text{C min}^{-1}$

As expected, the low molecular weight P(Ric-C12) presents a semi-crystalline behavior with a  $T_g$  about  $-61^\circ\text{C}$  and a melting temperature at  $-37^\circ\text{C}$ . This crystalline behavior disappeared with the grafting of phenyl ethyl pendant chains, leading to fully amorphous copolymers. A blend with 50 wt.% of P(Ric-C12) and 50 wt.% of P(Ric-Ph) was prepared and evaluated by DSC. Two  $T_g$  were observed, at  $-60^\circ\text{C}$  and  $-48^\circ\text{C}$  which correspond to the  $T_g$  of the P(Ric-C12) and P(Ric-Ph), respectively, meaning that they are immiscible. Conversely, only one  $T_g$  was observed for all the copolyesters tested, confirming their random nature.

Table IV-2: Thermal behavior of Ph : C12 copoly(9-alkyl 12-hydroxystearate) with different ratios and a blend of PRic-C12 #1 and PRic-Ph #5. Measured by DSC during the second heating cycle at a rate of 10°C min<sup>-1</sup>

Entry	Ratio Ph : C12	M <sub>n</sub> <sup>1</sup> (g.mol <sup>-1</sup> )	M <sub>w</sub> <sup>1</sup> (g.mol <sup>-1</sup> )	Đ <sup>1</sup>	T <sub>g</sub> <sup>2</sup> (°C)	T <sub>melt</sub> <sup>2</sup> (°C)	T <sub>cris</sub> <sup>2</sup> (°C)
#1	0 : 100	6 400	10 300	1,6	-61	-37 (11 J/g)	-49 (18 J/g)
#2	25 : 75	3 000	6500	2.2	-61	-	-
#3	50 : 50	4 800	12 200	2.6	-57	-	-
#4	75 : 25	4 100	9 100	2.2	-54	-	-
#5	100 : 0	3 500	9 800	2.8	-49	-	-
Blend	50 : 50	-	-	-	-60/-48		

1 Obtained by SEC in THF – PS calibration

2 Obtained by DSC- first and second heating cycle at a rate of 10°C min<sup>-1</sup>

In addition, the T<sub>g</sub> increased by increasing the ratio of phenyl ethyl pendant chains in the copolyesters. This feature could be rationalized according to Fox equation (IV-1)<sup>8</sup>

$$\frac{1}{T_g} = \frac{w_1}{T_{g,1}} + \frac{w_2}{T_{g,2}} \quad (\text{IV-1})$$

where T<sub>g</sub> is the glass transition temperature of the copolymer, T<sub>g,1</sub> and T<sub>g,2</sub> the glass transition of P(Ric-Ph) and P(Ric-C12), respectively and w<sub>1</sub> and w<sub>2</sub> the weight fraction of MRic-Ph and MRic-C12 in the copolymer.

According to this equation, the T<sub>g</sub> of each copolyesters can be estimated and compared to the experimental T<sub>g</sub> obtained by DSC, see Figure IV-7.

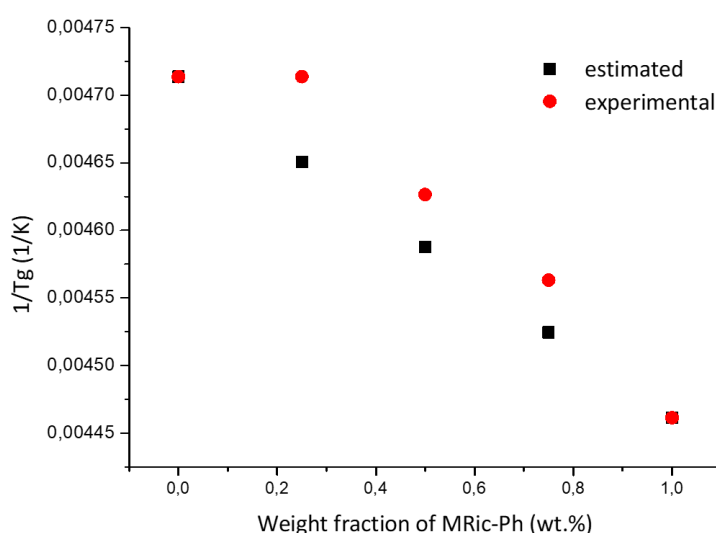


Figure IV-7: Glass transition temperature as a function of the weight fraction of phenyl ethyl- branched monomer. Comparison between experimental and estimated values determined by Fox equation

As expected,  $1/T_g$  decreases linearly with the increase of the phenyl monomer weight fraction in the copolymer. The estimated values determined with Fox equation and the measured data evolved similarly. The thermal behavior of the copolyesters evolve as a typical random copolymer with respect to their chemical composition.<sup>8</sup> As P(Ric-C12) is semi-crystalline, its glass transition temperature were overestimated, leading to a decrease of the estimated slope regarding to experimental values.

### 1.1.3. Solubility and behavior in mineral oil regarding to the temperature

The so-formed random copoly(9-alkyl 12-hydroxystearate)s were added in mineral oil, the Yubase 4+. First, the solubility of copolyesters was evaluated. The blends were stirred at 100 °C under magnetic stirring during 2 hours then cooled down at room temperature for 24 hours without stirring. It appeared that only the homopolymer P(Ric-C12) and the copolymer P(Ric-Ph<sub>0.25</sub>-*r*-Ric-C12<sub>0.75</sub>), with 25 wt.% of MRic-Ph and 75 wt.% of MRic-C12 were soluble in Yubase 4+, at a concentration of 3 wt.%. The other copolyesters precipitated in oil during the cooling step were not solubilized despite the heating at 100 °C. The two homogeneous systems were analyzed by viscometry using a densimeter-viscosimeter. Density, dynamic and kinematic viscosities were measured from 20 °C to 100 °C, see Table IV-A-1, allowing us determining the relative viscosities, the Viscosity Indexes and the Q values; data are reported in Table IV-3. The relative viscosities as a function of the temperature are displayed in Figure IV-8.

Table IV-3: Solubility, relative viscosity depending on the temperature, Viscosity Index and Q values of Yubase 4+ with 3 wt.% of comb copolyesters with various ratios of phenyl ethyl and dodecyl pendant chains

Ratio Ph : C12		0 : 100	25 : 75	50 : 50	75 : 25	100 : 0
$M_w$ (g.mol <sup>-1</sup> )		10 300	6 500	12 200	9 100	9 800
Solubility in Y		Yes	Yes	No	No	No
$\eta_{rel}$	20°C	1.129	1.139	-	-	-
	40°C	1.124	1.134	-	-	-
	60°C	1.120	1.128	-	-	-
	80°C	1.116	1.127	-	-	-
	100°C	1.112	1.120	-	-	-
VI	R=145	160	160	-	-	-
Q		0.91	0.90	-	-	-

The viscosity of the two solutions tested behaves similarly regarding to the temperature. The relative viscosity values are really close. Surprisingly, P(Ric-Ph<sub>0.25</sub>-*r*-Ric-C12<sub>0.75</sub>)s have a higher

impact on the oil viscosity than the P(Ric-C12) despite a lower molecular weight. Still, the Viscosity Indexes and the Q values are similar. There is no significant impact of the presence of some phenyl pendant chains on P(Ric-C12) on its behavior as viscosity modifier.

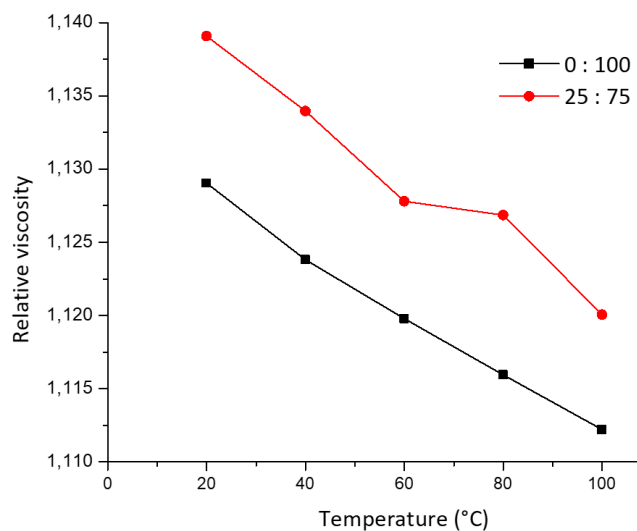


Figure IV-8: Relative viscosity as a function of temperature of Yubase 4+ with 3 wt.% of comb copolyesters with different ratios of phenyl ethyl and dodecyl pendant chain (Ph : C12)

#### 1.1.4. Conclusion

To conclude this part, methyl 9-phenyl ethyl 12-hydroxystearate and methyl 9-dodecyl 12-hydroxystearate were mixed following different ratios and polymerized by transesterification. Random copolyesters with molecular weight about  $10 \text{ kg}\cdot\text{mol}^{-1}$  were obtained. The copolyester glass transition temperatures were related to the copolyester composition. The presence of 50 wt.% of phenyl ethyl pendant chains or above in the copolyesters lead to their insolubility in mineral oil. As a result, only the impact of P(Ric-C12) and P(Ric-Ph<sub>0.25-r</sub>-Ric-C12<sub>0.75</sub>) on mineral oil viscosity was evaluated. It appeared that the two polymers behave similarly in oil with temperature; no influence of the presence of phenyl ethyl pendant chains in the copolymer was noticed.

## 1.2. Second series of comb copolyesters with $M_w > 50 \text{ kg.mol}^{-1}$

### 1.2.1. Copoly(9-alkyl 12-hydroxystearate)s synthesis

Copolyesters P(Ric-Ph-*r*-Ric-C12) with molecular weight around  $10 \text{ kg.mol}^{-1}$  were synthesized and added in a mineral oil. Only copolymers with less than 50 wt.% of phenyl ethyl branched moiety were found soluble. As a result, only copolyesters with a percentage of phenyl ethyl moieties between 0 and 50 wt.% were synthesized. MRic-Ph and MRic-C12 monomers were mixed and polymerized at  $180 \text{ }^\circ\text{C}$  for 48 hours under vacuum with 1 wt.% of  $\text{Ti}(\text{OiPr})_4$  as catalyst using mechanical stirring, according to the optimized reaction previously described. The structures were confirmed by  $^1\text{H}$  NMR spectroscopy, see Figure IV-A-2. The copolymer molecular weights were determined both by  $^1\text{H}$  NMR and SEC analyses with PS calibration. Results are reported in Table IV-4.

Table IV-4: Ratio of pendant chains, reactive functions conversion and copoly(9-alkyl 12-hydroxystearate)s P(Ric-Ph-*r*-Ric-C12) molecular weights

Entry	Ratio (wt.%) Ph : C12	Ratio (mol.%) Ph : C12	Ratio (mol.%) <sup>1</sup> Ph : C12	$P^2$	$\text{DPn}^2$	$M_n^2$ (g.mol <sup>-1</sup> )	$M_n^3$ (g.mol <sup>-1</sup> )	$M_w^3$ (g.mol <sup>-1</sup> )	$\text{Đ}^3$
#6	0 : 100	0 : 100	0 : 100	0.983	58	28 000	24 000	55 000	2.2
#7	15 : 85	17 : 83	19 : 81	0.971	35	11 800	22 000	70 500	3.2
#8	25 : 75	28 : 72	26 : 74	0.980	49	16 700	21 500	72 000	3.4
#9	30 : 70	33 : 67	30 : 70	0.976	42	14 400	23 800	85 000	3.6
#10	35 : 65	38 : 62	34 : 66	0.978	45	15 500	19 600	60 600	3.1
#11	40 : 60	44 : 56	41 : 59	0.977	44	15 000	20 000	56 400	2.8

Reaction conditions:  $180^\circ\text{C}$ , 1wt.% of  $\text{Ti}(\text{OiPr})_4$  in the melt under vacuum, mechanical stirring, 48 hours

1 Obtained by  $^1\text{H}$  NMR using  $H_h$  peak at 2.4 ppm and  $H_f$  peak at 2.9 ppm

2 Obtained by  $^1\text{H}$  NMR using  $\text{OCH}_3$  peak at 3.6 ppm for calculation

3 Obtained by SEC in THF – PS calibration

The composition of the copoly(9-alkyl 12-hydroxystearate)s determined by  $^1\text{H}$  NMR analyses are in accordance with the initial monomer weight concentrations. The molecular weights determined by  $^1\text{H}$  NMR spectroscopy are generally lower than the ones obtained by SEC measurements. As a result, the molecular weight obtained by SEC will be used as a reference. As it is displayed in Figure IV-9, all the copolyesters synthesized are in the same  $M_w \approx 60 \text{ kg.mol}^{-1}$ . As it was observed for the previous polyesters prepared, some oligomers and potential cyclization may be present in copolymers mixture.

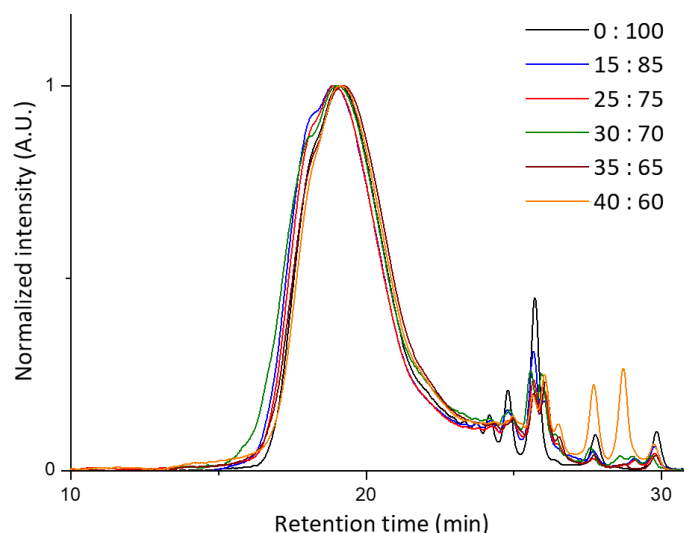


Figure IV-9: SEC traces of copoly(9-alkyl 12-hydroxystearate)s with different ratio of phenyl ethyl and dodecyl pendant chains – Performed in THF

### 1.2.2. Behavior in oil with temperature

The copolyesters prepared were blended in Yubase 4+ and the solubility of the polymers in Yubase 4+ was evaluated. The homogeneous blends were then analyzed by viscometry. Density, dynamic and kinematic viscosities were measured from 20 °C to 100 °C, see Table IV-A-2, allowing us determining the relative viscosities, the Viscosity Indexes and the Q values, see data reported in Table IV-5. The relative viscosities as a function of the temperature are displayed in Figure IV-10.

Table IV-5: Solubility, relative viscosity depending on the temperature, Viscosity Index and Q values of Yubase 4+ with 3 wt.% of comb copolyesters with various ratio of phenyl and dodecane pendant chains

Ratio Ph : C12	0 : 100	15 : 85	25 : 75	30 : 70	35 : 65	40 : 60
$M_w$ (g.mol <sup>-1</sup> )	55 000	70 500	72 000	85 000	60 600	56 400
Solubility in Y	Yes	Yes	Yes	No	No	No
$\eta_{rel}$	20°C	1.278	1.272	1.269	-	-
	40°C	1.279	1.277	1.276	-	-
	60°C	1.277	1.280	1.285	-	-
	80°C	1.276	1.284	1.292	-	-
	100°C	1.276	1.288	1.298	-	-
VI	R=145	181	186	189	-	-
Q		0.99	1.04	1.08	-	-

The P(Ric-Ph-*r*-Ric-C12)s were insoluble in mineral oil when the weight percentage of phenyl ethyl functionalized monomer was about 30 wt.% or above. As a result, only homopolymer P(Ric-C12) and copolyesters with 15 and 25 wt.% of MRic-Ph could be evaluated as viscosity

modifiers in Yubase 4+. As illustrated in Figure IV-10, the relative viscosity of the two oil solutions containing copolyesters at 3wt.% increase with the temperature while the solution with homopolyester remains stable over the temperature. Indeed, the relative viscosity at 20°C of the oil containing 3 wt.% of copolymers 15 : 85 and 25 : 75, with  $M_w = 70 \text{ kg.mol}^{-1}$  is lower than the one of the oil containing P(Ric-C12) of  $M_w$  of  $55 \text{ kg.mol}^{-1}$ . Moreover, the higher the percentage of phenyl ethyl pendant chains in the copolymer, the higher the impact on the oil V-T behavior. It was then speculated that the grafting of phenyl ethyl group could lead to contracted or aggregated polymer coils at low temperature. It is supposed that the copolyester solubility increases with the temperature leading to the relative viscosity increase. The oil Viscosity Index is enhanced by the addition of polyesters. The homopolyester addition increases the oil VI from 145 to 181 and the copolyester addition leads to VI of 186 for 15 : 85 and of 189 for 25 : 75 copolymers. The Q values of solutions with 15 : 85 and 25 : 75 copolyesters are 1.04 and 1.08, respectively while with the P(Ric-C12),  $Q = 0.99$ . The latter can be then considered as a thickener while the copolyesters are Viscosity Index improvers with a positive impact on the oil V-T behavior.

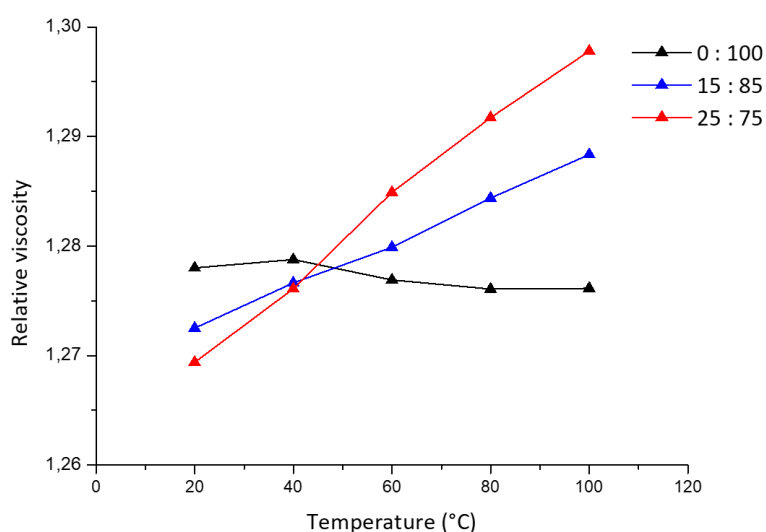


Figure IV-10: Relative viscosity as a function of temperature of Yubase 4+ with 3 wt.% of second series of comb copolyesters with different ratios of phenyl ethyl and dodecyl pendant chains (Ph : C12)

### 1.3. Conclusion

Random copoly(9-alkyl 12-hydroxystearate)s with various ratios of phenyl ethyl and dodecyl pendant chains synthesized by polycondensation of functionalized methyl ricinoleate, MRic-Ph and MRic-C12. A series of P(Ric-Ph-*r*-Ric-C12) with  $M_w \approx 10 \text{ kg.mol}^{-1}$  were first prepared

and their behaviors in oil investigated. It appeared that copolyesters with 50 wt.% of phenyl ethyl moiety are not soluble in mineral oil. The soluble homopolymer P(Ric-C12) and copolyester with 25 wt.% of phenyl ethyl group behave similarly in solution regarding to the temperature. However, a strong impact of the copolymer composition was observed for P(Ric-Ph-*r*-Ric-C12) with  $M_w \approx 60 \text{ kg}\cdot\text{mol}^{-1}$ . Indeed, it was shown that the copolyesters with phenyl ethyl moieties act as Viscosity Index improvers in oil with a positive impact on oil V-T behavior while the homopolymer acts as a thickener. It was then anticipated that grafting of phenyl ethyl moieties in the copolyester affects its solubility in Yubase 4+ regarding to the temperature, leading to contracted or aggregated polymer coils at room temperature which can expand or disaggregate with the temperature increase, thus leading to the oil viscosity increase.

## 2. Variation of copolyesters pendant chain moieties

---

Some random copoly(9-alkyl 12-hydroxystearate)s with appropriate ratios of phenyl ethyl- and dodecyl- pendant chains could act as Viscosity Index improvers in mineral oil. Those two types of pendant chains were selected as an example but other combinations with various types of insoluble and soluble pendant alkyl chains were also synthesized and evaluated as viscosity modifiers in mineral oil. As illustrated in Figure IV-11, first, methyl 9-phenyl ethyl 12-hydroxystearate was selected as the “insoluble” monomer and copolymerized with hydrogenated methyl ricinoleate (MHS) and methyl 9-ethyl hexyl 12-hydroxystearate (MRic-EH). Then, methyl 9-butyl 12-hydroxystearate (MRic-C4) was selected as “insoluble” moieties and copolymerized successively with MRic-C12 and MRic-EH as “soluble” counterpart. For each copolymer synthesized, several “insoluble : soluble” ratios were investigated in order to determine the copolymer solubility limit in mineral oil. Finally, the soluble copolyesters in oil were evaluated as viscosity modifiers.

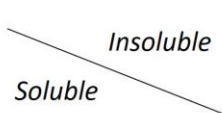
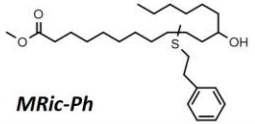
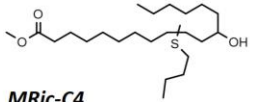
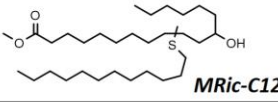
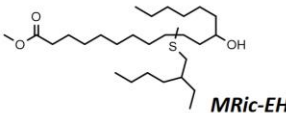
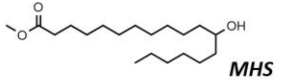
	<i>Insoluble</i>	 <b>MRic-Ph</b>	 <b>MRic-C4</b>	
<i>Soluble</i>		 <b>MRic-C12</b>	 <i>P(Ric-C12-r-Ric-Ph)</i>	 <i>P(Ric-C12-r-Ric-C4)</i>
		 <b>MRic-EH</b>	 <i>P(Ric-EH-r-Ric-Ph)</i>	 <i>P(Ric-EH-r-Ric-C4)</i>
		 <b>MHS</b>	 <i>P(HS-r-Ric-Ph)</i>	

Figure IV-11 : Copolymerization of various methyl 9-alkyl 12-hydroxystearate with « insoluble » or « soluble » pendant chains

## 2.1. Copoly(9-alkyl 12-hydroxystearate)s synthesis and solubility in oil

### 2.1.1. Copolymers with phenyl ethyl pendant chains and various soluble pendant chains

Copoly(9-alkyl 12-hydroxystearate)s were synthesized with successively MHS and MRic-EH at different ratios. All the copolyester structures were confirmed by <sup>1</sup>H NMR spectroscopy, an example for each type of copolyester is illustrated in Figure IV-12 and the copolyester molecular weights were determined by SEC analyses. The copolyesters were then added to with Yubase 4+ following the same protocol as previously described in order to evaluate their solubility in mineral oil. Results are reported in Table IV-15.

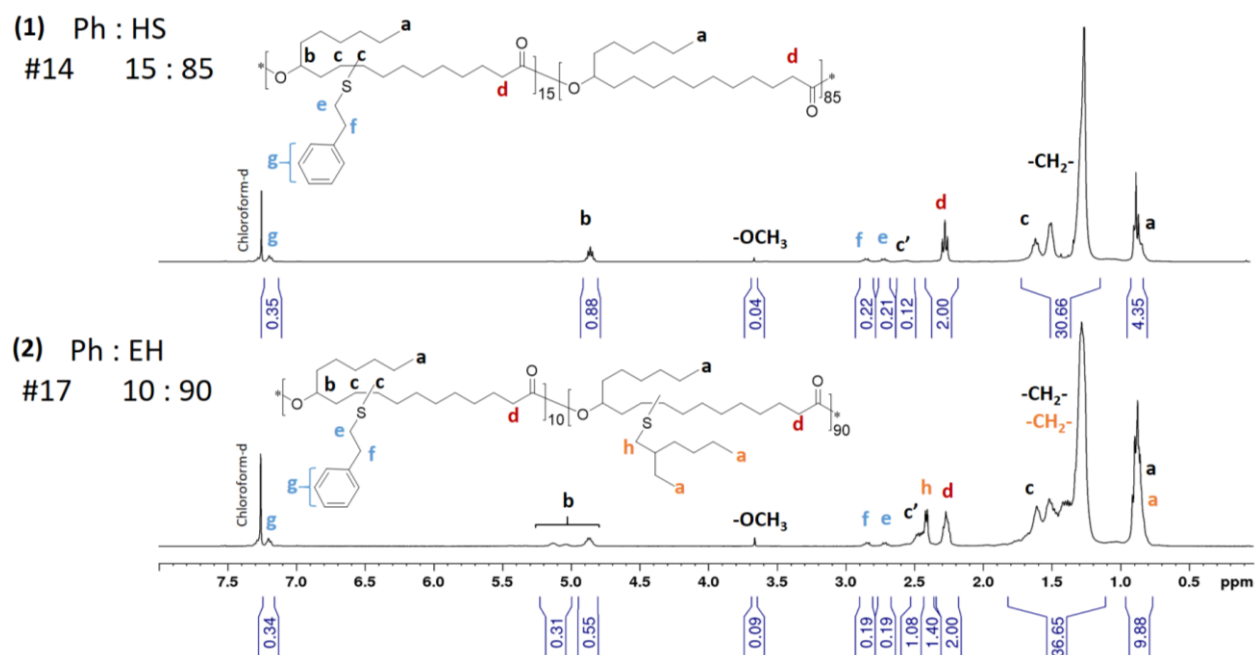


Figure IV-12:  $^1\text{H}$  NMR spectra in  $\text{CDCl}_3$  of copoly(9-alkyl 12-hydroxystearate) with  $M_w = 60 \text{ kg.mol}^{-1}$  (1) P(Ric-Ph<sub>0.15</sub>-r-HS<sub>0.85</sub>) and (2) P(Ric-Ph<sub>0.1</sub>-r-Ric-EH<sub>0.9</sub>)

Table IV-15 : Ratio of pendant chains, molecular weights and solubility in mineral oil of P(Ric-Ph-r-HS) and P(Ric-Ph-r-Ric-EH)

Entry	Ratio (wt.%) Ph : HS	$M_n^1$ (g.mol <sup>-1</sup> )	$M_w^1$ (g.mol <sup>-1</sup> )	$\bar{D}^1$	Solubility in Y
#12	0 : 100	25 600	63 000	2.4	Yes
#13	10 : 90	34 500	86 900	2.5	No
#14	15 : 85	20 200	68 600	3.4	No

Entry	Ratio (wt.%) Ph : EH	$M_n^1$ (g.mol <sup>-1</sup> )	$M_w^1$ (g.mol <sup>-1</sup> )	$\bar{D}^1$	Solubility in Y
#15	0 : 100	20 400	41 300	2	Yes
#16	5 : 95	23 200	64 700	2.9	Yes
#17	10 : 90	16 500	37 800	2.3	Yes
#18	15 : 85	25 200	62 800	2.5	No
#19	20 : 80	27 600	78 200	2.8	No

180°C, 1wt.% of  $\text{Ti}(\text{OiPr})_4$  in the melt under vacuum, mechanical stirring, 48 hours

1 Obtained by SEC in THF –PS calibration

Poly(hydroxystearate) is soluble in a large  $M_w$  range in mineral oil, see Chapter 2. The aim was then to introduce some phenyl pendant chains to reduce its solubility. MHS and MRic-Ph were then copolymerized by transesterification. Molecular weights of  $63 \text{ kg.mol}^{-1}$  and above were obtained. The P(HS-r-Ric-Ph) performed were found insoluble in mineral oil, even at  $100^\circ\text{C}$ . As a result, the effect of the addition of phenyl ethyl pendant chains on PHS behavior in oil could not be investigated.

MRic-Ph was also copolymerized with MRic-EH at different weight ratios. The copoly(9-alkyl 12-hydroxystearate) molecular weights are in the range 38 – 72 kg.mol<sup>-1</sup>. It was observed that P(Ric-Ph-*r*-Ric-EH) lost its solubility in mineral oil when the percentage of MRic-Ph was superior or equal to 10 wt.%. In the case of P(Ric-Ph-*r*-Ric-C12), the solubility limit was about 25 wt.% of MRic-Ph. As MRic-EH has shorter pendant chains than MRic-C12, the corresponding copolyester has probably less affinity with the aliphatic mineral oil than dodecyl-based copoly(9-alkyl 12-hydroxystearate).

### 2.1.2. Copolymers with butyl pendant chains and various soluble pendant chains

In the previous chapter, it was observed that the grafting of butyl chains on polyricinoleate avoid the polymer solubilisation in mineral oil. As a result, copoly(9-alkyl 12-hydroxystearate)s with butyl functionalized methyl ricinoleate (MRic-C4) as comonomer were synthesized following the same methodology as previously described. MRic-C12 and MRic-EH were selected as the second monomers representing the “soluble” moieties. The ratio between MRic-C4 and MRic-C12 or MRic-EH were varied in order to reach the solubility limit of each copolyester. The structures were confirmed by <sup>1</sup>H NMR spectroscopy; two spectra are displayed in Figure IV-13 as examples.

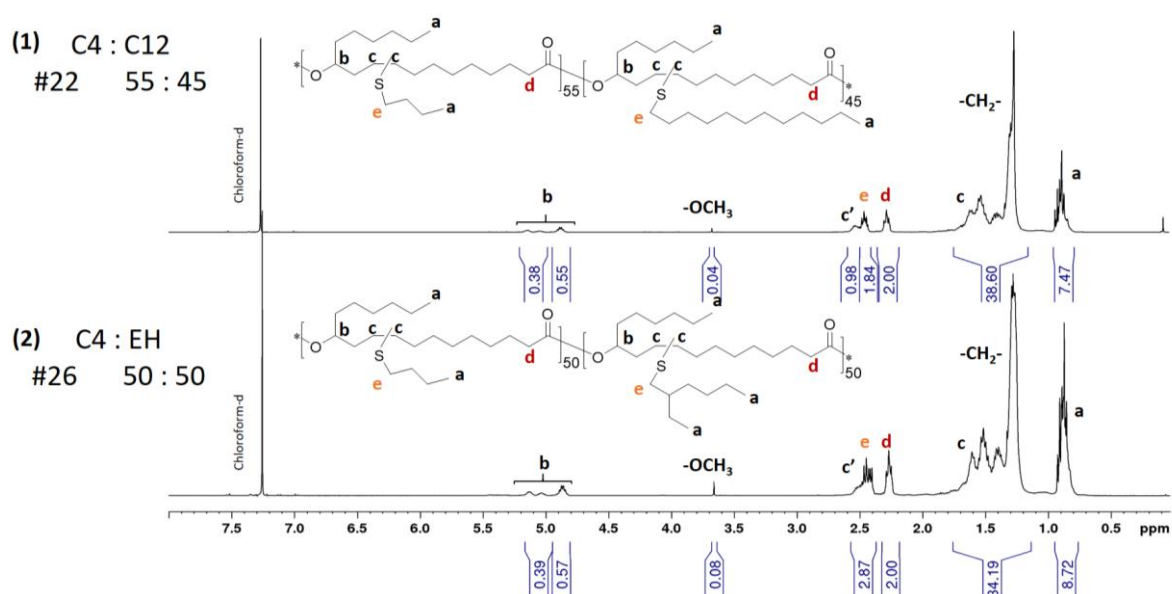


Figure IV-13: <sup>1</sup>H NMR spectra in CDCl<sub>3</sub> of copoly(9-alkyl 12-hydroxystearate) with M<sub>w</sub> = 60 kg.mol<sup>-1</sup> (1) P(Ric-C4<sub>0.55</sub>-*r*-C12<sub>0.45</sub>) and (2) P(Ric-C4<sub>0.5</sub>-*r*-Ric-EH<sub>0.5</sub>)

Molecular weights were determined by SEC measurements using PS calibration. Copoly(9-alkyl 12-hydroxystearate)s were then blended with Yubase 4+. The dilution protocol was the same as previously described. Results are reported in Table IV-7.

Table IV-7: Ratio of pendant chains, molecular weights and solubility in mineral oil of copolyesters P(Ric-C4-*r*-C12) and P(Ric-C4-*r*-Ric-EH)

Entry	Ratio (wt.%) C4 : C12	$M_n^1$ (g/mol)	$M_w^1$ (g/mol)	$\bar{D}^1$	Solubility in Y
#6	0 : 100	24 000	55 000	2.2	Yes
#20	25 : 75	5 700	17 000	3	Yes
#21	50 : 50	24 500	85 500	4.6	Yes
#22	55 : 45	23 000	64 200	2.8	Yes
#23	60 : 40	22 800	47 100	2.1	No

Entry	Ratio (wt.%) C4 : EH	$M_n^1$ (g/mol)	$M_w^1$ (g/mol)	$\bar{D}^1$	Solubility in Y
#15	0 : 100	20 400	41 300	2	Yes
#24	25 : 75	23 500	60 000	2.6	Yes
#25	40 : 60	15 500	40 500	2.6	Yes
#26	50 : 50	17 100	43 000	2.5	Yes
#27	55 : 45	23 600	70 700	2.8	No
#28	60 : 40	16 000	49 000	3	No

*Reaction conditions: 180°C, 1wt.% of Ti(OiPr)<sub>4</sub> in the melt under vacuum, mechanical stirring, 48 hours*  
*1 Obtained by SEC in THF –PS calibration*

For the two types of synthesized copoly(9-alkyl 12-hydroxystearate), i.e. P(Ric-C4-*r*-Ric-C12) and P(Ric-C4-*r*-Ric-EH), molecular weights are in the range of 40 – 85 kg.mol<sup>-1</sup>. In the case of P(Ric-C4-*r*-Ric-C12), the insolubility appears for copolymer containing more than 55 wt.% of MRic-C4 as monomer. As  $M_w$  55:45 >  $M_w$  60:40, it is concluded that the loss of solubility is due to the amount of insoluble butyl pendant chains and not to the copolymer molecular weight. As a result, the copolyester solubility in mineral oil is mostly related to the nature of both the insoluble and soluble pendant alkyl chains. The solubility limits were defined for each type of copolymers by varying the ratios between the two comonomers. Results are summarized in Figure IV-14.

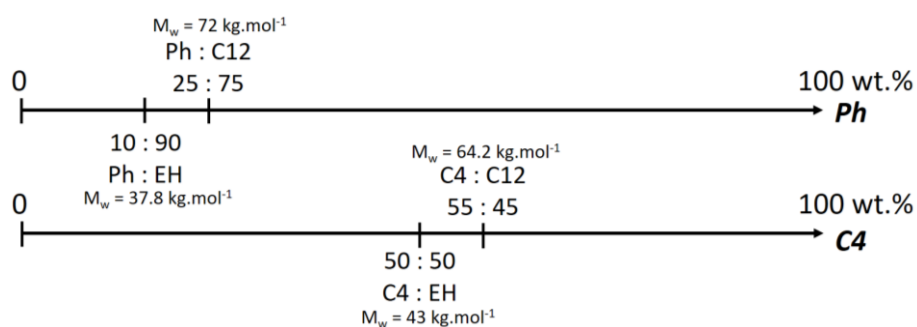


Figure IV-14 : Copolyester solubility limit in mineral oil regarding to the ratio of insoluble / soluble monomers

The nature of the soluble and insoluble pendant alkyl chains has an effect on the copoly(9-alkyl 12-hydroxystearate)s solubility in Yubase 4+. For instance, copolyesters with phenyl ethyl pendant chains are less soluble than copolyesters with butyl chains, due to the closer structure of butyl than phenyl ethyl moieties regarding to the oil structure. Similarly, as dodecyl chains are long aliphatic carbon chains, they provide good affinity with oil leading to the solubilisation of copolyesters with higher insoluble part than for 2-ethylhexyl branched ones. To conclude, copoly(9-alkyl 12-hydroxystearate)s with various types and amounts of pendant chains were designed, leading to copolyesters soluble in oil or not. The behavior in oil of the soluble copolyesters was then investigated.

## 2.2. Copoly(9-alkyl 12-hydroxystearate)s behavior in Yubase 4+ with temperature

The Yubase 4+ with 3 wt.% of added polyesters were analyzed by viscometry as a function of temperature. Density, dynamic and kinematic viscosities were measured from 20 °C to 100 °C, see Table IV-A-3, allowing us determining the relative viscosities, the Viscosity Index and the Q values; data are reported in Table IV-8 and Table IV-9. The relative viscosities as a function of the temperature are displayed in Figure IV-15.

Table IV-8: Relative viscosity depending on the temperature, Viscosity Index and Q values of Yubase 4+ with 3 wt.% of comb copolyesters with various ratios of phenyl ethyl and dodecyl or 2-ethylhexyl pendant chains

		Ratio Ph : C12			Ratio Ph : EH		
		0 : 100	15 : 85	25 : 75	0 : 100	5 : 95	10 : 90
<b>M<sub>w</sub></b>	<b>(g.mol<sup>-1</sup>)</b>	55 000	70 500	72 000	41 300	64 700	37 800
<b>η<sub>rel</sub></b>	<b>20°C</b>	1.278	1.272	1.269	1.391	1.286	1.240
	<b>40°C</b>	1.279	1.277	1.276	1.396	1.287	1.238
	<b>60°C</b>	1.277	1.280	1.285	1.402	1.284	1.233
	<b>80°C</b>	1.276	1.284	1.292	1.403	1.282	1.226
	<b>100°C</b>	1.276	1.288	1.298	1.390	1.282	1.196
<b>VI</b>	<b>R=145</b>	<b>181</b>	<b>186</b>	<b>189</b>	<b>190</b>	<b>182</b>	<b>164</b>
<b>Q</b>		<b>0.99</b>	<b>1.04</b>	<b>1.08</b>	<b>0.98</b>	<b>0.93</b>	<b>0.82</b>

Table IV-9: Relative viscosity depending on the temperature, Viscosity Index and Q values of Yubase 4+ with 3 wt.% of comb copolyesters with various ratios of butyl and dodecyl or 2-ethylhexyl pendant chains

		Ratio C4 : C12				Ratio C4 : EH			
		0 : 100	25 : 75	50 : 50	55 : 45	0 : 100	25 : 75	40 : 60	50 : 50
<b>M<sub>w</sub></b> (g.mol <sup>-1</sup> )		55 000	17 000	85 500	64 200	41 300	60 000	40 500	43 000
<b>η<sub>rel</sub></b>	20°C	1.278	1.210	1.283	1.329	1.391	1.318	1.235	1.275
	40°C	1.279	1.213	1.295	1.349	1.396	1.328	1.228	1.272
	60°C	1.277	1.206	1.303	1.359	1.402	1.331	1.222	1.268
	80°C	1.276	1.197	1.309	1.367	1.403	1.331	1.216	1.267
	100°C	1.276	1.165	1.311	1.370	1.390	1.333	1.213	1.266
<b>VI</b>	<b>R=145</b>	<b>181</b>	<b>158</b>	<b>189</b>	<b>195</b>	<b>190</b>	<b>188</b>	<b>172</b>	<b>180</b>
<b>Q</b>		<b>0.99</b>	<b>0.78</b>	<b>1.06</b>	<b>1.06</b>	<b>0.98</b>	<b>1.01</b>	<b>0.93</b>	<b>0.98</b>

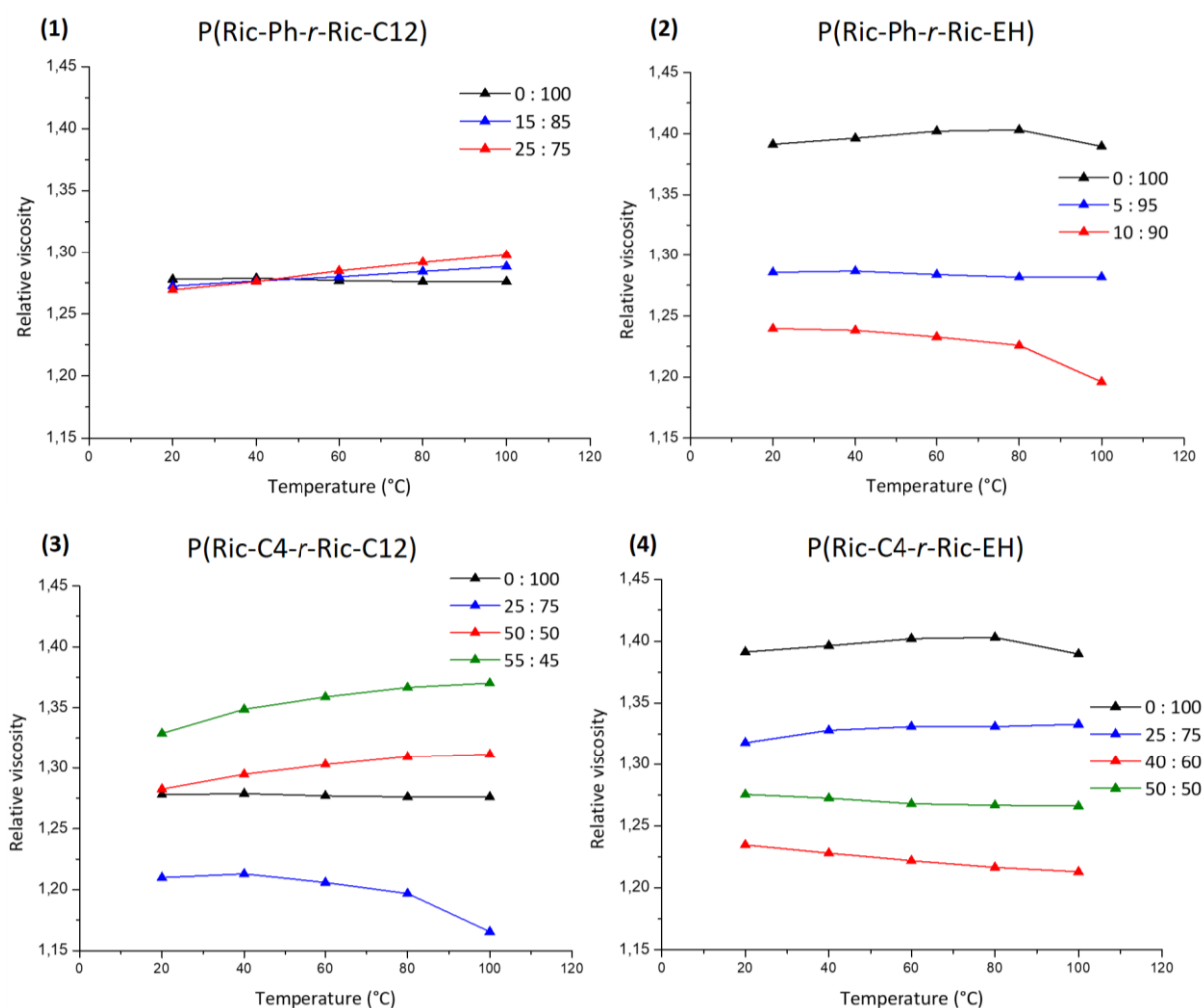


Figure IV-15: Relative viscosity as a function of temperature of Yubase 4+ with 3 wt.% of several comb copolyesters: (1)P(Ric-Ph-r-Ric-C12), (2) P(Ric-Ph-r-Ric-EH), (3) P(Ric-C4-r-Ric-C12) and (4) P(Ric-C4-r-Ric-EH)

As a general trend, an increase of the relative viscosity with the temperature is observed in the case of copolymers bearing dodecyl- soluble pendant chains. Both for copoly(9-alkyl 12-hydroxystearate)s with phenyl ethyl- and butyl- insoluble pendant chains, the highest the fraction of ‘insoluble’ moiety in the copolymer composition, the highest is the copolymer

impact on V-T behavior. For instance, Q values of 1.08 and VI = 189 for P(Ric-Ph<sub>25</sub>-*r*-Ric-C12<sub>75</sub>) and Q = 1.06 and VI = 195 for P(Ric-C4<sub>55</sub>-*r*-Ric-C12<sub>45</sub>) in oil are obtained. These copolymers are then considered as Viscosity Index improvers. Conversely, no positive impact of the copolyesters with 2-ethylhexyl pendant chains on oil V-T behavior was observed with Q values close to 1, whatever the amount of insoluble pendant chains. It is then speculated that the branched structure of 2-ethylhexyl forces the polymer coil expansion whatever the temperature.

However, the grafting of insoluble pendant chains has an impact on the thickening efficiency of the copolyester bearing EH pendant chains. For instance, P(Ric-Ph-*r*-Ric-EH),  $n_{rel\ 0:100}$  is superior to  $n_{rel\ 5:95\ EH}$  while  $M_w\ 0:100 = 41\ kg.mol^{-1}$  is below  $M_w\ 5:95 = 66\ kg.mol^{-1}$ . Similarly, the relative viscosity of the oil containing the PRic-EH is superior to the one containing the P(Ric-C4<sub>25</sub>-*r*-Ric-EH<sub>75</sub>) while the latter molecular weight is about  $60\ kg.mol^{-1}$ . It is assumed that the branched structure of EH increases the polymer coil size in solution. By grafting insoluble pendant chain, the amount of branched side chains decreases, leading to a decrease of the coil size and thus of the relative viscosity. In the case of copolyesters based on MRic-C12 as soluble part, the impact on the relative viscosity is conversely related mostly to the polymer molecular weight and not to its composition. An exception is noticed for P(Ric-C4<sub>55</sub>-*r*-Ric-C12<sub>45</sub>) which increases generally more the oil viscosity than other copolymer with lower molecular weight.

Finally, it appeared that the copolyesters with butyl pendant chains have a better thickening efficiency than the one with phenyl ethyl pendant chains. For instance, at 100 °C the relative viscosity reach 1.37 for P(Ric-C4<sub>55</sub>-*r*-Ric-C12<sub>45</sub>) while  $\eta_{rel} < 1.3$  for P(Ric-Ph<sub>25</sub>-*r*-Ric-C12<sub>75</sub>) with a superior molecular weight. As it was mentioned about copolyesters solubility in Yubase 4+, phenyl ethyl groups have lower affinity with the mineral oil than butyl pendant chains. As a result, once grafted to the copoly(9-alkyl 12-hydroxystearate), phenyl ethyl groups decrease the polymer affinity with the oil and then its thickening efficiency.

### 2.3. Conclusion

Copoly(9-alkyl 12-hydroxystearate)s with various types of pendant alkyl chains were synthesized. The grafting of phenyl ethyl- and butyl- pendant chains lead to a decrease of the

polymer solubility in mineral oil. The solubility limit of each type of copolyester is related to the balance between insoluble and soluble pendant chains. It appears that phenyl ethyl moieties have less affinity with mineral oil than butyl ones. As a result, copolyesters with more than 25 wt.% of MRic-Ph could not be solubilized in oil while copolyesters with 55 wt.% of MRic-C4 were still soluble in oil. The presence of dodecyl pendant chains permitted higher copolyester solubility in oil than by the presence of 2-ethylhexyl pendant chains in the copolyester composition.

Once the copoly(9-alkyl 12-hydroxystearate) solubility in mineral oil was determined, its effect on the oil viscosity was evaluated. The copolyester thickening efficiency was impacted by the pendant chain nature. The mineral oil V-T behavior was also enhanced by P(Ric-Ph-*r*-Ric-C12) and P(Ric-C4-*r*-Ric-C12) addition, with Q values > 1. The higher the percentage of insoluble pendant chains, the higher the copolymer impact on oil V-T relationship. Consequently, these two types of copoly(9-alkyl 12-hydroxystearate) can be considered as Viscosity Index improvers. However, it could be interesting to understand how the polymer behaves in solution regarding to the temperature and to possibly relate this behavior to one of the mechanisms reported in literature.

### 3. Study in model solvent: conformational behavior

---

It was assumed that the mineral oil V-T behavior was impacted by some copoly(9-alkyl 12-hydroxystearate)s such as P(Ric-Ph<sub>25</sub>-*r*-Ric-C12<sub>75</sub>) due to their low solubility in oil, the latter increasing with the temperature. Conversely, P(Ric-C12), which is more soluble than the copolymer due to the absence of phenyl ethyl pendant group, did not change the oil viscosity regarding to the temperature. As a result, some impacts of the polymer addition on oil V-T relationship were noticed but no further information about how the two polymers behave in oil regarding to the temperature were brought.

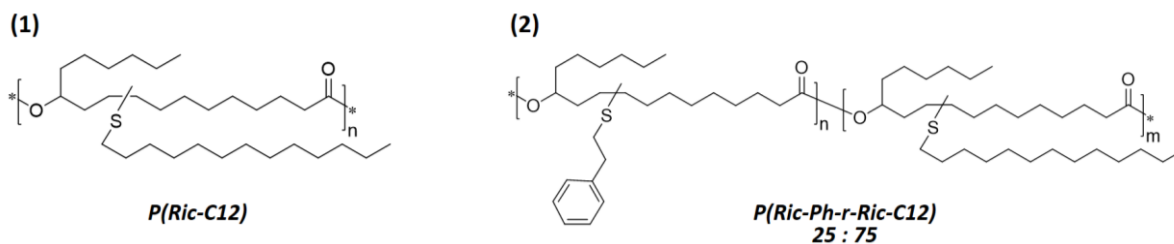


Figure IV-16: Chemical structure of homopoly(9-alkyl 12-hydroxystearate) P(Ric-C12) and copoly(9-alkyl 12-hydroxystearate) P(Ric-Ph-r-Ric-C12)

In order to understand the behavior in solution of these two polymers, illustrated in Figure IV-16, with temperature, a study was performed in model solvent. They were added in dodecane which presents close structure to mineral oil. First, the variation of the relative viscosity regarding to the temperature was investigated. Then, the dilute regime was evaluated in order to determine the intrinsic viscosity of the polymer in solution with temperature. Finally, the polymer coil size variation with the temperature was determined by SANS (Small Angle Neutrons Scattering) measurements.

### 3. 1. Behavior of homo- and copoly(9-alkyl 12-hydroxystearate)s in dodecane with the temperature

P(Ric-C12) and P(Ric-Ph<sub>0.25</sub>-r-Ric-C12<sub>0.75</sub>) were added in dodecane at concentrations from 0.3 wt.% to 3 wt.%. The polymers were solubilized at 100°C for two hours and cooled down at room temperature without stirring for 24 hours. Then, the density, dynamic viscosity and kinematic viscosity of the different solutions at temperatures from 20 °C to 100 °C were measured using a densimeter-viscosimeter, see data in Table IV-A-4 in Appendix. From these values, the relative viscosities were calculated as well as the Q values; the latter are reported in Table IV-10. The relative viscosities with respect to the temperature are illustrated in Figure IV-17.

Table IV-10: Relative viscosity regarding to the temperature and Q values of homopoly(9-alkyl 12-hydroxystearate) and copoly(9-alkyl 12-hydroxystearate) at several concentrations in dodecane

In dodecane	P(Ric-C12) $M_w = 55 \text{ kg.mol}^{-1}$						P(Ric-C12-r-Ric-Ph) $M_w = 72 \text{ kg.mol}^{-1}$					
Conc. (wt.%)	0.526	0.68	1	1.3	2	3	0.3	0.5	0.7	0.98	2.1	3
$\eta_{rel}$ 20°C	1.057	1.075	1.125	1.175	1.279	1.503	1.027	1.058	1.085	1.136	1.351	1.454
40°C	1.052	1.071	1.121	1.167	1.271	1.493	1.024	1.045	1.069	1.119	1.352	1.458
60°C	1.053	1.071	1.122	1.168	1.269	1.489	1.029	1.070	1.073	1.124	1.358	1.464
80°C	1.057	1.074	1.125	1.169	1.267	1.478	1.033	1.078	1.078	1.128	1.362	1.465
100°C	1.065	1.081	1.132	1.174	1.270	1.436	1.042	1.064	1.086	1.134	1.371	1.454
Q	1.257	1.149	1.091	1.037	0.994	0.884	1.75	1.426	1.232	1.129	1.056	0.991

As expected, the relative viscosity increases with the increase of the polymer concentration in dodecane. For similar concentration of P(Ric-C12) or P(Ric-Ph-*r*-Ric-C12), the relative viscosity is generally similar. No effect of the poly(9-alkyl 12-hydroxystearate) composition is noticed on their general thickening efficiency. The Viscosity Index improver effect was higher in the case of the copolymer than for homopolymer, with higher Q values at similar concentrations. This feature may be due to the presence of phenyl ethyl pendant chains, as it was observed in the case of polymer addition in mineral oil.

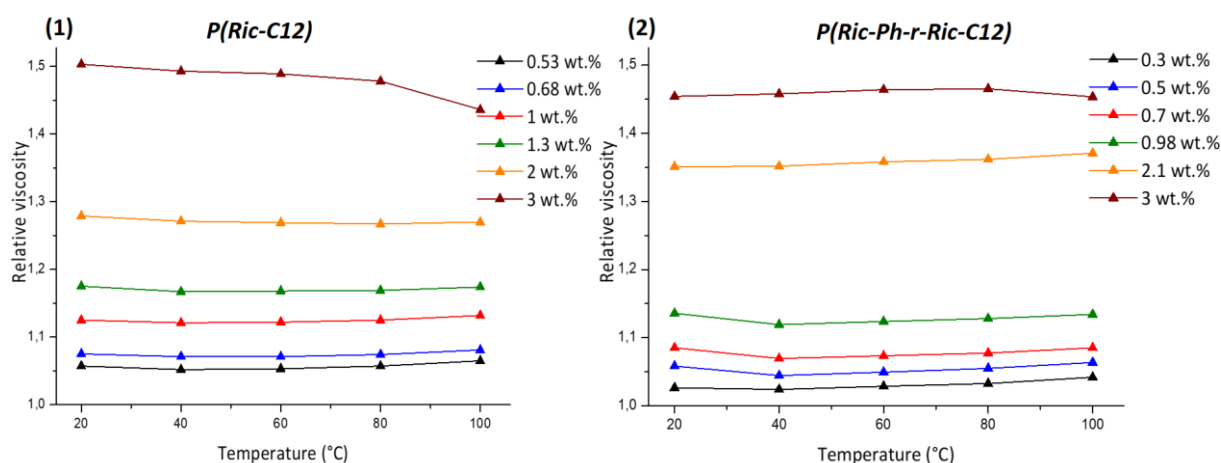


Figure IV-17: Relative viscosity regarding to the temperature for (1) homopoly(9-alkyl 12-hydroxystearate) and (2) copoly(9-alkyl 12-hydroxystearate) added in dodecane at various concentrations

Surprisingly, Q values decrease with the concentration increase for the two polymers. Both polymers impact positively the dodecane V-T behavior for concentrations below or equal to 1.3 wt.% for P(Ric-C12) and 2.1 wt.% for P(Ric-Ph-*r*-Ric-C12), with  $Q > 1$ . For higher concentrations, the Q values decrease below one. This could be due to the regime of dilution. The variation of the relative viscosity does not give information about the proper behavior of polymer in dodecane. However, following the literature, the two main phenomena described are the coil expansion and the aggregation/disaggregation behavior. In dilute solution, polymer coils are hypothetically not in contact with each other. Then, they may be able either to expand or to disaggregate with temperature, leading to an increase of the relative viscosity. Conversely, in dilute regime close to the overlap concentration,  $C^*$ , or above, polymer coil interaction or contact may limit either the coil expansion or the disaggregation, leading to lower impact on oil V-T behavior and Q values.

To conclude, similar thickening efficiency was observed for P(Ric-C12) and P(Ric-Ph-*r*-Ric-C12). However, at a same concentration, the oil V-T behavior was more impacted by the addition of

copolymer than homopolymer. This was attributed to the presence of phenyl ethyl pendant chains in P(Ric-Ph-*r*-Ric-C12) which decrease the polymer solubility in dodecane as it was observed in mineral oil. Moreover, the increase of the relative viscosity with temperature is strongly related to the concentration. Still, no information about the proper behavior in solution was given and further investigation should be performed such as the variation of the polymer intrinsic viscosity regarding to the temperature. The dilute regime should be preliminary determined because the concentration has a strong impact on the polymer behavior in solution.

### 3.2. Evolution of the intrinsic viscosity regarding to the temperature

#### 3.2.1. Evaluation of the dilute regime

In order to evaluate the intrinsic viscosity of P(Ric-C12) and P(Ric-Ph<sub>0.25</sub>-*r*-Ric-C12<sub>0.75</sub>) tested in dodecane, the polymer concentration in solution should be below C\*. In other words, the two polymers should be in a dilute regime. To determine this regime, solutions of dodecane with P(Ric-C12) and P(Ric-Ph<sub>0.25</sub>-*r*-Ric-C12<sub>0.75</sub>) at concentrations from 2 mg.mL<sup>-1</sup> to 21 mg.mL<sup>-1</sup>, i.e. 0.3 wt.% - 3 wt.%, were analyzed by Dynamic Light Scattering (DLS). The derived count rates obtained regarding to the polymer concentration are expressed in Figure IV-18.

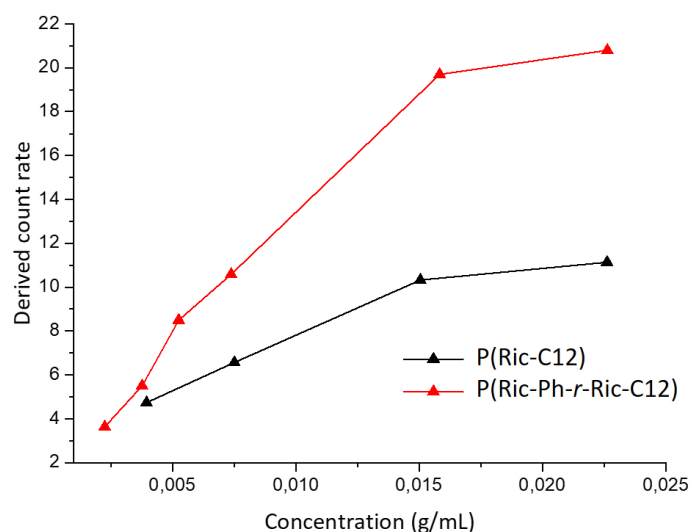


Figure IV-18 : Derived count rate regarding to the concentration for homo- and co-poly(9-alkyl 12-hydroxystearate) at 20°C, performed by DLS measurements

For both polymers in dodecane, the intensity increased linearly with the concentration for  $C \leq 0.016 \text{ g.mL}^{-1}$ , i.e. 2 wt.%. The polymer coils act as single particles in solution without polymer-polymer interaction, and the increase of the amount of polymer in solution leads to a direct

increase of the intensity signal. It can then be deduced that the polyesters are in the dilute regime. Conversely, the intensity seems to reach a plateau for  $C > 0.016 \text{ g}\cdot\text{mL}^{-1}$ , meaning that the polymer chains may not act as isolated coil in solution and could potentially start to interact with each other. The concentration is probably close to the overlap concentration. As a result, concentrations above  $C = 0.016 \text{ g}\cdot\text{mL}^{-1}$  were not considered in the following studies. A higher refracted intensity is noticed for P(Ric-Ph-r-Ric-C12) solutions than P(Ric-C12) ones. This may be due to the presence of phenyl pendant chains in the copolymer composition.

In dilute regime, the polymer solution viscosity increases linearly with the concentration. Then, once  $C^*$  is reached, a slope break is observed and the viscosity increase rate as a function of the concentration changes; the polymer is then in a semi-dilute regime. The kinematic viscosity was evaluated against the concentration of P(Ric-C12) and P(Ric-Ph-r-Ric-C12) in dodecane for concentration range  $0.002 \text{ g}\cdot\text{mL}^{-1} - 0.014 \text{ g}\cdot\text{mL}^{-1}$  and temperature from  $20^\circ\text{C}$  to  $100^\circ\text{C}$ . The kinematic viscosities were expressed as a function of the polymer concentration in Figure IV-19. A linear slope is obtained for the two types of solution whatever the temperature. The linear fits are obtained with R square value close to 1. The dilute regime is then confirmed for this range of concentration.

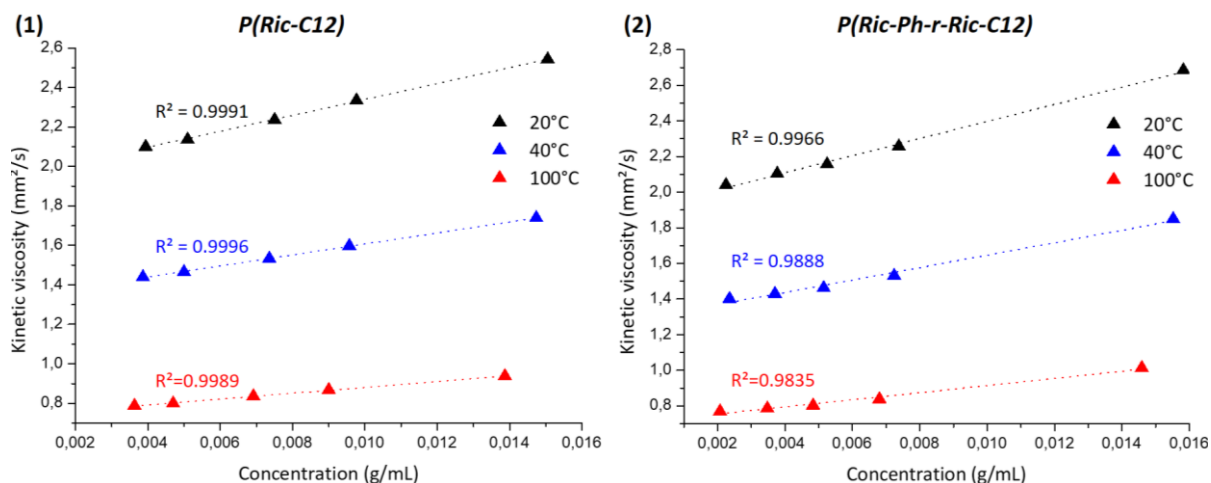


Figure IV-19 : Kinematic viscosity of dodecane solution depending on the concentration of additives, i.e. homopoly(9-dodecyl 12-hydroxystearate) and copoly(9-alkyl 12-hydroxystearate) with dodecyl and phenyl ethyl pendant chains

### 3.2.2. Intrinsic viscosity determination

As it was previously mentioned, the kinematic viscosities of dodecane solution with P(Ric-C12) and P(Ric-Ph-r-Ric-C12) in concentration range of 0.002 g.mL<sup>-1</sup> – 0.014 g.mL<sup>-1</sup> were determined for temperatures from 20 °C to 100 °C. Then, the reduced viscosity was calculated according to equation (IV-2).

$$\eta_{red} = \frac{\eta_{spe}}{c} = \frac{(\eta - \eta_0)/\eta_0}{c} \quad (IV-2)$$

where  $\eta_{red}$  the reduced viscosity,  $\eta_{spe}$  the specific viscosity,  $c$  the polymer concentration in g.mL<sup>-1</sup>,  $\eta$  the solution kinematic viscosity in mm<sup>2</sup>.s<sup>-1</sup> and  $\eta_0$  the dodecane kinematic viscosity in mm<sup>2</sup>.s<sup>-1</sup>. The reduced viscosity was expressed as a function of the polymer concentration in solution for several temperatures in Figure IV-20.

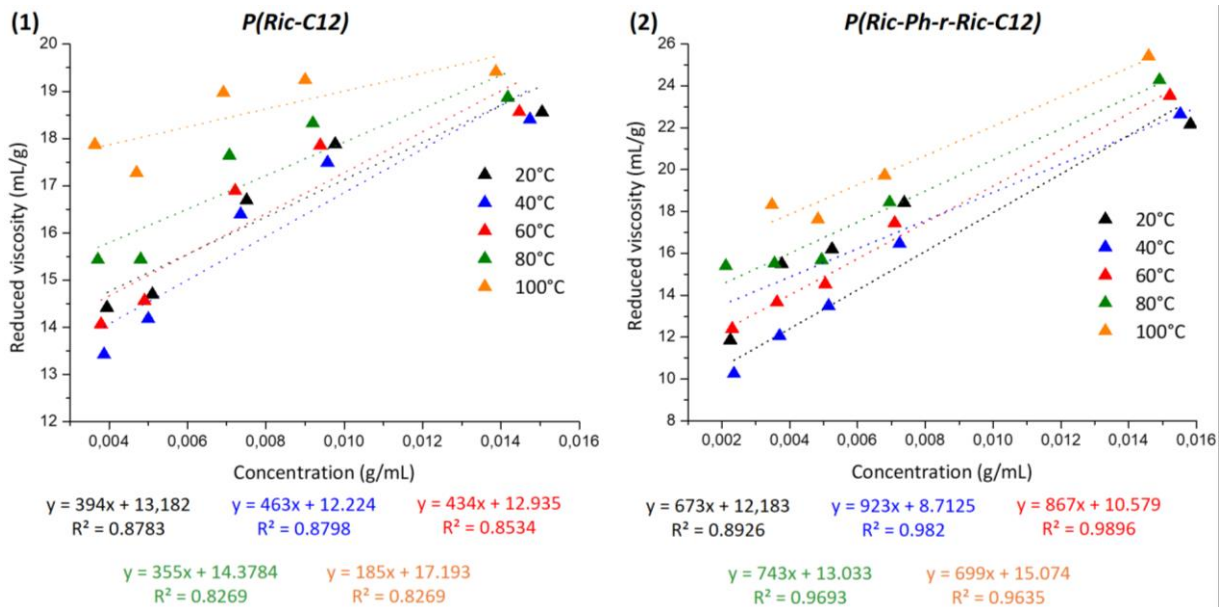


Figure IV-20 : Reduce viscosity as a function of the (1) PRic and (2) P(Ric-Ph-r-Ric-Ph) concentrations in dodecane at several temperatures

As the polymers are in dilute regime, it is possible to use the Huggins equation (IV-3) to determine the polymer intrinsic viscosity.

$$\eta_{red} = [\eta] - K_H[\eta]^2c \quad (IV-3)$$

where  $[\eta]$  the intrinsic viscosity in mL.g<sup>-1</sup> and  $K_H$  the Huggins constant. Using a linear fit of the reduced viscosity as a function of the temperature,  $[\eta]$  can be obtained as the reduced viscosity for  $c \rightarrow 0$ . Then, the Huggins constant are calculated from the slope values divided by  $[\eta]^2$ . The values obtained for PRic-C12 and P(Ric-Ph-r-Ric-C12) are reported in Table IV-11.

Table IV-11: Intrinsic viscosity and Huggins constant at several temperatures of dodecane solutions containing P(Ric-C12) and P(Ric-Ph-*r*-Ric-C12)

	P(Ric-C12) $M_w = 55 \text{ kg.mol}^{-1}$		P(Ric-C12- <i>r</i> -Ric-Ph) $M_w = 72 \text{ kg.mol}^{-1}$	
	$[\eta]$ (mL.g <sup>-1</sup> )	$K_H$	$[\eta]$ (mL.g <sup>-1</sup> )	$K_H$
<b>20°C</b>	13.18 ± 0.70	2.27 ± 0.49	12.18 ± 1.13	4.53 ± 0.91
<b>40°C</b>	12.22 ± 0.89	3.10 ± 0.66	8.71 ± 0.59	12.16 ± 0.95
<b>60°C</b>	12.94 ± 0.91	2.59 ± 0.62	10.58 ± 0.4	7.75 ± 0.45
<b>80°C</b>	14.38 ± 0.80	1.72 ± 0.45	13.03 ± 0.6	4.38 ± 0.45
<b>100°C</b>	17.19 ± 0.64	0.62 ± 0.25	15.07 ± 0.82	3.08 ± 0.80

Generally, the polymer intrinsic viscosity increases with the temperature. As a result, the polyester coils may expand by increasing the temperature due to a better solubility in dodecane. The intrinsic viscosity of P(Ric-Ph-*r*-Ric-C12) is lower than the one of P(Ric-C12) despite the higher molecular weight of the copolymer, e.g. at 40 °C,  $[\eta] = 8.7 \text{ mL.g}^{-1}$  with  $M_w = 72 \text{ kg.mol}^{-1}$  and  $[\eta] = 12.22 \text{ mL.g}^{-1}$  with  $M_w = 55 \text{ kg.mol}^{-1}$ , respectively. It is then assumed that, due to the presence of phenyl ethyl pendant chains, P(Ric-Ph-*r*-Ric-C12) is less soluble in dodecane than P(Ric-C12), thus leading to lower intrinsic viscosity.

In the case of P(Ric-C12) the Huggins constant varies from 3 at 40 °C to 0.6 at 100 °C. This variation in the opposite sense to the intrinsic viscosity was already observed in literature for Viscosity Index improvers.<sup>5,9</sup> The latter  $K_H = 0.6$  is close to 0.5, the mean value generally found for isolated polymers in solution. The larger  $K_H$  values indicate the presence of aggregation in solution.<sup>10</sup> As a result, P(Ric-C12) may be aggregated at low temperature and disaggregate with the temperature to isolated coils in solution at 100 °C. In parallel to the disaggregation, the polymer affinity with solvent may be enhanced leading to an increase of the intrinsic viscosity.

A decrease of the  $K_H$  values with temperature is also observed for the copolyester, from 12 at 40 °C to 3 at 100 °C. These values are much higher than the ones obtained with P(Ric-C12) solutions, whatever the temperature. It is then assumed that the P(Ric-Ph-*r*-Ric-C12) is much more aggregated in dodecane than P(Ric-C12), leading then to lower  $[\eta]$  values. By increasing the temperature, the copolymer may start to disaggregate. Still,  $K_H = 3$  at 100 °C, some aggregations may remain and the copolyester coils are not fully dispersed in solution.

To conclude, both polyesters may aggregate at room temperature and disaggregate progressively with the temperature increase. The copolymer with phenyl ethyl pendant chains seems less soluble in solution, leading to higher aggregation and lower intrinsic viscosity in dodecane.

### 3.3. Determination of the polymer size with respect to the temperature

Homopoly(9-dodecyl 12-hydroxystearate) P(Ric-C12) and copoly(9-alkyl 12-hydroxystearate) with 25 wt.% of phenyl ethyl and 75 wt.% of dodecyl pendant chains, P(Ric-Ph<sub>0.25</sub>-*r*-Ric-C12<sub>0.75</sub>), were added in dodecane at several concentrations below C\*. Regarding to the viscosity study, it was assumed that both polymers may present an aggregation-disaggregation behavior as a function of the temperature. This phenomenon may be enhanced by the presence of phenyl ethyl moieties. In order to evaluate this effect, a third polymer with a higher percentage of phenyl ethyl moieties, P(Ric-Ph<sub>0.4</sub>-*r*-Ric-C12<sub>0.6</sub>) will be compared to the P(Ric-C12) and P(Ric-Ph<sub>0.25</sub>-*r*-Ric-C12<sub>0.75</sub>) previously studied.

In order to confirm or not the aggregation-disaggregation behavior, the size of these three polyesters with the temperature was investigated by Small Angle Neutrons Scattering (SANS). The three polymers were added in deuterated-dodecane at 0.75 wt.% and 3 wt.%, i.e. below and close to the overlap concentration, respectively. The solutions were stirred at 100°C for two hours and cooled down for 24 hours. Samples with polymers at 3 wt.% in solution were analyzed at 36 °C and 72 °C. The samples of deuterated dodecane with 0.75 wt.% of polymers were analyzed following the successive temperatures of 20°C, 84°C, 72°C, 36 °C and then 20 °C for a second time. These samples were also analyzed 3 months after solubilization at 20°C, 100°C, 72°C, 36 °C and then 20 °C. An example of the neutrons scattered intensity as a function of the wave vectors is illustrated in Figure IV-21 and the R<sub>g</sub> obtained using a Debye model fitting is reported in Table IV-16.<sup>11,12</sup>

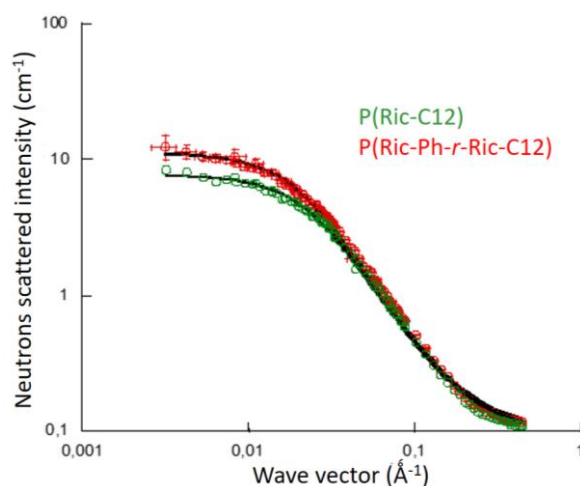


Figure IV-21 : Neutrons scattered intensity as a function of wave vector for solutions of d-dodecane with 3 wt.% of P(Ric-C12) and P(Ric-Ph-r-Ric-C12) at 36°C

For the polyesters tested, the radius of gyration decreased by increasing the temperature, whatever the concentration. For instance, when blended at 0.75 wt.% with dodecane, the P(Ric-Ph<sub>0.25</sub>-r-Ric-C12<sub>0.75</sub>) present a radius of gyration of 72 Å at 20 °C which decreased to 58 Å at 100 °C This decrease may be due to a progressive disaggregation of the polymer with the temperature, as it was previously observed in literature.<sup>6</sup> The other copolymer behaves similarly.

Table IV-16 : Radius of gyration determined by SANS of P(Ric-C12), P(Ric-Ph<sub>0.25</sub>-r-Ric-C12<sub>0.75</sub>) and P(Ric-Ph<sub>0.4</sub>-r-Ric-C12<sub>0.6</sub>) in deuterated dodecane

Conc (wt.%)		P(Ric-C12) M <sub>w</sub> =55 kg.mol <sup>-1</sup>			P(Ric-C12 <sub>0.25</sub> -r-Ric-Ph <sub>0.75</sub> ) M <sub>w</sub> =72 kg.mol <sup>-1</sup>			P(Ric-C12 <sub>0.4</sub> -r-Ric-Ph <sub>0.6</sub> ) M <sub>w</sub> =51 kg.mol <sup>-1</sup>			
		0.75	0.75*	3	0.75	0.75*	3	0.75	0.75*	3	3*
20°C	R <sub>g</sub> (Å)	65.7	57.7	-	73.8	65.1	-	58.5	52.9	66.1	59
	M <sub>w</sub> kg.mol <sup>-1</sup>	47	41	-	64	53	-	46	42	50	45
100°C	R <sub>g</sub> (Å)	-	57.3	-	-	65.4	-	-	50.8	-	47.3
	M <sub>w</sub> kg.mol <sup>-1</sup>	-	36	-	-	45	-	-	31	-	24
84°C	R <sub>g</sub> (Å)	60.1	-	-	67.5	-	-	54.6	-	52.4	-
	M <sub>w</sub> kg.mol <sup>-1</sup>	37	-	-	44	-	-	35	-	29	-
72°C	R <sub>g</sub> (Å)	58.7	57.2	55.3	68.1	63.9	67.0	52	51.5	52.3	48.9
	M <sub>w</sub> kg.mol <sup>-1</sup>	36	36	30	44	44	42	33	33	29	27
36°C	R <sub>g</sub> (Å)	59.2	56.6	65.4	68.5	63.9	77.2	53.7	49.3	56.5	52.7
	M <sub>w</sub> kg.mol <sup>-1</sup>	38	37	45	48	46	62	37	33	38	33
20°C	R <sub>g</sub> (Å)	58.7	54	-	68	64.6	-	54.3	50.9	59.5	60.5
	M <sub>w</sub> kg.mol <sup>-1</sup>	38	36	-	53	51	-	41	37	44	43

\* Sample (polymer dissolved in deuterated dodecane) analyzed after 3 months

In addition, the R<sub>g</sub> value obtained at 20°C right after the heating is lower than the one at the beginning of the measurement. It is then speculated that aggregation occurred at 20°C only after a certain time. The aggregation is slightly enhanced by increasing the polymer

concentration. For instance, at 72°C, P(Ric-Ph<sub>0.25</sub>-*r*-Ric-C12<sub>0.75</sub>)  $R_g = 58 \text{ \AA}$  at 0.75 wt.% and  $R_g = 67 \text{ \AA}$  at 3 wt.%. The highest the polymer concentration, the highest the aggregation. The sample have been analyzed after three months aging. In the case of P(Ric-C12), the radius of gyration is stable regarding to the temperature. The value is close to the  $R_g$  at high temperatures obtained during the first measurement. It is then assumed that the homopolymer progressively disaggregated with time. Conversely, an aggregation-disaggregation is still observed with temperature for the two copolyesters, suggesting a reversibility of the phenomenon.

## Conclusion

---

It appeared in the previous chapters than some comb poly(9-alkyl 12-hydroxystearate)s were soluble or insoluble in mineral oil depending on the nature of the pendant side chains. It was also shown that the soluble poly(9-alkyl 12-hydroxystearate), despite a thickening efficiency, did not impact on the oil V-T behavior. It was then assumed that a decrease of the polyester solubility by adding some “insoluble” pendant chains in the polymer could provide a Viscosity Index improver effect to the polymer. Consequently, poly(9-alkyl 12-hydroxystearate)s with various ratios of phenyl ethyl and dodecyl pendant chains were synthesized and added in mineral oil. The random copolymers lost their solubility in mineral oil when the amount of phenyl ethyl branched monomer was higher than 25 wt.%. The soluble copolyesters with  $M_w = 10 \text{ kg.mol}^{-1}$  did not impact the oil V-T behavior. However, a Viscosity Index improver effect was noticed when the polymer molecular weight was above  $50 \text{ kg.mol}^{-1}$ . It was also observed that the highest the percentage of phenyl pendant chains, the highest the polymer impact on the mineral oil V-T behavior.

Poly(9-alkyl 12-hydroxystearate)s with other nature of pendant chains were thus synthesized and evaluated in mineral oil. The copolymer with 55 wt.% of butyl and 45 wt.% of dodecyl pendant chains also impact positively the oil V-T behavior. It appeared that copolymer with 2-ethylhexyl pendant chains do not have a VI improver effect, maybe due to the steric hindrance of the branched side chain.

Finally, a poly(9-dodecyl 12-hydroxystearate) with 100% of dodecyl pendant chains and a copoly(9-alkyl 12-hydroxystearate) with 25 wt.% of phenyl ethyl and 75 wt.% of dodecyl pendant chains were added in dodecane as a model solvent. In mineral oil, only the latter showed a Viscosity Index improver behavior. However, in that case, both polymers impacted the dodecane V-T behavior. Surprisingly, a significant impact of the polymer concentration on their Viscosity Index improvement efficiency was noticed. It was then supposed that the polymer impacted positively the oil V-T behavior only in dilute regime. After determination of the latter, the intrinsic viscosity of the two polymers in dodecane was evaluated against temperature. For both polymers, the intrinsic viscosity increased with the temperature while the Huggins constant decreased. An aggregation-disaggregation behavior was then assumed for both polymers. The polymer radius of gyration was then determined by SANS measurements. A decrease of the radius of gyration regarding to the temperature was observed for both polymers, in accord with the aggregation – disaggregation behavior observed previously. This behavior was even more pronounced for the copolymer with phenyl moieties.

## References

---

- 1 T. W. Selby, *ASLE Trans.*, 1958, **1**, 68–81.
- 2 M. J. Covitch and K. J. Trickett, *Adv. Chem. Eng. Sci.*, 2015, **5**, 134–151.
- 3 P. Cusseau, N. Bouscharain, L. Martinie, D. Philippon, P. Vergne and F. Briand, *Tribol. Trans.*, 2017, **0**, 1–11.
- 4 C. Price and D. Woods, *Polymer (Guildf.)*, 1974, **15**, 389–392.
- 5 P. Bezot, B. Elmakoudi, B. Constans, D. Faure and P. Hoornaert, *J. Appl. Polym. Sci.*, 1994, **51**, 1715–1725.
- 6 M. T. Savoji, D. Zhao, R. J. Muisener, K. Schimossek, K. Schoeller, T. P. Lodge and M. A. Hillmyer, *Ind. Eng. Chem. Res.*, 2018, **57**, 1840–1850.
- 7 A. Martini, U. S. Ramasamy and M. Len, *Tribol. Lett.*, 2018, **66**, 58.
- 8 P. C. Hiemenz and T. P. Lodge, *Polymer Chemistry - Second edition*, CRC Press., 2007.
- 9 E. Maderek and B. A. Wolf, *Angew. Makromol. Chemie*, 1988, **161**, 157–173.
- 10 A. S. Yeung and C. W. Frank, *Polymer (Guildf.)*, 1990, **31**, 2089–2100.
- 11 P. Debye, *J. Phys. Colloid Chem.*, 1947, **51**, 18–32.
- 12 J. S. Pedersen, *Adv. Colloid Interface Sci.*, 1997, **70**, 171–210.

## Experimental

---

### ***Monomer synthesis***

All the methyl 9-alkyl 12-hydroxystearate were prepared following the same methodology as described in Chapter III. As a typical example, 10 g of methyl ester ricinoleate (32 mmol, 1 eq.) was mixed with 1-dodecanethiol (19.48 g, 96 mmol, 3 eq.), DMPA was added to the mixture (0.082 g, 0.32 mmol, 0.01 eq.). Photochemical thiol-ene reaction was performed in a 100 mL round bottom flask with a magnetic stirring under UV irradiation. A Lightningcure spot light source L9588-06A from Hamamatsu and a filter A9616-05 wavelength 350 to 400nm was used as UV source. During reaction, the conversion of double bonds was monitored by  $^1\text{H}$  spectroscopy (vinyl proton signals at 5.40 ppm). The irradiation was stopped once the double bond was no more detectable by  $^1\text{H}$  NMR.

After reaction, the viscous liquid was dissolved in 10 mL of dichloromethane (DCM) and the methyl ester ricinoleate with a thiol pendant group was purified by Flash column chromatography, using a gradient of cyclohexane (100 %) to ethyl acetate (100 %) eluent mixture. Product was recovered with a yield in the range of 62% - 84% by solvent evaporation and dried overnight under vacuum (0.22 mBar) at 80 °C.

The same methodology was used for all the thiol-ene reaction performed on methyl ricinoleate, with yield in the range of 62% - 84%. In the case of octadecane-1-thiol addition, 5 mL of cyclohexane were added to solubilize the solid thiol.

### ***Procedure of polymerization***

The polycondensation were performed following the methodology developed in Chapter II. For the first series of  $M_w = 10 \text{ kg.mol}^{-1}$  targeted, as an example, the methyl 9-dodecyl 12-hydroxystearate, MRic-C12, (1.5 g, 4.8 mmol) was dried overnight under vacuum at 70 °C with magnetical stirring in 50 mL Schlenk flask at 200 rpm. The mixture was cooled at room temperature under static vacuum and a 5 wt.% solution of  $\text{Ti}(\text{O}i\text{Pr})_4$  in DCM (0.015 g of catalyst, 0.053 mmol, 1 wt.%) was added under nitrogen flow. The mixture was stirred at room temperature for 30 min under static nitrogen then put under vacuum and heated at 70 °C for

30min. Then the mixture was heated at 120 °C for one hour, 140 °C for another hour and 180 °C for 5 hours still under dynamic vacuum to remove the MeOH sub-product and magnetic stirring at 200 rpm. After 8hours reaction, stirring was stopped, the highly viscous mixture was cooled to room temperature and the flask was opened to air in order to stop the reaction. No purification was performed on the final product. The higher molecular weight polymers were obtained using mechanical stirring during 48 hours reacting.

### ***Preparation of oil blended with additives***

As it was described in the two previous chapter, all the polymers were solubilized in oil following the same methodology: the oil with polyesters added was heated at 100 °C overnight under magnetic stirring to promote the solubilisation and then cooled down without stirring at room temperature during 24 hours. The solubility of the additive in the oil was evaluated macroscopically. Samples were degassed under vacuum and magnetic stirring for 30 minutes right before to be analysed by LOVIS 2000 densimeter-viscometer. In the case of dodecane, the solutions were heated for 2 hours and then cooled down without stirring at room temperature during 24 hours. The samples were not degassed for viscometry, DSL and SANS analysed.

## Appendix

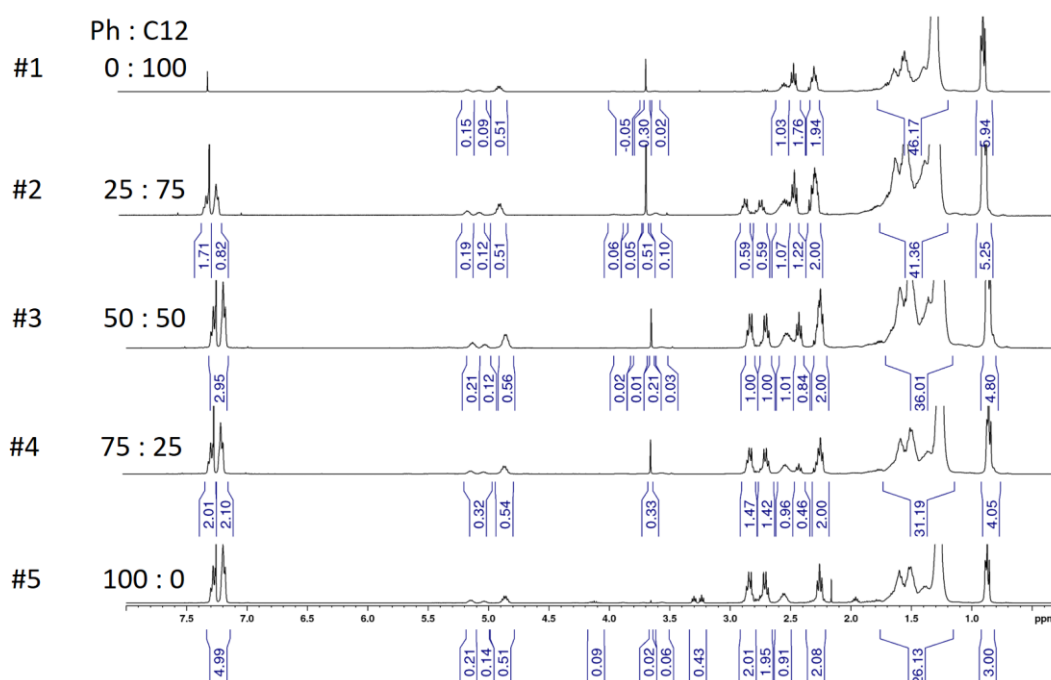


Figure IV-A-1:  $^1\text{H}$  NMR spectra in  $\text{CdCl}_3$  of copoly(9-alkyl 12-hydroxystearate) with phenyl and dodecane pendant chains at different ratios of each.  $M_w = 10 \text{ kg}\cdot\text{mol}^{-1}$

Table IV-A-1: Yubase 4+ with 3 wt.% copolyesters with  $M_w = 10 \text{ kg}\cdot\text{mol}^{-1}$ . Density, dynamic and kinematic values from 20 °C to 100 °C

	Temperature	20°C	40°C	60°C	80°C	100°C
<b>Yubase 4+</b>	<b>Density</b>	0.8226	0.8099	0.7973	0.7846	0.7720
	$\eta_{\text{dyn}}$ ( $\text{mPa}\cdot\text{s}^{-1}$ )	34.41	15.16	7.97	4.82	3.35
	$\eta_{\text{kin}}$ ( $\text{mPa}\cdot\text{s}^{-1}$ )	41.82	18.71	9.99	6.14	4.34
<b>+3 wt.% Viscoplex</b>	<b>Density</b>	-	-	-	-	-
	$\eta_{\text{dyn}}$ ( $\text{mPa}\cdot\text{s}^{-1}$ )	-	-	-	-	-
	$\eta_{\text{kin}}$ ( $\text{mPa}\cdot\text{s}^{-1}$ )	-	22.552	-	-	5.082
<b>#1 +3 wt.% P(Ric-C12)</b>	<b>Density</b>	0.8254	0.8127	0.8001	0.7874	0.7748
	$\eta_{\text{dyn}}$ ( $\text{mPa}\cdot\text{s}^{-1}$ )	38.98	17.09	8.95	5.39	3.74
	$\eta_{\text{kin}}$ ( $\text{mPa}\cdot\text{s}^{-1}$ )	47.22	21.03	11.19	6.85	4.824
<b>#2 +3 wt% P(Ric-Ph-r-Ric-C12) Ratio 25 : 75</b>	<b>Density</b>	0.8264	0.8139	0.801	0.7884	0.7757
	$\eta_{\text{dyn}}$ ( $\text{mPa}\cdot\text{s}^{-1}$ )	39.36	17.27	9.02	5.45	3.77
	$\eta_{\text{kin}}$ ( $\text{mPa}\cdot\text{s}^{-1}$ )	47.64	21.22	11.27	6.92	4.86

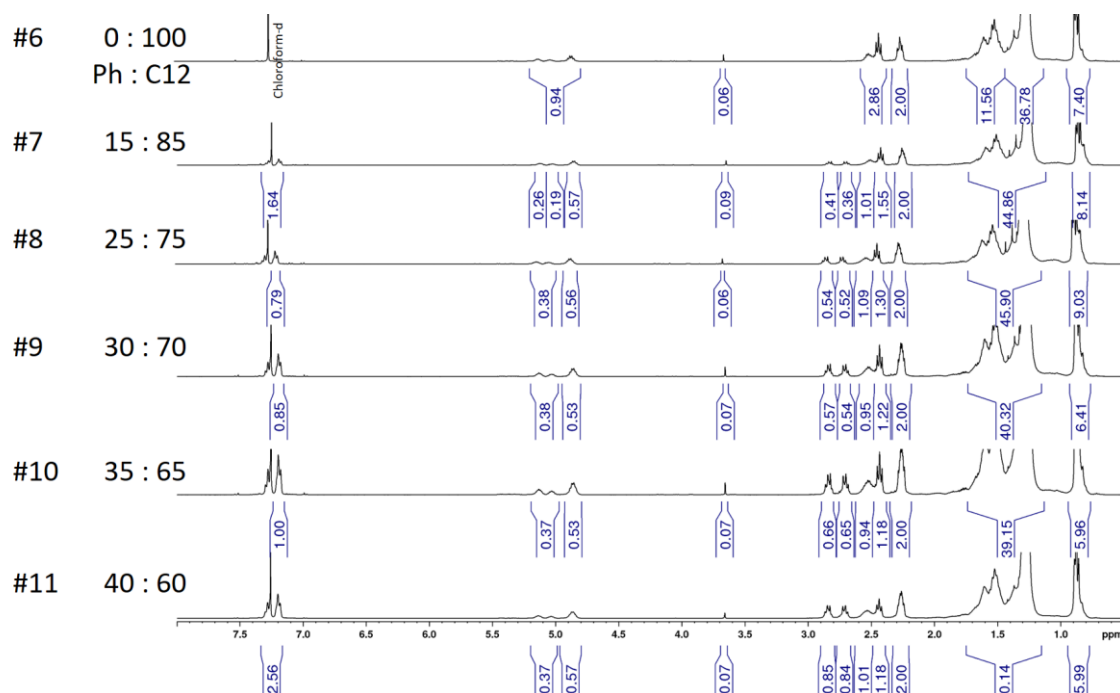


Figure IV-A-2:  $^1\text{H}$  NMR spectra in  $\text{CdCl}_3$  of of copoly(9-alkyl 12-hydroxystearate) with phenyl and dodecane pendant chains at different ratios of each.  $M_w = 60 \text{ kg}\cdot\text{mol}^{-1}$

Table IV-A-2: Yubase 4+ with 3 wt.% copolyesters with  $M_w = 50 \text{ kg}\cdot\text{mol}^{-1}$ . Density, dynamic and kinematic values at several temperatures

	Temperature	20°C	40°C	60°C	80°C	100°C
<b>Yubase 4+</b>	<b>Density</b>	0.8226	0.8099	0.7973	0.7846	0.7720
	$\eta_{\text{dyn}} \text{ (mPa}\cdot\text{s}^{-1}\text{)}$	34.41	15.16	7.97	4.82	3.35
	$\eta_{\text{kin}} \text{ (mPa}\cdot\text{s}^{-1}\text{)}$	41.82	18.71	9.99	6.14	4.34
<b>Y+3 wt.% Viscoplex</b>	<b>Density</b>	-	-	-	-	-
	$\eta_{\text{dyn}} \text{ (mPa}\cdot\text{s}^{-1}\text{)}$	-	-	-	-	-
	$\eta_{\text{kin}} \text{ (mPa}\cdot\text{s}^{-1}\text{)}$	-	22.552	-	-	5.082
<b>#6 Y+3 wt.% P(Ric-C12)</b>	<b>Density</b>	0.8255	0.8128	0.8001	0.7875	0.7748
	$\eta_{\text{dyn}} \text{ (mPa}\cdot\text{s}^{-1}\text{)}$	44.12	19.45	10.21	6.17	4.29
	$\eta_{\text{kin}} \text{ (mPa}\cdot\text{s}^{-1}\text{)}$	53.45	23.93	12.76	7.83	5.54
<b>#7 Y+3 wt% P(Ric-Ph-r-Ric-C12) Ratio 15 : 85</b>	<b>Density</b>	0.8259	0.8132	0.8005	0.7879	0.7753
	$\eta_{\text{dyn}} \text{ (mPa}\cdot\text{s}^{-1}\text{)}$	43.96	19.43	10.24	6.21	4.33
	$\eta_{\text{kin}} \text{ (mPa}\cdot\text{s}^{-1}\text{)}$	53.22	23.89	12.79	7.88	5.59
<b>#8 Y+3 wt% P(Ric-Ph-r-Ric-C12) Ratio 25 : 75</b>	<b>Density</b>	0.826	0.8133	0.8007	0.788	0.7754
	$\eta_{\text{dyn}} \text{ (mPa}\cdot\text{s}^{-1}\text{)}$	43.86	19.42	10.28	6.25	4.36
	$\eta_{\text{kin}} \text{ (mPa}\cdot\text{s}^{-1}\text{)}$	53.09	23.88	12.84	7.93	5.63

Table IV-A-3: Yubase 4+ with 3 wt.% copolyesters with  $M_w = 60 \text{ kg.mol}^{-1}$  and various pendant chains Density, dynamic and kinematic values at several temperatures

	Temperature	20°C	40°C	60°C	80°C	100°C
<b>Yubase 4+</b>	<b>Density</b>	0.8226	0.8099	0.7973	0.7846	0.7720
	$\eta_{\text{dyn}}$ ( $\text{mPa.s}^{-1}$ )	34.41	15.16	7.97	4.82	3.35
	$\eta_{\text{kin}}$ ( $\text{mPa.s}^{-1}$ )	41.82	18.71	9.99	6.14	4.34
<b>#15</b> Y+3 wt.% P(Ric-EH) Ratio 0 : 100	<b>Density</b>	0.8259	0.8132	0.8006	0.7879	0.7753
	$\eta_{\text{dyn}}$ ( $\text{mPa.s}^{-1}$ )	48.06	21.25	11.22	6.79	4.67
	$\eta_{\text{kin}}$ ( $\text{mPa.s}^{-1}$ )	58.19	26.13	14.01	8.61	6.03
<b>#16</b> Y+3 wt% P(Ric-Ph-r-Ric-EH) Ratio 5 : 95	<b>Density</b>	0.826	0.8133	0.801	0.790	0.780
	$\eta_{\text{dyn}}$ ( $\text{mPa.s}^{-1}$ )	44.42	19.58	10.27	6.20	4.31
	$\eta_{\text{kin}}$ ( $\text{mPa.s}^{-1}$ )	53.77	24.08	12.83	7.87	5.56
<b>#17</b> Y+3 wt% P(Ric-Ph-r-Ric-EH) Ratio 10 : 90	<b>Density</b>	0.8261	0.8134	0.801	0.790	0.780
	$\eta_{\text{dyn}}$ ( $\text{mPa.s}^{-1}$ )	42.84	18.85	9.866	5.93	4.02
	$\eta_{\text{kin}}$ ( $\text{mPa.s}^{-1}$ )	51.85	23.17	12.32	7.53	5.19
<b>#6</b> Y+3 wt.% P(Ric-C12) Ratio 0 :100	<b>Density</b>	0.8255	0.8128	0.8001	0.7875	0.7748
	$\eta_{\text{dyn}}$ ( $\text{mPa.s}^{-1}$ )	44.12	19.45	10.21	6.17	4.29
	$\eta_{\text{kin}}$ ( $\text{mPa.s}^{-1}$ )	53.45	23.93	12.76	7.83	5.54
<b>#20</b> Y+3 wt% P(Ric-C4-s-Ric-C12) Ratio 25 : 75	<b>Density</b>	0.8257	0.813	0.800	0.790	0.780
	$\eta_{\text{dyn}}$ ( $\text{mPa.s}^{-1}$ )	41.78	18.45	9.641	5.79	3.92
	$\eta_{\text{kin}}$ ( $\text{mPa.s}^{-1}$ )	50.6	22.7	12.05	7.35	5.06
<b>#21</b> Y+3 wt% P(Ric-C4-s-Ric-C12) Ratio 50 : 50	<b>Density</b>	0.8258	0.8131	0.801	0.790	0.780
	$\eta_{\text{dyn}}$ ( $\text{mPa.s}^{-1}$ )	44.29	19.7	10.42	6.33	4.41
	$\eta_{\text{kin}}$ ( $\text{mPa.s}^{-1}$ )	53.64	24.23	13.02	8.04	5.69
<b>#22</b> Y+3 wt% P(Ric-C4-s-Ric-C12) Ratio 55 : 45	<b>Density</b>	0.826	0.8133	0.801	0.790	0.780
	$\eta_{\text{dyn}}$ ( $\text{mPa.s}^{-1}$ )	45.91	20.53	10.87	6.61	4.61
	$\eta_{\text{kin}}$ ( $\text{mPa.s}^{-1}$ )	55.58	25.24	13.58	8.39	5.94
<b>#24</b> Y+3 wt% P(Ric-C4-s-Ric-EH) Ratio 25 : 75	<b>Density</b>	0.8259	0.8132	0.801	0.790	0.780
	$\eta_{\text{dyn}}$ ( $\text{mPa.s}^{-1}$ )	45.52	20.21	10.65	6.44	4.48
	$\eta_{\text{kin}}$ ( $\text{mPa.s}^{-1}$ )	55.12	24.85	13.3	8.17	5.78
<b>#25</b> Y+3 wt% P(Ric-C4-s-Ric-EH) Ratio 40 : 60	<b>Density</b>	0.8255	0.8128	0.8	0.790	0.770
	$\eta_{\text{dyn}}$ ( $\text{mPa.s}^{-1}$ )	42.63	18.08	9.772	5.88	4.08
	$\eta_{\text{kin}}$ ( $\text{mPa.s}^{-1}$ )	51.64	22.98	12.21	7.47	5.26
<b>#26</b> Y+3 wt% P(Ric-C4-s-Ric-EH) Ratio 50 : 50	<b>Density</b>	0.8261	0.8134	0.801	0.790	0.780
	$\eta_{\text{dyn}}$ ( $\text{mPa.s}^{-1}$ )	44.06	19.37	10.14	6.14	4.26
	$\eta_{\text{kin}}$ ( $\text{mPa.s}^{-1}$ )	53.34	23.81	12.67	7.78	5.49

Table IV-A-4: Dodecane with P(Ric-C12) or P(Ric-Ph-r-Ric-C12) at several concentrations. Density, dynamic and kinematic values from 20 °C to 100 °C.

	Temperature	20°C	40°C	60°C	80°C	100°C
<b>Dodecane 99%</b>	<b>Density</b>	0.7494	0.7349	0.7202	0.7054	0.6903
	$\eta_{\text{dyn}} \text{ (mPa}\cdot\text{s}^{-1}\text{)}$	1.459	1.005	0.757	0.628	0.51
	$\eta_{\text{kin}} \text{ (mPa}\cdot\text{s}^{-1}\text{)}$	1.987	1.368	1.050	0.890	0.739
<b>D + 0.53 wt.% P(Ric-C12)</b>	<b>Density</b>	0.75	0.7355	0.7208	0.706	0.691
	$\eta_{\text{dyn}} \text{ (mPa}\cdot\text{s}^{-1}\text{)}$	1.575	1.058	0.797	0.665	0.544
	$\eta_{\text{kin}} \text{ (mPa}\cdot\text{s}^{-1}\text{)}$	2.100	1.439	1.106	0.941	0.787
<b>D + 0.68 wt.% P(Ric-C12)</b>	<b>Density</b>	0.7503	0.7357	0.7211	0.7063	0.6912
	$\eta_{\text{dyn}} \text{ (mPa}\cdot\text{s}^{-1}\text{)}$	1.602	1.078	0.811	0.675	0.552
	$\eta_{\text{kin}} \text{ (mPa}\cdot\text{s}^{-1}\text{)}$	2.136	1.465	1.125	0.956	0.799
<b>D + 1 wt.% P(Ric-C12)</b>	<b>Density</b>	0.7508	0.7363	0.7217	0.7069	0.6918
	$\eta_{\text{dyn}} \text{ (mPa}\cdot\text{s}^{-1}\text{)}$	1.679	1.129	0.85	0.708	0.578
	$\eta_{\text{kin}} \text{ (mPa}\cdot\text{s}^{-1}\text{)}$	2.236	1.533	1.178	1.001	0.836
<b>D + 1.3 wt.% P(Ric-C12)</b>	<b>Density</b>	0.7514	0.7369	0.7223	0.7075	0.6924
	$\eta_{\text{dyn}} \text{ (mPa}\cdot\text{s}^{-1}\text{)}$	1.754	1.177	0.885	0.735	0.600
	$\eta_{\text{kin}} \text{ (mPa}\cdot\text{s}^{-1}\text{)}$	2.334	1.597	1.226	1.040	0.867
<b>D + 2 wt.% P(Ric-C12)</b>	<b>Density</b>	0.7525	0.738	0.7234	0.7086	0.6936
	$\eta_{\text{dyn}} \text{ (mPa}\cdot\text{s}^{-1}\text{)}$	1.913	1.283	0.964	0.799	0.651
	$\eta_{\text{kin}} \text{ (mPa}\cdot\text{s}^{-1}\text{)}$	2.542	1.739	1.332	1.128	0.938
<b>D + 3 wt.% P(Ric-C12)</b>	<b>Density</b>	0.7538	0.7394	0.7247	0.71	0.695
	$\eta_{\text{dyn}} \text{ (mPa}\cdot\text{s}^{-1}\text{)}$	2.252	1.511	1.133	0.934	0.737
	$\eta_{\text{kin}} \text{ (mPa}\cdot\text{s}^{-1}\text{)}$	2.987	2.043	1.563	1.315	1.061
<b>D + 0.3 wt% P(Ric-Ph-r-Ric-C12) Ratio 25 : 75</b>	<b>Density</b>	0.7496	0.735	0.7204	0.7055	0.6904
	$\eta_{\text{dyn}} \text{ (mPa}\cdot\text{s}^{-1}\text{)}$	1.529	1.030	0.778	0.649	0.532
	$\eta_{\text{kin}} \text{ (mPa}\cdot\text{s}^{-1}\text{)}$	2.040	1.401	1.080	0.919	0.770
<b>D + 0.5 wt% P(Ric-Ph-r-Ric-C12) Ratio 25 : 75</b>	<b>Density</b>	0.7497	0.7351	0.7204	0.7056	0.6906
	$\eta_{\text{dyn}} \text{ (mPa}\cdot\text{s}^{-1}\text{)}$	1.577	1.050	0.793	0.662	0.542
	$\eta_{\text{kin}} \text{ (mPa}\cdot\text{s}^{-1}\text{)}$	2.103	1.429	1.102	0.939	0.786
<b>D + 0.7 wt% P(Ric-Ph-r-Ric-C12) Ratio 25 : 75</b>	<b>Density</b>	0.7501	0.7356	0.7209	0.7061	0.691
	$\eta_{\text{dyn}} \text{ (mPa}\cdot\text{s}^{-1}\text{)}$	1.617	1.076	0.812	0.677	0.554
	$\eta_{\text{kin}} \text{ (mPa}\cdot\text{s}^{-1}\text{)}$	2.156	1.463	1.127	0.959	0.802
<b>D + 0.98 wt% P(Ric-Ph-r-Ric-C12) Ratio 25 : 75</b>	<b>Density</b>	0.7508	0.7363	0.7217	0.7068	0.692
	$\eta_{\text{dyn}} \text{ (mPa}\cdot\text{s}^{-1}\text{)}$	1.694	1.128	0.851	0.710	0.580
	$\eta_{\text{kin}} \text{ (mPa}\cdot\text{s}^{-1}\text{)}$	2.257	1.531	1.180	1.004	0.838
<b>D + 2.1 wt% P(Ric-Ph-r-Ric-C12) Ratio 25 : 75</b>	<b>Density</b>	0.7536	0.7392	0.7246	0.7099	0.6948
	$\eta_{\text{dyn}} \text{ (mPa}\cdot\text{s}^{-1}\text{)}$	2.023	1.367	1.033	0.860	0.704
	$\eta_{\text{kin}} \text{ (mPa}\cdot\text{s}^{-1}\text{)}$	2.684	1.849	1.426	1.212	1.013
<b>D + 3 wt% P(Ric-Ph-r-Ric-C12) Ratio 25 : 75</b>	<b>Density</b>	0.754	0.7395	0.7249	0.7101	0.6951
	$\eta_{\text{dyn}} \text{ (mPa}\cdot\text{s}^{-1}\text{)}$	2.178	1.475	1.114	0.926	0.747
	$\eta_{\text{kin}} \text{ (mPa}\cdot\text{s}^{-1}\text{)}$	2.889	1.994	1.537	1.304	1.074



## General conclusion and perspectives

---

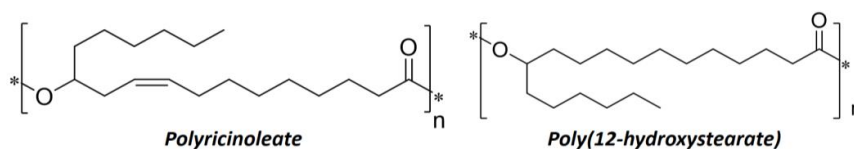
Lubricants are complex formulations based on oil containing various additives. They are used in many sectors, such as automotive, marine, aeronautic and industrial equipment. Nowadays, the main challenge of lubricants is to decrease their negative impact on the environment. In this frame, the aim of this thesis was to design new bio-based viscosity control additives and notably as viscosity modifiers and pour point depressants.

First, a literature survey was presented to evaluate the requirements for a polymer to act as a viscosity modifier (VM) or a pour point depressant (PPD). The most common polymer structures already described in the literature and their behavior in solution was discussed. It appeared that VM should thicken the oil, impact the oil viscosity-temperature relationship and resist to the shear. A good thickening efficiency is provided by polymers with high molecular weights and linear aliphatic structures such as poly(alphaolefin)s (OCP). However, they do not impact the oil viscosity against temperature; they are only considered as thickeners. They are also sensitive to the shear due to their linear structure. Conversely, comb and star-shaped polymers such as PAMAs present a higher shear stability but a lower thickening efficiency. Viscosity Index improvers impact positively the oil V-T behavior by coil expansion, such as comb PAMAs do, or by aggregation-disaggregation behavior like hydrogenated styrene-diene copolymer behave and some other OCP-grafted-PAMA copolymers.

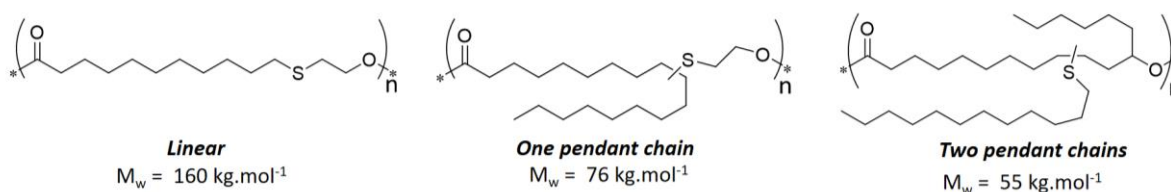
As far as pour point depressants are concerned, the most commonly used polymers are comb PAMAs with long alkyl side chains and semi-crystalline polymers as ethyl vinyl acetate copolymers and OCPs with high ethylene contents. Generally, those polymers are able to co-crystallize with oily wax compounds at low temperature. The presence of an amorphous phase in the mentioned polymers permits the dispersion of crystals thus limiting the oil gelation.

Finally, some bio-based viscosity modifiers have been developed but the research in this field is still at an infancy stage. Ethyl cellulose or poultry chicken feather were investigated as viscosity modifiers but the most developed bio-based additives are vegetable oil derivatives.

In this context, it was decided to develop fatty acid-based polyesters as viscosity modifiers. Methyl ricinoleate was selected as the appropriate monomer due to its aliphatic structure and the presence of natural internal double bond, hydroxyl group and ester function that can be further derivatized.

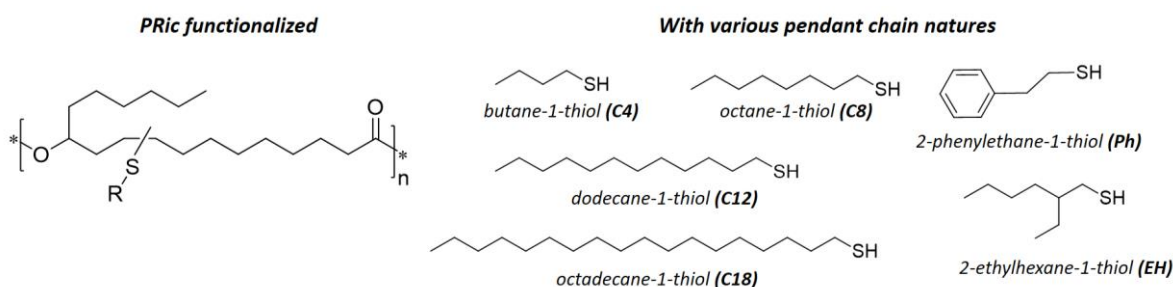


This A-B type monomer (methyl ricinoleate), as well as its saturated homologous the methyl 12-hydroxystearate, were polymerized through polycondensation. Data are collected in Chapter 2. Polyricinoleate (PRic) and polyhydroxystearate (PHS) could be obtained with molecular weights ranging from 10 to 130 kg.mol<sup>-1</sup>. PRic is a fully amorphous polymer with a glass transition temperature about -60 °C while PHS is semi-crystalline, with  $T_g = -40$  °C,  $T_{cris} = -30$ °C and  $T_m = -22$ °C. Both polymers exhibit a good thermal stability till 300 °C. The rheological behavior of the polyricinoleate in bulk condition was then evaluated regarding to PRic molecular weight. An entanglement of PRic chains was observed for  $M_w > 25$  kg.mol<sup>-1</sup>. The two polyesters were blended with an organic oil (Radialube 7368) and a mineral oil (Yubase 4+) in order to evaluate their efficiency as viscosity modifiers. High molecular weight PRic was neither soluble in mineral oil nor in organic one. However, soluble PRic with  $M_w = 32$  kg.mol<sup>-1</sup>, shows a thickening efficiency similar to the commercial additive tested, the Priolube 3986, with an increase of the relative viscosity of 1.5 at 20°C and an increase of the Viscosity Index from 152 to 175 in organic oil. Best results were obtained with PHS of  $M_w = 73$  kg.mol<sup>-1</sup>; in this case, the oil viscosity was doubled and the VI increases from 145 to 209 and from 152 to 204 for blends at 3 wt.% in mineral and organic oil, respectively. As a result, PHS appeared as a promising thickener. However, no impact on the oil V-T behavior was observed, avoiding the use of such polyester as Viscosity Index improver.



In the third chapter, the polyester structure was varied from linear to comb polyricinoleate derivatives with two aliphatic side chains. 2-mercaptoethanol (ME) was added on methyl undecenoate (MU) and methyl oleate (MO) in order to obtain linear and branched A-B monomer, respectively. The A-B monomer with two pendant alkyl chains, i.e. the poly(9-dodecyl 12-hydroxystearate) was obtained by thiol-ene addition of dodecane-1-thiol on methyl ricinoleate. The so-formed monomers were then polymerized by transesterification. The nature (primary or secondary) of the hydroxyl function as well as the presence of alkyl side chains affected the kinetics of polymerization. As expected, the linear MU-ME monomer, i.e. the methyl 11-(2-hydroxyethylthio)undecenoate, was the most reactive leading to polyesters with  $M_w > 160 \text{ kg}\cdot\text{mol}^{-1}$ . Both the presence of a thio-ether linkage and pendant alkyl chains in the repetitive unit affected the polyester properties. For instance, the linear polyester was semi-crystalline ( $T_g = -33 \text{ }^\circ\text{C}$ ,  $T_m = 53^\circ\text{C}$  and  $T_{cris} = 35 \text{ }^\circ\text{C}$ ) while comb polyesters were fully amorphous ( $T_g = -60 \text{ }^\circ\text{C}$ ). It appeared that only the comb poly(9-dodecyl 12-hydroxystearate) (PRic-C12) was soluble in both mineral and organic oils.

A series of comb poly(9-alkyl 12-hydroxystearate)s was thus developed with various nature of pendant alkyl chains and molecular weights. The nature of alkyl side chains did not impact the polyester thermal stability but affected the glass transition temperature. Indeed, the longest the alkyl chain length, the highest the  $T_g$ . For instance, P(Ric-C4) has a  $T_g = -66 \text{ }^\circ\text{C}$  while P(Ric-C12)  $T_g$  is about  $-61 \text{ }^\circ\text{C}$ . Interestingly, poly(9-octadecyl 12-hydroxystearate) (P(Ric-C18)) appeared to be semi-crystalline with a  $T_g$  about  $-28 \text{ }^\circ\text{C}$ , a  $T_{cris}$  of  $-12 \text{ }^\circ\text{C}$  and a  $T_m = -5 \text{ }^\circ\text{C}$ . Added at 0.1 wt.% in mineral oil, this comb polyester was able to co-crystallize with the oil waxy compounds at low temperature and to decrease the pour point about  $11 \text{ }^\circ\text{C}$ . P(Ric-C18) is thus a promising bio-based pour point depressant.

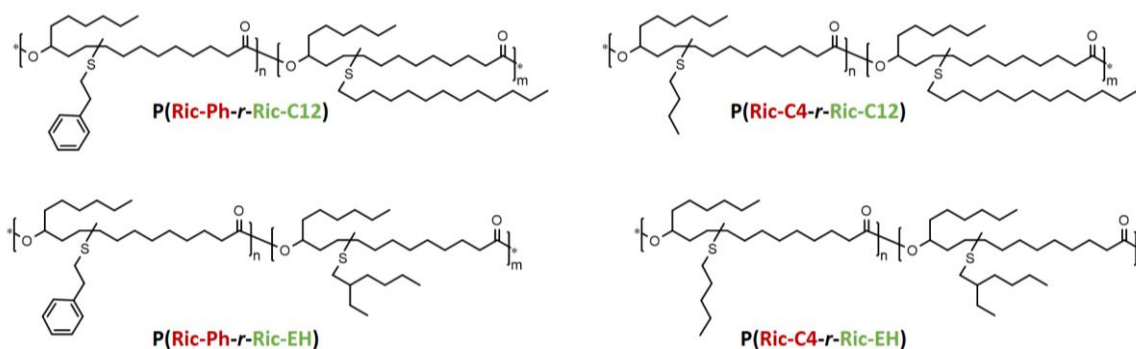


These comb poly(10-alkyl 12-hydroxystearate)s were also evaluated as viscosity modifiers in mineral and organic oils. In organic oil, the comb polymers act as a thickener, whatever the

side chains nature. Conversely, the poly(9-alkyl 12-hydroxystearate) behavior in mineral oil was affected by the nature of the pendant chains. For instance, PRic-C4 and PRic-Ph were insoluble in mineral oil. Among the soluble comb poly(9-alkyl 12-hydroxystearate) in mineral oil, P(Ric-EH) with a 2-ethylhexyl side chains appeared to have the best thickening efficiency with an increase of the oil viscosity about 1.4 times and a VI increase from 145 to 190. Still, no impact on the oil V-T behavior was observed.

In a nutshell, a promising pour point depressant behavior was obtained with comb PRic-C18. In addition, promising bio-based thickeners were developed such as PHS and P(Ric-EH) which increase the VI above 50 points. However, no impact of the prepared bio-based polyesters on the oil Viscosity-Temperature behavior was noticed, avoiding their use as Viscosity Index improvers.

The aim of the last chapter was then to design polyesters which can enhance the oil V-T behavior. It was observed in the previous chapter that some comb polyesters were soluble or not regarding to the nature of the grafted side chain. As a result, comb copoly(9-alkyl 12-hydroxystearate)s comprising some “insoluble” and “soluble” side chains were synthesized and evaluated as Viscosity Index improvers in mineral oil. Firstly, a series of random P(Ric-Ph-*r*-Ric-C12), was obtained with various ratio of phenyl ethyl- and dodecyl- pendant chains and added at 3 wt.% in mineral oil. The random copolymers lost their solubility in oil when the amount of phenyl ethyl- branched monomer was higher than 25 wt.%. For the others, an increase of the relative viscosity with respect to temperature was observed as a proof of the polymer impact on the oil V-T behavior ( $Q > 1$ ).



In the following, copoly(9-alkyl 12-hydroxystearate)s with other pendant chains were synthesized and added to mineral oils. The copolymer with 55 wt.% of butyl and 45 wt.% of

dodecyl pendant chains also impacted positively the oil V-T behavior, with a Q value superior to 1. It appeared that copolymer with 2-ethylhexyl pendant chains do not have a VI improver effect, probably due to the steric hindrance of the branched side chain.

Finally, a polyricinoleate with 100% of dodecyl- side chains and a copoly(9-alkyl 12-hydroxystearate) with 25% of phenyl ethyl- and 75% of dodecyl- side chains were added in dodecane, used as a model solvent. Surprisingly, both polymers impacted the dodecane V-T behavior while only the copolymer had this effect in mineral oil. The intrinsic viscosity of both polyesters in dodecane increased with the temperature while the Huggins constant decreased, traducing a disaggregation with the temperature. For P(Ric-C12) between 40 °C and 100 °C,  $[\eta]$  varied from 13 to 17 mL.g<sup>-1</sup> and  $K_H$  decreased from 3 to 0.6. Similarly, in the same range of temperature, the P(Ric-Ph-*r*-Ric-C12) intrinsic viscosity increased from 8 to 15 mL.g<sup>-1</sup> and  $K_H$  decreased from 12 to 3. In addition, a decrease of their radius of gyration with temperature was observed. As a result, it is speculated that both P(Ric-C12) and P(Ric-Ph-*r*-Ric-C12) aggregate at room temperature then disaggregate with the temperature increase. This behavior, even more pronounced for P(Ric-Ph-*r*-Ric-C12) than P(Ric-C12), led to a progressive increase of the oil viscosity, thus affected the V-T relationship.

In conclusion, the designed bio-based polyricinoleates derivatives are able to thicken oils to impact the oil V-T behavior and even to decrease the oil pour point, depending on the structure selected. Still, the possibilities of improvement of these systems are numerous. First, it could be interested to design copoly(9-alkyl 12-hydroxystearate)s with phenyl ethyl- and octadecyl- side chains to potentially combine their potential use as Viscosity Index improvers and Pour point depressants. Regarding the P(Ric-C18) efficiency as pour point depressant, it could be also interesting to use a normed test, such as ASTM D97 in order to have comparative data with commercial additives. In addition, microscopy and WAXS analyses at low temperature should be performed to fully analyze the co-crystallization with the oily waxy compounds.

The developed polyesters reached a good thickening efficiency and some were able to impact positively the oil V-T behavior through an aggregation-disaggregation behavior. Still, this impact was not really significant and should be improved. The design of block copoly(9-alkyl

12-hydroxystearate) instead of random ones in order to enhance the aggregation-disaggregation behavior could be also a strategy to develop. Some preliminary tests were performed but the obtained block P(Ric-C12-*b*-Ric-C4) did not reach sufficient molecular weights thus leading to a low thickening efficiency. Another way could be to force the polymer aggregation at low temperature through physical or chemical pendant chains interactions which can break at high temperature, leading to disaggregation. In that sense, the addition of pendant chains with hydrogen bonding such as sulfonate or urethane functions was investigated. Some preliminary results (not presented in this manuscript) were not convincing and require further investigations. In a same way, the integration of moieties enabling supramolecular interactions could be envisioned.

Finally, it could be interesting to more largely test the prepared polyricinoleate derivatives. Indeed, these bio-based polyesters designed as viscosity control additives could eventually ensure other properties required for lubricant applications. For instance, it is well-known that fatty acids are efficient as friction modifiers due to their polar head. In addition, sulfur compounds have good affinity with metal pieces. As a result, functionalized comb polyesters could also be evaluated as friction modifiers and anti-wear additives. Moreover, these polymers have a natural polarity due to the presence of ester bonds and could thus be tested as dispersants.

Through this work, bio-based functionalized polyricinoleates derivatives were obtained using simple and not harmful process following as much as possible the principles of green chemistry. Even if the biodegradability of the prepared polyesters was not tested, polyricinoleate is described in literature as a biodegradable polymer. Finally, promising bio-based viscosity control additives were designed, in accordance with new requirements in lubricant technology with respect to environmental issues. This work certainly opens new opportunities in this field.

# Materials and methods

---

## 1. Materials

Two different bio-based methyl ricinoleates (96%, kindly provided by ITERG; Nu-chek-prep, >99%) and methyl hydroxystearate (Nu-check-prep, >99%) were used without further purification for polyesters synthesis. Methyl oleate with 99% purity was supplied by Nu-chek-prep and methyl-10-undecanoate with 99% purity was purchased from Sigma-Aldrich.

Thiols were used as received: 2-mercaptoethanol (99%, TCI Europe), 1-butanethiol (99%, Sigma-Aldrich); 1-octanethiol (>98.5 %, Sigma-Aldrich), 1-dodecanethiol (>98%, Sigma-Aldrich); 1-octadecanethiol (98%, Sigma-Aldrich); 2-phenylethane-1-thiol (98%, Sigma-Aldrich) and 2-ethylhexane-1-thiol (>98%, TCI Europe).

Titanium isopropoxide ( $Ti(OiPr)_4$ , 99.99 %, Acros Organics); Triazabicyclodecene (TBD, 98%, Sigma-Aldrich); Sodium methoxide (NaOMe, 98%, Acros Organics) and Zinc Acetate ( $Zn(OAc)_2$ , 99.99%, Sigma-Aldrich) were used as catalyst as received. 2,2-Dimethoxy-2-phenylacetophenone (DMPA, 99 %, Aldrich) was used as received for photoinitiation. Reagent grade quality solvents were used as received. Deuterated solvents were purchased from Eurisotop and used as received.

Priolube 3986 was kindly provided from Croda. HOSO and Radialube 7368 were kindly provided by Oleon and Yubase 4+ from Total.

## 2. Methods

### ***Nuclear Magnetic Resonance (NMR)***

All the  $^1H$  and 1D  $^{13}C$ -NMR (DEPT) spectra were recorded on Bruker Avance 400 spectrometer (400 MHz and 100.63 MHz for  $^1H$  and  $^{13}C$ , respectively) by using  $CDCl_3$  as a solvent at room temperature.  $^1H$  NMR analyses were performed with 16 scans. Multiplicity dependent 1D  $^{13}C$ -NMR experiment (DEPT) was performed with deptsp135 pulse program (256 scans) Two-dimensional analysis such as  $^1H$ - $^1H$  COSY (COrrrelation Spectroscopy) was also performed.

### ***Size Exclusion Chromatography in THF (SEC)***

Polymer molecular weight were determined by Size Exclusion Chromatography (SEC) using tetrahydrofuran (THF) as the eluent. Measurements in THF were performed on an Ultimate 3000 system from ThermoScientific equipped with diode array detector DAD. The system also includes a multi-angles light scattering detector MALS and differential refractive index detector dRI from Wyatt technology. Polymers were separated on three G2000, G3000 and G4000 TOSOH HXL gel columns (300 x 7.8 mm) (exclusion limits from 1000 Da to 400 000 Da) at a flowrate of 1 mL.min<sup>-1</sup>. Columns temperature was held at 40°C. Polystyrene was used as the standard.

### ***Differential Scanning Calorimetry (DSC)***

Differential Scanning Calorimetry (DSC) measurements were performed on DSC Q100 (TA Instruments). The sample was heated from -130°C to 150°C at a rate of 10°C.min<sup>-1</sup>. Consecutive cooling and second heating run were also performed at 10°C.min<sup>-1</sup>. The glass transition temperatures and melting points were calculated from the second heating run.

### ***Thermogravimetric analysis (TGA)***

Thermogravimetric analyses were performed on TGA-Q500 system from TA instruments at a heating rate of 10 °C.min<sup>-1</sup> under nitrogen atmosphere from room temperature to 600°C.

### ***Rheological measurements***

Rheological measurements were monitored using an Anton Paar Physica MCR302 operating in the parallel plates geometry. The measurements were performed under nitrogen flow in the environmental chamber to avoid potential moisture effect. The temperature was controlled by Peltier device. The top plate has a diameter of 8 mm and the gap between plates was fixed at 1mm for the measurement in bulk. For the samples of oils blended with polymers, a cone plate with a diameter of 50 mm with 1° angle and the gap between plates was fixed at 1mm. Samples were loaded at room temperature. The sample was stabilized at the desirable temperature for 5 min before the measurement started. To evaluate the viscosity regarding to the temperature, a temperature ramp was applied from 20 °C to -30 °C with a decrease rate of 1 °C.min<sup>-1</sup>. A constant shear frequency of 1 rad.s<sup>-1</sup> was applied during the measurement.

***Density and viscosity analyses***

The viscosimetric tests were performed on a LOVIS 2000 apparatus from Anton Paar at several calibrated temperatures: 20 °C, 40 °C, 60 °C, 80 °C and 100 °C. Around 3 mL of solution were added in the density meter cell and the capillary tube ( $\varnothing$  1.8 mm for oils and  $\varnothing$  1.59 mm for dodecane) containing a steel ball ( $\varnothing$ 1.5mm,  $d=7.68 \text{ g.cm}^{-3}$ ). The density, the dynamic viscosity ( $\text{mPa.s}^{-1}$ ) and the kinematic viscosity ( $\text{mPa.s}^{-1}$ ) are determined directly from the apparatus.

***UV initiated reactions***

Photo-crosslinking were performed using a UV lamp HAMAMATSU equipped with a LC8 lamp (full power of  $4000 \text{ mW.cm}^{-1}$ ) and an A9616-03 filter transmitting in the range 280-400 nm, avoiding the heating of the mixture reaction. The lamp was placed in contact of the shlenk.

***Flash chromatography***

Flash chromatography was performed on a Grace Reveleris apparatus, employing silica cartridges from Grace. Cyclohexane: ethyl acetate gradients were used as eluents. The detection was performed through ELSD and three UV detectors at 254, 265 and 280 nm.

***Dynamic light scattering***

Dynamic light scattering measurements were performed at 25°C with a Malvern Instrument Nano-ZS equipped with a He-Ne laser ( $I \frac{1}{4} 632.8 \text{ nm}$ ). Samples were introduced into cells (pathway: 10 mm). The measurements were performed at a scattering angle of 90° at 20 °C

***Small angle Neutrons Scattering analyses (SANS)***

SANS measurements were performed on the PACE spectrometer of the Laboratoire Léon Brillouin (CEA-Saclay, France). Three configurations were used to cover overlapping wave vector  $q$  ranges of  $3.2 \times 10^{-3} - 3.4 \times 10^{-2}$ ,  $8.3 \times 10^{-3} - 8.8 \times 10^{-2}$ , and  $4.4 \times 10^{-2} - 0.45 \text{ \AA}^{-1}$ , with the following values of sample-to-detector distance  $D$  and neutron wavelength  $\lambda$ :  $D=4.56 \text{ m}$  and  $\lambda=13 \text{ \AA}$ ,  $D=4.56 \text{ m}$  and  $\lambda=5 \text{ \AA}$ ,  $D=0.86 \text{ m}$  and  $\lambda=5 \text{ \AA}$ . Each samples were measured successively at 20 °C, 84°C, 72°C, 36 °C and 20°C back.

By analysing the scattering intensity, it is possible to obtain the characteristic sizes and the shape and the interactions, represented by the form factor  $P(q)$  and the structure factor  $S(q)$ . The classical expression of the scattering intensity per unit volume of spherically symmetric particles writes

$$I(q) = n \Delta\rho^2 V_{\text{part.}}^2 P(q) S(q) \quad (1)$$

where  $n$  is the number density of particles,  $\Delta\rho$  is the difference in the neutron scattering length density between the particles and the solvent, and  $V_{\text{part.}}$  is the unit volume of the particles. The form factor describes the structure of particles and fulfills  $P(q = 0) = 1$  while the structure factor describes the interaction between particles. In the absence of interactions,  $S(q) = 1$ . Introducing the volume fraction of particles,  $\Phi = n V_{\text{part.}}$ ,

$$I(q) = \Phi \Delta\rho^2 V_{\text{part.}} P(q) \quad (2)$$

For individual chains, the volume  $V_{\text{part.}}$  is defined by the weight average molecular weight  $M_w$  of one mole of chains, the molar mass  $m$  and the volume  $v$  of one monomer as  $V_{\text{chain}} = M_w \cdot v/m$ . Thus, for a dilute solution of polymer of weight concentration  $c$ , occupying a volume fraction  $\Phi = N_A \cdot v \cdot c/m$ , where  $N_A$  is the Avogadro number ( $6.02 \cdot 10^{23}$ ), Eq. 2 becomes:

$$I(q) = v^2 \Delta\rho^2 \frac{c}{m^2} N_A M_w P(q) \quad (3)$$

By introducing the mass density of the polymer  $d = m/(N_A \cdot v)$ , we obtain:

$$I(q) = \Delta\rho^2 \frac{c}{d^2 N_A} M_w P(q) \quad (4)$$

Generally, the weight average molecular weight  $M_w$  and the radius of gyration  $R_G$  can be deduced from the fit to this equation using the so called Debye function as form factor:

$$P_{\text{Debye}}(q, R_G) = \frac{2}{(q^2 R_G^2)^2} (\exp(-q^2 R_G^2) + q^2 R_G^2 - 1) \quad (5)$$





## Nouveaux polyesters biosourcés comme additifs pour moduler les propriétés rhéologiques des lubrifiants

**Résumé :** L'objectif de ces travaux de thèse a été de développer des polyesters issus de ressources oléagineuses pour les utiliser comme additifs pour moduler la viscosité d'huiles lubrifiantes. Pour ce faire, l'approche par polycondensation de monomères de type hydroxy-acide a été privilégiée. Dans un premier temps, le poly(ricinoléate de méthyle) et son homologue saturé, le poly(12-hydroxystéarate de méthyle), ont été synthétisés dans une large gamme de masses molaires et leur utilisation comme épaississant d'huiles lubrifiantes a été démontrée. Dans un second temps, des polyesters dérivés du poly(ricinoléate de méthyle) et présentant des architectures de polymère en peigne ont été synthétisés par addition thiol-ène et polycondensation. Une étude de l'impact de l'architecture de ces polyesters sur leur comportement en solution a permis de prouver que les structures en peigne étaient les plus adaptées pour des applications visant, à la fois, un épaississement et une diminution du point d'écoulement de l'huile lubrifiante. Par la suite, des copoly(9-alkyl 12-hydroxystéarate)s en peigne possédant différentes chaînes pendantes ont été synthétisés afin de contrôler leur solubilité dans une huile minérale, la Yubase 4+, et ont permis de réduire la diminution de viscosité de cette huile avec la température. Finalement, l'étude dans le dodécane de deux copoly(9-alkyl 12-hydroxystéarate)s en peigne a révélé un phénomène d'agrégation des chaînes polymères lesquelles se désagrègent avec l'augmentation de la température, ce qui est en accord avec un des mécanismes d'action des additifs modulant la viscosité des huiles lubrifiantes décrit dans la littérature.

**Mots clés :** Poly(ricinoléate de méthyle), polyesters, biosourcé, polycondensation, réaction thiol-ène, additifs rhéologiques, lubrifiants

## New fatty acids based polyesters as viscosity control additives for lubricants

**Abstract:** The aim of this thesis was to promote the use of polyesters from oleaginous resources as viscosity control additives for lubricants. The hydroxyl-acid type monomers were polymerized through polycondensation route. First, poly(methyl ricinoleate) and its homologous poly(methyl-12-hydroxystearate) were synthesized in a large range of molecular weights and their use as thickeners of lubricant oils was demonstrated. Secondly, comb polyesters derived from poly(methyl ricinoleate) were designed *via* thiol-ene addition and polycondensation process. The effect of the polyester architecture on their behavior in solution was investigated and revealed that comb polymers are the most suitable for applications that required a thickening efficiency and a pour point depressant effect. Then, comb (co)poly(9-alkyl 12-hydroxystearate)s with various pendant alkyl chains were designed in order to control their solubility in a mineral oil, the Yubase 4+, and to limit the oil viscosity decrease of these oils with temperature. Finally, the behavior in dodecane of two comb (co)poly(9-alkyl 12-hydroxystearate)s revealed that the polymer chains tend to aggregate at low temperature and to disaggregate with the temperature increase. This phenomenon is in accordance with one of the oil Viscosity Index Improver behaviors, described in literature.

**Keywords:** Poly(methyl ricinoleate), fatty acid-based polyesters, biosourced, polycondensation, thiol-ene, viscosity control additives, lubricants

Laboratoire de Chimie des Polymères Organique, UMR5629  
16, avenue Pey-Berland, F-33607 PESSAC

